National Library of Canada
Acquisitions and Bibliographic Services Branch
395 Wellington Street
Ottawa, Ontario
K1A 0N4

Bibliothèque nationale du Canada
Direction des acquisitions et des services bibliographiques
395, rue Wellington
Ottawa (Ontario)
K1A 0N4

Your file Votre référence

Our file Notre référence

NOTICE

The quality of this microform is heavily dependent upon the quality of the original thesis submitted for microfilming. Every effort has been made to ensure the highest quality of reproduction possible.

If pages are missing, contact the university which granted the degree.

Some pages may have indistinct print especially if the original pages were typed with a poor typewriter ribbon or if the university sent us an inferior photocopy.

AVIS

La qualité de cette microforme dépend grandement de la qualité de la thèse soumise au microfilmage. Nous avons tout fait pour assurer une qualité supérieure de reproduction.

S'il manque des pages, veuillez communiquer avec l'université qui a conféré le grade.

La qualité d'impression de certaines pages peut laisser à désirer, surtout si les pages originales ont été dactylographiées à l'aide d'un ruban usé ou si l'université nous a fait parvenir une photocopie de qualité inférieure.

Canada

ATTITUDE DYNAMICS AND MANEUVERING OF FLEXIBLE SPACE SYSTEMS

By

M. Jafar Sadigh D.

Department of Mechanical Engineering

McGill University

Montreal, Canada

March 1995

A Thesis submitted to the Faculty of Graduate Studies and Research
in partial fulfillment of the requirements for the degree of
Doctor of Philosophy

ISBN 0-612-05786-0

Dedicated to my parents,

and to the memory of

Dr. F. Ghahremani

Abstract

In this thesis, the problem of attitude dynamics and maneuvering of flexible, multibody space systems is studied. A formulation for deriving the equations of motion of these systems, based on Kane's method, is presented. In this formulation the concepts of constrained motion and the effect of nonlinear coupling between rigid-body motion and the elastic vibrations are examined in depth.

Dynamics of constrained systems is studied with the main objective of deriving the complete, minimum-dimension set of equations of motion. A class of constraints is identified whose associated constraint forces, unknown quantities, remain in the minimum-order set of equations obtained by conventional methods. In this case, the minimum-order set of equations is incomplete, i.e., these equations have more unknowns than the number of equations, and can not be solved. A novel method, based on Kane's equations, is presented which is capable of generating the complete, minimum-order set of equations even for this class of constrained motion. As a spin-off, the formulation sheds some light on aspects such as adequacy and redundancy of constraint forces.

The effect of rigid-body motion on the dynamic behavior of flexible systems, known as dynamic or geometric stiffening effect, is examined in detail. An analytical development based on Kane's method is presented which shows that, in general, the equations of motion of a flexible system which undergoes rigid body motion might have some terms missing if the elastic motions are expressed as *linear* combinations of the generalized coordinates. The analysis precisely identifies which terms will be missed in a general case. It specifically shows that if the rigid-body motion is not prescribed, certain blocks of the generalized mass matrix might also miss some terms. Finally, a novel method based on nonlinear strain-displacement

relations is presented which can be used either to derive the correct equations directly, or to find the correction terms for an incorrect set of equations developed using conventional methods. The method is geometry-independent and can be used for different elastic elements such as beams, plates and shells.

Taking advantage of the above mentioned developments, a formulation is developed and implemented in a symbolic computer code, FLXSIM, for deriving the analytical form of the equations of motion. The code can handle constrained systems which are congregations of rigid bodies, beams, and plates connected through arbitrary joints, even flexible joints. Defining intermediate parameters to minimize the length of the equations, the code has been successful in simulating complex systems even on PC computers. The features such as easy incorporation of actuators, even along elastic members, and analytical linearization in the presence of intermediate parameters makes the code a powerful tool in control synthesis of complex systems.

Application of artificial constrained motion to devise open-loop control laws for tracking problems is proposed. Using this approach, to track the desired output trajectory, the states of the system do not have to track prescribed trajectories. Interesting applications of this method in semi-manual control of manipulators and in fine tracking of flexible manipulators are presented.

A perturbation technique in conjunction with a phase-plane based optimal control analysis is proposed for near-minimum-time maneuvering of flexible multibody systems moving along a prescribed trajectory. The idea is successfully employed to devise a control law for a typical retrieval maneuver performed by a Shuttle-based three link, flexible manipulator.

Résumé

Cette thèse étudie le problème de la manoeuvrabilité et du contrôle des manipulateurs spaciaux. La formulation utilisée pour obtenir les équations de mouvement de ces systèmes est basée sur la méthode de Kane. Avec cette formulation, les concepts de mouvement contraint "constrained motion" et l'effet d'accouplement entre le mouvement de corps rigide "rigid body motion" et les vibrations élastiques sont examinés en profondeur.

La dynamique de systèmes contraints est étudiée avec pour objectif principal de minimiser la dimension du système d'équations de motion. Une classe de contraintes pour laquelle le système d'équations possède plus de forces contraignantes que d'équations est identifiée. Pour cette classe de systèmes, les équations possède plus d'inconnus que d'équations et ne peuvent donc être résolues. La methode présentée est basée sur la dynamique de Kane et peut générer un système d'équations d'un ordre minimum même pour cette classe de système. De plus, cette formulation apporte des éclaircissements sur certains aspects tel que la pertinence et la redondance de contraintes.

Les effets de déplacements de corps sur la réponse dynamique d'un système flexible, aussi connu sous raidissement dynamique "dynamic stiffening", sont examinés en detail. Le développement analytique présenté démontre que généralement, les équations de motion d'un système flexible qui exécute une manoeuvre rigide peuvent perdre certains termes si la motion flexible est exprimé sous forme d'une combinaison linéaire des coordonnés généralisées. L'analyse identifie avec précision quels termes sont susceptible de disparaître. Elle démontre que si la motion rigide n'est pas prescrite, certaines blocs de la matrice de mass généralisée peuvent aussi manquer certain termes. De plus, une nouvelle methode basée sur une relation non-linéaire entre les deformations et les déplacements, permet de soit dériver correctement les

équations de motion ou d'établir des corrections pour des systèmes d'équations incorrectes basés sur des methodes conventionnelles. Cette methode est indépendante de la géométrie et peut être utilisée pour différents primitifs tel que plaques, poutres et autres.

Un programme symbolic, FLXSIM, utilise les développements mentionés ci-haut et dérive analytiquement les équations de motion. Le programme supporte des systèmes contraints qui sont composés de primitifs, poutres et de plaques connectés par des joints arbitraires. Le programme a été utilisé avec succès pour la simulation de systèmes complexes sur un ordinateur personnel (PC). La facilité d'implémentation de servomoteur (même au long du membre flexible) et la linéarisation analytique en présence de paramètres intermédiaires font de ce programme un outil puissant en matière de synthèse de contrôle de systèmes complexes.

Une application artificielle de contrainte est proposée pour la conception de boucle de contrôle "feed forward" de trajectoire. En utilisant cette approche, les variables du système n'ont pas besoin de suivre une trajectoire prescrite. Des applications intéressentes de cette méthode en contrôle semi-manuelle de manipulateur et en manipulation précise de manipulateur flexible sont présentées.

Une technique de perturbation en conjonction avec une analyse du plan de phase optimal est proposé pour manoeuvrer des systèmes flexibles sur une trajectoire prescrite en un temps presque minimum "near-minimum-time". Cette technique a été utilisée avec succès pour déterminer une fonction de contrôle pour des manoeuvres typiques de récupération par un manipulateur (trois membres) de la navette spaciale.

Acknowledgments

I would like to express my sincere gratitude to Professor A.K. Misra for his encouragement and advice during the course of the research. Also, his help in proof reading the manuscript and editorial suggestions were invaluable.

I gratefully acknowledge the scholarship provided by the Ministry of Culture and Higher Education of Iran, the financial support granted by the Natural Science and Engineering Research Council of Canada (NSERC), and the Max Bell Open Fellowship awarded by McGill University.

Sincere thanks are due to all of my professors and colleagues, among them special thanks are due to Mr. M. Keshmiri, for everything I learned from valuable discussions we had.

Finally, I wish to express my special thanks to my wife for her constant encouragement and support. I would like to thank my family, particularly my mother, for their kindness and belief in me.

Claim of Originality

To the best of the author's knowledge, the following developments presented in this thesis are original and have not been presented elsewhere.

- Development of a new method based on the introduction of *modified nonholonomic partial velocities* for deriving the complete minimum-order set of equations for systems with artificial and/or natural constraints.
- Development of some analytical measures for testing the adequacy and redundancy of constraint forces.
- Development of a formulation which precisely identifies the terms which might be missed from the equations of motion of elastic systems undergoing rigid-body motion.
- Development of a geometry-independent method –applicable to any type of elastic media– for calculation of second-order terms of elastic displacements based on the nonlinear strain-displacement relations, and presentation of specialization of this method to Euler beams and thin plates.
- Development of a versatile symbolic computer code (FLXSIM) for deriving dynamic equations of motion of flexible multibody systems in open or closed kinematic chain configuration.
- Application of feedback linearization technique to a system subjected to simple nonholonomic constraints.
- Development of a modified feedback linearization technique for handling under-actuated systems.

- Proposition of an approach for deriving an open-loop control law, based on artificially constrained motion, for tracking maneuver of flexible systems.
- Proposition of an algorithm for near-minimum-time control of flexible multibody systems with fairly general configuration along a prescribed trajectory, and application of the method to the problem of retrieval of a satellite by a spacecraft mounted flexible manipulator in minimum time.

Contents

Abstract i

Résumé iii

Acknowledgments v

Claim of Originality vi

Contents viii

List of Figures xii

List of Tables xvi

Nomenclature xvii

1 Introduction 1

1.1 Literature Review 6

1.1.1 Multibody dynamics 7

1.1.2 Dynamic stiffening effect 9

1.1.3 Constrained motion 12

1.1.4 Minimum-time control 14

1.2 Motivation and Objectives 19

1.3 Thesis Organization 20

2 Dynamics 23

2.1 Introduction 23

2.2 General Formulation 24

2.2.1 Specialization for rigid bodies 26

2.2.2 Specialization to Timoshenko beams 27

2.2.3 Specialization to the plates 33

2.3 Linearization 35

3 Constrained Motion **38**

3.1 Introduction 38

3.2 Classification of Constraints 39

3.3 Dynamic Equations for Constrained Motion: Conventional Methods 40

3.3.1 Lagrange's method 41

3.3.2 Kane's method 42

3.4 Natural and Artificial Constraints 42

3.5 Dynamic Equations for Constrained Motion: a New Method 45

3.5.1 Basic formulation 46

3.5.2 Calculation effort 51

3.5.3 Standard form of equations governing constrained motion 52

3.5.4 Extension of the formulation for continuous systems 52

3.6 Constraint Forces 54

3.6.1 Contributing forces 54

3.6.2 Determination 55

3.6.3 Adequacy 55

3.6.4 Redundancy 55

4 Kinematic Analysis **57**

4.1 Introduction 57

4.2 Kinematical Differential Equations 58

4.3 Modified Recursive Method 59

5 The Effect of Nonlinear Coupling Between Elastic and Rigid-Body Motions **64**

5.1 Introduction 64

5.2 Improper Linearization, the Source of Error 66

5.2.1 A simple example 66

5.2.2 General formulation 67

5.3 Comparison of Different Remedies 74

5.4 A Method for Direct Accommodation of the Missing Terms 75
5.4.1 General formulation 75
5.4.2 Specialization to the Euler beams 79
5.4.3 Specialization to thin plates 80
5.5 Illustrative Examples 81
5.5.1 Cantilever beam with longitudinal base motion 81
5.5.2 Planar two-bar linkage 84
5.5.3 RAE satellite 86
5.5.4 Rotating cantilever plate 88
6 Applications 93
6.1 Introduction 93
6.2 Capture of a Spinning Satellite 94
6.2.1 Uncontrolled motion simulation 95
6.2.2 Controlled motion simulation 96
6.3 Stabilizing Tethered Satellite Systems Using Space Manipulators 98
6.3.1 Equations of motion 99
6.3.2 Control of the system during stationkeeping 101
6.3.3 Control of the system during retrieval 102
6.4 Modeling and Simulation of a Redundant Space Manipulator 104
7 Application of Constrained Motion in Control of Flexible Structures 127
7.1 Introduction 127
7.2 Analytical Development 129
7.3 Illustrative Examples 130
7.3.1 A rigid, two-link manipulator 130
7.3.2 Control of a flexible manipulator 132
8 Time-Optimal Maneuvering of Flexible Multibody Systems 141
8.1 Introduction 141

8.2 Theoretical Development 142
8.2.1 Perturbation technique 143
8.2.2 Minimum-time, rigid-body maneuver 145
8.2.3 Vibration suppression 150
8.2.3.1 Vibration suppression during the minimum-time maneuver 151
8.2.3.2 Vibration suppression after finishing the minimum-time maneuver 152
8.3 Application: Retrieving a Satellite in Minimum Time, Using a Flexible Manipulator 153
9 Conclusions and Recommendations for Future Work 160
9.1 Summary and Conclusions 160
9.2 Suggestions for Future Work 164
Bibliography 167
Appendix A: Proof of Equation 3.10 174
Appendix B: Independent Additional Equations for Constraint Forces 175

List of Figures

1.1 A schematic diagram showing one of the possible configurations during the evolution of Space Station Alpha (taken from Modi and Suleman [1991]). 2

1.2 The general configuration of a TSS being controlled using a manipulator. 5

2.1 A multibody system. 24

2.2 Schematic of a rigid body B 26

2.3 Schematic of a cantilever beam. 28

2.4 Displacement of the neutral axis. 30

2.5 Schematic of a thin plate. 33

3.1 Two different type of constraints: (a) natural; (b) artificial. 43

4.1 Relative configuration of a frame B and an auxiliary frame A in the inertial frame 59

5.1 A simple pendulum. 90

5.2 Schematic of a general system. 90

5.3 Schematic of an Euler beam. 90

5.4 Schematic of a thin plate. 90

5.5 A Vertical Cantilever with moving base. 90

5.6 Simulation results, third correction method (present theory), for a(t) = 0, and different values of 91

5.7 Simulation results, third correction method (present theory), for g = 0, and different values of 91

5.8 Schematic of a two-bar linkage, ... 91

5.9 Schematic of the RAE satellite. 92

5.10 Simulation results for y'=201;a- premature linearization (booms 1 &3), b- nonlinear strain energy correction method (booms 1 &3), c- present theory (boom 1), d- present theory (boom 3) 92

5.11 Frequencies of a rotating cantilever plate; dotted lines: conventional theory; solid lines: present theory 92

6.1 Capturing a spinning satellite, the system configuration 109

6.2 Simulation of the uncontrolled capturing process with a rigid manipulator: (a) case 1, spacecraft center of mass has the prescribed orbit; (b) case 3, entire system's center of mass has the prescribed orbit. 110

6.3 Time history of the uncontrolled capturing process: (a) joint angles, cases 1, 2, and 3; (b) tip deflection, case 2; (c) spacecraft position, case 3. 111

6.4 Simulation of the controlled motion during the post-capture phase: (a) joint angles, cases 1 and 3; (b) spacecraft position, case 3. 112

6.5 Time history of the actuator torques in the post-capture phase, cases 1 and 3. 113

6.6 Simulation of the controlled motion in the post-capture phase, case 2: (a) joint angles; (b) tip deflection. 114

6.7 Time history of the actuator torques in the post-capture phase, case 2. 115

6.8 The general configuration of a TSS being controlled using a manipulator. 116

6.9 Gravitational forces applied on a rigid body, considering the effect of gravity gradient. 116

6.10 Uncontrolled motion of a tethered satellite system; dotted line: stationkeeping; dashed line: retrieval with exponential rate; solid line: retrieval with constant rate. 116

6.11 Stationkeeping at L=100 m, controlled motion, with different feedback gains; dotted line: Q1, solid line: Q2, dash-dotted line: Q3. Time history of tether length, DOFs, end effector position in the orbital frame (Xe and Ye), and torques. 117

6.12 Stationkeeping at L=1000 m, controlled motion, with different feedback gains; dotted line: Q1, solid line: Q2, dash-dotted line: Q3. Time history of tether length, DOFs, end effector position in the orbital frame (Xe and Ye), and torques. 118

6.13 Comparison between one-step and multi-step retrieving; dotted line: single-step, solid line: multi-step. Time history of tether length, DOFs, end effector position in orbital frame (Xe and Ye), and torques. 119

6.14 Comparison of different retrieval profiles; dotted line: constant rate, solid line: exponential rate. Time history of tether length, DOFs, end effector position in orbital frame (Xe and Ye), and torques. 120

6.15 Schematic of a spatial, seven-revolute-joint manipulator in straight-out configuration 121

6.16 Schematic of a flexible joint, definition of the motor and joint angles 121

6.17 Schematic of a flexible joint: (a) the mass-spring model; (b) the free-body diagram of the elements of the joint 122

6.18 Simulation of the seven-revolute-joint, flexible manipulator: time history of the joint angles 123

6.19 Simulation of the seven-revolute-joint, flexible manipulator: time history of elastic deflections of the joints as seen from the gearbox output 124

6.20 Simulation of the seven-revolute-joint, flexible manipulator: time history of the elastic deflections of the long booms 125

6.21 Simulation of the seven-revolute-joint, flexible manipulator: time history of the actuator torques 126

7.1 Schematic of a rigid, two-link manipulator 136

7.2 Schematic of a flexible, three-link manipulator 136

7.3 Simulation results for maneuver of a flexible manipulator, while keeping the end effector tip on the Y axis; time history of the generalized coordinates 137

7.4 Simulation results for maneuver of a flexible manipulator, while keeping the end effector tip on the Y axis; time history of the position of the end effector tip and the actuator torques 138

7.5 Simulation results for maneuver of a flexible manipulator, while keeping the end effector parallel to the X axis; time history of the generalized coordinates 139

7.6 Simulation results for maneuver of a flexible manipulator, while keeping the end effector parallel to the X axis; time history of the position of the end effector tip and the actuator torques 140

8.1 Minimum-time trajectory construction; a single-switching case 156

8.2 Minimum-time trajectory construction; a multi-switching case 156

8.3 Retrieval of a satellite by a spacecraft mounted manipulator; a schematic of the system 157

8.4 Simulation results for moving the satellite along the local horizontal, time history of the generalized coordinates. 158

8.5 Simulation results for moving the satellite along the local horizontal, time history of the position of the satellite and the actuator torques. 159

List of Tables

2.1 Possible simplifications from Timoshenko beam. 32

6.1 Redundant space manipulator, the characteristic data. 108

7.1 Three-link flexible manipulator; the physical data. 133

7.2 Initial and final conditions for moving the end effector of a flexible manipulator along the Y axis 134

7.3 Initial and final conditions for moving the end effector of a flexible manipulator parallel to the X axis 135

8.1 Spacecraft mounted flexible manipulator: the physical data. 155

8.2 Time-optimal retrieval maneuver: the initial and final conditions. 155

Nomenclature

Bold	bold face letters indicate arrays (matrices and column vectors).
Italic	scalars are shown in italic letters.
$()^{a}$	right superscripts refer to the points and bodies of interest
${}^{B}()$	left superscripts stand for the reference frames
$()_{i}$	right subscripts are numeric indices except for the index 't'
$(\vec{\ })$	a vector quantity.
$(\tilde{\ })$	a quantity associated with nonholonomic partial velocities
$(\tilde{\tilde{\ }})$	a quantity associated with modified nonholonomic partial velocities
$(\hat{\ })$	linearized form of the quantity ( )
$(\bar{\ })$	nominal value of the quantity ( )
$(\breve{\ })$	small deviation form the nominal value of the quantity ( )
$()^{*}$	prematurely linearized items and the terms associated with them
A	auxiliary frame
A, B	matrices defining the explicit form of the constraint equations
${}^{A}\mathbf{a}^{p}$	acceleration of particle *p* in frame *A*
a	origin of frame *A*
${}^{A}\mathbf{a}_{t}^{p}$	remainder of acceleration of particle *p* in frame *A*
B	a rigid body and the body frame
b	center of mass of rigid body *B* and origin of frame *B*
C^{j}	magnitude of the j-th constraint force
${}^{A}C^{B}$	rotation matrix of frame B in frame A
D^{s}	domain of the system S
E	modulus of elasticity

$\mathbf{E}$	correction constraint matrix defined in Eq.(3.23)
$\mathbf{F}^i$	resultant of all contributing active forces, excluding the constraint forces, acting on the i-th particle
$\mathbf{f}$	generalized force vector
$\mathbf{f}^j$	contribution of the j-th body to the generalized force vector
G	shear modulus
$\mathbf{G}$	geometric stiffness matrix
h	plate thickness
I	inertia frame
$\mathbf{I}^B$	centroidal inertia matrix
$\mathbf{J}$	matrix of the second moment of area of the cross section of beams
L, ℓ	beam length
L_1, L_2, l_1, l_2	plate dimensions
$\mathbf{M}$	generalized mass matrix
$\mathbf{M}^j$	contribution of the j-th body to the generalized mass matrix
m^s	mass of the system S
N	number of degrees of freedom of the system S
N_E	number of elastic degrees of freedom
N^R	number of rigid-body DOFs
n	number of bodies in the system S
P	number of constraints
$\mathbf{q}$	vector of generalized coordinates
$\mathbf{q}_0, \dot{\mathbf{q}}_0$	initial conditions
$\mathbf{q}^d, \dot{\mathbf{q}}^d$	desired final conditions
$\mathbf{q}^E$	generalized coordinates associated with elastic DOFs
$\mathbf{q}_f, \dot{\mathbf{q}}_f$	final conditions
$\mathbf{q}^R$	generalized coordinates associated with rigid-body DOFs

$\mathbf{R}$	resultant of all contributing forces acting on a rigid body
$\mathbf{R}^p$	resultant of all contributing forces acting on particle p
${}^B\bar{\mathbf{r}}^p$	position vector of point p in frame B
S	a multibody continuous system
$\mathbf{T}$	resultant torque of all contributing forces acting on a rigid body
$\mathbf{T}^p$	resultant torque of all contributing forces acting on particle p
t^f	final time for a minimum time maneuver
$\bar{t}^f$	final time of the minimum-time rigid-body maneuver
t^s	settling time
U	elastic strain energy
$\mathbf{u}$	vector of generalized speeds
$\mathbf{u}^E$	generalized speeds associated with elastic DOFs
$\mathbf{u}^R$	generalized speeds associated with rigid-body DOFs
${}^A\mathbf{V}^p$	velocity of particle p in frame A
${}^A\mathbf{V}_r^p$	r-th partial velocity of particle p in frame A
${}^A\mathbf{V}_t^p$	remainder of velocity of particle p in frame A
w_1, w_2, w_3	elastic deflections
$\mathbf{z}$	array of intermediate parameters
${}^A\boldsymbol{\alpha}^B$	angular acceleration of frame B in frame A
${}^A\boldsymbol{\alpha}_t^B$	remainder of angular acceleration of frame B in frame A
ε_{ijk}	permutation symbol
μ	number of inputs (actuator forces) of the system S
ν	number of particles of the system S
ρ	mass density
$\theta_1, \theta_2, \theta_3$	rotations due to elastic deformations
${}^A\boldsymbol{\omega}^B$	angular velocity of frame B in frame A
${}^A\boldsymbol{\omega}_r^B$	r-th partial angular velocity of frame B in frame A

${}^{i}\omega_{t}^{ij}$	remainder of angular velocity of frame B in frame A
$\mathcal{A}, \mathcal{B}$	matrices defining the implicit form of the constraint equations
$\mathcal{C}^{i}$	resultant of all contributing constraint forces acting on the i-th particle
$\mathcal{E}$	correction term for prematurely linearized set of equations of motion
$\mathcal{F}$	generalized active force vector
$\mathcal{F}^{j}$	contribution of the j-th body to the generalized active force vector
$\mathcal{L}$	Lagrangian
$\mathcal{S}$	a system of particles
$\tilde{\mathcal{T}}, \mathcal{T}'$	influence matrices of constraint forces defined in Eqs.(3.14) and (3.17)

Chapter 1

Introduction

Increasing demand on precise orientation, and re-orientation, of satellites has resulted in an area of scientific endeavor referred to as attitude dynamics and maneuvering. The need for attitude maneuvering of a spacecraft starts as soon as the spacecraft is inserted into the orbit, and lasts until the end of the in-orbit mission. For example, a communication satellite must be initially oriented toward a specific direction, once it is inserted into the orbit, and the same orientation must be maintained as long as the satellite is functional. This means that a series of attitude maneuvers must be performed regularly to compensate for the angular drift due to the environmental effects such as solar radiation torque, magnetic torque, and meteoroidal impact. Other examples are the maneuvers involving retargeting an antenna or manipulating an object with a spacecraft mounted manipulator, while keeping the rest of the system undisturbed. These examples, showing the importance of attitude maneuvering in a space mission, imply that the success of a space mission is very much dependent on a correct analysis and design of attitude maneuvers.

In the early stage of space exploration, the space systems tended to be small, mechanically simple and rigid. However, a modern spacecraft such as the Space Station Alpha, shown in Figure 1.1, can be composed of several flexible and rigid components arranged in a tree topology with both closed and open chains. On the other hand, a modern large space

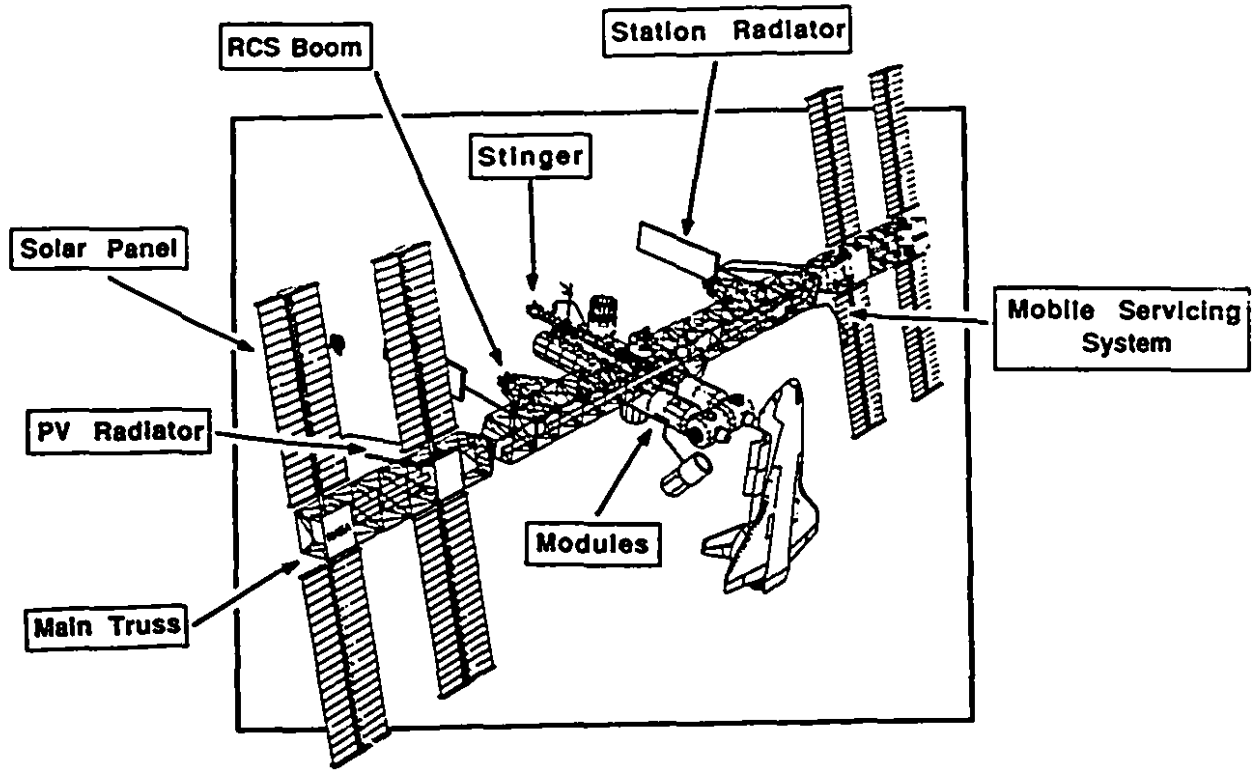

Figure 1.1 A schematic diagram showing one of the possible configurations during the evolution of Space Station Alpha (taken from Modi and Suleman [1991]).

system might be multitasking, i.e., it may perform several different activities simultaneously. Any of these features (flexibility, presence of closed loop chains in the system configuration, and capability for multitasking) can drastically increase the difficulty of the problem at hand.

The solution to a typical attitude maneuvering problem consists of two major parts as follows: (1) To develop a mathematical model describing the motion of the system, i.e., the equations of motion, provided that the orbital motion of the system is known and is not affected by attitude dynamics. (2) To devise a control law so that certain objectives are satisfied during the maneuver. The motion of the controlled system can then be simulated using the developed equations of motion to verify the validity of the devised control law. Each of the two parts of the solution has its associated difficulties which are steadily being increased by ambitious space missions requiring more complex spacecraft.

Since the equations of motion governing the attitude dynamics of a multibody system are usually lengthy and of highly nonlinear form, it is almost impossible to generate them for a system possessing more than two bodies without simplifying assumptions or usage of computers. This transforms the problem of obtaining the equations of motion to writing a suitable formalism, an algorithm for generating the equations of motion using computers.

Most of the existing formalisms and their associated computer codes have been designed to satisfy the needs for simulation purposes, i.e., to have a computationally better performance. However, in addition to the performance, capability of proper linearization, easy incorporation of actuators (discrete or distributed), especially in the case of flexible bodies, automatic elimination of algebraic constraint equations, yielding a minimum dimension set of ordinary differential equations, ODEs – *not a hybrid set of ODEs and algebraic equations* – as the equations of motion, are some other crucial points to the versatility of a formalism developed for control purposes.

Flexibility of the space systems is one of the important issues in spacecraft dynamics. The necessity for considering the flexibility effect in the dynamic analysis was first realized when the anomalous behavior of Explorer-I and Alouette-I was attributed to their flexible appendages. Explorer-I was passively spin-stabilized about its minimum-moment of inertia axis. The motion of a spacecraft spinning around its minimum-moment of inertia axis, which is stable if the system is rigid, was later proved to be unstable for flexible systems. The instability of Explorer-I was attributed to its flexible antennas. Alouette-I, a satellite with a compact central body and four long flexible antennas, was also destabilized due to the energy dissipation associated with the structural motion of the appendages caused by solar heating.

An important issue in analyzing the flexible systems undergoing large rigid motion is the effect caused by coupling of the elastic and rigid degrees of freedom (DOFs). Modeling a

system of this type while neglecting the effect of coupling may result in faulty equations of motion.

Constrained motion is another important issue in spacecraft dynamics, even if there is no real closed kinematic loop in the system. As an example, the motion of a free floating spacecraft, under no external forces or moments except the gravity while neglecting the gravity gradient effect, can be considered as a constrained motion with the simple non-holonomic constraint of *constant angular momentum* and the holonomic constraint of *prescribed orbital motion for the entire system's center of mass*. In the case of spatial motion, for instance, either of these constraints can reduce the degrees of freedom of the system by three, which may make the analysis of the system a lot easier.

Apart from the above mentioned constraints and those associated with closed kinematic chains, constrained motion can be encountered when the motion of some of the DOFs of the system are prescribed through the appropriate application of actuator forces – not through the interaction with the prescribed surrounding environment. This type of constraints, which can be called *artificial constraints*, are likely to be encountered in space robotics where a manipulator may be employed to imitate the motion of a certain mechanism. Figure 1.2 shows a typical problem in which the manipulator may be required to move the point O along the local horizontal to ensure the librational stability of a tethered satellite system (TSS). In this case, the system has three DOFs and one artificial constraint, as opposed to four DOFs for the unconstrained motion.

Clearly if one can generate the equations of motion of a constrained system as a set of explicit ODEs, not differential and algebraic equations (DAEs), it can save a lot of efforts in control analysis and simulation; moreover, it ensures that the motion would follow the prescribed pattern.

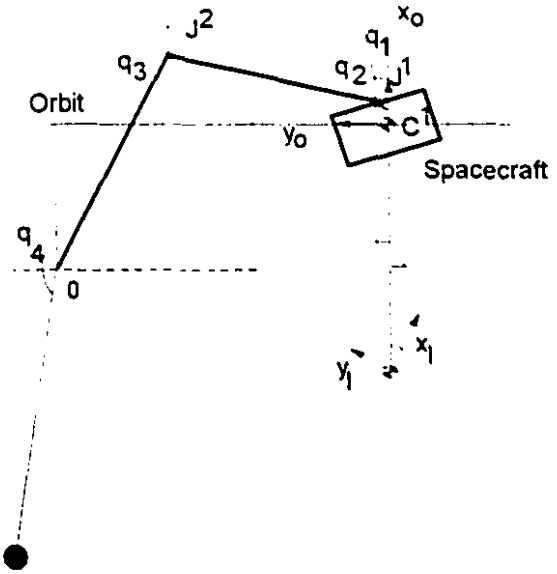

Figure 1.2 The general configuration of a TSS being controlled using a manipulator.

Once the equations of motion are generated, a control law can be devised based on the objective of the maneuver. Different methods and algorithms of control might be used, depending on the maneuver and the objectives, to accomplish the task. For example, the stationkeeping maneuver of a satellite can be performed by utilizing a control law obtained from linear control methods. In this case, the controller can be designed based on LQR method to optimize some cost function, like the consumed energy, or it can be simply a PD controller which is clearly easier to implement practically. Another example is the docking maneuver which can be accomplished using a controller designed using the feedback linearization technique, a nonlinear controller, or one based on the LQR method with time dependent gains. The same task can be done, while optimizing a cost function such as maneuvering time, using the nonlinear optimal control methods.

Optimal solutions, which are usually too difficult to implement in practice, are of academic interest. In reality, they provide the lower/upper limits for a specific maneuver and give a measure to define the performance of a practical solution.

In spite of the considerable amount of research done, the problems of dynamic stiffening effect and constrained motion, which are vital in analysis of spacecraft attitude dynamics, have not been solved completely. These problems are tackled in this thesis. In addition, development of a formalism, and a computer code based on that, capable of generating the equations of motion analytically and in a form suitable for control purposes is also attempted. Finally, this thesis aims at applying existing algorithms of control such as feedback linearization technique, and nonlinear optimal control, perhaps with some improvements, to maneuver and control of complex space systems.

1.1 Literature Review

Due to the fact that the analysis and design of space systems have to be very precise, research on many relevant subjects has been pioneered, or at least elaborated, by researchers working on problems related to space. This is true for dynamics and maneuvering of spacecraft too. Nevertheless, these subjects have also been studied by researchers with other interests. For instance, the research on multibody dynamics in a modern context was first initiated by researchers working on spacecraft dynamics; however, the same subject has also been studied by other researchers working in other areas such as robotics and mechanisms.

To obtain a better perspective of the previous research works, the literature review has been categorized under four topics as follows:

(1) multibody dynamics;

(2) dynamic stiffening effect;

(3) constrained motion;

(4) minimum-time maneuvering and control.

Although this is not the way the story was unfolded chronologically, we have chosen this path to share the benefits of research work done by people in other disciplines. We believe that this will provide a better means to spot the difficulties and unresolved problems.

1.1.1 Multibody dynamics

The last three decades have witnessed considerable efforts towards formulation of dynamical equations of multibody systems, conducted by investigators in three different fields: spacecraft dynamics, robotics, and mechanisms. The multibody dynamics in a modern context was first studied by Hooker and Margulies [1965]. In this study, they considered a system of interconnected rigid bodies in a tree configuration. On the other hand, the very fundamental contributions to this field can be attributed to Likins [1966, 1974], Meirovitch [1966, 1970, 1973], and Hughes [1970, 1972]. Likins, with his comprehensive papers, provided a good physical insight to the problem and inspired extensive research activities. Precise modeling and elegant mathematical analyseis were carried out by Meirovitch. Besides presenting generalized formulation procedures, Hughes performed extensive work on analysis and control of space systems. These studies provided a strong background to the subject of the effect of flexibility on attitude dynamics.

While most of the above-mentioned works were directed towards spacecraft dynamics, research on multibody dynamics with applications in mechanism dynamics and, particularly, manipulators dynamics was also undertaken. Uicker [1965] derived the equations of motion of closed-loop linkages. His work was later modified by Kahan [1969] to include open-loop mechanisms. In the seventies, researchers were trying to use the dynamical models of manipulators in their control analysis. The works of Paul [1972], Bejczy [1974], Raibert [1977], and Horn [1978] can be mentioned as some examples in which they employed different simplified mathematical models in the control analysis. The models were simplified to

overcome the computational difficulties due to complicated equations of motion of the manipulators, which at that time was a bottleneck to the problem.

In the early stages, researchers were more concerned with developing the theoretical foundation of the problem. However, in recent years, the research is conducted more and more towards developing formalisms, i.e., algorithms suitable for automatic generation of equations of motion using computers, and improving their performance. Some of these works are concerned with more specific problems, e.g., tethered satellite systems and ground-based robots, while some others have tried to produce formalisms with a broader area of application. However, none of the formalisms can claim to be equally suitable for different areas of interest, nor are they equally well designed for both control and simulation purposes.

There is a vast body of literature on multibody dynamics. To avoid diverting from our objective, we focus our attention on general purpose formalism and refer the interested reader to the comprehensive reviews of multibody dynamics by Modi [1974], and Likins [1988].

MBDY, developed by Flisher and Likins [1974] based on Hooker-Margulies formulation, was one of the first computer codes for simulating multibody dynamics. Frisch [1975] developed NBOD2 to generate and solve the equations of motion of N coupled flexible bodies and point masses. Bodley et al.[1978] produced a computer code called DISCOS which was capable of incorporating control in the simulation of the dynamics of structures. TREETOPS was another computer code which was developed by Singh et al.[1985] to simulate the dynamics of flexible multibody systems. Unlike most of the previously-mentioned computer codes, extensive control simulation capabilities were built into the TREETOPS program. Cyril et al.[1991] developed a computer code, FLEXLINK, for serial manipulators with flexible links. In all these codes the formalism is implemented numerically.

Another branch of multibody computer codes evolved as a result of the development of symbolic computer languages such as MATHEMATICA and MAPLE. Several symbolic

computer codes were developed for multi-rigid-body systems, such as NEWEUL by Schiehlen and Kreuzer [1977], MESA VERDE by Wittenburg and Wolz [1985], SD/EXACT by Rosenthal and Sherman [1986], AUTOLEV by Schaechter and Levinson [1988], and AUTOSIM by Sayers [1991]. These codes are capable of analytically generating the explicit form of the equations of motion. However, the advantage of having analytical, explicit form of equations comes with the difficulty of increasing the length of the equations as the number of the bodies in the system grows. This difficulty, which becomes drastically worse for systems with flexible members, can be identified as the bottleneck for using symbolic multibody codes.

Symbolic multi-rigid-body computer codes such as SD/EXACT and AUTOSIM, despite their fair capabilities, are not suitable for today's space systems due to the inherent flexibility of light weight space structures. Most of the multi-flexible-body formalisms, on the other hand, are implemented numerically which makes it necessary to pre-define the system configuration, i.e., the kind of joints and links, the position of the actuators, etc. Simpler definitions result in better performance of the formalism, but restrict it in scope, while defining more complete systems results in weaker performance. Moreover, completely numerical implementation is not suitable for control purposes, for numerical linearization is difficult to perform and the implementation of arbitrary placement of actuators becomes very difficult, if not impossible. Also, incorporation of different control schemes becomes a difficult task.

1.1.2 Dynamic stiffening effect

Study of the behavior of flexible bodies attached to a moving support has been vigorously pursued for almost fifty years in connection with a number of diverse disciplines such as machine design, helicopter dynamics, robotics, and spacecraft dynamics. The problem can be stated as the disagreement between the results predicted by conventional modeling methods and the experimental results. The researchers have tried to find a method to make appropriate corrections to the equations of motion of such systems to obtain correct results. The

scope of the published studies on this subject varies from the simple case of vibration of rotating bars with constant angular velocity to very complicated problems of the motion of flexible spacecraft antennas with arbitrary base motion.

Meirovitch [1967], in his monograph, discussed the problem of transverse vibration of a rotating bar with prescribed angular velocity, as well as transverse vibration of a bar under axial forces. Vigneron [1970] also studied the effect of dynamic stiffening in multibody dynamics. He studied the dynamics of a spinning satellite with crossed-dipole configuration. Likins [1974] who probably coined the words "geometric stiffening" of rotating beams, carried out an illuminating study on this subject by considering the problem of rotating elastic appendages.

Hoa [1979] investigated the vibrational frequencies of a rotating beam with a tip mass. The effects of the root offset and the setting angle (the angle between the spin axis and the beam axis) were also considered. The papers by Peters and Hodges [1980] and Kammer and Schlack [1986] have considered planar vibration of a rotating beam and determined the critical spin rate for buckling. Fox and Burdess [1978], in a similar study, calculated the limits on the natural frequencies of a rotating beam.

The problem of an elastic beam undergoing arbitrary base motion was studied by Kane et al. [1987]. They proposed to retain the second order terms, in terms of elastic generalized coordinates, in the expression for the axial elastic displacement of the beam. In spite of reasonable results obtained, their approach suffers from a confusion in using the deformed and undeformed-configuration coordinates. In developing the equation governing the coupling of the elastic deflections, from which the second order terms are extracted, they assumed that the transverse deflections are functions of deformed-configuration coordinates. However, the transverse elastic deflections supplied to this equation, as well as the rest of calculations, were expressed in terms of undeformed coordinates. This inconsistency violates the above-mentioned crucial equation from which the expression for the second-order longitudinal elastic deflection

was calculated. The same deficiency remained in the study of plates undergoing large overall motion carried out by Banerjee and Kane [1989]. This drawback has been clearly pointed out and discussed by Hanagud and Sarkar [1989] who, instead, used a fourth order expression for the elastic strain energy to compensate for the missing terms in the equations of motion.

Ider and Amirouche [1989] investigated the effect of geometric stiffening on the dynamics of multibody elastic systems. They chose to use a third-order expression for the elastic strain energy to accommodate the dynamic stiffening effect.

Most of the work done in this area suffers from the drawback of *direct use of geometry* in establishing the relations governing the interaction of the elastic deflections, irrespective of whether these relations are used later in calculation of nonlinear velocities or nonlinear strain energy. The direct use of geometry, which is a case-dependent approach, has been a major obstacle in developing general methods capable of handling more complicated elastic elements such as plates and shells.

As an attempt to circumvent this obstacle, Banerjee and Dikens [1990], in a fairly complete study, considered the problem of a general elastic body undergoing arbitrary base motion. They proposed a method based on compensating for the missing terms by means of a geometric stiffness matrix. The matrix must be generated using a finite element approach and defining the zero-order inertia forces as an external force field acting on the elastic body. Although the study is a significant advancement, it is difficult to use the method for complex multibody systems, for which the definition of the generalized coordinates and generalized speeds associated with base motion are different from those used in their paper.

A better idea was proposed by Padilla and von Flotow [1992]. Attributing the missing terms to premature linearization (linearization prior to the calculation of velocities), they suggested the use of nonlinear strain-displacement relations to prevent loss of any terms in the equations of motion. Their study, however, fell short of developing a general formulation

applicable to different elastic media. They confined their study to the beams and for more complicated cases suggested the use of *ruthlessly linearized* equations, equations in which all nonlinear terms involving the elastic deflections and their time rate of change are ignored, instead of using improperly linearized equations.

1.1.3 Constrained motion

In the past decade there has been a growing interest in modeling and simulation of large mechanical systems with constrained motion and closed kinematic loops. This has been motivated by applications in diverse areas such as astrodynamics, robotics, mechanisms, and biosystems.

The method of using Lagrange's multipliers to generate the equations governing the motion of a constrained system is well known – see Goldstein [1950] for example. However, this method has the disadvantage of producing a hybrid set of differential and algebraic equations (DAEs), which may not be convenient in many cases. Moreover, for a system with P independent constraints, this hybrid set of equations has $2P$ additional equations (and unknowns) compared to the minimum number of equations which are conceptually sufficient to describe the motion of the system. Hence, a considerable amount of effort has been devoted to find methods to eliminate the unwanted variables and reduce the order of the equations of motion to its minimum, which at the same time reduces the hybrid set of DAEs to a set of ODEs.

Within the past few decades, several related methods have been proposed that first derive the hybrid set of equations and subsequently reduce the system, by means of a matrix transformation, to the minimal order form. In a procedure developed by Uicker [1969], the dependent variables are calculated from the algebraic constraint equations numerically. The independent coordinates are integrated then using these initial values. The necessity for proper

choice of the independent coordinates and the high cost of iterations for calculation of the dependent coordinates are some of the drawbacks of this method. Wehage and Haug [1982] suggested a method which uses a Lagrangian approach and Gaussian elimination to identify the independent generalized coordinates. Nikravesh and Haug [1983] used Gaussian elimination with full pivoting to accomplish the same task. Their work was modified by Mani [1984] who employed singular value decomposition to identify the independent generalized coordinates. This technique showed better stability characteristics. His work was further improved by Kim and Vanderploeg [1986] on the numerical efficiency by introducing "null-space updating" based on *QR* decomposition.

As opposed to these Lagrangian-based methods, another set of algorithms have been developed based on Kane's method. Kane [1961] presented an elegant approach which can be used to directly generate the minimal set of equations. This method will be discussed in detail in the fourth chapter. The drawback of this method can be identified as the lack of a constraint force evaluation approach as systematic as the Lagrangian multiplier method and the necessity for predetermining the independent generalized speeds.

A series of research works were conducted to modify Kane's approach to determine the independent coordinates of a constrained system automatically. Kamman and Huston [1984] introduced the zero-eigenvalue technique, which was based on a matrix theorem given by Walton and Steeves [1969], to calculate the orthogonal complement of the constraint Jacobian matrix. This orthogonal complement matrix is used then to identify the independent coordinates as well as to reduce the equations of motion to its minimal form. Singh and Likins [1985] used singular-value decomposition to do the same task. Angeles and Lee [1988] used the method of natural orthogonal complement to eliminate the Lagrange multipliers. To improve the numerical efficiency, Amirouche et al. [1988] used a pseudo-upper-triangular decomposition of the constraint matrix based on successive multiplication of Householder transformations to compute the orthogonal complement matrix. Ider and Amirouche [1988] presented a similar

method based on equivalence transformation of the constraint matrix to an upper-triangular form. The transformation matrix was generated by simple Gaussian elimination technique.

All of the above methods presume the constraints to be implemented *naturally*. While the methods for generating the equations of motion of naturally constrained systems is rather well developed, no method is available to derive the equations of motion of *artificially* constrained systems (as defined in Section 3.4).

1.1.4 Minimum-time control

Rapid maneuvering has long been part of many space missions. For an actual system, with actuator saturation limit, the time elapsed to accomplish a certain motion cannot be shorter than a certain value. The time-optimal-maneuvering problem deals with finding the time-history of the control inputs, actuator torques, which can accomplish the desired motion in the shortest interval of time.

This optimization problem can be formulated using Pontryagin's minimum principle (see Kirk [1970]) with the final time as the objective function, the function to be minimized. The problem has no closed-form solution except in the simplest cases such as a single DOF system with a single controller. Moreover, the problem for complicated nonlinear systems yields acceptable results, even to numerical approaches, only when certain simplifying restrictions are applied. Taking the effect of flexibility into account increases the complexity of the problem by increasing both the DOFs of the system and introducing the necessity for suppressing the elastic motions.

Many researchers have devoted their efforts towards developing numerical methods to solve the two-point boundary-value problem (TPBVP) arising from Pointryagin's minimum principle. Most of these methods are the shooting methods, based on iteration, to find correct initial conditions for the costates of the system.

Robert et al. [1969] introduced a perturbation technique to solve the nonlinear TPBVP The method is based on making the system increasingly nonlinear through a sequence of linear problems, while using the solution to each step as the forcing function for the next order of equations. In a similar approach, Subrahmanyam [1986] uses Newton's method to make successive approximations by linearizing the system through a discretization procedure. Miele and Iyer [1970], using the method of particular solution tried to approximate the "true" set of initial conditions by a linear combination of a set of initial conditions used in the previous steps to determine the independent solutions. Quasilinearization is another technique which is used by several researchers when addressing the problem of nonlinear TPBVP. Yeo et al. [1974] introduced a method for choosing the initial multipliers for quasilinearization in an optimal way to achieve the fastest convergence as well as an accurate solution. Li and Bainum [1990] employed the quasilinearization technique to minimize a blended-function of time and energy while shortening the final time successively to arrive at the minimum time solution. Bainum et al. used the results of this method as the initial guess for a multiple shooting method to arrive at a more accurate solution to the minimum time problem of multi-axis maneuvering of a flexible spacecraft [1992].Unlike the previously mentioned methods, which need a relatively good initial guess to converge, the direct methods such as the steepest descent method employed by Storm [1973] lead to very fast convergence within a few steps. However, the convergence rate decays as the desired accuracy increases. The steepest decent algorithm was recently modified by Meier and Bryson [1990] to develop the switch time optimization (STO) method. The method assumes that the controls are saturated during the maneuver and takes the number of switches as the input to solve for the switch times.

Another method which seems to be promising in solving optimal control problems is the method of collocation and nonlinear programming. Collocation was developed by Dikmanns and Well [1975] and combined with nonlinear programming by Hargreaves and Paris [1987]. The method, which was recently employed by Scrivener and Thompson [1993] to find the time-

optimal attitude maneuver of a rigid spacecraft, has the advantage of converging within the desired accuracy in a reasonable amount of time, even with a relatively poor initial guess.

The problem of rest to rest maneuvering of rigid spacecraft has received considerable attention in the past. In an early attempt, Kamton [1970] studied the minimum time maneuver of a rigid spacecraft, while assuming the angular velocity vector to remain fixed in the inertial frame. In a similar way, D'Amario and Stubbs [1979] used Euler's theorem on rotation to perform rapid reorientation of rigid spacecraft. This problem was also studied by several other researchers. One may mention the works by Chen and Kane [1980], Carrington and Junkins [1986], Vadali and Junkins [1983,1984], Wie and Barbara [1985], and Vadali [1986] as typical examples. For more detailed information, the interested reader is referred to the comprehensive review on this subject by Singh et al. [1989] and Scrivener and Thompson [1992].

Flexible spacecraft slewing problems, like their rigid-body counterparts, have received considerable attention. Most of the researchers in this area studied the problem of single-axis maneuvering of a rigid hub with flexible appendages.

Dods and Williamson [1984] studied the problem of single-axis maneuvering of a flexible, single-controller spacecraft. They came up with an algorithm suitable for systems with a low fundamental frequency. Ben-Asher and Burns [1987] presented a solution to a nonlinear optimization problem based on the solution to the linearized problem as an initial guess. It was found that the minimum times for both linear and nonlinear systems were similar, but symmetry of switching times was destroyed in the nonlinear model. The same problem was solved through phase-plane analysis by Barbieri and Oguner [1988].

Perturbation technique was used by Meirovitch and Quinn [1987], Meirovitch and Sharony [1990] and Meirovitch and Kwak [1990]. Using the perturbation technique, they subdivided the equations of motion to two sets: (1) the zero-order set, a nonlinear set governing the rigid-body motion; (2) the first-order set, a linear time-varying set associated with the

elastic motion. The system was controlled by a combination of open-loop and closed-loop control. The bang-bang input torque resulting from the time-optimal solution of the zero-order system was applied by the hub actuator as the open-loop control to produce the reference motion. At the same time, the actuators located on the flexible appendages applied the input torques of the feedback control, calculated using state feedback approaches, to suppress the elastic vibrations.

The problem of time-optimal, open-loop control of a single-axis maneuver of a rigid hub with flexible appendages was also studied by Thompson et al. [1989]. To meet hardware constraints in generating instantaneous switches and to avoid excitation of higher flexible modes, they chose to avoid instantaneous switching by smoothing the bang-bang control profile. In this approach, the ability to control the degree of sharpness of the switches, has provided a good means to evaluate the tradeoffs with respect to maneuver time and residual energy.

This work was later on improved by Junkins et al. [1990]. They employed the Lyapounov method to devise an asymptotically stable feedback control to suppress the elastic vibrations. The input to the system, applied by a single actuator to the hub, was the sum of this feedback and a reference smoothed-bang-bang control, obtained based on the analysis presented by Thompson et al.[1989]. The method was subsequently validated by them experimentally [1991]. This method was also applied by Bell and Junkins [1993] to solve the minimum time and minimum fuel, three dimensional maneuvering of a flexible spacecraft with general configuration, and by Hecht and Junkins [1992] to solve the time optimal problem of a flexible two-link manipulator. In a recent work, Bang et al. [1993] took the near-minimum-time maneuver resulting from smoothed input and optimized the control with respect to the smoothing parameters .The resulting profile involves less smoothing, to achieve a short maneuver, but the vibrational excitation is also reduced.

Bainum and Li [1991] employed the method of quasilinearization and particular solution to address the problem of optimal large angle maneuvers of a flexible spacecraft. The same method was also used by Tan et al. [1991] to solve the problem of minimum time slewing of a flexible shallow spherical shell system. They used the solution to the linearized problem as a nominal solution for the nonlinear TPBVP.

In a recent paper, Li and Bainum [1993] presented an analytical solution to the minimum time control of a fourth-order linear system near the origin. The system under consideration, which has two real zeros and two imaginary eigenvalues, represents a flexible structure with one rigid mode and one elastic mode.

Banerjee and Singhose [1994] studied the problem of slewing and vibration control of a highly flexible structure. They used the innovative method of "preshaping input command" presented by Singer and Seering [1990] to find the multi-switch bang-bang control law which can accomplish a rest-to-rest maneuver in minimum time while suppressing the elastic vibration at the same time. In addition to this open-loop control, they also presented the results of an augmented closed-loop control.

The multi-dimensional optimal control problem has also been studied extensively by researchers in the field of robotics. Although most of the algorithms developed by researchers in this field are meant to be used for rigid, earth-bound robots, they can be commonly applied to other multi-dimensional optimal control problems. The STO algorithm, developed by Meier and Bryson [1990], is an example of the algorithms developed originally to solve time-optimal control problem of a two-link manipulator that have found applications in other areas of research.

For the sake of brevity, only one algorithm which is of particular interest to this thesis is discussed here and for more references, the interested reader is refereed to the excellent reviews on this subject by Shiller and Dubowsky [1989] and Wie et al. [1990]. Babrow et al.

[1985] developed the above-mentioned algorithm for the special case of the time-optimal motion of a manipulator along a specified path. This method uses the phase-plane analysis to find the optimal velocity profile of the manipulator along a given path subject to actuator constraints. The method considers the full nonlinear dynamics of the manipulator and permits actuator constraints to be expressed as complex functions of the system states. The algorithm is quite straight forward and computationally efficient in the case of single-switching maneuver. However, in the case of multi-switching controls, which can occur frequently, an inefficient shooting method was suggested for calculation of switching points.

This work was extended by Shiller [1984] to include the constraint of maximum speeds that a manipulator can sustain without losing its grasp of the payload. Shiller and Dubowsky [1989] extended the method further to find the optimal path itself.

1.2 Motivation and Objectives

The primary objective of this work is to study different aspects of the dynamics of flexible, multibody space-structures during rapid maneuvering and to produce a computer code which can correctly develop the equations of motion of such systems in a form suitable for control analysis.

Constrained motion is the first concept which is discussed in this thesis. While *naturally* constrained motion has gained considerable attention in the past, *artificially* constrained motion has almost been untouched. In fact, almost no attention has been paid to the *method of implementation* of constraint forces which is the main point of difference between natural and artificial constraints. One of the specific objectives of this study is to develop a method which can uniquely generate the minimum dimension set of equations of motion for systems subject to artificial and/or natural constraints.

Effect of rigid-body base motion on the dynamic response of flexible systems is another point of interest in this study. Although this has been studied by several researchers, there is still a debate over what is the exact source of flaw in the equations (kinetic or strain energy), or what remedy is the best. Above all, the lack of a general theory which can be applied to a multibody system with different kinds of elastic members (beams, plates, and shells) is also evident.

Having developed the above methods for handling constrained motion and flexible systems undergoing rigid-body motion, development of a symbolic computer code armed with these theories is attempted. The code should be capable of introducing some intermediate parameters to keep the size of the equations of motion as small as possible, and carrying out proper linearization of equations in the presence of intermediate parameters. It should also facilitate easy incorporation of actuators in any arbitrary location, even on the elastic bodies.

The second objective of this work is to study some issues related to the control and maneuvering of flexible multibody space systems. The application of constrained motion, specially artificial constraints, in control of flexible multibody systems is studied. Although the control of constrained systems has been studied in the past, the idea of using artificial constraints to devise control algorithms is new. Time-optimal motion of flexible, multibody systems along a specified path is the last subject to be studied in this thesis.

1.3 Thesis Organization

The thesis can be divided into two parts. The first part, Chapters 2-5, analyses the dynamics of the system and the relevant issues, while the second part, Chapters 6-8, deals with control and simulation of the system.

In particular, Chapter 2 presents the overall structure and formulation of the equations governing constrained motion of a flexible multibody system. The dynamical model for a

general member of the system is presented along with the specialization for rigid bodies, Timoshenko beams, and plates. Linearization of equations of motion in the presence of intermediate parameters is also discussed in this chapter.

Chapter 3 is devoted to the study of constrained motion. Natural and artificial constraints are first introduced and their difference is discussed. Conventional methods for generating the equations of motion of naturally constrained systems is presented briefly. Next, a method is developed which can be employed to generate the minimum-order set of equations for systems with artificial and/or natural constraints. This chapter ends with the discussion of some related issues such as determination, adequacy and redundancy of constraint forces.

In Chapter 4, the kinematical equations of motion and the modified recursive method, used to calculate angular velocities and partial velocities necessary in developing the equations of motion, are presented. Most of the material covered in Chapters 2 and 4 are not new developments and are presented briefly for the sake of completeness and continuity of the discussion.

The effect of rigid-body base motion on dynamic response of elastic systems is studied in Chapter 5. The discussion starts with a proof to show that incorrect kinetic energy (due to early linearization of velocities) is the source of the error in the equations developed by using the conventional methods of discretization. Different remedies for this problem are then examined and compared. Finally, a general method for generating the correct equations of motion based on the nonlinear strain-displacement relations is presented. Specialization of the method, which can be virtually applied to any elastic medium, are given for beams and plates. Several examples are provided to illustrate some rather unusual phenomena in elastic bodies undergoing large base motion (such as missing terms in the mass matrix or experiencing a softening effect).

The formalism developed in Chapters 2-5 is employed in Chapter 6 to solve three problems. Capture of a spinning satellite by a flexible two-link manipulator is the first problem studied. In the second problem, the feasibility of using a two-link space manipulator for stabilizing tethered satellite systems is investigated. The last problem studied deals with the retrieval of a large payload by a redundant space manipulator, which possesses seven revolute joints; in this study the effects of flexibility of both the joints and links of the manipulator are taken into account.

The idea of using constrained motion in control of multibody systems is presented in Chapter 7 through presentation of some examples. It is shown that the method can find interesting applications in semi-manual control of manipulators and in fine tracking of flexible manipulators.

Chapter 8 presents an approach for near-minimum-time maneuvering of flexible multibody systems moving along a prescribed trajectory. The idea is successfully employed to perform a retrieval maneuver by a Shuttle-based three link, flexible manipulator.

Chapter 9 concludes this thesis by presenting some concluding remarks and suggestions for future work.

Chapter 2

Dynamics

2.1 Introduction

As stated in Chapter 1, development of a computer code for generating the equations of motion of a flexible multibody system is one of the objectives of this study. This chapter presents the formulation, based on which the computer code (FLXSIM) is produced. Most of the material presented in this chapter are not new developments and are presented briefly for the sake of continuity and completeness. In this chapter, it is assumed that the system has no closed kinematic loop or prescribed motion, i.e., the motion is unconstrained. The study of constrained motion is left for Chapter 3.

The formulation is based on Kane's method and the equations of motion are found by superposing the contribution of each body to the generalized mass and force matrices. Since each body is being considered as a part of the whole system, not a separate body, and since the formalism is based on an energy-based method, the non-working constraint forces (e.g., joint forces) do not come into the picture.

Before starting the discussion, it is useful to define some of the conventions used in this thesis. The right subscripts are numeric indices except for the index 't', the right superscripts refer to the points and bodies of interest, and the left superscripts stand for the reference

frames; for example, ${}^{A}\mathbf{V}^{P}$ is the velocity of point p in frame A. The left superscript is omitted in the case of the inertia frame. The elements of a column are components of the corresponding vector in the frame shown by the left superscript, except for the rotational quantities which are the components of the vector in the frame shown by the right superscript. Thus, if $\bar{\mathbf{a}}_i$ and $\bar{\mathbf{b}}_i$ denote unit vectors in frames A and B, respectively, then ${}^{A}r_i^P = \bar{\mathbf{a}}_i \cdot {}^{A}\vec{\mathbf{r}}^P$ (the i-th component of the position vector of point p in frame A, ${}^{A}\vec{\mathbf{r}}^P$, projected in frame A); however, ${}^{A}\omega_i^B = \bar{\mathbf{b}}_i \cdot {}^{A}\vec{\boldsymbol{\omega}}^B$ (the i-th component of the projection of the relative angular velocity vector ${}^{A}\vec{\boldsymbol{\omega}}^B$ in frame B); similarly ${}^{A}\alpha_i^B = \bar{\mathbf{b}}_i \cdot {}^{A}\vec{\boldsymbol{\alpha}}^B$, and so on.

2.2 General Formulation

Consider a system S with N degrees of freedom which is a congregation of n rigid and flexible bodies connected through a set of arbitrary joints (Figure 2.1). The system is driven by μ inputs, i.e., actuator forces and torques, denoted by $\boldsymbol{\tau} = \tau_1,\ldots,\tau_\mu$. The motion of the system can be fully described in terms of $2N$ independent scalars as follows: $\mathbf{q} = q_1,\ldots,q_N$, the

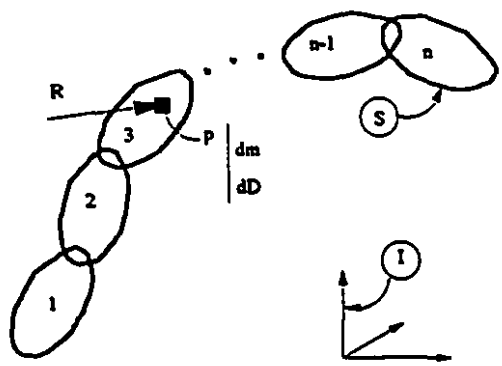

Figure 2.1 A multibody system.

generalized coordinates; and $\mathbf{u} = u_1,\ldots,u_N$, the generalized speeds. The generalized speeds are defined as linear combinations of the time rates of the generalized coordinates:

$$u_r = \sum_{s=1}^{N} Y_{rs}(\mathbf{q},t)\dot{q}_s + Z_r(\mathbf{q},t), \quad r = 1,\ldots,N, \tag{2.1}$$

such that Eq. (2.1) can be solved uniquely for $\dot{q}_1,\ldots,\dot{q}_N$.

Kane's equations of motion for the continuous system S, shown in Figure 2.1, can be written as

$$\int_{D^s} \mathbf{V}_r^p \cdot \mathbf{R}^p \, dD - \int_{m^s} \mathbf{V}_r^p \cdot \mathbf{a}^p \, dm = 0, \quad r = 1,\ldots,N, \tag{2.2}$$

in which D^s, m^s and $\mathbf{a}^p$ are, respectively, the entire domain of S, the mass of S, and the acceleration of the element p; also, $\mathbf{R}^p$ is the resultant contributing force acting on the element dD (see Kane and Levinson [1985]), while $\mathbf{V}_r^p$ is the r-th partial velocity of element p, defined as

$$\mathbf{V}_r^p = \partial \mathbf{V}^p(\mathbf{q},\mathbf{u},t)/\partial u_r, \quad r = 1,\ldots,N. \tag{2.3}$$

The acceleration of point p has the general form of

$$\mathbf{a}^p = \sum_{s=1}^{N} \mathbf{V}_s^p(\mathbf{q},t)\,\dot{u}_s + \mathbf{a}_t^p(\mathbf{q},\mathbf{u},t), \tag{2.4}$$

in which $\mathbf{a}_t^p$, the remainder of acceleration of point p, denotes the portion of the acceleration which is independent of time derivatives of the generalized speeds. Substituting Eq. (2.4), one can rewrite Eq.(2.2) as:

$$\mathbf{M}(\mathbf{q},t)\,\dot{\mathbf{u}} = \mathbf{f}(\mathbf{q},\mathbf{u},\tau,t), \tag{2.5}$$

where $\mathbf{M}$ and $\mathbf{f}$ are the generalized mass and force matrices which can be written in the form

$$\begin{aligned} \mathbf{M} &= \sum_{j=1}^{n} \mathbf{M}^j, \\ \mathbf{f} &= \sum_{j=1}^{n} \mathbf{f}^j. \end{aligned} \tag{2.6}$$

Here the elements of $\mathbf{M}^j$ and $\mathbf{f}^j$ are given by

$$M_{rs}^j = \int_{m^j} \mathbf{V}_r^p \cdot \mathbf{V}_s^p \, dm, \quad r,s = 1,\ldots,N \;,\; j = 1,\ldots,n, \tag{2.7.a}$$

$$f_r^j = \mathcal{F}_r^j - \int_{m^j} \mathbf{V}_r^p \cdot \mathbf{a}_t^p \, dm, \quad r = 1,\ldots,N \;,\; j = 1,\ldots,n \tag{2.7.b}$$

where

$$\mathcal{F}_r^j = \int_{D^j} \mathbf{V}_r^P \cdot \mathbf{R}^P \, dD, \quad r = 1,\ldots,N \ , \ j = 1,\ldots,n \tag{2.7c}$$

The main task of the formalism is to produce $\mathbf{M}^j$ and $\mathbf{f}^j$, which are the contributions of individual members to the mass matrix and force column. Equations (2.7) are sufficient for the calculation of the above mentioned terms in the most general case which is an arbitrary elastic body. In the calculation procedure, there are two main steps: (i) calculation of the kinematical terms, $\mathbf{V}_r^P$, $\mathbf{a}_t^P$, as well as determination of the resultant contributing force $\mathbf{R}^P$ acting on the element dD, and (ii) integration over the domain of each body, necessary in Eqs. (2.7).

The procedure for calculation of the kinematical terms is given in Chapter 4; on the other hand, the difficulty of evaluating volume integrals can be circumvented in special cases by carrying out the closed form solution or at least by reducing the dimension of integration. What follows in this section presents such simplifications for cases when the j-th body is either a rigid body, a beam type member, or a plate. Nevertheless, the same simplifications can be performed for other types of members such as shells.

2.2.1 Specialization for rigid bodies

Let the j-th member of the previously defined system S be a rigid body B, shown in Figure 2.2. Defining a set of mutually perpendicular unit vectors $\bar{\mathbf{b}}_1, \bar{\mathbf{b}}_2, \bar{\mathbf{b}}_3$, fixed in B with the origin at its center of mass, b , one can express the partial velocity $\mathbf{V}_r^P$ and the remainder of acceleration $\mathbf{a}_t^P$ in terms of centroidal quantities $\mathbf{V}_r^b$, $\mathbf{a}_t^b$, $\boldsymbol{\omega}_r^B$, $\boldsymbol{\alpha}_t^B$, and $\boldsymbol{\omega}^B$ as follows:

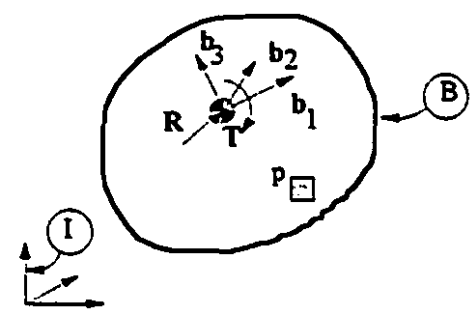

Figure 2.2 Schematic of a rigid body B

$$\mathbf{V}_r^P = \mathbf{V}_r^b + \mathbf{C}^B(\boldsymbol{\omega}_r^B \times {}^B\mathbf{r}^P + {}^B\mathbf{V}_r^P), \quad r = 1,\ldots,N, \tag{2.8}$$

$$\mathbf{a}_t^P = \mathbf{a}_t^b + \mathbf{C}^B(\boldsymbol{\alpha}_t^B \times {}^B\mathbf{r}^P + {}^B\mathbf{a}_t^P) + \dot{\mathbf{C}}^B(\boldsymbol{\omega}^B \times {}^B\mathbf{r}^P + 2\,{}^B\mathbf{V}^P). \tag{2.9}$$

In the above relations, $\mathbf{C}^B$, whose elements C_{ij}^B are given by $\vec{\mathbf{i}}_i \cdot \vec{\mathbf{b}}_j$, is the rotation matrix for frame B relative to the inertial frame I, while $\boldsymbol{\omega}^B$ denotes the angular velocity of B in I. Furthermore, $\boldsymbol{\omega}_r^B$ and $\boldsymbol{\alpha}_t^B$, respectively, can be written as the r-th partial angular velocity and the remainder of angular acceleration of B in I,

$$\boldsymbol{\omega}_r^B = \partial \boldsymbol{\omega}^B(\mathbf{q},\mathbf{u},t)/\partial u_r, \quad r = 1,\ldots,N, \tag{2.10}$$

$$\boldsymbol{\alpha}^B = \sum_{r=1}^{N} \boldsymbol{\omega}_r^B(\mathbf{q},t)\dot{u}_r + \boldsymbol{\alpha}_t^B(\mathbf{q},\mathbf{u},t). \tag{2.11}$$

Thus $\boldsymbol{\alpha}_t^B$ is the part of $\boldsymbol{\alpha}^B$ that does not depend on the time rate of the generalized speeds. Substituting Eqs. (2.8-2.9) into Eqs.(2.7), and noting that $\int_{m^B} \rho\, dm = 0$ and $\int_{m^B} {}^B\mathbf{r}^P \times (\boldsymbol{\omega}^B \times {}^B\mathbf{r}^P)\, dm = \mathbf{I}^B\boldsymbol{\omega}^B$ ($\boldsymbol{\omega}^B$ can be replaced with other quantities such as $\boldsymbol{\omega}_r^B$ and $\boldsymbol{\alpha}_t^B$), where $\mathbf{I}^B$ is the centroidal inertia matrix of B corresponding to the axes aligned with the unit vectors $\vec{\mathbf{b}}_1$,$\vec{\mathbf{b}}_2$,and $\vec{\mathbf{b}}_3$, one obtains

$$M_{rs}^B = m^B\, \mathbf{V}_r^b \cdot \mathbf{V}_s^b + \boldsymbol{\omega}_r^B \cdot (\mathbf{I}^B\, \boldsymbol{\omega}_S^B), \quad r,s = 1,\ldots,N, \tag{2.12.a}$$

$$f_r^B = \mathbf{V}_r^b \cdot (\mathbf{R} - m^B\, \mathbf{a}_t^b) + \boldsymbol{\omega}_r^B \cdot [\mathbf{T} - \mathbf{I}^B\, \boldsymbol{\alpha}_t^B - \boldsymbol{\omega}^B \times (\mathbf{I}^B\, \boldsymbol{\omega}^B)], \quad r = 1,\ldots,N, \tag{2.12.b}$$

in which the torque **T** and the force **R** whose line of action passes through the point *b*, are the equivalent set for all the contributing forces acting on B. We may recall that **R** stands for the components of $\vec{\mathbf{R}}$ in the inertial frame I, whereas, **T** contains the components of $\vec{\mathbf{T}}$ in the body frame B.

2.2.2 Specialization to Timoshenko beams

Suppose the j-th member of the system is a one dimensional elastic body (i.e., the properties of the member are only functions of a single variable x); beams, bars, and strings are examples of this kind of members. In this section, Eqs. (2.7) are simplified for a Timoshenko

beam, the most comprehensive one dimensional elastic body. Table 2.1 gives the possible simplifications from a Timoshenko beam to other one-dimensional elastic bodies.

Consider a Timoshenko beam (Figure 2.3) characterized by a natural length L, material properties $E(x)$, $G(x)$, $\rho(x)$, and cross sectional properties $A(x)$, $\mathbf{J}(x)$, $\alpha_2(x)$, $\alpha_3(x)$, $\kappa(x)$, and $\Gamma(x)$. The above properties are defined as follows. Let x be the distance from the root of the beam, point o, to the centroid of a generic cross section of the beam, which in this analysis is assumed to coincide with the center of twist, the flexure center and the elastic center; then $E(x)$, $G(x)$, and $\rho(x)$ represent the modulus of elasticity, the shear modulus and the mass per unit length of the beam at x, respectively. The area of cross section, the Saint Venant torsion factor, and the warping factor are denoted by A, κ and Γ respectively. Hereafter the functional representation '(x)' is omitted.

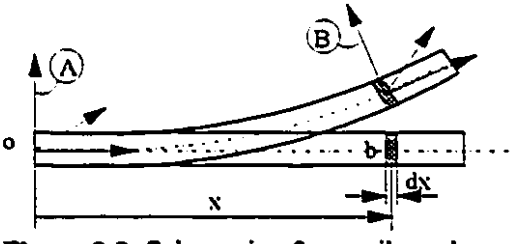

Figure 2.3 Schematic of a cantilever beam.

To define the quantities $\mathbf{J}, \alpha_2, \alpha_3$, we define a set of mutually perpendicular unit vectors $\bar{\mathbf{b}}_1, \bar{\mathbf{b}}_2, \bar{\mathbf{b}}_3$, fixed in the plane of the cross section at x with its origin, b, at the centroid and oriented such that $\bar{\mathbf{b}}_1$ is along the elastic axis of the beam and $\bar{\mathbf{b}}_2, \bar{\mathbf{b}}_3$ are located in the plane of the cross section; then, $\mathbf{J}$ is the matrix of the second moment of area of the cross section associated with axes along the unit vectors $\bar{\mathbf{b}}_1, \bar{\mathbf{b}}_2, \bar{\mathbf{b}}_3$ and α_2 and α_3 are the shear area ratios for $\bar{\mathbf{b}}_2$ and $\bar{\mathbf{b}}_3$ directions (see Kane et al. [1987]). To generate the contribution of this member to $\mathbf{M}$ and $\mathbf{f}$,we consider an element of the beam with a length of dx. This element, dB, can be treated as an infinitesimal rigid body, so that using the corresponding expressions for rigid bodies (Eqs.(2.12)), we may derive the expressions for $\mathbf{dM}$ and $\mathbf{df}$, the contribution of the

element to the system mass and force matrices. The centroidal inertia and mass of the element, needed in Eqs.(2.12), can be related to $\mathbf{J}$ and ρ as follows

$$\mathbf{I}^B = \frac{\rho}{A}\mathbf{J}\,dx \quad , \quad m^B = \rho\,dx. \tag{2.13}$$

Substituting Eqs.(2.13) into Eqs(2.12) and integrating over the length of the beam, one gets the contribution of the entire beam to the total mass matrix and force column as:

$$M_{rs}^j = \int_0^L \rho\left[\mathbf{V}_r^b \cdot \mathbf{V}_s^b + \frac{1}{A}\boldsymbol{\omega}_r^B \cdot (\mathbf{J}\,\boldsymbol{\omega}_s^B)\right]dx, \quad r,s = 1,\ldots,N, \tag{2.14}$$

$$f_r^j = \mathcal{F}_r^j - \int_0^L \rho\left[\mathbf{V}_r^b \cdot \mathbf{a}_t^b + \frac{1}{A}\boldsymbol{\omega}_r^B \cdot [\mathbf{J}\,\boldsymbol{\alpha}_t^B + \boldsymbol{\omega}^B \times (\mathbf{J}\,\boldsymbol{\omega}^B)]\right]dx, \quad r = 1,\ldots,N, \tag{2.15}$$

where F_r^j denotes the contribution of the j-th member to the generalized active force column defined in Eq.(2.7.c). As opposed to the rigid bodies, calculation of $\mathcal{F}_r^j$ for elastic members needs further elaboration. There are two sources of contributing forces in $\mathcal{F}_r^j$, the first is the external contributing forces and the second is the internal ones, where external and internal are defined with respect to the entire beam, not the element dB. Thus we can write

$$\mathcal{F}_r^j = \int_0^L \left[\mathbf{V}_r^b \cdot (\mathbf{R}^e + \mathbf{R}^i) + \boldsymbol{\omega}_r^B \cdot (\mathbf{T}^e + \mathbf{T}^i)\right]dx, \quad r = 1,\ldots,N, \tag{2.16}$$

where, $\mathbf{R}^e$ and $\mathbf{T}^e$ are the density of the equivalent set of all contributing external forces and moments acting on the element dB, while $\mathbf{R}^i$ and $\mathbf{T}^i$ form the density of the equivalent set for the internal ones. Hence, we may write

$$\mathcal{F}_r^j = (\mathcal{F}_r^j)^e + (\mathcal{F}_r^j)^i, \quad r = 1,\ldots,N. \tag{2.17}$$

The contribution of the internal forces and moments, $(\mathcal{F}_r^j)^i$, can be derived by utilizing the strain energy function as follows:

$$(\mathcal{F}_r^j)^i = -\partial U/\partial q_r, \quad r = 1,\ldots,N. \tag{2.18}$$

One should note that the elastic strain energy is a function of elastic generalized coordinates only, so $(\mathcal{F}_r^*)^* = 0$ for all non-elastic generalized coordinates. Equation (2.18) is based on the assumption that the generalized speeds are defined such that $\dot{q}_i = u_i$ for all q_i belonging to the elastic DOFs. A similar relation for the general definition of generalized speeds can be found in Kane and Levinson [1985].

The strain energy is a function of the deformation of the beam. To establish this function we need to define the relative orientation and position of a generic element dB in the frame A, located at the root of the beam. The two frames, A and B, are parallel when the beam is undeformed. In fact, frame A is undergoing the same rigid motion as the beam. The element dB can be brought into a general orientation from the orientation of A by three successive rotations of $\theta_1, \theta_2, \theta_3$, about $\bar{\mathbf{b}}_1, \bar{\mathbf{b}}_2, \bar{\mathbf{b}}_3$; furthermore, the element can be brought into a general position from its undeformed position by an elastic displacement of $w_1\bar{\mathbf{a}}_1 + w_2\bar{\mathbf{a}}_2 + w_3\bar{\mathbf{a}}_3$. Based on the above definitions, the strain energy function is :

$$U = \frac{1}{2}\int_0^L \left\{ EA\left(\frac{\partial \eta(x,t)}{\partial x}\right)^2 + EJ_{22}\left(\frac{\partial \theta_2(x,t)}{\partial x}\right)^2 + EJ_{33}\left(\frac{\partial \theta_3(x,t)}{\partial x}\right)^2 + G\kappa\left(\frac{\partial \theta_1(x,t)}{\partial x}\right)^2 + \frac{GA}{\alpha_2}\left(\frac{\partial w_2(x,t)}{\partial x} - \theta_3(x,t)\right)^2 + \frac{GA}{\alpha_3}\left(\frac{\partial w_3(x,t)}{\partial x} + \theta_2(x,t)\right)^2 \right\} dx \qquad (2.19)$$

In the above relation, η denotes the displacement of the element along the axial direction of the beam, as shown in an exaggerated fashion in Figure 2.4. Note that η is equal to w_1 only up to the first order of the elastic generalized coordinates, but they are not equal if the second order

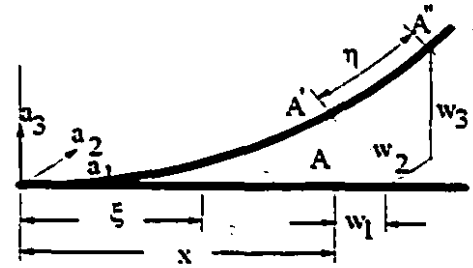

Figure 2.4 Displacement of the neutral axis.

terms of the generalized coordinates are taken into account. This will be discussed in more detail in Chapter 5, where the dynamic stiffening effect is addressed.

There might be two kinds of external forces, namely distributed (e.g. gravitational), and concentrated (e.g. actuators) forces and torques acting on the beam. In this case $(\mathcal{F}_r^f)^e$ can be calculated as:

$$(\mathcal{F}_r^f)^e = \int_0^L \left[\mathbf{V}_r^b \cdot \mathbf{R}^d + \boldsymbol{\omega}_r^B \cdot \mathbf{T}^d \right] dx + \sum_{k=1}^{n^p} \mathbf{V}_r^{p^k} \cdot \mathbf{R}^k + \sum_{k=1}^{n^p} \boldsymbol{\omega}_r^{p^k} \cdot \mathbf{T}^k, \quad r = 1,\ldots,N, \quad (2.20)$$

in which, p^k is the element of the beam on which the external point force/torque, $\mathbf{R}^k/\mathbf{T}^k$, is acting, and $\mathbf{R}^d$ and $\mathbf{T}^d$ are the density of distributed external forces and moments per unit length of the beam. Equation (2.20) makes the implementation of any type of external forces easy.

So far, the relations governing the contribution of an elastic beam to the total mass and force matrices are established, but these relations are in terms of the spatial coordinates of the elements of the beam, $\mathbf{w}, \boldsymbol{\theta}$, which need an infinite number of generalized coordinates to be described. Clearly it can not be a practical way, so one needs to discretize these quantities to obtain some finite number of DOFs. The assumed modes method is used here to relate the spatial coordinates to the generalized coordinates as:

$$\begin{aligned} \eta(x,t) &= \sum_{i=\mu_1+1}^{\mu_1+\nu_1} \varphi_{1i}\, q_i \\ w_k(x,t) &= \sum_{i=\mu_k+1}^{\mu_k+\nu_k} \varphi_{ki}\, q_i, \quad k = 2,3 \\ \theta_k(x,t) &= \sum_{i=\mu_{(k-3)}+1}^{\mu_{(k-3)}+\nu_{(k-3)}} \varphi_{(k-3)i}\, q_i, \quad k = 1,2,3 \end{aligned} \quad (2.21)$$

which represent linear combinations of the elastic generalized coordinates, $q_i(t)$, and some admissible functions, $\varphi_{ji}(x)$, which must satisfy at least the geometric boundary conditions. ν_k are arbitrary numbers which signify the number of shape functions employed, whereas μ_k and

$\mu_{...}$ denote the number of generalized coordinates previously defined. One should note that no special boundary condition has been assumed so far, and hence the same formulation can be used for different types of boundary conditions.

The use of the assumed modes method or finite elements is equivalent to the assumption of linearity for the *elastic* DOFs, for these methods are good only if the motion due to each mode is not affected by the others. This can be true only if all *elastic* DOFs are small enough, so that a set of ODEs linear in *elastic* DOFs and non-linear in rigid DOFs is the best we can get from a discretized elastic system. However, to get a properly linearized set of equations, we may start linearizing only after the calculation of the partial velocities.

When discretization techniques are used by defining the elastic displacements w_1, w_2, w_3 as linear combinations of the elastic generalized coordinates, the linearization has inevitably started prematurely, prior to the calculation of the partial velocities. In the absence of a large rigid motion, this premature linearization would not cause any problem. But, for an elastic body undergoing large rigid motions, premature linearization might result in the loss of some *first-order terms* in the equations of motion. A detailed discussion of this subject can be found in Chapter 5 of this thesis, where it is shown that in the case of beams, this problem can be avoided by considering terms up to the second-order in the elastic generalized coordinates in the expressions for w_1 as follows:

$$w_1 = \eta - \int_0^x \left[\left(\partial w_2 / \partial \xi\right)^2 + \left(\partial w_3 / \partial \xi\right)^2 \right] d\xi. \qquad (2.22)$$

Table 2.1 Possible simplifications from Timoshenko beam.

To Neglect	Set	Euler Beam	String	Bar
Extension	$\varphi_{1i} = 0$, $i = \nu_1,\ldots,\nu_2$			
Bending in a_2 dir.	$\varphi_{2i} = 0$, $i = \nu_2+1,\ldots,\nu_3$			■
Bending in a_3 dir.	$\varphi_{3i} = 0$, $i = \nu_3+1,\ldots,\nu_4$			■
Torsion	$\varphi_{4i} = 0$, $i = \nu_4+1,\ldots,\nu_5$		■	
Rotary Inertia	$I_{22} = I_{33} = 0$	■	■	■
Shear	$1/\alpha_2 = 1/\alpha_3 = 0$	■	■	■
Warping restraint	$\Gamma = 0$	■	■	■

2.2.3 Specialization to plates

The specialization for plates can be carried out in a similar fashion as for beams. Consider that the j-th member of the system Σ is a thin plate, shown in Figure 2.5, with the thickness h, which is much smaller than the other two dimensions of the plate (L_1 and L_2). The plate is characterized by its mass density per unit area ρ, modulus of elasticity E, and Poisson's ratio ν. In the following analysis, both mid-plane stretch and transverse vibration of the plate are considered. Besides, the effect of rotary inertia is taken into account; however, the shear deformation is ignored. To find the contribution of the plate in the equations of motion of the system, i.e., $\mathbf{M}^j$ and $\mathbf{f}^j$, we consider an infinitesimal element of the plate (see Figure 2.5) with the area of $dx_1\,dx_2$ and height of h.

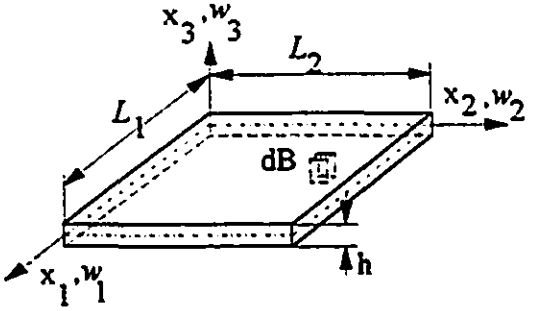

Figure 2.5 Schematic of a thin plate

To describe the motion of the plate we define two frames. The frame A is located at the point of attachment of the plate to the lower body in the chain such that the unit vector $\bar{\mathbf{a}}_3$ is normal to the mid-plane of the plate. Frame A follows the rigid-body motion of the plate. On the other hand, the frame B is attached to the element dB with its origin at the centroid of the element. This frame, which is parallel to the frame A when the plate is undeformed, follows all motions of the element dB. The frame B can be brought into a general orientation from the orientation of A by three successive rotations of $\theta_1,\theta_2,\theta_3$, about $\bar{\mathbf{b}}_1,\bar{\mathbf{b}}_2,\bar{\mathbf{b}}_3$, respectively; furthermore, the element can be brought into a general position from its undeformed position by an elastic displacement of $w_1\bar{\mathbf{a}}_1 + w_2\bar{\mathbf{a}}_2 + w_3\bar{\mathbf{a}}_3$.

The infinitesimal element, dB, can be regarded as a rigid body with centroidal moment of inertia and mass defined as

$$\mathbf{I}^B = \frac{\rho h^2}{12}\mathbf{K}\,dx_1\,dx_2 \quad , \quad m^B = \rho\,dx_1\,dx_2, \tag{2.23}$$

where

$$\mathbf{K} = \begin{bmatrix} 1 & 0 & 0 \\ 0 & 1 & 0 \\ 0 & 0 & 0 \end{bmatrix}. \tag{2.24}$$

Substituting Eqs.(2.23) into Eqs.(2.12) and integrating over the area of the plate, one gets the contribution of the entire plate to the total mass matrix and force column as:

$$M_{rs}^j = \int_0^{L_1}\int_0^{L_2} \rho\left[\mathbf{V}_r^b \cdot \mathbf{V}_s^b + \frac{h^2}{12}\boldsymbol{\omega}_r^B \cdot (\mathbf{K}\,\boldsymbol{\omega}_s^B)\right] dx_2\,dx_1, \quad r,s = 1,\ldots,N, \tag{2.25}$$

$$f_r^j = \mathcal{F}_r^j - \int_0^{L_1}\int_0^{L_2} \rho\left[\mathbf{V}_r^b \cdot \mathbf{a}_t^b + \frac{h^2}{12}\boldsymbol{\omega}_r^B \cdot [\mathbf{K}\,\boldsymbol{\alpha}_t^B + \boldsymbol{\omega}^B \times (\mathbf{K}\,\boldsymbol{\omega}^B)]\right] dx_2\,dx_1, \quad r = 1,\ldots,N. \tag{2.26}$$

In the above equations, $\mathcal{F}_r^j$ denotes contribution of the j-th member to the generalized active force column defined in Eq.(2.7.c). This term, using the same methodology presented for beams, can be calculated as

$$\mathcal{F}_r^j = -\partial U/\partial q_r + \int_0^{L_1}\int_0^{L_2}\left[\mathbf{V}_r^b \cdot \mathbf{R}^d + \boldsymbol{\omega}_r^B \cdot \mathbf{T}^d\right] dx_2\,dx_1 + \sum_{k=1}^{\mu^P} \mathbf{V}_r^{p^k} \cdot \mathbf{R}^k + \sum_{k=1}^{\mu^T} \boldsymbol{\omega}_r^{p^k} \cdot \mathbf{T}^k, \quad r = 1,\ldots,N, \tag{2.27}$$

in which, p^k is the element of the plate on which the external point force/torque, $\mathbf{R}^k/\mathbf{T}^k$, is acting, and $\mathbf{R}^d$ and $\mathbf{T}^d$ are the density of distributed external forces and moments per unit area of the plate. The strain energy of the plate, denoted in Eq.(2.27) by U, is given by

$$U = \int_{a_1}^{b_1}\int_{a_2}^{b_2}\left\{\frac{Eh}{1-\nu^2}\left[w_{1,1}^2 + w_{2,2}^2 + 2\nu w_{1,1}w_{2,2} + \frac{1-\nu}{2}(w_{1,2}+w_{2,1})^2\right] + \right.$$
$$\left.\frac{Eh^3}{12(1-\nu^2)}\left[w_{1,11}^2 + w_{2,22}^2 + 2\nu w_{1,11}w_{2,22} + 2(1-\nu)w_{1,12}^2\right]\right\} dx_2\, dx_1 . \qquad (2.28)$$

where

$$w_{i,j} = \frac{\partial w_i}{\partial x_j} \quad , \quad w_{i,jk} = \frac{\partial^2 w_i}{\partial x_j \partial x_k} \qquad (2.29)$$

The spatial coordinates of the plate can be related to the elastic generalized coordinates using assumed modes method as:

$$w_k(x,t) = \sum_{i=\mu_k+1}^{\mu_k+\nu_k} \varphi_{ki}\, q_i , \quad k = 1,2,3 ,$$
$$\theta_k(x,t) = \sum_{i=\mu_{(k-3)}+1}^{\mu_{(k-3)}+\nu_{(k-3)}} \varphi_{(k-3)i}\, q_i , \quad k = 1,2,3 , \qquad (2.30)$$

in which ν_k are arbitrary numbers which signify the number of shape functions employed; whereas, μ_k denotes the number of generalized coordinates previously defined. It is shown in Chapter 5 that to obtain correct results for a plate undergoing large rigid-body motion, this linear relations must be corrected to include second order terms of the elastic generalized coordinates.

2.3 Linearization

The equations of motion can be linearized after obtaining them, or by starting linearization only after calculating the partial velocities based on *nonlinear* expressions for velocities. Any attempt to start the linearization prior to this stage would lead to a premature linearization, which may result in the loss of some linear terms in the equations of motion.

Here, the linearization is carried out analytically after obtaining the nonlinear form of the equations of motion. This has the advantage of obtaining both nonlinear and linear forms of the equations of motion; moreover, the difficulty of extending the formalism to make it capable of

direct generation of the linear form of the equations is removed. This way, the burden of linearization is left to the computer, and it is done using the symbolic computer language, MAPLE-V.

The non-linear equations of motion, however, are often very lengthy, which makes either the introduction of some intermediate parameters necessary or the use of symbolic language impractical. The code developed here is capable of analytical linearization of the equations generated in terms of intermediate parameters using the chain rule for differentiation. This makes the use of the code for generating linear and non-linear equations of motion of large systems practical.

To discuss the method of linearization, a few words about the intermediate parameters are necessary. The general form of the equations of motion, with intermediate parameters, can be written as

$$\mathbf{M}(\mathbf{q},\mathbf{z},t)\,\dot{\mathbf{u}} = \mathbf{f}(\mathbf{q},\mathbf{u},\mathbf{z},\tau,t). \tag{2.31}$$

in which $\mathbf{z}$ is the vector of intermediate parameters. The intermediate parameters are collected in a way such that the i-th intermediate parameter is a function of the first (i-1) intermediate parameters, the generalized coordinates, the generalized speeds, and the inputs of the system as follows:

$$z_i = z_i(z_1,\ldots,z_{i-1},\mathbf{q},\mathbf{u},\tau,t). \tag{2.32}$$

The linearized form of the equations of motion can then be written as:

$$\overline{\mathbf{M}}\,\dot{\tilde{\mathbf{u}}} = [\bar{\mathbf{f}}_q - (\overline{\mathbf{M}\dot{\mathbf{u}}})_q]\tilde{\mathbf{q}} + \bar{\mathbf{f}}_u\,\tilde{\mathbf{u}} + \bar{\mathbf{f}}_\tau\,\tilde{\tau} + [\bar{\mathbf{f}}_z - (\overline{\mathbf{M}\dot{\mathbf{u}}})_z]\tilde{\mathbf{z}}. \tag{2.33}$$

In the above relation, $\bar{\mathbf{q}}, \bar{\mathbf{u}}$, and $\dot{\bar{\mathbf{u}}}$ are the trim condition or nominal values of the generalized coordinates, the generalized speeds, and time-rate of the generalized speeds. Similarly, $\overline{\mathbf{M}}$ denotes the value of the mass matrix evaluated at the trim condition, i.e., $\overline{\mathbf{M}} = \mathbf{M}(\bar{\mathbf{q}},\bar{\mathbf{z}},t)$. On

the other hand, $\tilde{\mathbf{q}}, \tilde{\mathbf{u}}, \dot{\tilde{\mathbf{u}}}, \tilde{\boldsymbol{\tau}}$, and $\tilde{\mathbf{z}}$ represent the small deviations of the corresponding variables from their trim-condition values. The other terms appearing in Eq.(2.33) can be defined as

$$\bar{\mathbf{f}}_{\mathbf{q}} = \left.\frac{\partial \mathbf{f}}{\partial \mathbf{q}}\right|_{\mathbf{q},\mathbf{u},\mathbf{z},\boldsymbol{\tau}}, \quad \bar{\mathbf{f}}_{\mathbf{u}} = \left.\frac{\partial \mathbf{f}}{\partial \mathbf{u}}\right|_{\mathbf{q},\mathbf{u},\mathbf{z},\boldsymbol{\tau}}, \quad \bar{\mathbf{f}}_{\mathbf{z}} = \left.\frac{\partial \mathbf{f}}{\partial \mathbf{z}}\right|_{\mathbf{q},\mathbf{u},\mathbf{z},\boldsymbol{\tau}}, \quad \bar{\mathbf{f}}_{\boldsymbol{\tau}} = \left.\frac{\partial \mathbf{f}}{\partial \boldsymbol{\tau}}\right|_{\mathbf{q},\mathbf{u},\mathbf{z},\boldsymbol{\tau}}$$
$$\overline{(\mathbf{M}\dot{\mathbf{u}})}_{\mathbf{q}} = \left.\frac{\partial (\mathbf{M}\dot{\mathbf{u}})}{\partial \mathbf{q}}\right|_{\mathbf{q},\mathbf{z},\dot{\mathbf{u}}}, \quad \overline{(\mathbf{M}\dot{\mathbf{u}})}_{\mathbf{z}} = \left.\frac{\partial (\mathbf{M}\dot{\mathbf{u}})}{\partial \mathbf{z}}\right|_{\mathbf{q},\mathbf{z},\mathbf{u}}. \tag{2.34}$$

where $\bar{\mathbf{z}}$ is the value of $\mathbf{z}$ evaluated at the trim condition.

To complete the linearization procedure, $\bar{\mathbf{z}}$ and $\tilde{\mathbf{z}}$ must be computed. Taking advantage of the special arrangement of the vector $\mathbf{z}$ (see Eq.(2.32)), one can use the following recursive formulas to accomplish this task.

$$\bar{z}_i = z_i(\bar{z}_1, \ldots, \bar{z}_{i-1}, \bar{\mathbf{q}}, \bar{\mathbf{u}}, \bar{\boldsymbol{\tau}}, t), \tag{2.35}$$

$$\tilde{z}_i = \sum_{j=1}^{i-1} \overline{z_{i,j}}\, \tilde{z}_j + (z_i)_{\mathbf{q}}\, \mathbf{q} + (z_i)_{\mathbf{u}}\, \mathbf{u} + (z_i)_{\boldsymbol{\tau}}\, \boldsymbol{\tau}, \tag{2.36}$$

in which $\overline{z_{i,j}}$, $(z_i)_{\mathbf{q}}$, $(z_i)_{\mathbf{u}}$, and $(z_i)_{\boldsymbol{\tau}}$ are defined as:

$$\overline{z_{i,j}} = \left.\frac{\partial z_i}{\partial z_j}\right|_{\mathbf{z},\bar{\mathbf{q}},\bar{\mathbf{u}},\bar{\boldsymbol{\tau}}}, \quad (z_i)_{\mathbf{q}} = \left.\frac{\partial z_i}{\partial \mathbf{q}}\right|_{\bar{\mathbf{z}},\bar{\mathbf{q}},\bar{\mathbf{u}},\bar{\boldsymbol{\tau}}}, \quad (z_i)_{\mathbf{u}} = \left.\frac{\partial z_i}{\partial \mathbf{u}}\right|_{\bar{\mathbf{z}},\bar{\mathbf{q}},\bar{\mathbf{u}},\bar{\boldsymbol{\tau}}}, \quad (z_i)_{\boldsymbol{\tau}} = \left.\frac{\partial z_i}{\partial \boldsymbol{\tau}}\right|_{\bar{\mathbf{z}},\bar{\mathbf{q}},\bar{\mathbf{u}},\bar{\boldsymbol{\tau}}}. \tag{2.37}$$

Chapter 3

Constrained Motion

3.1 Introduction

In Chapter 2 a formulation for unconstrained motion of multibody systems was developed . In this chapter we extend the formalism to systems with constrained motion. The motion of a system is said to be constrained when, irrespective of the time history of driving forces, the generalized coordinates of the system and their time derivatives are related to each other through some algebraic relations. If P constraints are imposed on a system with $\mathcal{N}$ degrees of freedom (DOFs), then the DOFs of the system are reduced to $N = \mathcal{N} - P$. In this case, one may expect that an independent set of $\mathcal{N} + N$ first-order differential equations, $\mathcal{N}$ kinematical and N dynamical equations, suffices to describe the dynamics of the system, that is to determine $\mathcal{N}$ generalized coordinates and N independent generalized speeds. Unlike the kinematics analysis which is quite straight-forward, the procedure of deriving a complete, minimum-order set of dynamical equations of motion may pose a challenging problem. Discussion of the formulation of these equations is the subject of this chapter.

In this context, by "minimum-order set of equations" we mean a set of dynamical equations with as many equations as the number of independent generalized speeds. On the other hand, a "complete set of equations" is a set which has as many unknowns as the number of equations. In general, a minimum-order set of equations may not be complete.

In this chapter we first classify the constraints; then, two most popular, existing methods for deriving the minimum-order set of equations governing the motion of constrained systems are briefly explained. Afterwards, we identify a class of constraints for which the constraint forces, unknown quantities, remain in the minimum-order set of equations obtained by conventional methods. In this case, the minimum-order set of equations is incomplete, i.e., have more unknowns than the number of equations, and cannot be solved. A novel method, based on Kane's equations, is presented which is capable of generating the complete, minimum-order set of equations even for this class of constrained motion. The essence of the method is to make some modifications to the nonholonomic partial velocities. Use of these *modified partial velocities* eliminates the contributing constraint forces automatically and includes their effect in the equations of motion at the same time. As a spin-off, the formulation sheds some light on aspects such as adequacy and redundancy of constraint forces.

3.2 Classification of Constraints

For a dynamical system, the function $g(\mathbf{q},\mathbf{u},t)=0$ represents a constraint, where $\mathbf{q}$ and $\mathbf{u}$ denote the arrays of generalized coordinates and generalized speeds of the system, while t represents time.

A constraint is called *holonomic* if the constraint equation is integrable, i.e., it can be represented as $g(\mathbf{q},t)=0$. On the other hand, a constraint with non-integrable equation is called *nonholonomic*. The constraint is *simple nonholonomic* if the function $g(\mathbf{q},\mathbf{u},t)$ is a linear function of generalized speeds. The constraints may also be classified as *rheonomic* and *scleronomic*, according to whether the function g does, or does not contain t explicitly.

In addition to the above kinematic classifications, which are well-known to dynamicists, constraints can be classified based on their dynamic nature as artificially and naturally imposed constraints. *Artificially imposed constraints* are those constraints which are maintained by

applying constraint forces through actuators; these constraint forces need to be evaluated and supplied artificially. On the other hand, natural constraints are those constraints whose associated forces are applied naturally, through reaction of the elements of the system with each other and with the surrounding environment. These two types of constraints and their differences are discussed in more detail in the following sections.

The scope of the study here is confined, from the kinematic point of view, to systems with *simple* nonholonomic constraints. This, however, can include holonomic constraints as well, because any holonomic constraint equation can be differentiated to yield a form similar to that of a simple nonholonomic one. On the other hand, both categories of natural and artificial constraints are studied.

3.3 Dynamic Equations for Constrained Motion: Conventional Methods

Consider a system $\mathcal{S}$, comprised of ν particles, with N DOFs which is subjected to P independent simple nonholonomic constraints described by

$$\left[[\mathcal{A}_1(\mathbf{q},t)]_{P\times N} \quad [\mathcal{A}_2(\mathbf{q},t)]_{P\times P}\right]\begin{bmatrix}[\mathbf{u}_1]_N\\ [\mathbf{u}_2]_P\end{bmatrix}=[\mathcal{B}(\mathbf{q},t)]_P, \tag{3.1}$$

in which $\mathbf{q}=q_1,\ldots,q_{N+P}$ is an array of the generalized coordinates, and $\mathbf{u}_1=u_1,\ldots,u_N$ and $\mathbf{u}_2=u_{N+1},\ldots,u_{N+P}$ denote the independent and dependent sets of generalized speeds of the system, respectively. Here, $\mathcal{A}_2$ is an invertible matrix, by virtue of the independence of constraints. The constraints are enforced by P constraint forces whose magnitudes are designated by $\mathbf{C}=C_1,\ldots,C_P$.

The objective is to find a set of N dynamical equations of motion. This task can be accomplished using either Lagrange's method or Kane's method. We discuss both methods here; however, the second one, Kane's method, is the one adopted in the formulation and

computer code developed in this study. Both of the above-mentioned methods, which can be readily found in the literature, are briefly presented here for the sake of continuity and completeness.

3.3.1 Lagrange's method

Lagrange's equations of motion for the constrained system S can be written as (see Meirovitch [1970])

$$\frac{d}{dt}\left(\frac{\partial \mathcal{L}}{\partial \dot{q}_r}\right)-\frac{\partial \mathcal{L}}{\partial q_r}=Q_r+\sum_{i=1}^{P}\mathcal{A}_{ri}\lambda_i, \quad r=1,\ldots,N+P, \tag{3.2}$$

in which $\mathcal{L}$, Q_r, and $\mathcal{A}=[\mathcal{A}_1 \quad \mathcal{A}_2]$ are, respectively, the Lagrangian of the system, the r-th generalized active force of the system, and the constraint matrix defined in Eq.(3.1). The quantity λ_i denotes the i-th Lagrange's multiplier, which is an indication of the i-th constrained force of the system. The set of $N+P$ equations of motion, Eq.(3.2), can be transformed into a set of N equations independent of the Lagrange multipliers. To this end, Eq.(3.2) must be premultiplied by the transpose of the matrix $\mathcal{A}^c$ defined as

$$\mathcal{A}^c=\begin{bmatrix}[\mathbf{I}]_{N\times N}\\ -[\mathcal{A}_2^{-1}]_{P\times P}[\mathcal{A}_1]_{P\times N}\end{bmatrix}, \tag{3.3}$$

in which $[\mathbf{I}]$ denotes the identity matrix. The matrix $\mathcal{A}^c$ is clearly an orthogonal complement matrix of $\mathcal{A}$ (i.e., $\mathcal{A}\mathcal{A}^c=0$). As stated in Chapter 1, several procedures for the numerical calculation of the matrix $\mathcal{A}^c$ are available in the literature. Using this transformation one may write the minimum-order set of equations of motion, which is now independent of Lagrange multipliers, as

$$\sum_{r=1}^{N+P}\mathcal{A}_{rj}^c\left[\frac{d}{dt}\left(\frac{\partial \mathcal{L}}{\partial \dot{q}_r}\right)-\frac{\partial \mathcal{L}}{\partial q_r}\right]=\sum_{r=1}^{N+P}\mathcal{A}_{rj}^c Q_r, \quad j=1,\ldots,N. \tag{3.4}$$

3.3.2 Kane's method

Kane's equations of motion (Kane and Levinson [1985]) for the constrained system S can be written as

$$\sum_{i=1}^{\nu} m^i \tilde{\mathbf{V}}_r^i \cdot \mathbf{a}^i = \sum_{i=1}^{\nu} \tilde{\mathbf{V}}_r^i \cdot \mathbf{R}^i, \quad r = 1,\ldots,N, \tag{3.5}$$

where m^i, $\mathbf{a}^i$, and $\mathbf{R}^i$ denote the mass and the acceleration of the i-th particle, and the resultant of all contributing active forces applied on particle i, respectively. Here, $\tilde{\mathbf{V}}_r^i$ denotes the r-th nonholonomic partial velocity of the i-th particle defined as

$$\tilde{\mathbf{V}}_r^i = \partial \mathbf{V}^i(\mathbf{q}, \mathbf{u}_1, t)/\partial u_r, \quad r = 1,\ldots,N, \tag{3.6}$$

where $\mathbf{V}^i$ is the absolute velocity of particle i. One can readily see that, in this formulation, the introduction of the Lagrange multipliers is not necessary, so the minimum-order set of equations can be generated directly.

In spite of their differences, which may make one of the above-mentioned methods more convenient for a certain problem, either of them can be applied equally well to solve most of the constrained motion problems encountered in practice. There are cases, however, when some of the constraint forces remain in the minimum–order equations of motion obtained by either one of the above two methods. The presence of these constraint forces (which are called *contributing constraint forces*) causes the number of unknowns to exceed the number of equations. This phenomenon is discussed in more detail in the next section, where an important class of constraints which normally exhibit this behavior is introduced.

3.4 Natural and Artificial Constraints

Equation (3.1) ($\mathcal{A}\,\mathbf{u} = \mathcal{B}$) describes completely the simple nonholonomic constraints from the kinematics point of view; however, it does not say anything about the method of imposition of these constraints. One should note that two identical systems moving under

kinematically equivalent constraints may exhibit completely different dynamic behavior depending on the method of imposition of constraints –natural or artificial. A simple example which illustrates this point is given below.

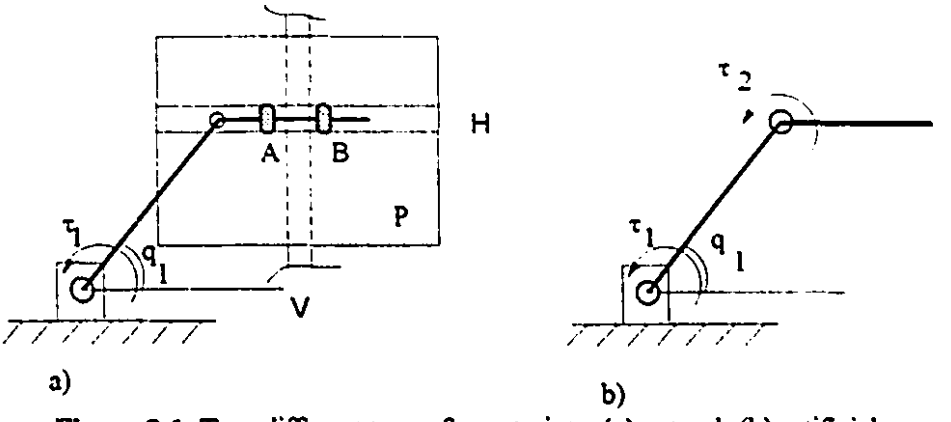

Figure 3.1 Two different type of constraints: (a) natural; (b) artificial.

Figure 3.1-a depicts a mechanism which keeps the second link of a rigid manipulator parallel to the X axis, during the course of its motion, by forcing it to move between two frictionless guides at A and B. The motion of the guides themselves in the Y direction is made possible by the motion of the plate P in the guide V. Since the constraint forces –reaction forces at A and B– are provided through natural interaction of the system with its surrounding environment, the motion can be considered as an example of a ***natural constrained motion.*** The motion takes place in the horizontal plane. In this case, the constraint forces do not contribute in the minimum-order set of equations of motion which is

$$(4m\ell^2/3)\dot{u}_1 = \tau_1, \tag{3.7}$$

where m and ℓ are the mass and the length of each link, and $u_1 = \dot{q}_1$ is the generalized speed of the system. Here τ_1 is the input to the system and there are as many equations as unknowns.

On the other hand, Figure 3.1-b shows a two-link manipulator whose second link is intended to remain horizontal through application of the torque τ_2. This model is a typical example of systems with *artificial constraints*, for the constraint torque is applied through the

actuator located at the elbow joint (it needs to be evaluated and supplied artificially). In this case, regardless of the employed method, the constraint torque τ_2 remains in the minimum-order set of equations of motion, which is

$$(4m\ell^2/3)\dot{u}_1 = \tau_1 - \tau_2. \tag{3.8}$$

Clearly, in this case, τ_2 cannot be regarded as a free input parameter, as opposed to τ_1, for it has to be provided in such a manner that the second link always remains horizontal. Comparison of Eqs.(3.7) and (3.8) reveals that the method of imposition of constraints affects the dynamics of the system. Note that Eq.(3.8) is identical to Eq.(3.7) except for a term τ_2 which obviously is not identically zero. It also shows that the minimum-order set of equations generated for the system with the artificial constraint is not *complete*, it has more unknowns than equations, as opposed to the equations generated for the system with the natural constraint.

All previous methods for reducing the order of equations share the basic short-coming of just taking advantage of the kinematical definition of constraints, i.e., Eq.(3.1). These approaches do not account for the dynamic nature of the constraints, so they end up with the same equations of motion for a constrained system regardless of the type of the constraint, natural or artificial.

A point which is worth mentioning before leaving the discussion is that there are cases where the constraint forces associated with artificial constraints do not appear in the minimum-order set of equations generated using the conventional methods (presented in Section 3.3). As an example, we may think of prescribing the motion of the first link of a planar two link manipulator as a function of time. In this case the torque τ_1 has to be evaluated, as a certain function of time based on the dynamics of the system, and then would be applied through an actuator. However, this torque would not appear in the minimum-order set of equations generated using the conventional order-reduction methods, i.e., the constraint torque τ_1 is non-contributing even if the constraint itself is artificial. Now, one might ask how to find out if the

constraint forces for a complicated motion are contributing or not. The answer to this question will be given in Section 3.6.1.

3.5 Dynamic Equations for Constrained Motion: a New Method

In this section, we use Kane's equations of motion to develop a method which can handle the constrained motion regardless of the type of imposition of constraints, natural or artificial. First the basic formulation is developed; then the calculation effort involved in generating the equations of motion using this method is assessed, and finally the standard form of the equations and its specialization for continuous systems is presented. The analysis is based on the following assumptions:

- The directions of the applied constraint forces are known (as functions of time and generalized coordinates), although their magnitudes are unknown.
- Constraint forces are adequate to enforce the specified constrained motion –except for some singular configurations which can be avoided in practice.
- Constraint forces are not redundant.

The above assumptions are made to make the discussion more concise, and by no means they restrict the scope of this formulation, specially in practical situations. The first assumption does not restrict the generality of the analysis, because any constraint force with unknown direction, which is rare in practice, can be resolved into a set of components with known directions and unknown magnitudes. Also, any constrained system must satisfy the second assumption, otherwise it can not follow the prescribed constrained motion. On the other hand, redundancy of the constraint forces, which might be encountered in practice, would bring some aspects of mechanics of materials into the analysis of motion, which is usually avoided in the

analysis of multibody systems. Having stated the assumptions, we may now present the equations of motion.

3.5.1 Basic formulation

Consider the system S, described in Section 3.3. It would be shown that the *complete minimum-order* equations of motion for this system can be obtained using the following equation:

$$\sum_{i=1}^{\nu} m^i \tilde{\tilde{\mathbf{V}}}_r^i \cdot \mathbf{a}^i = \sum_{i=1}^{\nu} \tilde{\tilde{\mathbf{V}}}_r^i \cdot \mathbf{R}^i, \quad r = 1,\ldots,N, \tag{3.9}$$

in which m^i, and $\mathbf{a}^i$ are the mass and the absolute acceleration of the i-th particle, respectively, while $\tilde{\tilde{\mathbf{V}}}_r^i$ is the *r*-th *modified nonholonomic partial velocity* (MNPV) of particle *i*, (as defined later). Also, $\mathbf{R}^i$ denotes the resultant of all contributing forces, including the constraint forces, which is acting on particle *i*. This includes the contact forces (like friction), the body forces (such as gravity and magnetic forces), and the actuator forces.

The completeness of Eq.(3.9) implies that the use of $\tilde{\tilde{\mathbf{V}}}_r^i$ in generating the equations of motion causes all constraint forces to vanish from the equations of motion. In other words

$$\sum_{i=1}^{\nu} \tilde{\tilde{\mathbf{V}}}_r^i \cdot \mathbf{C}^i = 0 . \tag{3.10}$$

The proof of Eq.(3.10) is given in Appendix A. The term $\mathbf{C}^i$, appearing in the above equation, is the resultant of all contributing constraint forces acting on the *i*-th particle. One has to distinguish between C_j, the magnitude of the j-th constraint force (a scalar), and $\mathbf{C}^i$, the resultant of all contributing constraint forces applied on particle *i* (a vector). In fact, C_j and $\mathbf{C}^i$ are related to each other through the following equation:

$$\mathbf{C}^i = \sum_{j=1}^{p} C_j \mathbf{n}^{ij}, \tag{3.11}$$

where $\mathbf{n}^{ij}$ denotes the array of the direction cosines of the j-th constraint force applied on the i-th particle; it is zero if the j-th constraint force is not acting on the i-th particle.

In order to define the *modified nonholonomic partial velocities*, $\tilde{\tilde{\mathbf{V}}}_r^i$, and to show that Eq.(3.9) represents N *independent* equations governing the motion of the constrained system, we start with the conventional nonholonomic equations of motion, discussed in Section 3.3.2. These equations, which are generated using the nonholonomic partial velocities, can be stated for the system $\mathcal{S}$ as

$$\sum_{i=1}^{\nu} m^i \tilde{\mathbf{V}}_r^i \cdot \mathbf{a}^i = \sum_{i=1}^{\nu} \tilde{\mathbf{V}}_r^i \cdot \mathbf{F}^i + \sum_{i=1}^{\nu} \tilde{\mathbf{V}}_r^i \cdot \mathcal{C}^i, \quad r = 1,\ldots,N, \tag{3.12}$$

where $m^i, \mathbf{a}^i, \tilde{\mathbf{V}}_r^i$, and $\mathcal{C}^i$ are as defined earlier, and $\mathbf{F}^i = \mathbf{R}^i - \mathcal{C}^i$ is the resultant of all contributing active forces, excluding the constraint forces, applied on particle i.

Equation (3.12) represents N independent equations of motion. In the case of systems with *natural* constraints, these equations are complete, i.e., the number of equations is the same as the number of unknowns (the independent generalized speeds). That is because the second term on the right hand side (RHS) of Eq.(3.12) vanishes (Kane and Levinson [1985]). This means that Eq.(3.12) can be solved in conjunction with kinematical equations to determine the dynamics of the system, i.e. to determine $q_1,\ldots,q_{N+P}$ and $u_1,\ldots,u_N$ as functions of time. Equally well, in the case of systems with *artificial* constraints, Eq.(3.12) represents N independent equations of motion. However, in this case the second term on the RHS of Eq.(3.12) may not vanish which, as stated earlier, makes the set of dynamical equations incomplete. Substituting Eq.(3.11), one can rewrite Eq.(3.12) as follows

$$\sum_{i=1}^{\nu} m^i \tilde{\mathbf{V}}_r^i \cdot \mathbf{a}^i = \sum_{i=1}^{\nu} \tilde{\mathbf{V}}_r^i \cdot \mathbf{F}^i + \sum_{j=1}^{P} \tilde{\mathcal{T}}_{rj} C_j, \quad r = 1,\ldots,N. \tag{3.13}$$

where

$$\tilde{\mathcal{T}}_{rj} = \sum_{i=1}^{\nu} \tilde{\mathbf{V}}_r^i \cdot \mathbf{n}^{ij}, \quad r = 1,\ldots,N, j = 1,\ldots,P, \tag{3.14}$$

while $\mathcal{T}_{rj}$ can be defined as the contribution of the unit magnitude of the j-th constraint force in the r-th nonholonomic equation of motion.

P additional independent equations, with no additional unknowns, are clearly necessary from which the constraint forces, C_j, are to be found and substituted into Eq.(3.13) to yield a complete set of N independent equations of motion.

These additional equations can be obtained by introducing P additional generalized speeds such that they violate the constraints. These additional generalized speeds are used only in the calculation of modified partial velocities, while they are all set to zero in determining the velocities and accelerations. The partial velocities associated with these new generalized speeds can be used to generate the P additional independent equations. This procedure, which is parallel to the procedure of "bringing non-contributing constraint forces into evidence" discussed by Kane and Levinson [1985], is detailed in Appendix B. The procedure presented here, as opposed to the one suggested by Kane and Levinson which leaves the burden of properly introducing the additional generalized speeds to the user, provides an algorithmic method of introducing some P *independent* additional generalized speeds which forces the motion to violate all of the above-mentioned constraints. In Appendix B it is shown that the partial velocities associated with the new, constraint-violating generalized speeds, $\tilde{\mathbf{V}}''_{s\sim N}$, can be related to the partial velocities of the system through the following relation

$$\tilde{\mathbf{V}}''_{s\sim N} = \sum_{k=1}^{P} A'_{ks}\, \mathbf{V}'_{k\sim N}, \qquad s = 1,\ldots,P \tag{3.15}$$

in which $\mathbf{A}' = \mathcal{A}_c^{-1}$, while $\mathcal{A}_c$ is the matrix defined in Eq.(3.1). It is also proven in Appendix B that the equations of motion generated using $\tilde{\mathbf{V}}''_{s\sim N}$ would provide P additional equations independent of Eq.(3.12) as follows:

$$\sum_{i=1}^{\nu} m^i\, \tilde{\mathbf{V}}''_{s\sim N} \cdot \mathbf{a}^i = \sum_{i=1}^{\nu} \tilde{\mathbf{V}}''_{s\sim N} \cdot \mathbf{F}^i + \sum_{i=1}^{\nu} \tilde{\mathbf{V}}''_{s\sim N} \cdot \mathbf{C}^i, \qquad s = 1,\ldots,P. \tag{3.16}$$

Defining the elements of the matrix $\mathcal{T}'_{P\times P}$ as

$$\mathcal{T}_{sj}^{t} = \sum_{i=1}^{N} \tilde{\mathbf{V}}_{s+N}^{i} \cdot \mathbf{n}^{i}, \quad s, j = 1, \ldots, P. \tag{3.17}$$

and using Eq.(3.11), one can rewrite Eq.(3.16) as

$$\sum_{i=1}^{N} m^{i} \tilde{\mathbf{V}}_{s+N}^{i} \cdot \mathbf{a}^{i} = \sum_{i=1}^{N} \tilde{\mathbf{V}}_{s+N}^{i} \cdot \mathbf{F}^{i} + \sum_{j=1}^{P} \mathcal{T}_{sj}^{t} C_{j}, \quad s = 1, \ldots, P. \tag{3.18}$$

The existence of the inverse of the matrix $\mathcal{T}^{t}$ is guaranteed by the assumption of adequacy of the constraint forces (this is discussed in more detail in Section 3.6.3). Considering this, we may premultiply the set of Eqs.(3.18) by $-\tilde{\mathcal{T}}\,\mathcal{T}^{t-1}$ and add the result to Eq.(3.13) to get

$$\sum_{i=1}^{N} m^{i} \left(\tilde{\mathbf{V}}_{r}^{i} - \sum_{j=1}^{P} \sum_{s=1}^{P} \tilde{\mathcal{T}}_{\eta} \left(\mathcal{T}^{t-1}\right)_{js} \tilde{\mathbf{V}}_{s+N}^{i} \right) \cdot \mathbf{a}^{i} =$$

$$\sum_{i=1}^{N} \left(\tilde{\mathbf{V}}_{r}^{i} - \sum_{j=1}^{P} \sum_{s=1}^{P} \tilde{\mathcal{T}}_{\eta} \left(\mathcal{T}^{t-1}\right)_{js} \tilde{\mathbf{V}}_{s+N}^{i} \right) \cdot \mathbf{F}^{i}, \quad r = 1, \ldots, N. \tag{3.19}$$

Now, we define $\tilde{\tilde{\mathbf{V}}}_{r}^{i}$ as

$$\tilde{\tilde{\mathbf{V}}}_{r}^{i} = \tilde{\mathbf{V}}_{r}^{i} - \sum_{j=1}^{P} \sum_{s=1}^{P} \tilde{\mathcal{T}}_{\eta} \left(\mathcal{T}^{t-1}\right)_{js} \tilde{\mathbf{V}}_{s+N}^{i}, \quad r = 1, \ldots, N, \tag{3.20}$$

which reduces Eq.(3.19) to

$$\sum_{i=1}^{N} m^{i} \tilde{\tilde{\mathbf{V}}}_{r}^{i} \cdot \mathbf{a}^{i} = \sum_{i=1}^{N} \tilde{\tilde{\mathbf{V}}}_{r}^{i} \cdot \mathbf{F}^{i}, \quad r = 1, \ldots, N. \tag{3.21}$$

Note that since Eqs (3.16) are independent of Eqs(3.13) the result of solving them together, Eqs.(3.21), represents N independent equations governing the motion of the constrained system. Finally, Eq.(3.9) can be obtained by adding Eq.(3.10) to Eq.(3.21) and noting that $\mathbf{R}^{i} = \mathbf{F}^{i} + \mathbf{C}^{i}$.

As one can see, the key element in this formulation is the definition of the ***modified nonholonomic partial velocities*** $\tilde{\tilde{\mathbf{V}}}_{r}^{i}$, defined in Eq.(3.20). Recalling the definition of $\tilde{\mathbf{V}}_{s+N}^{i}$ in

Eq.(3.15), we may relate the modified nonholonomic partial velocities to the partial velocities of the system as follows

$$\tilde{\tilde{\mathbf{V}}}_r^t = \tilde{\mathbf{V}}_r^t - \sum_{s=1}^{P} E_{rs}\, \mathbf{V}_{s-N}^t, \quad r = 1,\ldots,N, \tag{3.22}$$

where

$$E_{rs} = \sum_{k=1}^{P}\sum_{j=1}^{P} \tilde{\mathcal{T}}_{rj}\, (\mathcal{T}'^{-1})_{jk}\, A_{sk}^t, \quad r = 1,\ldots,N,\ s = 1,\ldots,P. \tag{3.23}$$

On the other hand, the nonholonomic partial velocities of the system defined by Kane and Levinson [1985] can be written as

$$\tilde{\mathbf{V}}_r^t = \mathbf{V}_r^t + \sum_{s=1}^{P} A_{sr}\mathbf{V}_{s-N}^t, \tag{3.24}$$

in which $\mathbf{A} = -\mathcal{A}_2^{-1}\,\mathcal{A}_1$. Substituting for $\tilde{\mathbf{V}}_r^t$ from Eq.(3.24) into Eq.(3.22), one may more conveniently write

$$\tilde{\tilde{\mathbf{V}}}_r^t = \mathbf{V}_r^t + \sum_{s=1}^{P} (A_{sr} - E_{rs})\, \mathbf{V}_{s-N}^t. \tag{3.25}$$

As opposed to the definition of $\tilde{\mathbf{V}}_r^t$, which only accounts for the effects of kinematics of constraint, the effect of constraint forces is also included in the definition of $\tilde{\tilde{\mathbf{V}}}_r^t$, through the appearance of $\tilde{\mathcal{T}}$ and $\mathcal{T}'$ in the definition of matrix **E** (see Eq.(3.23)). This, indeed, is the reason why the present approach is successful in dealing with systems with artificial constraints.

It is evident from Eqs.(3.24) and (3.25) that for a system with no constraints ($P = 0$), both $\tilde{\tilde{\mathbf{V}}}_r^t$ and $\tilde{\mathbf{V}}_r^t$ are equivalent to $\mathbf{V}_r^t$. This suggests that Eq.(3.9) can be employed to develop the equations of motion of unconstrained systems as well as constrained ones.

3.5.2 Calculation effort

The calculation effort necessary to generate the equations of motion based on the MNPVs, the method presented in this section, differs from that of generating nonholonomic equations of motion based on the conventional methods, e.g., Eq.(3.13), by the amount of work necessary to produce the matrix **E**. Out of the three elements forming the matrix **E**, the matrix $\mathbf{A}' = \mathcal{A}_r^{-1}$ is necessary in calculation of the nonholonomic partial velocities as well. The other two matrices, ($\tilde{\mathcal{T}}$ and $\mathcal{T}'$) are very easy to calculate, despite their appearance as summations over the whole domain of the system. This is due to the fact that the term $\mathbf{n}^{ij}$ appearing in their definition is zero at all points of the system except for a few, the points of application of constraint forces. With this in mind, one has to carry out the summations only over the points of application of the constraint forces.

The other fact which simplifies the calculation even further is that the artificial constraint forces usually appear in pairs (action and reaction) with $\mathbf{n}^{ij} = -\mathbf{n}^{(i+1)j}$ where i and $i+1$ depict the points of application of the j-th contributing constraint force. Observing this fact one may avoid the burden of calculating the partial velocities ($\mathbf{V}_r^i$ and $\mathbf{V}_r^{i+1}$), necessary in calculation of $\tilde{\mathcal{T}}$ and $\mathcal{T}'$. One may, instead, calculate the partial velocity of the differences, i.e.,

$$\mathbf{V}_r^i - \mathbf{V}_r^{i+1} = \partial(\mathbf{V}^i - \mathbf{V}^{i+1})/\partial u_r, \quad r = 1,\ldots,N+P. \tag{3.26}$$

The simplifying effect of Eq.(3.26) can be better understood by considering that normally the i-th and $(i+1)$-th points are adjacent, so, no matter how complex the system is, $\mathbf{V}^i - \mathbf{V}^{i+1}$ has a simple relation with the DOFs and generalized speeds, as opposed to $\mathbf{V}^i$ and $\mathbf{V}^{i+1}$ which may have very complicated expressions.

3.5.3 Standard form of equations governing constrained motion

To obtain the standard form of the equations of motion, we may expand the acceleration of the i-th particle as

$$\mathbf{a}^i = \sum_{r=1}^{N} \tilde{\mathbf{V}}_r^i \dot{u}_r + \tilde{\mathbf{a}}_t^i \tag{3.27}$$

in which $\tilde{\mathbf{a}}_t^i$, the remainder of acceleration of the i-th particle, is the portion of $\mathbf{a}^i$ which does not contain the time derivative of the generalized speeds. Substituting for $\mathbf{a}^i$ from Eq.(3.27) in Eq.(3.9), we may write the standard form of equations of motion as

$$\sum_{s=1}^{N} \tilde{\tilde{M}}_{rs} \dot{u}_s = \tilde{\tilde{f}}_r, \quad r = 1,\ldots,N \tag{3.28}$$

in which $\tilde{\tilde{\mathbf{M}}}$ and $\tilde{\tilde{\mathbf{f}}}$, the mass matrix and generalized force column associated with modified nonholonomic partial velocities, are defined as

$$\begin{aligned} \tilde{\tilde{M}}_{rs} &= \sum_{i=1}^{\nu} m^i \tilde{\tilde{\mathbf{V}}}_r^i \cdot \tilde{\mathbf{V}}_s^i, \quad r,s = 1,\ldots,N, \\ \tilde{\tilde{f}}_r &= \sum_{i=1}^{\nu} \tilde{\tilde{\mathbf{V}}}_r^i \cdot (\mathbf{R}^i - m^i \tilde{\mathbf{a}}_t^i), \quad r = 1,\ldots,N. \end{aligned} \tag{3.29}$$

3.5.4 Extension of the formulation for continuous systems

Let us once again consider the system S, described in Chapter 2, which is a congregation of n bodies and has N DOFs. Besides, we consider that the system is subjected to P simple nonholonomic constraints, described by Eq.(3.1). The system, in this case, has $N+P$ generalized coordinates ($\mathbf{q} = q_1,\ldots,q_{N+P}$), N independent generalized speeds ($\mathbf{u}_1 = u_1,\ldots,u_N$), and P dependent generalized speeds ($\mathbf{u}_2 = u_{N+1},\ldots,u_{N+P}$).

Equation (3.28) represents the dynamical equations of motion of this system. The mass matrix and force column for this system can be obtained by changing the summations in Eqs.(3.29) to integrals over the entire domain of S as

$$\begin{aligned} \tilde{\tilde{M}}_{rs} &= \int_{m^s} \tilde{\tilde{\mathbf{V}}}_r^p \cdot \tilde{\mathbf{V}}_s^p \, dm, \qquad r,s = 1,\ldots,N, \\ \tilde{\tilde{f}}_r &= \int_{D^s} \tilde{\tilde{\mathbf{V}}}_r^p \cdot \mathbf{R}^p \, dD - \int_{m^s} \tilde{\tilde{\mathbf{V}}}_r^p \cdot \tilde{\mathbf{a}}_t^p \, dm, \qquad r = 1,\ldots,N, \end{aligned} \tag{3.30}$$

in which D^s, m^s and $\mathbf{a}^p$ are, respectively, the entire domain of S, the mass of S, and the acceleration of a sample infinitesimal element p; also, $\mathbf{R}^p$ is the resultant contributing force acting on the element p. Dividing the domain of integrals, one can find the contribution of the *j-th* member of the system to $\tilde{\tilde{\mathbf{M}}}$ and $\tilde{\tilde{\mathbf{f}}}$ as

$$\begin{aligned} \tilde{\tilde{M}}_{rs}^j &= \int_{m^j} \tilde{\tilde{\mathbf{V}}}_r^p \cdot \tilde{\mathbf{V}}_s^p \, dm, \qquad r,s = 1,\ldots,N, \\ \tilde{\tilde{f}}_r^j &= \int_{D^j} \tilde{\tilde{\mathbf{V}}}_r^p \cdot \mathbf{R}^p \, dD - \int_{m^j} \tilde{\tilde{\mathbf{V}}}_r^p \cdot \tilde{\mathbf{a}}_t^p \, dm, \qquad r = 1,\ldots,N, \end{aligned} \tag{3.31}$$

and

$$\begin{aligned} \tilde{\tilde{\mathbf{M}}} &= \sum_{j=1}^{n} \tilde{\tilde{\mathbf{M}}}^j, \\ \tilde{\tilde{\mathbf{f}}} &= \sum_{j=1}^{n} \tilde{\tilde{\mathbf{f}}}^j. \end{aligned} \tag{3.32}$$

Similar specializations as those given in Section 2.2 can be made for Eqs.(3.31) in the case of the *j*-th member of the system being a rigid body, a beam, or a plate. For instance, if the *j*-th member of the system is a rigid body, denoted by B, Eqs.(3.31) can be simplified to

$$\tilde{\tilde{M}}_{rs}^B = m^B \tilde{\tilde{\mathbf{V}}}_r^b \cdot \tilde{\mathbf{V}}_s^b + \tilde{\tilde{\boldsymbol{\omega}}}_r^B \cdot (\mathbf{I}^B \tilde{\boldsymbol{\omega}}_s^B), \qquad r,s = 1,\ldots,N, \tag{3.33.a}$$

$$\tilde{\tilde{f}}_r^B = \tilde{\tilde{\mathbf{V}}}_r^b \cdot (\mathbf{R} - m^B \tilde{\mathbf{a}}_t^b) + \tilde{\tilde{\boldsymbol{\omega}}}_r^B \cdot [\mathbf{T} - \mathbf{I}^B \tilde{\boldsymbol{\alpha}}_t^B - \boldsymbol{\omega}^B \times (\mathbf{I}^B \boldsymbol{\omega}^B)], \qquad r = 1,\ldots,N, \tag{3.33.b}$$

in which m^B and $\mathbf{I}^B$ are the mass and the centroidal inertia matrix of B corresponding to the local axes. Furthermore, the term $\mathbf{R}$ denotes the array of components of $\bar{\mathbf{R}}$ in the inertial frame I, whereas, $\mathbf{T}$ contains the components of $\bar{\mathbf{T}}$ in the body frame B. The torque $\bar{\mathbf{T}}$ and the force

$\vec{\mathbf{R}}$, whose line of action passes through the centroid of the rigid body B, are the equivalent set for all the contributing forces acting on B. The quantity $\tilde{\tilde{\omega}}_r^B$ which appears in Eqs.(3.33) is defined as

$$\tilde{\tilde{\omega}}_r^B = \tilde{\omega}_r^B - \sum_{s=1}^{p} E_{rs}\, \omega_{s,N}^B, \quad r = 1,\ldots,N. \tag{3.34}$$

where the matrix $\mathbf{E}$ is as defined in Eq.(3.23).

3.6 Constraint Forces

In this section we examine some issues relevant to the constraint forces such as contribution, determination, adequacy, and redundancy of the constraint forces. In the discussion of adequacy and redundancy, instead of giving rigorous proofs, we try to provide the reader with some insight and practical measures.

3.6.1 Contributing forces

A primary question which may arise in dealing with constrained systems can be whether a constraint force, say C_j, is a contributing one or not. The question can be answered, in some cases, based on the intuition and expertise of the dynamicist. However, a more reliable answer can be obtained by forming the j-th column of the matrix $\tilde{\mathcal{T}}$. The force is not contributing if and only if this column is identically zero. This suggests that if there is any doubt about a constraint force being contributing or not, the best way is to regard it as contributing and include it in the active forces, $\mathbf{R}^i$. One can also see that if all constraint forces are non-contributing then the matrix $\tilde{\mathcal{T}}$ would be identically zero, and consequently so would be matrix $\mathbf{E}$. In this case, the modified nonholonomic partial velocities, $\tilde{\tilde{\mathbf{V}}}_r$, reduce to the nonholonomic partial velocities, $\tilde{\mathbf{V}}_r$, which makes the use of the method presented here completely equivalent to the conventional method presented in the Section 3.3.2

3.6.2 Determination

The constraint forces can be simply calculated using Eq.(3.18) as follows

$$C_j = \sum_{i=1}^{P} (\mathcal{T}'^{-1})_{ji} \sum_{i=1}^{N} \tilde{\mathbf{V}}_{i,N}^{ri} \cdot (m^i \mathbf{a}^i - \mathbf{F}^i), \quad j = 1,\ldots,P. \tag{3.35}$$

One should be specially careful about using the active forces excluding all constraint forces, $\mathbf{F}^i$, in this equation.

3.6.3 Adequacy

For a system with P constraints we may say that the P constraint forces, $C_1,\ldots,C_P$, are adequate to enforce the constrained motion if for any arbitrary motion of the system $(\mathbf{q}(t), \mathbf{u}(t), \dot{\mathbf{u}}(t))$, one can find $C_1,\ldots,C_P$ such that Eq.(3.18) is satisfied. Note that violating Eq.(3.18) is equivalent to producing acceleration, and consequently velocities, which would violate the constraints. The adequacy of constraint forces can be achieved only if the matrix $\mathcal{T}'$ is invertible. Otherwise, one may always find some combination of $\mathbf{q}(t), \mathbf{u}(t)$, and $\dot{\mathbf{u}}(t)$ which violates Eq.(3.18).

3.6.4 Redundancy

A constraint force is said to be redundant if it does the same job as another constraint force, or a combination of some other constraint forces. In this case, removing the redundant constraint force should not have any effect on the dynamics of the system, except for the magnitude of the constraint forces which might be altered.

To avoid redundancy, the number of constraint forces should be equal to the number of constraints. However, this is not a sufficient condition. For instance, for a system with P constraints we may arrange P constraint forces in such a way that some of them repeat the same operation and become redundant; of course, in this case the system suffers from a lack of

adequacy of constraint forces too. The redundancy of constraint forces can be mathematically verified by checking the linear independence of the columns of the matrix $\mathcal{T}'$. To clarify this, let us assume that m columns of the matrix $\mathcal{T}'$ are linearly dependent (without loss of generality we may assume them to be the first m columns) such that

$$\mathcal{T}'_{im} = \sum_{j=1}^{m-1} \alpha_j \mathcal{T}'_{ij}, \quad i = 1,\ldots,P. \tag{3.36}$$

The contribution of $C_1,\ldots,C_m$ in Eq.(3.18) is

$$\sum_{j=1}^{m} \mathcal{T}_{ij} C_j = \sum_{j=1}^{m-1} \mathcal{T}_{ij} C_j + \mathcal{T}'_{im} C_m, \quad i = 1,\ldots,P \tag{3.37}$$

which can be rewritten using Eq.(3.36) as

$$\sum_{j=1}^{m} \mathcal{T}_{ij} C_j = \sum_{j=1}^{m-1} \mathcal{T}'_{ij}(C_j + \alpha_j C_m), \quad i = 1,\ldots,P \tag{3.38}$$

One can readily observe from Eq.(3.38) that a new set of constraint forces containing m-1 members (with the magnitudes of $C_j + \alpha_j C_m$) can have exactly the same contribution to the dynamics of the system as the constraint forces $C_1,\ldots,C_m$. This means that the m-th constraint force is redundant and can be removed without any effect on the dynamics of the system.

Chapter 4

Kinematic Analysis

4.1 Introduction

In the previous two chapters, a formulation was developed which can be employed to generate N independent dynamical equations of motion of the system S which has N DOFs and P simple nonholonomic constraints. In this chapter we complete the formalism by presenting the kinematic analysis of the system. Considering that any unconstrained motion can be modeled as a special case of constrained motion with zero constraints ($P = 0$), we may just focus on completing the formulation for constrained systems.

To solve for the $2N + P$ independent variables of the system S ($u_1,\ldots,u_N$ and $q_1,\ldots,q_{N-P}$), we need $N + P$ independent equations in addition to the N dynamical equations. Besides, the dynamical equations are functions of some kinematical terms which need to be calculated. The calculation of these terms, specially in the case of multibody systems, is an important part of the procedure of developing the equations of motion and has a great impact on the performance of the resultant equations of motion.

In this chapter, we first present the kinematical differential equations of the system, which provides the $N + P$ additional equations necessary to complete the set of $2N + P$

equations which describes the motion of the system. Then, a recursive formulation for calculation of the kinematical terms involved in the dynamical equations of motion is presented.

4.2 Kinematical Differential Equations

The differential kinematical equations of motion relate the time derivatives of the generalized coordinates to the generalized speeds of the system. These equations, for the constrained system S, can be found using the definition of the generalized speeds, $\mathbf{u} = \mathbf{Y}(\mathbf{q},t)\,\dot{\mathbf{q}} + \mathbf{Z}(\mathbf{q},t)$, and solving them for $\dot{\mathbf{q}}$ as follows:

$$\dot{q}_r = \sum_{s=1}^{N+P} W_{rs}(\mathbf{q},t)\,u_s + X_r(\mathbf{q},t), \quad r = 1,\ldots,N+P. \tag{4.1}$$

The kinematical equations can also be expressed in terms of independent generalized speeds. To this end, we recall the constraint equations, Eq.(3.1), which can be rewritten in an explicit form as

$$[\mathbf{u}_2]_P = [\mathbf{A}(\mathbf{q},t)]_{P\times N}\,[\mathbf{u}_1]_N + [\mathbf{B}(\mathbf{q},t)]_P. \tag{4.2}$$

The dependent generalized speeds, $\mathbf{u}_2$, can be substituted from Eq.(4.2) into Eq.(4.1) which yields

$$\dot{q}_r = \sum_{s=1}^{N} \tilde{W}_{rs}(\mathbf{q},t)\,u_s + \tilde{X}_r(\mathbf{q},t), \quad r = 1,\ldots,N+P, \tag{4.3}$$

where

$$\begin{aligned} \tilde{W}_{rs} &= W_{rs} + \sum_{k=1}^{P} W_{r(N+k)}\,A_{ks}, \quad r = 1,\ldots,N+P \ , \ s = 1,\ldots,N, \\ \tilde{X}_r &= X_r + \sum_{k=1}^{P} W_{r(N+k)}\,B_k, \quad r = 1,\ldots,N+P. \end{aligned} \tag{4.4}$$

Equations (4.3) and (3.28) form a set of $2N+P$ ordinary differential equations which can be solved to give the $2N+P$ unknowns of the system, $u_1,\ldots,u_N$ and $q_1,\ldots,q_{N+P}$.

4.3 Modified Recursive Method.

The equations of motion, presented in the previous chapter, are functions of the following kinematical terms: ω^B, $\tilde{\omega}_r^B, \tilde{\omega}_r^B, \tilde{\alpha}_t^B, \tilde{V}_r^b, \tilde{V}_r^b$ and $\tilde{a}_t^b$. In multibody systems the calculation of these terms for each body needs a lot of computational effort, most of which might have been repeated in the calculations related to the previous member in the chain. This is why utilizing a recursive method seems helpful in reducing the amount of kinematical calculations. In contrast to the usual recursive method, used widely in previous works, which uses the kinematical terms of the parent body, a *modified recursive method* is presented which is based on the usage of an *auxiliary frame* with known kinematical properties calculated in the previous step. This method offers a greater flexibility compared with the usual recursive method. As the auxiliary frame, one can choose the parent body-frame (the usual recursive method), the inertia frame or any other frame which suits the problem the best.

To show how the method works, we consider a frame B, i.e., a frame attached to a rigid body B (Figure 4.1) which is assumed to be part of the system S with N DOFs, and P simple nonholonomic constraints, defined as in Eq.(4.2). In addition to the frame B, we also consider an auxiliary frame A whose motion is assumed to be known; points b and a are, respectively, the origins of the frames B and A.

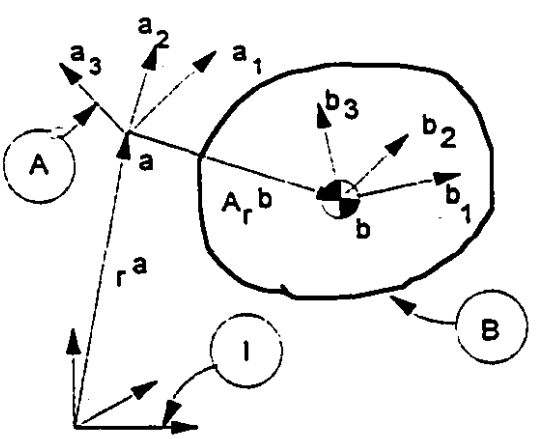

Figure 4.1 Relative configuration of a frame B and an auxiliary frame A in the inertial frame

The purpose is to calculate $\boldsymbol{\omega}^B, \tilde{\boldsymbol{\omega}}_r^B, \tilde{\tilde{\boldsymbol{\omega}}}_r^B, \tilde{\boldsymbol{\alpha}}_t^B$ (i.e., the angular velocity, the r-th nonholonomic and modified nonholonomic partial angular velocity, and the nonholonomic remainder of the angular acceleration of the frame B in the inertial frame), and $\tilde{\mathbf{V}}_r^b, \tilde{\tilde{\mathbf{V}}}_r^b, \tilde{\mathbf{a}}_t^b$ (i.e., the r-th nonholonomic and modified nonholonomic partial velocity, and the nonholonomic remainder of the acceleration of point b in the inertial frame), using the known kinematics of the auxiliary frame A. To this end, we may start with the following basic relations of relative motion:

$$\boldsymbol{\omega}^B = ({}^A\mathbf{C}^B)^T \boldsymbol{\omega}^A + {}^A\boldsymbol{\omega}^B, \tag{4.5}$$

$$\boldsymbol{\alpha}^B = ({}^A\dot{\mathbf{C}}^B)^T \boldsymbol{\omega}^A + ({}^A\mathbf{C}^B)^T \boldsymbol{\alpha}^A + {}^A\boldsymbol{\alpha}^B, \tag{4.6}$$

$$\mathbf{V}^b = \mathbf{V}^a + \mathbf{C}^A(\boldsymbol{\omega}^A \times {}^A\mathbf{r}^b + {}^A\mathbf{V}^b), \tag{4.7}$$

$$\mathbf{a}^b = \mathbf{a}^a + \dot{\mathbf{C}}^A(\boldsymbol{\omega}^A \times {}^A\mathbf{r}^b + 2\,{}^A\mathbf{V}^b) + \mathbf{C}^A(\boldsymbol{\alpha}^A \times {}^A\mathbf{r}^b + {}^A\mathbf{a}^b). \tag{4.8}$$

In above relations, ${}^A\mathbf{C}^B$ is the rotation matrix of frame B in frame A, defined by ${}^AC_{ij}^B = \bar{\mathbf{a}}_i \cdot \bar{\mathbf{b}}_j$, and ${}^A\mathbf{r}^b$ denotes the array of the components of the position vector of the point b in frame A. Similarly, $\mathbf{C}^A$, the rotation matrix of frame A in the inertial frame, is defined as $C_{ij}^A = \bar{\mathbf{I}}_i \cdot \bar{\mathbf{a}}_j$.

To obtain a recursive formulation for $\tilde{\boldsymbol{\omega}}_r^B$, the r-th nonholonomic partial angular velocity of B in the inertial frame, let us start with the following definition (Kane and Levinson [1985])

$$\boldsymbol{\omega}^B = \sum_{r=1}^{N} \tilde{\boldsymbol{\omega}}_r^B u_r + \tilde{\boldsymbol{\omega}}_t^B, \tag{4.9}$$

in which $\tilde{\boldsymbol{\omega}}_t^B$ is the part of $\boldsymbol{\omega}^B$ which is independent of generalized speeds. Expanding the right hand side of Eq.(4.5), using Eq.(4.9), and collecting the coefficients of generalized speeds, one can rewrite Eq.(4.5) as:

$$\boldsymbol{\omega}^B = \sum_{r=1}^{N} \left[({}^A\mathbf{C}^B)^T \tilde{\boldsymbol{\omega}}_r^A + {}^A\tilde{\boldsymbol{\omega}}_r^B \right] u_r + \sum_{r=1}^{N} \left[({}^A\mathbf{C}^B)^T \tilde{\boldsymbol{\omega}}_t^A + {}^A\tilde{\boldsymbol{\omega}}_t^B \right]. \tag{4.10}$$

The r-th nonholonomic partial angular velocity of frame B in inertial frame, $\tilde{\boldsymbol{\omega}}_r^B$, can be easily found by inspection from Eq.(4.10) to be

$$\tilde{\omega}_r^B = ({}^A\mathbf{C}^B)^T \tilde{\omega}_r^A - {}^A\tilde{\omega}_r^B, \quad r = 1,\ldots,N. \tag{4.11}$$

A similar relation can be established for the r-th holonomic partial angular velocity, which is needed in calculation of $\tilde{\tilde{\omega}}_r^B$, by expanding angular velocities in terms of all generalized speeds as follows:

$$\omega = \sum_{r=1}^{N+P} \omega_r u_r + \omega_t, \tag{4.12}$$

which results in

$$\omega_r^B = ({}^A\mathbf{C}^B)^T \omega_r^A + {}^A\omega_r^B, \quad r = 1,\ldots,N+P. \tag{4.13}$$

To obtain the relation for $\tilde{\tilde{\omega}}_r^B$, let us recall its definition

$$\tilde{\tilde{\omega}}_r^B = \tilde{\omega}_r^B - \sum_{s=1}^{P} E_{rs}\, \omega_{s+N}^B, \quad r = 1,\ldots,N. \tag{4.14}$$

Substituting for $\tilde{\omega}_r^B$ and ω_{s+N}^B from Eqs.(4.11) and (4.13) into Eq.(4.14), while collecting similar terms, one obtains

$$\tilde{\tilde{\omega}}_r^B = ({}^A\mathbf{C}^B)^T \left[\tilde{\omega}_r^A - \sum_{s=1}^{P} E_{rs}\, \omega_{s+N}^A\right] + \left[{}^A\tilde{\omega}_r^B - \sum_{s=1}^{P} E_{rs}\, {}^A\omega_{s+N}^B\right], \quad r = 1,\ldots,N, \tag{4.15}$$

which is equivalent to

$$\tilde{\tilde{\omega}}_r^B = ({}^A\mathbf{C}^B)^T\, \tilde{\tilde{\omega}}_r^A + {}^A\tilde{\tilde{\omega}}_r^B, \quad r = 1,\ldots,N. \tag{4.16}$$

Starting from Eqs.(4.6-4.8) and using a similar approach, one can develop the following recursive formulas for $\tilde{\alpha}_t^B$, $\tilde{\mathbf{V}}_r^b$, $\tilde{\tilde{\mathbf{V}}}_r^b$, and $\tilde{\mathbf{a}}_t^b$

$$\tilde{\alpha}_t^B = ({}^A\dot{\mathbf{C}}^B)^T \omega^A + ({}^A\mathbf{C}^B)^T \tilde{\alpha}_t^A + {}^A\tilde{\alpha}_t^B, \tag{4.17}$$

$$\tilde{\mathbf{V}}_r^b = \tilde{\mathbf{V}}_r^a + \mathbf{C}^A(\tilde{\omega}_r^A \times {}^A\mathbf{r}^b + {}^A\tilde{\mathbf{V}}_r^b), \quad r = 1,\ldots,N, \tag{4.18}$$

$$\tilde{\tilde{\mathbf{V}}}_r^b = \tilde{\tilde{\mathbf{V}}}_r^a + \mathbf{C}^A(\tilde{\tilde{\omega}}_r^A \times {}^A\mathbf{r}^b + {}^A\tilde{\tilde{\mathbf{V}}}_r^b), \quad r = 1,\ldots,N, \tag{4.19}$$

$$\tilde{\mathbf{a}}_t^b = \tilde{\mathbf{a}}_t^a + \dot{\mathbf{C}}^A(\omega^A \times {}^A\mathbf{r}^b + 2\,{}^A\mathbf{V}^b) + \mathbf{C}^A(\tilde{\alpha}_t^A \times {}^A\mathbf{r}^b + {}^A\tilde{\mathbf{a}}_t^b). \tag{4.20}$$

In the above relations two categories of terms can be identified as follows :

1. Terms which depend on both frames A and B, i.e., ${}^{A}\mathbf{r}^{b}$, ${}^{A}\mathbf{C}^{B}$, ${}^{A}\tilde{\mathbf{V}}_{r}^{b}$, ${}^{A}\tilde{\bar{\mathbf{V}}}_{r}^{b}$, ${}^{A}\tilde{\mathbf{a}}_{t}^{b}$, ${}^{A}\boldsymbol{\omega}^{B}$, ${}^{A}\tilde{\boldsymbol{\omega}}_{r}^{B}$, ${}^{A}\tilde{\boldsymbol{\alpha}}_{t}^{B}$ and ${}^{A}\dot{\mathbf{C}}^{B}$.

2. Terms which depend only on the choice of the auxiliary frame, i.e. $\tilde{\mathbf{V}}_{r}^{A}$, $\tilde{\bar{\mathbf{V}}}_{r}^{A}$, $\tilde{\mathbf{a}}_{t}^{A}$, $\boldsymbol{\omega}^{A}$, $\tilde{\boldsymbol{\omega}}_{r}^{A}$, $\tilde{\bar{\boldsymbol{\omega}}}_{r}^{A}$, $\tilde{\boldsymbol{\alpha}}_{t}^{A}$, $\mathbf{C}^{A}$, and $\dot{\mathbf{C}}^{A}$. These terms are assumed to be known from the previous step.

From the first category of terms, ${}^{A}\mathbf{r}^{b}$ and ${}^{A}\mathbf{C}^{B}$, which physically determine the position and orientation of B in A, must be introduced as inputs to the formalism, while the others must be calculated. Adopting ${}^{A}\mathbf{C}^{B}$ as the required input to the formalism, provides a flexibility over using different sets of orientation parameters (e.g., different sets of Euler angles, Euler parameters). The computer code, FLXSIM, provides several subroutines to compute the rotation matrix based on the given orientation parameters.

Knowing ${}^{A}\mathbf{R}^{b}$ and ${}^{A}\mathbf{C}^{B}$, one can calculate ${}^{A}\mathbf{V}^{b}$, ${}^{A}\mathbf{a}^{b}$, ${}^{A}\boldsymbol{\omega}^{B}$, ${}^{A}\boldsymbol{\alpha}^{B}$ as

$$ {}^{A}V_{t}^{B} = {}^{A}\dot{r}_{t}^{B}, \tag{4.21} $$

$$ {}^{A}a_{t}^{B} = {}^{A}\dot{V}_{t}^{B}, \tag{4.22} $$

$$ {}^{A}\omega_{t}^{B} = {}^{A}\bar{\omega}^{B}\cdot\bar{\mathbf{b}}_{t} = -\frac{1}{2}\sum_{j=1}^{3}\sum_{k=1}^{3}\varepsilon_{ijk}\,{}^{A}C_{ik}^{B}\,{}^{A}\dot{C}_{ij}^{B}, \tag{4.23} $$

$$ {}^{A}\alpha_{t}^{B} = {}^{A}\dot{\omega}_{t}^{B}, \tag{4.24} $$

in which ε_{ijk} is the permutation symbol. It is worth mentioning that in the above relations the time derivatives are frame independent, for ${}^{A}r_{t}^{b}$, ${}^{A}V_{t}^{b}$, and ${}^{A}\omega_{t}^{B}$ are scalars –components of vectors. Using the definition of nonholonomic partial velocities and remainder of acceleration, one can find them by inspection from the above relations or calculate them as follows:

$$ {}^{A}\mathbf{V}_{r}^{b} = \partial[{}^{A}\mathbf{V}^{b}(\mathbf{q},\mathbf{u},t)]/\partial u_{r}, \quad r = 1,\ldots,N+P, \tag{4.25} $$

$$ {}^{A}\tilde{\bar{\mathbf{V}}}_{r}^{b} = {}^{A}\mathbf{V}_{r}^{b} + \sum_{s=1}^{P} A_{sr}\,{}^{A}\mathbf{V}_{s+N}^{b}, \quad r = 1,\ldots,N, \tag{4.26} $$

$$ {}^{A}\tilde{\mathbf{V}}_{t}^{b} = {}^{A}\mathbf{V}^{b} - \sum_{r=1}^{N} {}^{A}\tilde{\mathbf{V}}_{r}^{b}\,u_{r}, \tag{4.27} $$

$$ {}^{A}\tilde{\mathbf{a}}_t^b = \sum_{r=1}^{N} {}^{A}\dot{\tilde{\mathbf{V}}}_r^b u_r + {}^{A}\dot{\tilde{\mathbf{V}}}_t^b . \tag{4.28} $$

$$ {}^{A}\boldsymbol{\omega}_r^B = \partial[{}^{A}\boldsymbol{\omega}^B(\mathbf{q},\mathbf{u},t)]/\partial u_r , \quad r = 1,\ldots,N+P. \tag{4.29} $$

$$ {}^{A}\tilde{\boldsymbol{\omega}}_r^B = {}^{A}\boldsymbol{\omega}_r^B + \sum_{s=1}^{P} A_{sr}\, {}^{A}\boldsymbol{\omega}_{s+N}^b , \quad r = 1,\ldots,N. \tag{4.30} $$

$$ {}^{A}\tilde{\boldsymbol{\omega}}_t^B = {}^{A}\boldsymbol{\omega}^B - \sum_{r=1}^{N} {}^{A}\boldsymbol{\omega}_r^b u_r , \tag{4.31} $$

$$ {}^{A}\tilde{\boldsymbol{\alpha}}_t^B = \sum_{r=1}^{N} {}^{A}\dot{\tilde{\boldsymbol{\omega}}}_r^B u_r + {}^{A}\dot{\tilde{\boldsymbol{\omega}}}_t^B . \tag{4.32} $$

On the other hand, the modified nonholonomic partial velocities can be found, using their definitions (equations (3.22) and (3.34))

$$ {}^{A}\tilde{\tilde{\mathbf{V}}}_r^b = {}^{A}\tilde{\mathbf{V}}_r^b - \sum_{s=1}^{P} E_{sr}\, {}^{A}\mathbf{V}_{s+N}^b , \quad r = 1,\ldots,N \tag{4.33} $$

$$ {}^{A}\tilde{\tilde{\boldsymbol{\omega}}}_r^B = {}^{A}\tilde{\boldsymbol{\omega}}_r^B - \sum_{s=1}^{P} E_{sr}\, {}^{A}\boldsymbol{\omega}_{s+N}^b , \quad r = 1,\ldots,N \tag{4.34} $$

The second category of terms - i.e., $\tilde{\mathbf{V}}_r^a, \tilde{\tilde{\mathbf{V}}}_r^a, \tilde{\mathbf{a}}_t^a, \boldsymbol{\omega}^A, \tilde{\boldsymbol{\omega}}_r^A, \tilde{\tilde{\boldsymbol{\omega}}}_r^A, \tilde{\boldsymbol{\alpha}}_t^A, \mathbf{C}^A$, and $\dot{\mathbf{C}}^A$ - can be calculated, simply, by substituting frame B in the above relation with the new auxiliary frame A'. This means to provide ${}^{A}\mathbf{r}^{A'}$ and, ${}^{A}\mathbf{C}^{A'}$ and to carry out similar calculations as above. The last point to mention is that the kinematical properties of the first auxiliary frame must be provided as the input to the formalism. Obviously, the inertia frame can serve as the first auxiliary frame to remove the burden of providing complicated relations.

Chapter 5

The Effect of Nonlinear Coupling Between Elastic and Rigid-Body Motions

5.1 Introduction

The effect of rigid-body base motion on the dynamic response of a flexible system was briefly addressed in Chapter 2, in the dynamic analysis of beams and plates. This chapter presents a detailed discussion of this subject.

For quite some time, researchers have recognized that the stiffness of an elastic beam, whose base is undergoing fast rotation around an axis normal to its center-line, increases with a rate proportional to the square of the angular velocity of rotation. This possibly was the reason why the phenomenon was called geometric or dynamic *stiffening*. In contrast to the experimental observations, the equations of motion obtained by the conventional approaches predict the beam to become softer. This contradiction was a reason for the researchers to look for the shortcomings of the conventional dynamic modeling and to find a way to compensate for the missing stiffness.

Some researchers attribute the source of this defect to the truncation of the strain energy expression in linear theory; therefore, they suggest retention of the nonlinear terms up to the third-order of elastic generalized coordinates in the strain energy expression. The second group considers the centrifugal field as an external, *pseudo-potential field* and finds the stiffness due to this field and adds it to the stiffness obtained from the linear elastic strain energy. The third group believes that the missing stiffness is due to premature linearization. The terms "premature linearization" and "improper linearization," which are interchangeably used in this thesis, refer to a linearization which is started prior to the calculation of partial derivatives in the process of deriving the equations of motion by an energy-based method. For instance, any linearization done prior to the calculation of partial velocities in Kane's method, or partial derivatives of kinetic and potential energy expressions in Lagrange's method, would be premature. This group suggests to retain up to the *second order terms of the elastic generalized coordinates* in the expressions for elastic deflections to avoid improper linearization. There is still some debate as to which approach is the best.

In this chapter, we first show that premature linearization may lead to the loss of some linear terms in the equations of motion that are generated using an energy-based method (e.g., Lagrange's or Kane's method). To this end, a general formulation of the equations of motion, based on Kane's equations, for a system that undergoes both rigid body motion and elastic motion, is presented. Both properly and prematurely linearized equations of motion are obtained and compared to learn which terms are lost in the equations of motion and where. Then, different remedies for compensating for the missing terms are compared. A method based on the nonlinear strain-displacement theory is presented afterward, which can be employed to derive the correct equations of motion of a general elastic system undergoing a general rigid body motion. A systematic procedure is introduced which can be used to specialize the method for different elastic media. The specialization of this method for beams and plates is given. Finally, the problem of an orbiting satellite with long flexible appendages

along with some other illustrative examples are solved using the presented theory. The examples show some interesting phenomena such as softening of a flexible beam due to its rigid-body base motion, or missing some terms from mass matrix due to improper linearization.

5.2 Improper Linearization, the Source of Error

In this section, we first explain, through a simple example, how the equations of motion might lose some terms as a result of improper linearization, and how it can be prevented. Then, a general formulation is given to identify which terms will be missing from the equations of motion, obtained by conventional methods, for elastic systems undergoing rigid body motion in a general case.

5.2.1 A simple example

Consider a hinged rigid bar, shown in Figure 5.1, which undergoes small oscillations around its equilibrium position in the vertical plane. The goal is to generate *the linear form of the equation of motion, using an energy-based method*. The position vector of an element of the bar can be written as (see Figure 5.1)

$$\mathbf{r} = x\cos(q)\mathbf{i} + x\sin(q)\mathbf{j}, \tag{5.1}$$

or, for small q,

$$\mathbf{r} \cong x\,\mathbf{i} + xq\,\mathbf{j}, \tag{5.2}$$

which is correct up to the first order. Using this *linearized* position vector, Eq.(5.2), one can find the kinetic energy and potential energy of the system as $T = ml^2\dot{q}^2/6$ and $V = -mgl/2$. Substituting these energy expressions in Lagrange's equation results in the following equation

$$(ml^2/3)\ddot{q} = 0. \tag{5.3}$$

One can readily see that the restoring term due to the gravity is absent in the prematurely linearized equation of motion of the pendulum, Eq.(5.3). This is exactly what happens when a

conventional method is employed to generate the equations of motion using energy-based methods. The conventional methods consider the position vector of an element of the elastic body as a linear combination of the elastic generalized coordinates, which is clearly a premature linearization.

To correct the above error, in the case of the simple pendulum, we might use either the nonlinear expression for position vector, Eq.(5.1), or the approximation of that correct up to the *second order*, Eq. (5.4), as follows

$$\mathbf{r} \cong x(1-q^2/2)\mathbf{i} + xq\,\mathbf{j}. \tag{5.4}$$

Using the *second-order* position vector, Eq.(5.4), we can develop the kinetic and potential energy as $T = ml^2\dot{q}^2/6$ and $V = -mgl(1-q^2/2)/2$, and consequently, the equation of motion as

$$(ml^2/3)\ddot{q} + (mgl/2)q = 0. \tag{5.5}$$

This *properly linearized* equation of motion is in total agreement with the results that can be obtained from linearizing the nonlinear equation of motion obtained by starting from Eq.(5.1).

In the case of elastic members, however, a complete nonlinear expression for the elastic deflections may not be achievable, but an expression correct up to the second order can be written using the nonlinear strain-displacement theory. This simple example reveals that the phenomenon of missing terms is not confined to the analysis of elastic systems. In other words, any set of prematurely linearized equations might suffer from the same defect.

5.2.2 General formulation

At this point, we present a general formulation, based on Kane's method, to identify the terms which might be omitted, due to premature linearization, in the equations of motion of a system with both zero-order and first-order DOFs (e.g., an elastic system undergoing rigid-

body motion). To this end, the partially-linearized equations of motion for the system are derived first by linearizing the nonlinear equations (proper linearization) and then by starting the linearization prior to the calculation of partial velocities (premature linearization). The comparison of these two sets of equations reveals the missing terms and their places in the equations of motion. Here, the terms "zero-order" and "first-order" refer to the quantities of the order of ε^0 and ε^1, respectively, where $\varepsilon^1 << \varepsilon^0$. For instance, the rigid-body motion is $O(\varepsilon^0)$, while the elastic motion is $O(\varepsilon^1)$. Besides, by "partially-linearized equations" we mean a set of equations which are linear functions of the first-order DOFs but nonlinear functions of the zero-order DOFs.

Before starting the discussion, it is useful to recall some of the conventions which are used in this chapter. Overhead symbols '^', '‾', and '~' are used to indicate, respectively, the linearized form, the nominal value, and the small deviation from the nominal value of the corresponding quantity. For instance, $\hat{\mathbf{V}} = \overline{\mathbf{V}} + \tilde{\mathbf{V}}$ indicates that the linearized velocity equals the nominal value $\overline{\mathbf{V}}$ plus the small deviation $\tilde{\mathbf{V}}$. Also, the prematurely linearized items and the terms associated with them are identified by an asterix, e.g., $\hat{\mathbf{V}}_r^*$ is the prematurely linearized r-th partial velocity.

Consider a system $\mathcal{S}$ consisting of ν particles with N degrees of freedom. The system can be identified by the definition of $2N$ scalars as follows: $q_1,\ldots,q_N$, the generalized coordinates, and $u_1,\ldots,u_N$, the generalized speeds. Assume that the first N_E generalized coordinates and generalized speeds are small compared to the others. The *nonlinear* equations of motion for this system, using Kane's method can be written as

$$\sum_{i=1}^{\nu} \mathbf{V}_r^i \cdot (\mathbf{R}^i - m^i \mathbf{a}^i) = 0, \tag{5.6}$$

where $\mathbf{V}_r^i$ is the r-th partial velocity of the particle p^i in the inertial frame, defined as $\partial \mathbf{V}^i / \partial u_r$, $\mathbf{R}^i$ represents the resultant contributing active forces acting on p^i, and m^i and $\mathbf{a}^i$ are the mass and acceleration of p^i, respectively.

The linearized form of $\mathbf{V}_r^i$, $\mathbf{R}^i$, and $\mathbf{a}^i$ can be written as

$$\hat{\mathbf{V}}_r^i = \overline{\mathbf{V}}_r^i + \breve{\mathbf{V}}_r^i, \quad r = 1,\ldots,N, \tag{5.7.a}$$

$$\hat{\mathbf{R}}^i = \overline{\mathbf{R}}^i + \breve{\mathbf{R}}^i, \tag{5.7.b}$$

$$\hat{\mathbf{a}}^i = \overline{\mathbf{a}}^i + \breve{\mathbf{a}}^i. \tag{5.7.c}$$

The equations of motion, Eq.(5.6), can be linearized by substituting the linearized form of $\mathbf{V}_r^i$, $\mathbf{R}^i$, and $\mathbf{a}^i$, Eqs.(5.7), and neglecting the second-order terms. This yields the properly linearized equations of motion as

$$\sum_{i=1}^{\nu} \overline{\mathbf{V}}_r^i \cdot (\overline{\mathbf{R}}^i - m^i \overline{\mathbf{a}}^i) + \sum_{i=1}^{\nu} \left[\overline{\mathbf{V}}_r^i \cdot (\breve{\mathbf{R}}^i - m^i \breve{\mathbf{a}}^i) + \breve{\mathbf{V}}_r^i \cdot (\overline{\mathbf{R}}^i - m^i \overline{\mathbf{a}}^i) \right] = 0, \quad r = 1,\ldots,N \tag{5.8}$$

In the above relation the first summation contains the zero-order terms, and the second summation contains the first-order terms of the linearized equations of motion. Each of these two parts can be equated to zero separately. The zero-order equations of motion are suitable for calculation of the nominal motion of the system. The first order equations are suitable for linear analysis such as linear control and stability analysis. The partially linearized form of the equations of motion, Eq.(5.8), is specially important for the purpose of simulation of elastic systems with zero-order degrees of freedom.

We get the prematurely linearized equations of motion by starting the linearization prior to the calculation of partial velocities. The general linearized form of the velocity expression is

$$\hat{\mathbf{V}}^i = \sum_{r=1}^{N_g} \overline{\mathbf{V}}_r^i u_r + \sum_{r=N_g+1}^{N} (\overline{\mathbf{V}}_r^i + \breve{\mathbf{V}}_r^i) u_r + \hat{\mathbf{V}}_t^{*i}, \tag{5.9}$$

where $\hat{\mathbf{V}}_r^{*i}$ is the part of $\hat{\mathbf{V}}^i$ that does not depend on the generalized speeds. Note that since $u_1,\ldots,u_{N_E}$ are of the first order, the $\bar{\mathbf{V}}_1^i,\ldots,\bar{\mathbf{V}}_{N_E}^i$ do not remain in the linearized velocity expression. The partial velocities of the system in this case are

$$\hat{\mathbf{V}}_r^{*i} = \begin{cases} \bar{\mathbf{V}}_r^i & r = 1,\cdots,N_E, \\ \hat{\mathbf{V}}_r^i = \bar{\mathbf{V}}_r^i + \tilde{\mathbf{V}}_r^i & r = N_E+1,\ldots,N, \end{cases} \tag{5.10}$$

which are already linear. However, the first N_E of them are different from those obtained by proper linearization (see Eq.(5.7.a)), i.e., linearization after the calculation of partial velocities. Premature linearization, thus, causes loss of the first-order terms of the partial velocities associated with the linear generalized speeds, $u_1,\ldots,u_{N_E}$.

The equations of motion with premature linearization are now

$$\sum_{i=1}^{\nu} \hat{\mathbf{V}}_r^{*i} \cdot (\mathbf{R}^i - m^i \hat{\mathbf{a}}^{*i}) = 0. \tag{5.11}$$

Considering the fact that differentiation with respect to time and linearization with respect to the generalized coordinates, generalized speeds, and input forces are commutative, we can write

$$\hat{\mathbf{a}}^{*i} = \dot{\hat{\mathbf{V}}}^i = \hat{\dot{\mathbf{V}}}^i = \hat{\mathbf{a}}^i = \bar{\mathbf{a}}^i + \tilde{\mathbf{a}}^i. \tag{5.12}$$

Substituting for $\hat{\mathbf{V}}_r^{*i}$ and $\hat{\mathbf{a}}^{*i}$ from Eqs.(5.10) and (5.12) into Eq.(5.11) and neglecting the second order terms, one gets the prematurely linearized equations of motion (which, in general, do not represent the correct equations of motion) as follows :

$$\sum_{i=1}^{\nu} \bar{\mathbf{V}}_r^i \cdot (\bar{\mathbf{R}}^i - m^i \bar{\mathbf{a}}^i) + \sum_{i=1}^{\nu} \tilde{\mathbf{V}}_r^i \cdot (\bar{\mathbf{R}}^i - m^i \bar{\mathbf{a}}^i) = 0 \quad r = 1,\ldots,N_E \tag{5.13.a}$$

$$\sum_{i=1}^{\nu} \bar{\mathbf{V}}_r^i \cdot (\bar{\mathbf{R}}^i - m^i \bar{\mathbf{a}}^i) + \sum_{i=1}^{\nu} \left[\bar{\mathbf{V}}_r^i \cdot (\tilde{\mathbf{R}}^i - m^i \tilde{\mathbf{a}}^i) + \tilde{\mathbf{V}}_r^i \cdot (\bar{\mathbf{R}}^i - m^i \bar{\mathbf{a}}^i) \right] = 0, \quad r = N_E+1,\ldots,N \tag{5.13.b}$$

Comparison of Eqs.(5.13) with Eq. (5.8) reveals that

- Premature linearization has no effect on the zero-order part of the equations of motion (first summation in the equations), as expected.
- Premature linearization has no effect on the equations of motion associated with the zero-order DOFs (rigid-body motion), $r = N_E + 1,\ldots,N$.
- Due to premature linearization, the equations of motion associated with the first-order DOFs, $r = 1,\ldots,N_E$, lose the following first order terms represented by $\mathcal{E}$:

$$\mathcal{E}_r = \sum_{i=1}^{\nu}\left[\tilde{\mathbf{V}}_r^i \cdot (\overline{\mathbf{R}}^i - m^i\,\overline{\mathbf{a}}^i)\right] \quad r = 1,\ldots,N_E. \tag{5.14}$$

Equations (5.9) and (5.10) suggest that to avoid premature linearization it is adequate to retain up to the second order terms in the expression for velocity. However, if premature linearization has already been done, then the equations can be corrected by adding the missing part given by Eq. (5.14) to them. This suggests another approach to generate the correct equations of motion: first, generate the prematurely linearized form of the equations, using conventional theories; then, generate the equations of motion for a similar system, which is moving only with second-order velocities under the action of a zero-order force field equal to the difference of the zero-order contributing active forces and inertia forces; then, add the two sets of equations.

Equations (5.8) and (5.13) can be used to generate the standard form of the equations of motion. Differentiation of Eq. (5.9) with respect to time gives

$$\hat{\mathbf{a}}^i = \sum_{s=1}^{N_E} \overline{\mathbf{V}}_s^i \dot{u}_s + \sum_{s=N_E+1}^{N} \hat{\mathbf{V}}_s^i \dot{u}_s + \hat{\mathbf{a}}_t^i\,, \tag{5.15}$$

in which $\hat{\mathbf{a}}_t^i$, the remainder of acceleration, is the portion of acceleration that is independent of time derivatives of the generalized speeds. Equation (5.15) can be equivalently written as:

$$\begin{aligned}\bar{\mathbf{a}}^i &= \sum_{s=N_E+1}^{N} \bar{\mathbf{V}}_s^i \dot{u}_s + \bar{\mathbf{a}}_t^i, \\ \bar{\mathbf{a}}^i &= \sum_{s=1}^{N_E} \bar{\mathbf{V}}_s^i \dot{u}_s + \sum_{s=N_E+1}^{N} \bar{\mathbf{V}}_s^i \dot{u}_s + \bar{\mathbf{a}}_t^i,\end{aligned} \tag{5.16}$$

Substituting Eq.(5.16) into Eq.(5.8) and collecting the coefficient of $\dot{u}_s$, one can rewrite Eq.(5.8), the set of properly linearized equations of motion, as

$$\mathbf{M}\,\dot{\mathbf{u}} = \mathbf{f} \tag{5.17.a}$$

where

$$M_{rs} = \begin{cases} \sum_{i=1}^{v} m^i \bar{\mathbf{V}}_r^i \cdot \bar{\mathbf{V}}_s^i, & r = 1,\ldots,N,\ s = 1,\ldots,N_E \\ \sum_{i=1}^{v} m^i \left[\bar{\mathbf{V}}_r^i \cdot \hat{\mathbf{V}}_s^i + \hat{\mathbf{V}}_r^i \cdot \bar{\mathbf{V}}_s^i \right], & r = 1,\ldots,N,\ s = N_E+1,\ldots,N \end{cases} \tag{5.17.b}$$

$$f_r = \sum_{i=1}^{v} \left[\bar{\mathbf{V}}_r^i \cdot (\hat{\mathbf{R}}^i - m^i \hat{\mathbf{a}}_t^i) + \hat{\mathbf{V}}_r^i \cdot (\bar{\mathbf{R}}^i - m^i \bar{\mathbf{a}}_t^i) \right], \quad r = 1,\ldots,N. \tag{5.17.c}$$

On the other hand, substitution of Eq.(5.16) in Eqs.(5.13) yields the prematurely linearized form of equations as

$$\mathbf{M}^* \dot{\mathbf{u}} = \mathbf{f}^* \tag{5.18.a}$$

where

$$M_{rs}^* = \begin{cases} \sum_{i=1}^{v} m^i \bar{\mathbf{V}}_r^i \cdot \bar{\mathbf{V}}_s^i, & r = 1,\ldots,N,\ s = 1,\ldots,N_E \\ \sum_{i=1}^{v} m^i \bar{\mathbf{V}}_r^i \cdot \hat{\mathbf{V}}_s^i, & r = 1,\ldots,N_E,\ s = N_E+1,\ldots,N \\ \sum_{i=1}^{v} m^i \left[\bar{\mathbf{V}}_r^i \cdot \hat{\mathbf{V}}_s^i + \hat{\mathbf{V}}_r^i \cdot \bar{\mathbf{V}}_s^i \right], & r = N_E+1,\ldots,N,\ s = N_E+1,\ldots,N \end{cases} \tag{5.18.b}$$

$$f_r^* = \begin{cases} \sum_{i=1}^{v} \bar{\mathbf{V}}_r^i \cdot (\hat{\mathbf{R}}^i - m^i \hat{\mathbf{a}}_t^i), & r = 1,\ldots,N_E \\ \sum_{i=1}^{v} \left[\bar{\mathbf{V}}_r^i \cdot (\hat{\mathbf{R}}^i - m^i \hat{\mathbf{a}}_t^i) + \hat{\mathbf{V}}_r^i \cdot (\bar{\mathbf{R}}^i - m^i \bar{\mathbf{a}}_t^i) \right], & r = N_E+1,\ldots,N \end{cases} \tag{5.18.c}$$

The equations of motion can be partitioned as

$$\begin{bmatrix} \mathbf{M}^{EE} & \mathbf{M}^{ER} \\ \mathbf{M}^{RE} & \mathbf{M}^{RR} \end{bmatrix} \begin{bmatrix} \dot{\mathbf{u}}^E \\ \dot{\mathbf{u}}^R \end{bmatrix} = \begin{bmatrix} \mathbf{f}^E \\ \mathbf{f}^R \end{bmatrix}, \tag{5.19}$$

in which the superscripts *E and R* indicate the terms associated with the first-order and zero-order DOFs, respectively. Comparison of Eqs. (5.17) and (5.18) shows that all blocks of the properly linearized equations are equal to their corresponding ones in prematurely linearized equations, except for the following two blocks†

$$\mathbf{M}^{ER} = \mathbf{M}^{*ER} + \left[\sum_{i=1}^{N} m^i \bar{\mathbf{V}}_r^i \cdot \bar{\mathbf{V}}_s^i\right], \quad r = 1,\ldots,N_E, s = N_E+1,\ldots,N \tag{5.20.a}$$

$$\mathbf{f}^E = \mathbf{f}^{*E} + \left[\sum_{i=1}^{N} \bar{\mathbf{V}}_r^i \cdot (\bar{\mathbf{R}}^i - m^i \bar{\mathbf{a}}_t^i)\right] = \mathbf{f}^{*E} + \mathbf{G}\mathbf{q}^E, \quad r = 1,\ldots,N_E \tag{5.20.b}$$

in which $\mathbf{G}$ is a $N_E \times N_E$ matrix whose elements are given by

$$G_{rs} = \sum_{i=1}^{N} \left(\overline{\partial \mathbf{V}_r^i / \partial q_s}\right) \cdot \left(\bar{\mathbf{R}}^i - m^i \bar{\mathbf{a}}_t^i\right) = G_{rs}(\mathbf{q}^R, \mathbf{u}^R, t), \quad r,s = 1,\ldots,N_E. \tag{5.21}$$

where $\mathbf{q}^R$ and $\mathbf{u}^R$ denote the vectors of zero-order generalized coordinates, $q_{N_E+1},\ldots,q_N$, and generalized speeds, $u_{N_E+1},\ldots,u_N$. This matrix becomes a function of time only, or a constant, if all zero-order motions of the system are prescribed (in which case $N_E = N$).

Padilla and von Flotow [1992] suggested that, in addition to the above mentioned blocks, some linear terms might be omitted from the $\mathbf{M}^{RR}$ block due to premature linearization. The above formulation (see also Eq.(5.14)) clearly shows that none of the blocks associated with the rigid-body motion, including $\mathbf{M}^{RR}$, might lose any term due to premature linearization. This is due to the fact that premature linearization has no effect on the partial velocities associated with the zero-order generalized speeds (see Eq.(5.10)).

The following facts can be concluded from Eqs.(5.17) to (5.21):

- In the case of *properly partially linearized* equations of motion, the mass matrix is not symmetric as can be seen in Eqs.(5.17.b).

† The missing terms shown within square brackets in Eqs.(5.20) could be generated directly by substituting Eqs.(5.16) into Eq.(5.14).

- Because the missing terms depend on $\tilde{\mathbf{V}}_r^i$, they are *linear* functions of $q_1, \ldots, q_{N_f}$, the first-order generalized coordinates.
- In the case of completely linearized equations (i.e., all the large motions are prescribed), the generalized force vector is the only part of the equations of motion that might lose some terms. Moreover, in this case, $N = N_g$, and the geometric stiffness matrix is independent of generalized coordinates and speeds.

5.3 Comparison of Different Remedies

In this section the three previously mentioned methods of compensation (see Section 5.1) are compared. The first method, nonlinear strain energy approach, proves to be the weakest, for it compensates for some missing *linear* stiffness terms with *non-linear* ones. The method can produce reasonably good results *only* if the elastic DOFs of the system are selected cautiously. For instance, in the case of beams, to obtain correct results, one *has to* consider at least one DOF for the longitudinal vibrations. This itself has two major difficulties. First, it increases the order of the system, if only the transverse motions are of interest, and second, it introduces some *unwanted high frequencies* due to the longitudinal vibrations, which makes the integration procedure more difficult. In addition to these difficulties, since the method cannot recover the missing terms explicitly, it is not convenient for the cases where the zero-order motion/force is either time or generalized coordinate-dependent. The example presented in Section 5.5.1 helps to shed some light on this discussion.

The second method, pseudo-potential field method, less frequently used for multibody systems, has the potential for correct compensation of the missing stiffness terms, but it is not recommended, because the difficulty of implementing the method grows drastically as the system and its rigid motions become more complicated. Besides, none of the above methods is capable of compensating for the missing terms in the mass matrix, for the elements of mass matrix, usually, are not rendered by a potential energy function. However, an extension of the

second method based on Eq.(5.14), similar to what Banerjee and Dickens [1990] have used, may compensate for missing terms in the mass matrix, although the implementation of this method is difficult in the case of complex multibody systems.

On the other hand, the third method, usually more convenient and rigorous, can be employed to derive the correct and complete form of the linearized equations of motion, which can be used for either linear analysis or nonlinear simulation. The example presented in Section 5.5.1 is devoted to clarify the above discussion. This method will be explained in more detail in the next section.

5.4 A Method for Direct Accommodation of the Missing Terms

5.4.1 General formulation

As suggested in the first section, the use of a nonlinear expression for the velocities, up to second order terms, results in the generation of the equations of motion correct up to the first order. This can be easily accomplished if the small DOFs are not *elastic* DOFs (see the example of the pendulum in the first section). But, in the case of an elastic body, it is not that easy to find the nonlinear expressions for velocities because the true nonlinear expressions for elastic deflections in terms of elastic generalized coordinates are not known.

In general, the elastic deflections (w_1, w_2, and w_3) can be expressed as

$$\mathbf{w} = \mathbf{w}(\mathbf{x}, \mathbf{q}^E) \tag{5.22}$$

where $\mathbf{w}$ denotes the vector of elastic deflections (see Figure 5.2), $\mathbf{q}^E = q_1,\ldots,q_{N_E}$ is the vector of the elastic generalized coordinates, which are functions of time, and $\mathbf{x}$ is the position vector in the undeformed configuration, a spatial variable. Now if the elastic deflections are small enough, one can use a Taylor expansion to express $\mathbf{w}$ as

$$w_i(\mathbf{x},t)=\sum_{j=1}^{N_E}\varphi_{ij}(\mathbf{x})\,q_j+\sum_{j=1}^{N_E}\sum_{k=1}^{N_E}\psi_{ijk}(\mathbf{x})\,q_j\,q_k+\cdots,\qquad i=1,2,3 \tag{5.23}$$

in which φ_{ij} and ψ_{ijk} are functions of the space variables. Conventional methods of discretization, like the assumed-mode method, consider only up to the first order terms of the above Taylor expansion. This might be a good approximation for describing w(x, t) itself, within a chosen domain. However, no matter how small w(x, t) is, we have to keep the second order terms to have the correct form of the equations of motion up to the first order, derived by an energy-based method for a system which undergoes rigid-body motion. Now the question remains as to how to find φ_{ij} and ψ_{ijk}.

In the conventional methods of discretization, φ_{ij}, the mode shapes, are approximated by some shape functions, which must at least satisfy the geometric boundary conditions. Although φ_{ij} can be approximated by any set of shape functions, the accuracy of the results is strongly dependent on how similar the chosen shape functions are to the actual mode shapes. In the same fashion, any set of functions which satisfy the geometric boundary conditions is acceptable as ψ_{ijk}. Similar to the case of φ_{ij}, the better the chosen ψ_{ijk} agrees with the physics of the system, the better the results obtained.

One of the best ways to find consistent shape functions for ψ_{ijk} is to take advantage of the nonlinear strain-displacement theory. Using this theory one can relate the nonlinear elastic displacements to the diagonal elements of the strain tensor, ε_{ii}, as (see Donaldson [1993])

$$\begin{aligned}
\varepsilon_{xx}&=\partial w_1/\partial x_1+\frac{1}{2}\left[(\partial w_2/\partial x_1)^2+(\partial w_3/\partial x_1)^2\right],\\
\varepsilon_{yy}&=\partial w_2/\partial x_2+\frac{1}{2}\left[(\partial w_1/\partial x_2)^2+(\partial w_3/\partial x_2)^2\right],\\
\varepsilon_{zz}&=\partial w_3/\partial x_3+\frac{1}{2}\left[(\partial w_1/\partial x_3)^2+(\partial w_2/\partial x_3)^2\right].
\end{aligned} \tag{5.24}$$

In this study the Lagrangian description is adopted, which means that everything is expressed in terms of the undeformed configuration. This has both the convenience of working with

practically preferred *undeformed* configuration as well as requiring much simpler algebra in deriving the theory.

In the method presented here, the strains ε_{ii}, not the displacements, are considered as linear functions of the elastic generalized coordinates, and the elastic displacements w_i are then calculated using the nonlinear strain-displacement theory. Since the strains are linear functions of elastic generalized coordinates, we may always choose them such that

$$\int \varepsilon_{ii}\, dx_i = \sum_{j=1}^{N_E} \varphi_{ij} q_j, \tag{5.25}$$

in which φ_{ij} are the first-order shape functions defined in Eq.(5.23). Using Eq.(5.25), one can rewrite Eq.(5.24) as

$$\begin{aligned}
w_1 &= \sum_{j=1}^{N_E} \varphi_{1j} q_j - \frac{1}{2}\int\left[(\partial w_2/\partial \xi_1)^2 + (\partial w_3/\partial \xi_1)^2\right] d\xi_1, \\
w_2 &= \sum_{j=1}^{N_E} \varphi_{2j} q_j - \frac{1}{2}\int\left[(\partial w_1/\partial \xi_2)^2 + (\partial w_3/\partial \xi_2)^2\right] d\xi_2, \\
w_3 &= \sum_{j=1}^{N_E} \varphi_{3j} q_j - \frac{1}{2}\int\left[(\partial w_1/\partial \xi_3)^2 + (\partial w_2/\partial \xi_3)^2\right] d\xi_3,
\end{aligned} \tag{5.26}$$

where ξ_i denotes a dummy variable for x_i. Equations (5.26) form a set of coupled partial differential equations. However, since we only need to retain up to second-order terms in the expression for w_1, w_2, and w_3, it is good enough to substitute the first-order part of their expressions in the integrals. This turns the problem to an explicit integration which results in:

$$\begin{aligned}
w_1 &= \sum_{j=1}^{N_E} \varphi_{1j} q_j - \frac{1}{2}\sum_{j=1}^{N_E}\sum_{k=1}^{N_E}\left[\int\left(\frac{\partial \varphi_{2j}}{\partial \xi_1}\frac{\partial \varphi_{2k}}{\partial \xi_1} + \frac{\partial \varphi_{3j}}{\partial \xi_1}\frac{\partial \varphi_{3k}}{\partial \xi_1}\right) d\xi_1\right] q_j q_k, \\
w_2 &= \sum_{j=1}^{N_E} \varphi_{2j} q_j - \frac{1}{2}\sum_{j=1}^{N_E}\sum_{k=1}^{N_E}\left[\int\left(\frac{\partial \varphi_{1j}}{\partial \xi_2}\frac{\partial \varphi_{1k}}{\partial \xi_2} + \frac{\partial \varphi_{3j}}{\partial \xi_2}\frac{\partial \varphi_{3k}}{\partial \xi_2}\right) d\xi_2\right] q_j q_k, \\
w_3 &= \sum_{j=1}^{N_E} \varphi_{3j} q_j - \frac{1}{2}\sum_{j=1}^{N_E}\sum_{k=1}^{N_E}\left[\int\left(\frac{\partial \varphi_{1j}}{\partial \xi_3}\frac{\partial \varphi_{1k}}{\partial \xi_3} + \frac{\partial \varphi_{2j}}{\partial \xi_3}\frac{\partial \varphi_{2k}}{\partial \xi_3}\right) d\xi_3\right] q_j q_k.
\end{aligned} \tag{5.27}$$

The method can now be summarized in the following two steps:

- Define $\tilde{w}_i$, the first-order components of the displacements as linear functions of the elastic generalized coordinates

$$\tilde{w}_i = \sum_{j=1}^{N_e} \varphi_{ij} q_j . \tag{5.28}$$

- Calculate the displacements w_i correct up to the second order using Eq. (5.27).

Although the above formulation is quite general and can be applied to any type of three-dimensional elastic member, it is more convenient to have specializations for some simpler cases. For instance, it is not an efficient approach to analyze a beam or a plate as a general three-dimensional elastic body. To derive the equations of motion of a general three-dimensional elastic body, one has to carry out triple integrals over the spatial domain of the body. However, for a beam only single integrals need to be evaluated. This simplification is due to the practical assumptions made in the beam theory.

To be practically useful, the above theory must be expressed using the same terminology as used in the related specified category (e.g. beams). It can be achieved by applying the assumptions made for that specific category of elastic bodies to the above theory. As a result, an improved theory for that category will be developed which has the conveniences of both simplicity and accuracy. To do this, one has to take the following steps: (1) find the general 3-D elastic displacement field based on the lower dimensional elastic displacement field and the assumptions made in that specific medium; (2) make the necessary second-order corrections to the 3-D elastic field using Eq.(5.27); (3) reversing the first step, find the correct special lower dimensional displacement field using the results of the second step and the assumptions made for the medium. The specializations of the above theory to Euler beams and thin plates are presented below as examples.

5.4.2 Specialization to Euler beams

Consider an Euler beam with a rigid infinitesimal element dB, shown in Figure 5.3. Transverse deflections, longitudinal vibration and torsion are different types of motion which the beam might experience. To analyze the motion of the beam, the elastic displacements of point b, and elastic rotations of the element dB should be expressed in terms of the elastic generalized coordinates. Using the conventional assumed-mode method, one can express the linear field of displacements as

$$\begin{aligned}
&\underline{\breve{w}}_i = \sum_{j=1}^{N_E} \varphi_{ij}(x_1) q_j \,, \quad i = 1,2,3, \\
&\underline{\breve{\theta}}_1 = \sum_{j=1}^{N_E} \varphi_{4j}(x_1) q_j \,, \\
&\underline{\breve{\theta}}_2 = -\partial \underline{w}_3 / \partial x_1 \,, \quad \underline{\breve{\theta}}_3 = \partial \underline{w}_2 / \partial x_1 \,.
\end{aligned} \tag{5.29}$$

Note that in Eqs.(5.29) the underlined variables, $\underline{\breve{w}}_i(x_1)$ and $\underline{\breve{\theta}}_i(x_1)$, denote the corresponding quantities evaluated at point b, with $x_2 = x_3 = 0$. These quantities do not represent the general three-dimensional field of displacements in the beam.

The second order expression for the above displacements and rotations can be obtained using the geometry of the beam. However, in this context, we would like to follow a general approach, which can be applied similarly to other categories of elastic bodies. To do so, we should first find the first-order three-dimensional displacement field, $\breve{w}_i(x_1, x_2, x_3)$, from which $\underline{\breve{w}}_i(x_1)$ and $\underline{\breve{\theta}}_i(x_1)$ can be derived; then the corrected field of displacements, $w_i(x_1, x_2, x_3)$, should be calculated, using Eqs.(5.27). Finally, the corrected displacements and rotations of dB, $\underline{w}_i(x_1), \underline{\theta}_i(x_1)$, should be calculated using w_i.

The three dimensional field $\breve{w}_i(x_1, x_2, x_3)$ can be found by applying the assumptions made in the slender-beam theory to a general field of displacements which results in (Ider and Amirouche [1989])

$$\begin{aligned}
\bar{w}_1 &= \underline{\bar{w}}_1 - (\partial \underline{\bar{w}}_2/\partial x_1)x_2 - (\partial \underline{\bar{w}}_3/\partial x_1)x_3 , \\
\bar{w}_2 &= \underline{\bar{w}}_2 - \underline{\bar{\theta}}_1 x_3 , \\
\bar{w}_3 &= \underline{\bar{w}}_3 + \underline{\bar{\theta}}_1 x_2 .
\end{aligned} \tag{5.30}$$

The linear three dimensional field $\bar{w}_i(x_1, x_2, x_3)$ is corrected using Eqs.(5.27), and the corrected one-dimensional displacements and rotations of dB, $\underline{w}_i$ and $\underline{\theta}_i$, are extracted from them as

$$\begin{aligned}
\underline{w}_1 &= \sum_{j=1}^{N_g} \varphi_{1j}(x_1) q_j - \frac{1}{2}\int \left[(\partial \underline{w}_2/\partial \xi_1)^2 + (\partial \underline{w}_3/\partial \xi_1)^2 \right] d\xi_1 , \\
\underline{w}_i &= \sum_{j=1}^{N_g} \varphi_{ij}(x_1) q_j , \quad i = 2,3 , \\
\underline{\theta}_1 &= \sum_{j=1}^{N_g} \varphi_{4j}(x_1) q_j , \quad \underline{\theta}_2 = -\partial \underline{w}_3/\partial x_1 , \quad \underline{\theta}_3 = \partial \underline{w}_2/\partial x_1 .
\end{aligned} \tag{5.31}$$

Use of the above nonlinear relations would result in generation of the equations of motion correct up to the first order. It is worth mentioning that although $\underline{\theta}_i$ are small, the second order terms involving them should be retained in the rotation matrix to prevent premature linearization.

5.4.3 Specialization to thin plates

The theory can be specialized for thin plates in a similar fashion as for beams. Consider the plate shown in Figure 5.4. The two–dimentional linear field of elastic displacements for thin plates, which relates the elastic motion of a 2–D infinitesimal rigid element dB of the plate to the elastic generalized coordinates, can be expressed as:

$$\begin{aligned}
\underline{\bar{w}}_i &= \sum_{j=1}^{N_g} \varphi_{ij}(x_1, x_2) q_j , \quad i = 1,2,3 \\
\underline{\bar{\theta}}_1 &= \partial \underline{w}_3/\partial x_2 , \quad \underline{\bar{\theta}}_2 = -\partial \underline{w}_3/\partial x_1 .
\end{aligned} \tag{5.32}$$

The corresponding 3–D elastic displacement field can be related to the above 2–D elastic field by (see Donaldson [1993])

$$\begin{aligned}
\bar{w}_1(x_1,x_2,x_3) &= \underline{\bar{w}}_1 - \left[\partial \underline{\bar{w}}_3(x_1,x_2)/\partial x_1\right]x_3 ,\\
\bar{w}_2(x_1,x_2,x_3) &= \underline{\bar{w}}_2 - \left[\partial \underline{\bar{w}}_3(x_1,x_2)/\partial x_2\right]x_3 ,\\
\bar{w}_3(x_1,x_2,x_3) &= \underline{\bar{w}}_3(x_1,x_2) .
\end{aligned} \tag{5.33}$$

This linear 3–D field is corrected using Eq.(5.27), and the results are evaluated at $x_3 = 0$ to yield the following corrected 2–D special field:

$$\begin{aligned}
\underline{w}_1 &= \sum_{j=1}^{N_g} \varphi_{1j}(x_1,x_2)q_j - \frac{1}{2}\int[(\partial \underline{w}_2/\partial \xi_1)^2 + (\partial \underline{w}_3/\partial \xi_1)^2]\,d\xi_1 ,\\
\underline{w}_2 &= \sum_{j=1}^{N_g} \varphi_{2j}(x_1,x_2)q_j - \frac{1}{2}\int[(\partial \underline{w}_1/\partial \xi_2)^2 + (\partial \underline{w}_3/\partial \xi_2)^2]\,d\xi_2 ,\\
\underline{w}_3 &= \sum_{j=1}^{N_g} \varphi_{3j}(x_1,x_2)q_j ,\\
\underline{\theta}_1 &= \partial \underline{w}_3/\partial x_2 \quad , \quad \underline{\theta}_2 = -\partial \underline{w}_3/\partial x_1
\end{aligned} \tag{5.34}$$

It should be mentioned here that the above specialized theories, established for beams and thin plates, are valid for any type of boundary conditions. However, the domain of the integral must be such that the geometric boundary conditions are met by the second–order shape functions. Furthermore, the specialization can be done similarly for the cases where shear deformations are important.

5.5 Illustrative Examples

5.5.1 Cantilever beam with longitudinal base motion

To clarify the discussion of the third section, "Comparison of the Three Different Remedies," the well-known problem of a cantilever beam with *longitudinal* base motion, shown in Figure 5.5, is considered. The elastic deflection of the beam, which is confined to the vertical plane, is described with one transverse mode as $\underline{\bar{w}}_2 = \varphi q$, where φ is a shape function satisfying the geometric boundary conditions, and q is the elastic generalized coordinate. The equation of motion obtained using this linear relation, prematurely linearized, is

$$\ddot{q} - \omega_1^2 q = 0 \tag{5.35}$$

which neither reflects the effect of the gravity nor the base motion. Here $\omega_1^2 = c_1 (EI/mL^3)$, where EI, L, and m are, respectively, the flexural rigidity, the length, and the mass of the beam, while c_1 is a constant whose value depends on the choice of the shape functions. For instance, for the shape function $\varphi(x)$, given in Eq.(5.36), which is used in the solution of this example, the value of c_1 is 12.36.

$$\varphi(x) = A\left[(\cosh(\lambda\xi) - \cos(\lambda\xi)) - \sigma(\sinh(\lambda\xi) - \sin(\lambda\xi))\right], \tag{5.36}$$

in which $A = 0.5$, $\lambda = 1.875$, $\sigma = (\cosh\lambda + \cos\lambda)/(\sinh\lambda + \sin\lambda)$, and $\xi = x/L$.

A second order correction can be made to the above first order displacement using Eq.(5.31), the nonlinear strain-displacement method, to give

$$\begin{aligned} \underline{\bar{w}}_1 &= \left[-\frac{1}{2}\int_0^{x_1}\left(\frac{\partial\varphi(\xi_1)}{\partial\xi_1}\right)d\xi_1\right]q^2, \\ \underline{\bar{w}}_2 &= \varphi q. \end{aligned} \tag{5.37}$$

Using the above nonlinear displacements, one can develop the properly linearized equation of motion for this beam as

$$\ddot{q} + \left[\omega_1^2 - \alpha_1(g/L) - \alpha_1(a(t)/L)\right]q = 0 \tag{5.38}$$

where g, $a(t)$, and α_1 are, respectively, the acceleration due to gravity, the base acceleration and a constant whose value depends on the choice of the shape function (for the shape function given by Eq.(5.36), $\alpha_1 = 2.259$). Equation (5.38) shows that for $a(t) = a_0 > 0$ the system becomes dynamically softer, and for $a(t) = a_0 < 0$ stiffer. On the other hand, if $a(t) = a_0\cos(\omega_0 t)$ the stiffness becomes time dependent, and the equation of motion can be transformed into the standard form of the Mathieu equation, which means even a statically unstable beam, with $(g/L) > (\omega_1^2/\alpha_1)$, can be stabilized by a proper choice of a_0 and ω_0; conversely, a statically stable beam might become unstable. Although the method of

stabilization with *lateral* base motion is well known, the present method of stabilization by *longitudinal* base motion could not be analyzed, unless the equations of motion are derived correctly.

On the other hand, using the first method of remedy, i.e. by employing a fourth-order strain energy expression and considering one *transverse* elastic DOF only, the equation of motion can be found as

$$\ddot{q} + \omega_1^2 q + \beta_1(\omega_1^2/L^2)\, q^3 = 0 \tag{5.39}$$

where β_1 is a constant, dependent on the choice of the shape function (with φ defined in Eq.(5.36), $\beta_1 = 0.818$). Obviously, the compensating term, $\beta_1(\omega_1^2/L^2)\, q^3$, always stiffens the system, regardless of the base motion, so it cannot describe the other effects discussed earlier, arising from different kinds of base motions. Of course, the nonlinear strain energy method can produce much better results if one considers the longitudinal motion of the beam as well. In this case, the equations of motion, considering one transverse and one longitudinal mode, are

$$\begin{aligned} &\ddot{q}_1 + \omega_1^2 q_1 + \beta_1(\omega_1^2/L^2)\, q^3 + (\gamma_1 \omega_2^2/L) q_1 q_2 = 0 \\ &\ddot{q}_2 + \omega_2^2 q_2 + (\beta_2 \omega_2^2/L) q_1^2 = \alpha_2 (g + a(t)) \end{aligned} \tag{5.40}$$

where q_1, and q_2 stand for the lateral and longitudinal generalized coordinates, ω_1 and β_1 are as defined earlier, and α_2, β_2, and γ_1 are some constants. The quantity ω_2, which is the fundamental frequency of the longitudinal vibration of the beam in absence of gravity and base motion, is given by $\omega_2^2 = c_2\, E A / m L$, where A denotes the cross-sectional area of the beam. The constants $\alpha_2, \beta_2, \gamma_1$ and c_2 are functions of the selected shape functions. Using the function given in Eq.(5.36) as the transverse shape function and $\sin(\pi x/2L)$ as the longitudinal shape function, one can evaluate $\alpha_2, \beta_2, \gamma_1$ and c_2 to -1.273, 0.355, 1.405, and 2.467, respectively.

Equations (5.40) can produce results similar to those of Eq.(5.38), but at the cost of increasing the order of the system and making the set of differential equations stiff by

Equations (5.40) can produce results similar to those of Eq.(5.38), but at the cost of increasing the order of the system and making the set of differential equations stiff by introducing a high frequency ω_2 into the system. One should also note that if $a(t)$ is constant, Eqs.(5.40) can predict the correct frequency for the lateral motion, taking advantage of linearization around $\bar{q}_2$ obtained from the solution for the fixed points. However if $a(t)$ is time dependent, this possibility is ruled out. The same difficulty arises when the zero-order motion/force is generalized-coordinate-dependent.

Typical simulation results (non-dimensional tip deflection, δ/L, versus the period of non-moving beam, τ_1) for two types of base motion, obtained using the presented theory (Eq.(5.38)), are shown in Figures 5.6 and 5.7. As can be seen, the response of the system to a typical initial condition varies both with changes in $(g/l)/\omega_1^2$ and the parameters of the base motion. Besides, Figure 5.6 shows that for a value of $(g/l)/\omega_1^2 = 0.5$ the linear solution becomes unstable. This linear instability is the phenomenon of buckling of the beam under its own weight.

5.5.2 Planar two-bar linkage

Figure 5.8 shows a system that serves as an example to show the possibility of terms missing in the generalized mass matrix of the system due to premature linearization. The system, which consists of two rigid bars connected through a revolute joint, has two degrees of freedom. The first degree of freedom, q_1, is intended to remain small, while the second one, q_2, can accept large values. The system is assumed massless except for the point masses m_1 and m_2, located at the tips of the bars.

Using the nonlinear expression of $\mathbf{r}_2 = L_1\bar{\mathbf{n}}_1 + L_2[-\sin(q_1)\bar{\mathbf{n}}_1 + \cos(q_1)\bar{\mathbf{t}}_1]$ to express the position vector of the point mass m_2, one gets the nonlinear equations of motion in vector form as

$$\begin{bmatrix} m_2 L_2^2 & m_2 L_2[L_2 - L_1 \sin(q_1)] \\ m_2 L_2[L_2 - L_1 \sin(q_1)] & L_1^2(m_1+m_2) + m_2 L_2[L_2 - 2L_1 \sin(q_1)] \end{bmatrix} \begin{bmatrix} \dot{u}_1 \\ \dot{u}_2 \end{bmatrix} = \begin{bmatrix} -K q_1 - m_2 L_1 L_2 u_2^2 \cos(q_1) \\ T_1 + m_2 L_1 L_2 u_1 (2u_2 + u_1)\cos(q_1) \end{bmatrix}. \tag{5.41}$$

On the other hand, the prematurely linearized equations of motion, obtained using the linearized form of the position vector of m_2 (i.e., $\mathbf{r}_2 = L_1 \mathbf{n}_1 + L_2[-q_1 \mathbf{n}_1 + \mathbf{t}_1]$), are

$$\begin{bmatrix} m_2 L_2^2 & m_2 L_2^2 \\ m_2 L_2^2 & L_1^2(m_1+m_2) + m_2 L_2(L_2 - 2L_1 q_1) \end{bmatrix} \begin{bmatrix} \dot{u}_1 \\ \dot{u}_2 \end{bmatrix} = \begin{bmatrix} -K q_1 - m_2 L_1 L_2 u_2^2 + m_2 L_2^2 u_2^2 q_1 \\ T_1 + 2m_2 L_1 L_2 u_1 u_2 \end{bmatrix}. \tag{5.42}$$

and the properly linearized equations of motion, obtained based on the position vector with second-order terms (i.e., $\mathbf{r}_2 = L_1 \bar{\mathbf{n}}_1 + L_2[-q_1 \bar{\mathbf{n}}_1 + (1 - q_1^2/2)\bar{\mathbf{t}}_1]$), are

$$\begin{bmatrix} m_2 L_2^2 & m_2 L_2(L_2 - \underline{L_1 q_1}) \\ m_2 L_2^2 & L_1^2(m_1+m_2) + m_2 L_2(L_2 - 2L_1 q_1) \end{bmatrix} \begin{bmatrix} \dot{u}_1 \\ \dot{u}_2 \end{bmatrix} = \begin{bmatrix} -K q_1 - m_2 L_1 L_2 u_2^2 + (m_2 L_2^2 u_2^2 q_1 - \underline{m_2 L_2^2 u_2^2 q_1}) \\ T_1 + 2m_2 L_1 L_2 u_1 u_2 \end{bmatrix}. \tag{5.43}$$

The missing terms in the generalized mass matrix and force vector are underlined. The form of these terms, linear in terms of elastic generalized coordinates and their places, are in complete agreement with the general results obtained in Section 5.2.2.

Either Eq.(5.14) or Eqs.(5.20) can be employed to determine the missing terms in the set of prematurely linearized equations of motion, Eq.(5.42). Adding the result of Eq.(5.14) to Eq.(5.42), one obtains the correct form of the equations of motion. For this system

$$\begin{aligned} &\bar{\mathbf{v}}_1^{(1)} = 0 \quad , \quad \bar{\mathbf{v}}_1^{(2)} = -L_2 q_1 \bar{\mathbf{t}}_1 \, , \\ &\bar{\mathbf{a}}^{(2)} = (L_1 \dot{u}_2 - L_2 u_2^2)\bar{\mathbf{t}}_1 - (L_2 \dot{u}_2 + L_1 u_2^2)\bar{\mathbf{n}}_1 \, , \\ &\bar{\mathbf{R}}^{(2)} = 0 \, , \end{aligned} \tag{5.44}$$

where the superscript (i) indicates quantities associated with the i-th point mass. Substitution of Eqs.(5.44) into Eq. (5.14) gives the correction terms to be added to the right hand side of Eq.(5.42) as follows:

$$\mathcal{E} = m_2 L_1 L_2 \dot{u}_2 \dot{q}_1 - m_2 L_2^2 u_2^2 q_1. \tag{5.45}$$

This lumped model was chosen to provide the possibility of comparison of the results of premature and proper linearization with the linearized equations obtained from nonlinear equations of motion, Eq. (5.41). A very similar problem can be considered by replacing the second rigid bar, the masses and the spring with an elastic cantilever beam clamped to the rigid massless first bar. Use of the conventional assumed-mode method for describing the elastic displacements of the beam causes similar terms to be missed from the equations of motion. As before, none of the methods of compensation is capable of compensating for these terms except the third one.

5.5.3 RAE satellite

The Radio Astronomy Satellite, launched by NASA in July 1968, had four 228.75 meters STEM type Be-Cu antennas, with 0.02 (Kg/m) density and bending stiffness of 6.033 ($N.m^2$). The antennas are located in the orbital plane. The planar motion of the system, depicted in Figure 5.9, is studied here. The center of mass moves on a 224 minute nominally circular orbit, but let us assume that it is subjected to a known orbital perturbation of y(t) in the local horizontal direction. The gravity gradient effect is taken into account, and the attitude of the satellite during the motion is assumed unchanged. Due to the small forces, the longitudinal elongation of the beam is negligible and is of no interest. So, the elastic displacements of the booms are described using one transverse DOF for each boom. Using the conventional assumed-mode method, one may write $\bar{w}_2^i = \varphi_i q_i, i = 1,\ldots,4$, where $\bar{w}_2^i$ stands for the lateral deflection of the i-th boom. The equations of motion for the system, obtained based on $\bar{w}_2^i$, are

$$
\begin{aligned}
&q_1'' + \left(1 - \alpha(\omega_0/\omega_1)^2\right)q_1 + \beta y''(t) = 0,\\
&q_2'' + \left(1 - \alpha(\omega_0/\omega_1)^2\right)q_2 + \gamma y'(t) = 0,\\
&q_3'' + \left(1 - \alpha(\omega_0/\omega_1)^2\right)q_3 - \beta y''(t) = 0,\\
&q_4'' + \left(1 - \alpha(\omega_0/\omega_1)^2\right)q_4 - \gamma y'(t) = 0,
\end{aligned}
\tag{5.46}
$$

in which ω_0 is the orbital rate and α, β, γ are some constants which are functions of the selected shape functions; moreover, prime and double prime stand for time derivatives with respect to the non-dimensionalized time, $\tau = t\omega_1$, where ω_1 denotes the fundamental frequency of the booms with a fixed base. As expected, the stiffness of the booms are reduced due to the rotation about the earth (recall that the prematurely linearized equation of motion predicts lower stiffness for a rotating beam compared to the non-rotating one). The terms $\beta y''$ and $\gamma y'$ in Eq.(5.46) act as forcing functions due to the translational and Coriolis acceleration of the base. Using the shape function given in Eq.(5.36), one can evaluate the constants α, β, γ, and ω_1 to be 0.215, 1340, 1.25, and 0.00117, respectively.

The correct form of the equations of motion could be generated directly using the third method. However, a more convenient approach may be to make corrections to Eqs.(5.46) by adding the results of Eqs.(5.14) to them. Taking similar steps as those taken in the previous example, one can calculate the correction terms using Eq.(5.14) as

$$
\mathcal{E} = \begin{bmatrix} (.74+.008y')q_1 \\ -.01y''q_2 \\ (.74-.008y')q_3 \\ .01y''q_4 \end{bmatrix} = \begin{bmatrix} .74+.008y' & 0 & 0 & 0 \\ 0 & -0.01y'' & 0 & 0 \\ 0 & 0 & .74-.008y' & 0 \\ 0 & 0 & 0 & 0.01y'' \end{bmatrix} \begin{bmatrix} q_1 \\ q_2 \\ q_3 \\ q_4 \end{bmatrix}, \tag{5.47}
$$

in which the data for RAE satellite have already been incorporated. As expected, the compensating terms appear in the form of a geometric stiffness matrix, for the zero-order motions are prescribed. The compensating terms show that the stiffness of the boom is, indeed, a function of y' and y''. This suggests that the booms might become softer and even buckle for

certain values of $\dot{\gamma}'$ and $\dot{\gamma}''$. This phenomenon is shown in Figure 5.10, which presents some typical simulation results for the booms 1 and 3 for the case of $\dot{\gamma}' = 0$ and $\dot{\gamma} = 0.235\,(m/s)$ ($\gamma' = 201$ *m rad*). In this case, the third boom buckles due to the effect of Coriolis acceleration of the base.

On the other hand, the first remedy, nonlinear strain energy expression, compensates for the missing stiffness by adding the cubic terms $1.56\times10^{5}q_i^3, i = 1,\ldots,4$ to the corresponding equations of motion, which does not account for the effect of the base motion. This method, however, can produce better results if one considers at least one longitudinal DOF for each boom. Clearly, the worst thing an analyst might do is to study a system with eight DOFs, while it *can be analyzed correctly* with only four DOFs. Furthermore, the method produces additional difficulties by introducing the longitudinal frequencies, almost 7000 times larger than the lateral frequencies, to the system of differential equations which makes the integration procedure more difficult.

5.5.4 Rotating cantilever plate

This example is given to verify the applicability of the presented theory to a two dimensional elastic media. Consider a rectangular cantilever plate (Figure 5.4), rotating about one of its edges, say the X_2 axis, with a constant angular velocity of ω_0. The dimensions of the plate are l_1, l_2, and h, respectively. Its material properties are characterized by Young's modulus E, Poisson's ratio ν, and mass per unit area ρ. The equations of motion for this system can be obtained using the following *linear* field of elastic displacement:

$$\begin{aligned} \underline{\breve{w}}_1 &= \underline{\breve{w}}_2 = 0, \\ \underline{\breve{w}}_3 &= \sum_{i=1}^{2} \varphi_i(x_1, x_2) q_i, \end{aligned} \tag{5.48}$$

in which

$$\begin{aligned} \varphi_1(x_1, x_2) &= \psi_{c1}(x_1)\,\psi_{f1}(x_2), \\ \varphi_2(x_1, x_2) &= \psi_{c2}(x_1)\,\psi_{f2}(x_2), \end{aligned} \tag{5.49}$$

while the shape functions $\psi_{\alpha}(x_1)$ and $\psi_{\beta}(x_2)$ are chosen as the i-th eigenfunctions of a cantilever and a free-free beam, respectively.

The above linear field of elastic deflections, Eqs.(5.48), can be corrected to a nonlinear one using Eqs.(5.34). The correct governing equations of motion, based on the nonlinear elastic displacement field, can be found as

$$\ddot{q}_i + (0.21\omega_0^2 + \overline{\omega}_i^2) q_i = 0, \quad i = 1,2, \tag{5.50}$$

in which $\overline{\omega}_1$ and $\overline{\omega}_2$, the frequencies of the non-rotating plate, are as follows

$$\begin{aligned} \overline{\omega}_1^2 &= 12.48(D/\rho l_1^4), \\ \overline{\omega}_2^2 &= [1 + 9.24(1-\nu) l_r^2]\overline{\omega}_1^2. \end{aligned} \tag{5.51}$$

In the above relations, $l_r = l_1/l_2$, denotes the ratio of the dimensions of the plate, while the flexural rigidity D is given by $Eh^3/12(1-\nu^2)$.

Figure 5.11 shows the variation in the non-dimensionalized frequencies of oscillation of the plate with the change in the non-dimensionalized angular velocity, $\omega_0/\overline{\omega}_1$, for a rectangular plate with $\nu = .3$ and $l_r = 1$. As expected, the results of the conventional theory, dotted lines, falsely show dynamic softening, while the results of the present theory, solid lines, correctly predict stiffening of the rotating plate.

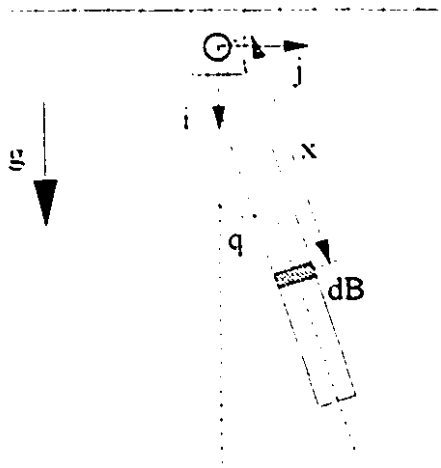

Figure 5.1 A simple pendulum.

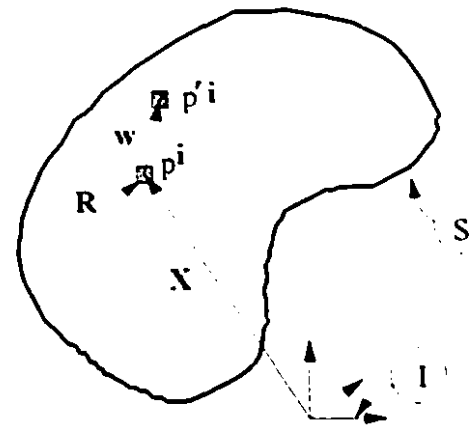

Figure 5.2 Schematic of a general system.

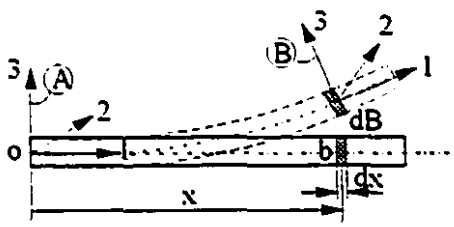

Figure 5.3 Schematic of an Euler beam.

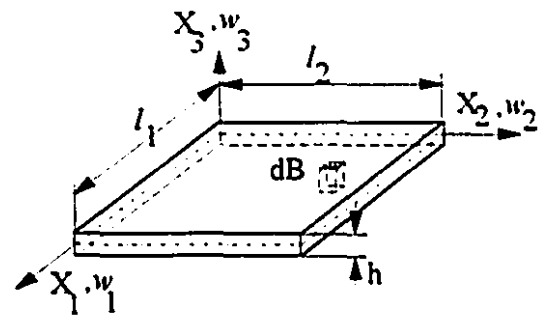

Figure 5.4 Schematic of a thin plate.

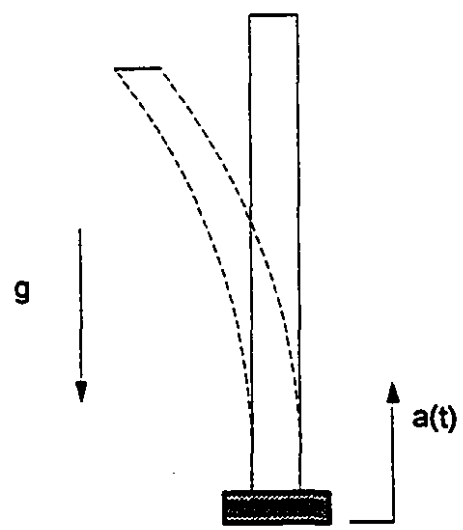

Figure 5.5 A Vertical Cantilever with moving base.

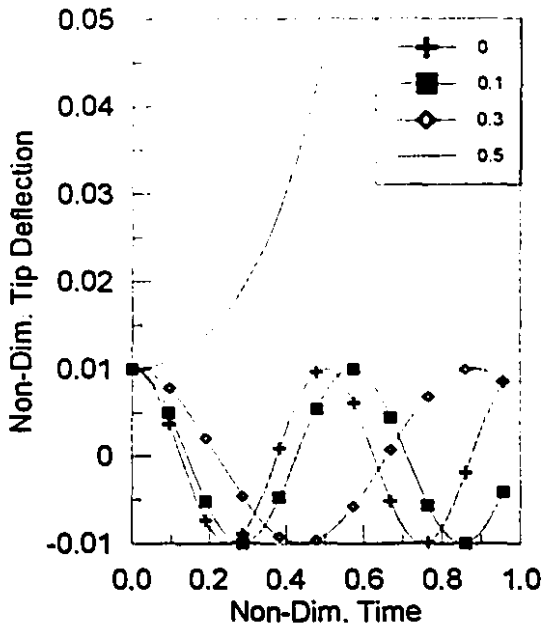

Figure 5.6 Simulation results, third correction method (present theory), for $a(t) = 0$, and different values of $(g/L)/\omega_1^2$.

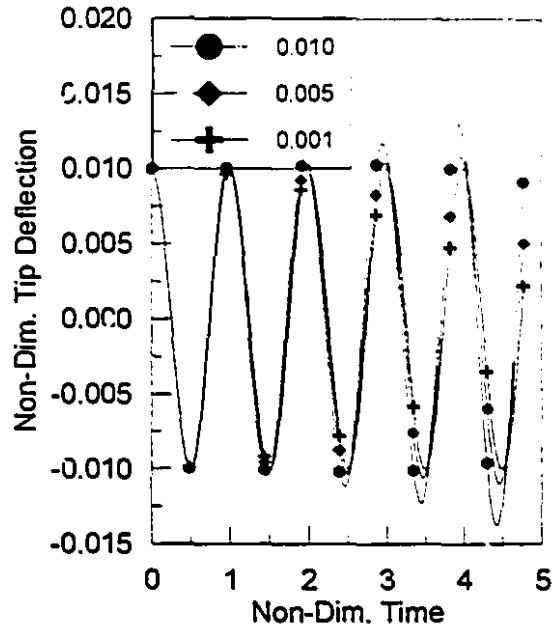

Figure 5.7 Simulation results, third correction method (present theory), for $g = 0$. $\omega_0/\omega_1 = 2$ and different values of $(a_0/L)/\omega_1^2$.

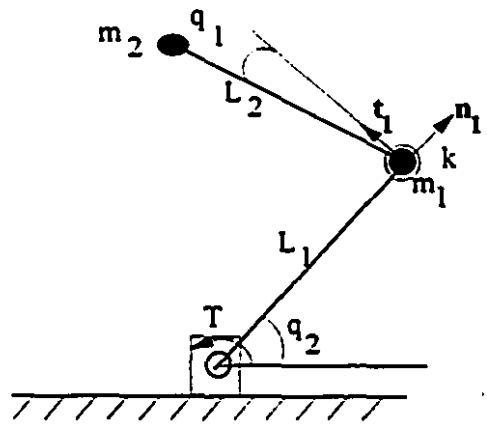

Figure 5.8 Two-bar linkage, $q_1 \ll q_2$.

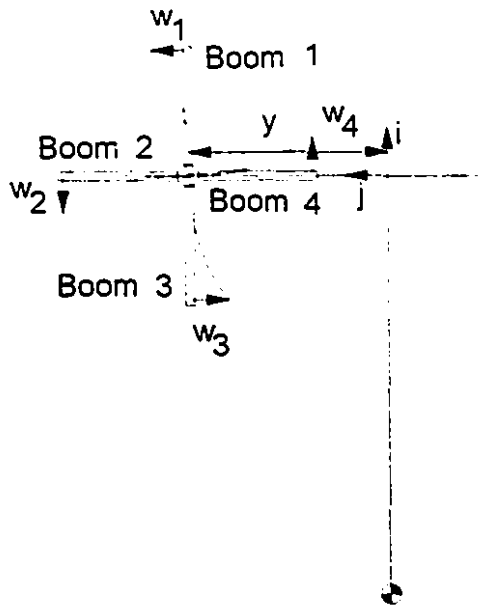

Figure 5.9 Schematic of the RAE satellite.

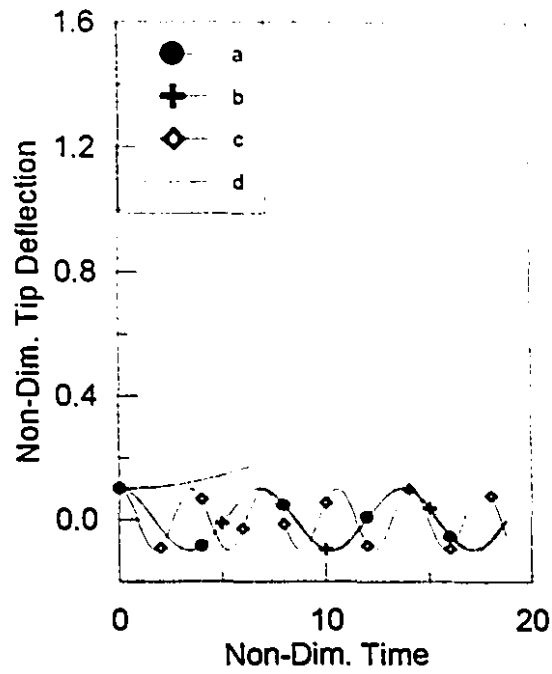

Figure 5.10 Simulation results for $y'=201$;
a- premature linearization (booms 1 &3),
b- nonlinear strain energy correction method (booms 1 &3),
c- present theory (boom 1),
d- present theory (boom 3).

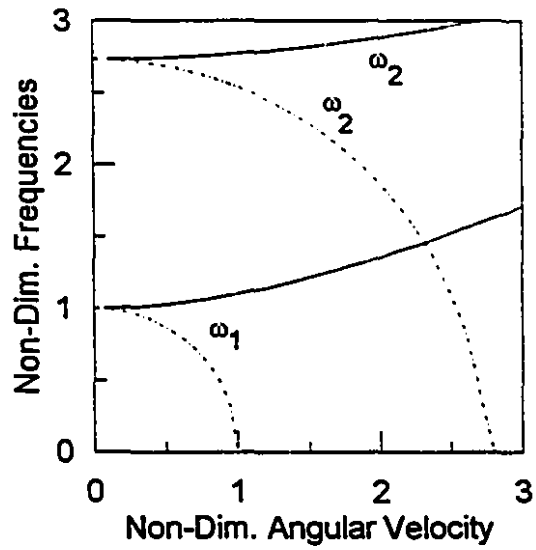

Figure 5.11 Frequencies of a rotating cantilever plate; dotted lines: conventional theory; solid lines: present theory

Chapter 6

Applications

6.1 Introduction

So far, we have completed a formulation for the dynamic analysis of flexible multibody systems, based on which the computer code FLXSIM has been developed. This chapter is devoted to the presentation of simulation results for three different problems, whose equations of motion are obtained using FLXSIM.

Capture of a spinning satellite by a flexible two-link manipulator is the first problem studied. In the second problem, the feasibility of using a two-link space manipulator for stabilizing tethered satellite systems is investigated. The last problem studied deals with the retrieval of a large payload by a redundant space manipulator, which possesses seven revolute joints; in this study the effects of flexibility of both the joints and links of the manipulator are taken into account.

The problems solved in this chapter may serve as a means to show some of the capabilities of the formalism developed in the previous chapters, and the computer code written based on that. For instance, the capabilities of deriving the minimum-order set of equations for a constrained system and analytical linearization of equations of motion in the presence of intermediate parameters are demonstrated in the first problem. On the other hand, the versatility

of the code in handling complex flexible multibody systems with flexible joints is shown through the solution of the third problem, a serial manipulator with twenty DOFs (rigid and flexible). In this problem, proper definition of intermediate parameters has made it possible to analyze the problem using a PC computer.

6.2 Capture of a Spinning Satellite

A two-link spacecraft-mounted manipulator, shown in Figure 6.1, is used to capture a spinning satellite. The purpose is to achieve a smooth berthing of the payload as it is captured by the end effector of the manipulator.

The problem is solved with three different sets of assumptions. In all three cases, a circular orbit, not affected by the attitude dynamics of the system during the capturing process, and planar motion, are assumed. In the first case, the manipulator links are considered to be rigid and the center of mass (c.m.) of the spacecraft, not of the entire system, is assumed to follow a circular orbit. In the second case, the assumption of rigidity is dropped and the elastic displacement of each beam is approximated by using only the first mode of a fixed base cantilever. The third case, an example of application of constrained motion analysis, is concerned with the same problem as the first case, but assumes that the *entire system's center of mass* is in the above-mentioned circular orbit.

The system, in the first case, has four holonomic DOFs (rigid). In the second case, there are six holonomic DOFs (four rigid and two elastic). In the third case, the center of mass of the entire system is considered to move in a circular orbit; hence even if the system has four holonomic DOFs, the definition of two *dependent pseudo-generalized coordinates* (q_5 and q_6), which describe the position of the spacecraft center of mass (see Figure 6.1) is necessary to make the analysis of the system easier. The constraint equation, obtained by making *the position vector of the whole system's center of mass in the orbital frame equal to zero*, is:

$$\sum_{i=1}^{n} \rho^i m^i = 0 \tag{6.1}$$

where ρ^i indicates the position vector of the center of mass of the i-th member in the orbital frame. Differentiation of Eq.(6.1) with respect to time yields two scalar functions linear in terms of the generalized speeds $u_1,\ldots,u_6$ which can be solved for u_5 and u_6 to give

$$u_{s+4} = \sum_{r=1}^{4} A_{sr}(q_1,\ldots,q_6)\, u_r, \qquad s = 1,2. \tag{6.2}$$

The system is treated as a simple nonholonomic one with $q_1,\ldots,q_6$ as the generalized coordinates and Eqs.(6.2) as the simple nonholonomic constraints.

The physical parameters of the system are: spacecraft mass =10000 kg, spacecraft moment of inertia about its center of mass=40000 kg.m^2, orbital rate =0.001 rad/sec, satellite (payload) mass =1000 kg, payload moment of inertia about its center of mass=500 kg.m^2, payload initial spin rate =0.5 rpm, link mass =20 kg, $(EI)_{link} = 8810$ N.m^2, link length =8.13 m, the distance from the spacecraft center of mass to the shoulder joint, $\overline{c^1 J^1} = 1$ m (Figure 6.1), the distance from satellite center of mass to the wrist joint, $\overline{c^2 J^3} = 1$ m (Figure 6.1).

The initial conditions are calculated by solving the inverse kinematics problem such that the satellite center of mass is located on local horizontal sixteen meters away from the spacecraft center of mass. Besides, to assure a smooth berthing process, the initial joint rates are chosen such that the grapple point on the satellite (payload) and the end effector have the same velocity.

6.2.1 Uncontrolled motion simulation

The uncontrolled motion of the system during the post-capturing phase is simulated here. Figure 6.2 compares the results of simulation for the cases one and three (spacecraft c.m. moves along the prescribed orbit and entire system c.m. moves along the prescribed orbit). The time history of the joint DOFs, for all three cases, are shown in Figure 6.3.a, while the tip

deflections of the beams (case 2) and the position of the spacecraft c.m. (case 3) are presented in Figures 6.3.b and 6.3.c, respectively. As can be seen from the results (Figure 6.3.a), there is almost no difference between the flexible and rigid cases; this is due to the smooth berthing process and absence of applied torques at the joints. The considerable difference between case 1, or case 2, (the spacecraft c.m. in a circular orbit) and case 3 (the entire system c.m. in a circular orbit), as seen in Figures 6.2 and 6.3, suggests that a free-flying case cannot be approximated arbitrarily as either case 1 or case 3. In other words, the spacecraft needs reaction jets to eliminates q_5 and q_6 variations and stay on a prescribed orbit.

The results also show the possibility of using the rotational kinetic energy of the captured satellite in the retrieval process. After being captured by the arm, the satellite moves towards the mother spacecraft even in the absence of any actuator forces (Figure 6.3.a). The results represent only one possible solution to the problem because the system is redundant and different sets of initial conditions, corresponding to different approach trajectories, may be chosen. Strong dependency of the system response on the initial conditions might induce a challenging problem of choosing the best set of initial conditions, i.e., best approach trajectory, to get the most desirable system response.

6.2.2 Controlled motion simulation

The purpose of control here is to maintain the pre-capture configuration of the system during post-capturing phase while reducing the satellite spin rate to zero. This is done for the three previously mentioned cases.

Case 1: Feedback linearization technique is employed to control the system in this case. To use this technique, the equations of motion should be written in the form $\mathbf{M}\dot{\mathbf{u}} = \mathbf{f} = \mathbf{Q} + \boldsymbol{\tau}$, in which $\boldsymbol{\tau}$ is the part of the generalized force vector associated with input torques, and $\mathbf{Q}$ is the part independent of them. This is done by the computer code automatically, which is

specially useful for complicated systems when definition of intermediate parameters is inevitable.

Having the equations of motion in the above form, one can choose

$$\tau = -\mathbf{Q} - \mathbf{M}[\mathbf{D}\mathbf{u} + \mathbf{K}(\mathbf{q} - \overline{\mathbf{q}})] \tag{6.3}$$

where $\mathbf{D}_{4\times4}, \mathbf{K}_{4\times4}$ and $\overline{\mathbf{q}}_{4\times1}$ are the specified damping and stiffness matrices associated with the controlled response, and the array of nominal values (trim condition) of the generalized coordinates. Choosing **D** and **K** as diagonal positive-definite matrices would asymptotically stabilize the system. The simulation results of the controlled motion for case 1 are presented in Figures 6.4 and 6.5.

Case 2: In this case, the equations of motion are analytically linearized around the trim condition, i.e., the pre-capture configuration. Then, an LQR method is used to stabilize the motion around the trim condition. The simulation results for this case are presented in Figures 6.6 and 6.7. Although the results show small deflections for the beam (Figure 6.6), this may not be the case for any arbitrary berthing scheme with impact or any arbitrary set of initial conditions. An interesting result obtained here is that the elastic DOFs can be controlled using the joint torques.

Case 3: Feedback linearization technique is used to control the motion of the system during the post-capture phase. The generated equations of motion are of the form

$$\sum_{s=1}^{4} \tilde{M}_{rs}\dot{u}_s = \tilde{f}_r = \tilde{Q}_r + \tilde{\tau}_r, \quad r = 1,\ldots,4 \tag{6.4}$$

in which $\tilde{\tau}$ denotes the part of the nonholonomic generalized force vector associated with input torques, and $\tilde{\mathbf{Q}}$ is the part independent of them. Choosing

$$\tilde{\tau} = -\tilde{\mathbf{Q}} - \tilde{\mathbf{M}}[\mathbf{D}\tilde{\mathbf{u}} + \overline{\mathbf{K}}(\mathbf{q} - \overline{\mathbf{q}})] \tag{6.5}$$

where $\mathbf{D}_{4\times4}$ and $\overline{q}_{6\times1}$ are as defined as before but the stiffness matrix, $\overline{\mathbf{K}}_{4\times6}$, is defined as

$$\overline{\mathbf{K}}_{4\times6} = [\mathbf{K}_{4\times4} \quad \mathbf{0}_{4\times2}] \tag{6.6}$$

where $\mathbf{K}_{4\times4}$ is a diagonal positive matrix. This way q_5, q_6, u_5 and u_6 are not controlled directly, however, since u_5 and u_6 are simple algebraic functions of $u_1,\ldots,u_4$ (Eq.(6.2)), they would be controlled once $u_1,\ldots,u_4$ are controlled. This, in turn, controls q_5 and q_6 which are related to $u_1,\ldots,u_6$ through the kinematical differential equations of motion.

The time history of the joint angles during the post-capture phase for cases 1 and 3 are compared in Figure 6.4.a. As one can see, using similar $\mathbf{K}$ and $\mathbf{D}_v$ we get similar solutions for joint angles in both cases. On the other hand, Figure 6.4.b shows that the system is maintained in the same configuration as in the first case, but without using the reaction jets which are necessary in the first case to maintain the spacecraft center of mass in the orbit. Using a similar approach, it is possible to reduce one more degree of freedom by introducing the simple non-holonomic constraint of constant angular momentum. This makes it possible to control the attitude of the spacecraft through the joint torques as well.

6.3 Stabilizing Tethered Satellite Systems Using Space Manipulators

Tethered satellite systems (i.e., orbiting bodies connected by a long tether) have the potential for a large number of applications. These systems can be shuttle-mounted, space station-based or free flyers. The applications cover a broad spectrum such as upper atmospheric measurements, electrodynamic experiments, providing microgravity environment, isolation of scientific platforms from the space station, etc. A detailed documentation of these applications has been done by von Tiesenhausen[1984].

There are three phases in the operation of tethered satellite systems: deployment phase, during which the subsatellite is deployed to the appropriate altitude; the stationkeeping phase during which experiments are conducted; and the retrieval phase in which the subsatellite is reeled back into the main satellite. The deployment phase is asymptotically stable if the

deployment rate is less than certain critical rate; the stationkeeping phase is marginally stable, while the retrieval phase is unstable (see Misra and Modi [1986]).This makes it necessary to devise some control schemes to stabilize the dynamics of tethered satellite systems.

The off-set control, proposed by Modi et al.[1990], is one of the several schemes devised for this purpose. This scheme, which is specially suitable for short tethers, involves changing the offset of the point of attachment of the tether. The objective of this study is to investigate the feasibility of using a space manipulator as a mechanism to implement the offset control during stationkeeping and retrieval.

To start with, a dynamical model is developed for the system consisting of a spacecraft-mounted manipulator and a tethered payload, using the computer code FLXSIM. Control laws are then developed using this dynamical model. Finally, computer simulations are carried out to validate the control laws developed.

6.3.1 Equations of motion

The system under consideration, shown in Figure 6.8, consists of a main spacecraft, the orbiter, a two-link spacecraft–mounted manipulator and a subsatellite, connected to the orbiter by a tether. In deriving the equations of motion, it is assumed that the spacecraft and the manipulator are rigid and the entire motion is coplanar with the orbital plane. The subsatellite is modeled as a point mass, while the tether is assumed to be massless and to remain straight during the motion.

With the above assumptions, the system has four degrees of freedom (DOFs) which are described by the following generalized coordinates: q_1, the pitch angle of the spacecraft; q_2, the shoulder joint angle; q_3, the elbow joint angle; and q_4, the librational angle of the tether. The generalized speeds are simply defined as the time derivatives of the generalized coordinates ($u_i = \dot{q}_i$, $i = 1,\ldots,4$). In addition to these four DOFs, the system has some prescribed motions

which are the motion of the spacecraft center of mass in a circular orbit, $R = R_0$, and $\theta = \theta(t)$, and the variation of the length of the tether, $L = L(t)$. It is assumed that these prescribed motions are not affected by the other motions of the system.

In the analysis of this system the *gravity gradient* plays an important role, due to the considerably large dimensions of the system. The gravitational forces applied on a rigid body, considering the effect of gravity gradient, can be replaced (see Hughes [1986]) by a force $\mathbf{W}_g$ passing through the center of mass of the body accompanied by a torque $\mathbf{T}_g$ where*

$$\mathbf{W}_g = -m^B g_0[1-2(\rho/R_0)\cos\alpha]\bar{\mathbf{n}} - [m^B g_0(\rho/R_0)\sin\alpha]\bar{\mathbf{t}} \tag{6.7}$$

$$\mathbf{T}_g = 3(g_0/R_0)[(\sin(2\alpha)(I_{11}^B - I_{22}^B)/2 + \cos(2\alpha)I_{12}^B]\bar{\mathbf{k}} \tag{6.8}$$

in which, ρ is the distance from the point o (see Figure 6.9) of the system which is moving in a prescribed orbit (e.g., spacecraft center of mass in this problem) and g_0 denotes the acceleration due to gravity measured at the point o.

The equations of motion for this system, which are obtained using the computer code FLXSIM, have the following general form

$$\mathbf{M}_{4\times4}(\mathbf{q}, L(t))\,\dot{\mathbf{u}}_{4\times1} = \mathbf{f}_{4\times1}(\mathbf{q}, \mathbf{u}, L, \dot{L}, \ddot{L}) + \mathcal{T}_{4\times3}\tau_{3\times1}, \tag{6.9}$$

in which $\tau = [\tau_1, \tau_2, \tau_3]^T$, where τ_1, τ_2 and τ_3 are the actuator torques applied on the spacecraft, shoulder joint, and elbow joint, respectively. The equations of motion of the system, Eqs.(6.9), have the following characteristics:

- The equations are highly nonlinear and coupled.
- The equations can have fixed points only when the length of the tether is either constant (in the stationkeeping phase) or an exponential function of time (during retrieval and deployment).

*Equations (6.7) and (6.8) represent simplified form of $\mathbf{W}_g$ and $\mathbf{T}_g$ for the planar case.

- The linearized equations of motion are time-invariant if the length of the tether is constant and time-varying if the length of the tether is changing.
- The uncontrolled response of the system is asymptotically stable during deployment, marginally stable during stationkeeping, and unstable during retrieval.
- The rank of matrix $\mathcal{T}$ is less than the number of DOFs, which means that the system is under-actuated (i.e., there are not as many free input parameters as the DOFs).

Figure 6.10 illustrates the uncontrolled motion of a tethered satellite system, with fixed manipulator. The following data were used in the numerical simulations presented in this study: $m^{orbiter} = 10^5\ kg$, $m^{links} = 20\ kg$, $m^{subsatellite} = 500\ kg$, $I_{11}^{orbiter} = 9.68 \times 10^6\ kg.m^2$, $I_{22}^{orbiter} = 1.29 \times 10^6\ kg.m^2$, $I_{33}^{orbiter} = 10.1 \times 10^6\ kg.m^2$, $I_{12}^{orbiter} = I_{13}^{orbiter} = I_{23}^{orbiter} = 0$, $L^{links} = 8.13\ m$. The stationkeeping phase is simulated for $L^{tether} = 500\ m$, and the retrieval phase for both $L^{tether} = 500e^{-0.22\theta}$ and $L^{tether} = 500 - 46\ \theta$, where θ denotes the orbital angle.

The dependence of the equations of motion on the tether length and its derivatives makes the equations of motion autonomous for the stationkeeping phase and non–autonomous for retrieval. Because of this difference in the nature of the equations, different control strategies are chosen for each phase. A standard LQR method is used to make the stationkeeping phase asymptotically stable. On the other hand, feedback linearization technique is employed to stabilize the retrieval. It is assumed that all of the states of the system are available and the actuator forces are unlimited.

6.3.2 Control of the system during stationkeeping

The equations of motion governing the stationkeeping phase have several fixed points. Here, the equations are *analytically linearized* around the fixed point $[0,0,0,0,\pi/2, \pi/4, 3\pi/4, \pi]$ to give

$$\begin{bmatrix} \overline{\mathbf{M}} & \mathbf{0} \\ \mathbf{0} & \mathbf{I} \end{bmatrix} \begin{bmatrix} \dot{\eta} \\ \dot{\xi} \end{bmatrix} = \begin{bmatrix} \overline{\mathbf{Df}}_u & \overline{\mathbf{Df}}_q \\ \mathbf{I} & \mathbf{0} \end{bmatrix} \begin{bmatrix} \eta \\ \xi \end{bmatrix} + \begin{bmatrix} \overline{\mathbf{Df}}_\tau \\ \mathbf{0} \end{bmatrix} \tau \tag{6.10}$$

in which ξ and η are small perturbations defined by $\mathbf{u} = \overline{\mathbf{u}} + \eta$, and $\mathbf{q} = \overline{\mathbf{q}} + \xi$, and $\mathbf{Df}_{\bullet}$ represents the Jacobian of $\mathbf{f}$ with respect to "$\bullet$" evaluated at the fixed point.

The fact that the linearized system is controllable permits the use of state feedback techniques. A standard LQR method is used here with different weight functions. Figures 6.11 and 6.12 show the response of the system for different values of the tether length and three different weight functions as follows:

$$\mathbf{Q} = \begin{bmatrix} k\,\overline{\mathbf{M}}_{4\times4} & 0 \\ 0 & \mathbf{H}_{4\times4} \end{bmatrix}, \qquad \mathbf{H} = \begin{bmatrix} 1 & 0 & 0 & 0 \\ 0 & 5 & 0 & 0 \\ 0 & 0 & 10 & 0 \\ 0 & 0 & 0 & 1 \end{bmatrix}, \qquad \mathbf{R} = \begin{bmatrix} 0.1 & 0 & 0 \\ 0 & 1 & 0 \\ 0 & 0 & 1 \end{bmatrix}$$

and

$\mathbf{Q}^{(1)} = \mathbf{Q}$ where $k = 1$
$\mathbf{Q}^{(2)} = \mathbf{Q}$ where $k = 25$
$\mathbf{Q}^{(3)} = \mathbf{Q}$ where $k = 50$

where $\mathbf{Q}$ is the weight function for the states and $\mathbf{R}$ is the weight function for the inputs in the objective function which is minimized in the LQR method.

The results in Figure 6.11 and 6.12 show the feasibility of using space manipulators to asymptotically stabilize the motion during stationkeeping. The rather small amount of control efforts shows that the flexibility of the manipulators would not be a major concern (elastic deformations would be small). However, for long tethers, where the required joint torques are large, the flexibility of the manipulator links should be included in the analysis.

6.3.3 Control of the system during retrieval

The equations of motion during retrieval is non-autonomous. The motion of the system during retrieval phase is unstable; moreover, it does not have, in general, any fixed point. With

this in mind, one may choose the feedback linearization technique to stabilize the system. However, no input has a direct access to the librational DOF of the tether, as can be seen from the dimension of τ in Eq.(6.9). This means that, the system is not completely feedback linearizable. One solution to this problem is to stabilize the tether motion using the other inputs, that is to linearize the equation associated with the librational tether angle using the other inputs. This, however shifts the instability from the tether to the rest of the system and cannot be considered as a good solution. Another approach, which has been successfully applied to some simple systems encountering the same problem, is to transform the equations under a specific nonlinear transformation, which makes the inputs capable of complete feedback linearization of the new system (for example, see Spong and Vidyasagar[1989]). The existence of the transformation is subject to the validity of certain conditions on the mass matrix and force vector. However, the complexity of this system leaves no room for this approach. Besides, even if one accepts to undertake the burden of the analysis, there is still no guarantee that the conditions are met or the nonlinear transformation can be found. A third approach is to use a *modified* feedback linearization technique as follows.

The set of nonlinear differential equations

$$\mathbf{M}\dot{\mathbf{u}} = \mathbf{f} + \mathcal{T}\tau \tag{6.11}$$

can be linearized by choosing τ such that

$$\mathcal{T}\tau = -\mathbf{f} - \mathbf{M}\mathbf{L} \tag{6.12}$$

where

$$\mathbf{L} = \mathbf{D}\mathbf{u} + \Lambda(\mathbf{q} - \overline{\mathbf{q}}) \tag{6.13}$$

in which, $\mathbf{D}$ and Λ are positive definite matrices, usually chosen to be diagonal. However, if the rank of $\mathcal{T}$ is less than the number of DOFs, then Eq.(6.12) would be an overdetermined set of equations and has no unique solution. In this case, we may choose to find $\overline{\tau}$ such that the index ε, defined as:

$$\varepsilon = (\mathcal{T}\bar{\tau} + \mathbf{f} + \mathbf{M}\mathbf{L})^T \mathbf{Q} (\mathcal{T}\bar{\tau} + \mathbf{f} + \mathbf{M}\mathbf{L}), \tag{6.14}$$

is minimized. The matrix $\mathbf{Q} > 0$ in Eq.(6.14) is the weight function, which can be simply chosen as the identity matrix. Using this $\bar{\tau}$ as the input to the system gives

$$\mathbf{M}\dot{\mathbf{u}} = \mathbf{f} + \mathcal{T}\bar{\tau} \equiv -\mathbf{M}\mathbf{L} \tag{6.15}$$

It is worth mentioning that this method does not guarantee the asymptotic stability of the system; instead, it tries to narrow the gap, in an optimum sense, between the response of the system with that of a completely linearized system, $\dot{\mathbf{u}} + \mathbf{L} = \mathbf{0}$.

Figures 6.13 and 6.14 present the simulation results for retrieval phases using the above method. The results show that the method can be used in a sequential retrieval-stationkeeping procedure to successfully retrieve the subsatellite. These results show some sharp jumps in the actuator torques, which occur at the beginning of each stationkeeping period. This suggests that, in practice, to avoid actuator saturation due to this sharp jumps, the maneuver should be scheduled such that the controlled stationkeeping phase starts before the system gains certain amount of energy during the retrieval phase. It is also evident that shorter tethers are easier to control (demand less control effort and induce smaller motion in the rest of the system). The results also reveal that a *multi-step* retrieval–stationkeeping gives better results than retrieving the same length in one step followed by a period of controlled stationkeeping (see Figure 6.13). Comparison of the simulation results for retrieving the subsatellite with exponential and constant rate (Figure 6.14) shows that the exponential rate gives better performance both in terms of the motion and the required actuator torques.

6.4 Modeling and Simulation of a Redundant Space Manipulator

The objective of this study is to develop the dynamical model of a system with several rigid and elastic degrees of freedom. This study may serve to verify the capability of the

computer code FLXISM in handling complicated dynamical systems. The system under consideration, shown in Figure 6.15, is a large space manipulator which has eight links connected through seven revolute joints, arranged in a three-dimensional configuration. This manipulator resembles the Space Station Remote Manipulator System (SSRMS) which is supposed to serve on the space station Alpha. Out of the eight links of the manipulator, links 4 and 5 (long booms) may, in practice, exhibit elastic behavior. Besides, due to the rather high gear ratio of the joints ($\omega_{in}/\omega_{out} = 1700$), the effect of joint flexibility is significant. Thus, even a basic, simplified dynamical model for this system must include the effects of joint and link flexibility.

The system has seven rigid DOFs, joint angles. To account for the effect of joint flexibility, the joints of the system, which are identical, are modeled as second order systems (mass-spring). This means that each joint has one additional DOF (flexible DOF). In addition to the above fourteen DOFs, the system has, at least, six elastic DOFs due to in-plane, out-of-plane, and rotational elastic vibrations of links 4 and 5 (assumed-mode method is used here to model the elastic behavior of the booms).

The motion of the system can be fully described by the definition of twenty generalized coordinates as follows:

$q_1,\ldots,q_7 \equiv \theta_1,\ldots,\theta_7$	joint angles,
$q_8,\ldots,q_{14} \equiv \gamma_1,\ldots,\gamma_7$	motor angles,
q_{15}	torsion of link 4 (tip deflection),
q_{16}	out-of-plane bending of link 4 (tip deflection),
q_{17}	in-plane bending of link 4 (tip deflection),
q_{18}	torsion of link 5 (tip deflection),
q_{19}	out-of-plane bending of link 5 (tip deflection),

q_{20} in-plane bending of link 5 (tip deflection).

The generalized speeds of the system are simply defined as the time derivatives of the generalized coordinates of the system (i.e., $u_i = \dot{q}_i$, $i = 1,\ldots,20$).

Figure 6.16 illustrates the definition of the joint and motor angles ($q_1,\ldots,q_{14}$). The joint and motor angles (θ_i and γ_i) are related as $\delta_i = \gamma_i - r\theta_i$, where r and δ_i are, respectively, the gear ratio of the gearbox and the elastic rotational deflection of the gearbox as seen from its input side. If the joint flexibility is neglected, then δ_i vanishes.

The long booms of the manipulator (links 4 and 5) are modeled as Euler-Bernoulli beams. As stated earlier, the assumed mode method is used to relate the elastic deflections to the elastic generalized coordinates as follows:

$$\begin{aligned} \phi_4 &= \varphi q_{15}, & \phi_5 &= \varphi q_{18}, \\ w_{4y} &= \psi q_{16}, & w_{5y} &= \psi q_{19}, \\ w_{4z} &= \psi q_{17}, & w_{5z} &= \psi q_{20}. \end{aligned} \tag{6.16}$$

in which ϕ_i, w_{iy}, and w_{iz} are, respectively, the elastic torsion and the elastic deflections in Y and Z directions associated with the i-th link. Moreover, φ, and ψ are shape functions which are chosen as follows:

$$\begin{aligned} \varphi &= \sin(\pi\xi/2) \\ \psi &= A\left[(\cosh(\lambda\xi) - \cos(\lambda\xi)) - \sigma(\sinh(\lambda\xi) - \sin(\lambda\xi))\right] \end{aligned} \tag{6.17}$$

in which $A = 0.5$, $\lambda = 1.875$, $\sigma = (\cosh\lambda + \cos\lambda)/(\sinh\lambda + \sin\lambda)$, and $\xi = x/L$, where x and L are the spatial variable and the length of the beam.

On the other hand, the joints of the system are modeled as mass-spring systems. Figure 6.17 illustrates a schematic of the i-th flexible joint of the manipulator. In this figure the torques τ_{m_i}, τ_{s_i}, and τ_i are the motor torque, the spring torque and the joint torque (the torque delivered to the i+1^{-st} link), respectively. It is assumed that:

- The gearbox inertia is included in J_m, the motor inertia.
- The stiffness of both motor and gearbox are replaced by a spring which is located between motor (pure inertia) and the gearbox (pure transformer), see Figure 6.17.

According to this model, the motor torque is the input to the system, the joint torque, $\tau_i = r\,\tau_{s_i}$, is the torque which drives the next link, and the spring torque, τ_{s_i}, is a function of the elastic rotational deflection, δ_i, defined as

$$\tau_{s_i} = \begin{cases} 0.07\ \mathrm{sgn}(\delta_i)\ \delta_i^2 & |\delta_i| < 1.5\,rad, \\ \mathrm{sgn}(\delta_i)(0.4\,\delta_i - 0.4425) & |\delta_i| \geq 1.5\,rad \end{cases} \tag{6.18}$$

where "sgn" denotes the sign function.

Figures 6.18 to 6.21 show the simulation results for a typical maneuver for the system. The data of the system, which are used in this simulation, are presented in Table 6.1. In this maneuver the manipulator is employed to retrieve a heavy payload along a straight line (here, X axis). This maneuver resembles the docking of Shuttle with the Space Station Alpha using the SSRMS. In this simulation it is assumed that both orbital and attitude motions of the Space Station are unchanged during the maneuver.

Initially, the manipulator is in straight-out configuration ($q_i = 0, i = 1,\ldots,20$), and both manipulator and payload are at rest, with respect to the Space Station. Although the nominal maneuver is planar, the actual maneuver is three dimensional. That is due to the presence of flexibility in joints and links and the spatial configuration of the manipulator. The maneuver is accomplished by an open-loop control, with the actuator torques evaluated using the inverse dynamics of the rigid model of the manipulator.

Table 6.1 Redundant space manipulator, the characteristic data.

Descr.	Mass (Kg)	Length (m)	Central moment of inertia (Kg. m^2)		
			I_{11}	I_{22}	I_{33}
Link 1	207	1.2	6.4	30.6	30.6
Link 2	90	0.6	8.4	8.1	2.1
Link 3	90	0.5	5.6	2.1	5.8
Link 4	160	7	-	-	-
Link 5	160	7	-	-	-
Link 6	90	0.5	5.6	2.1	5.8
Link 7	90	0.6	8.4	8.1	2.1
Link 8	207	1.2	6.4	30.6	30.6
Payload	90000	1.4	9.68×10^6	1.29×10^6	10.1×10^6

$r = 1700$ (m) Gearbox ratio

$J_m = 2\times10^{-4}$ (Kg.m^2) Motor inertia

$M_J = 90$ (Kg) Mass of joints (motor and gearbox)

$EI = 2.5\times10^6$ (N.m^2) Flexural rigidity of long booms

$GJ = 1.27\times10^6$ (N.m^2) Torsional rigidity of long booms

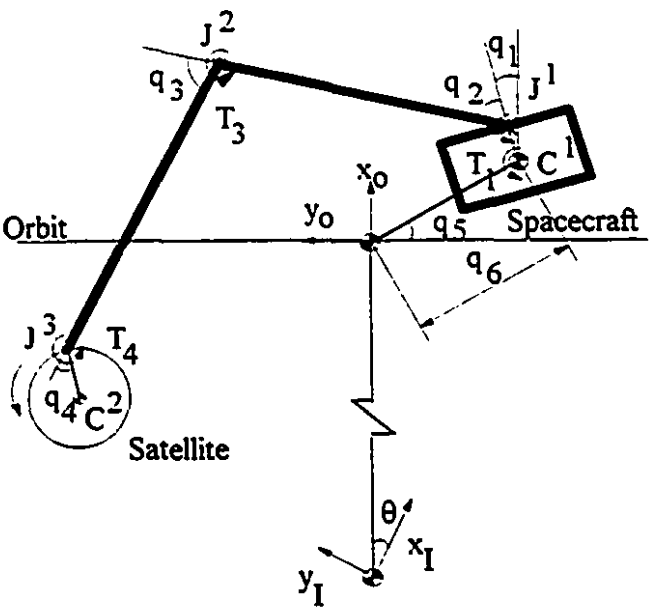

Figure 6.1 Capturing a spinning satellite, the system configuration

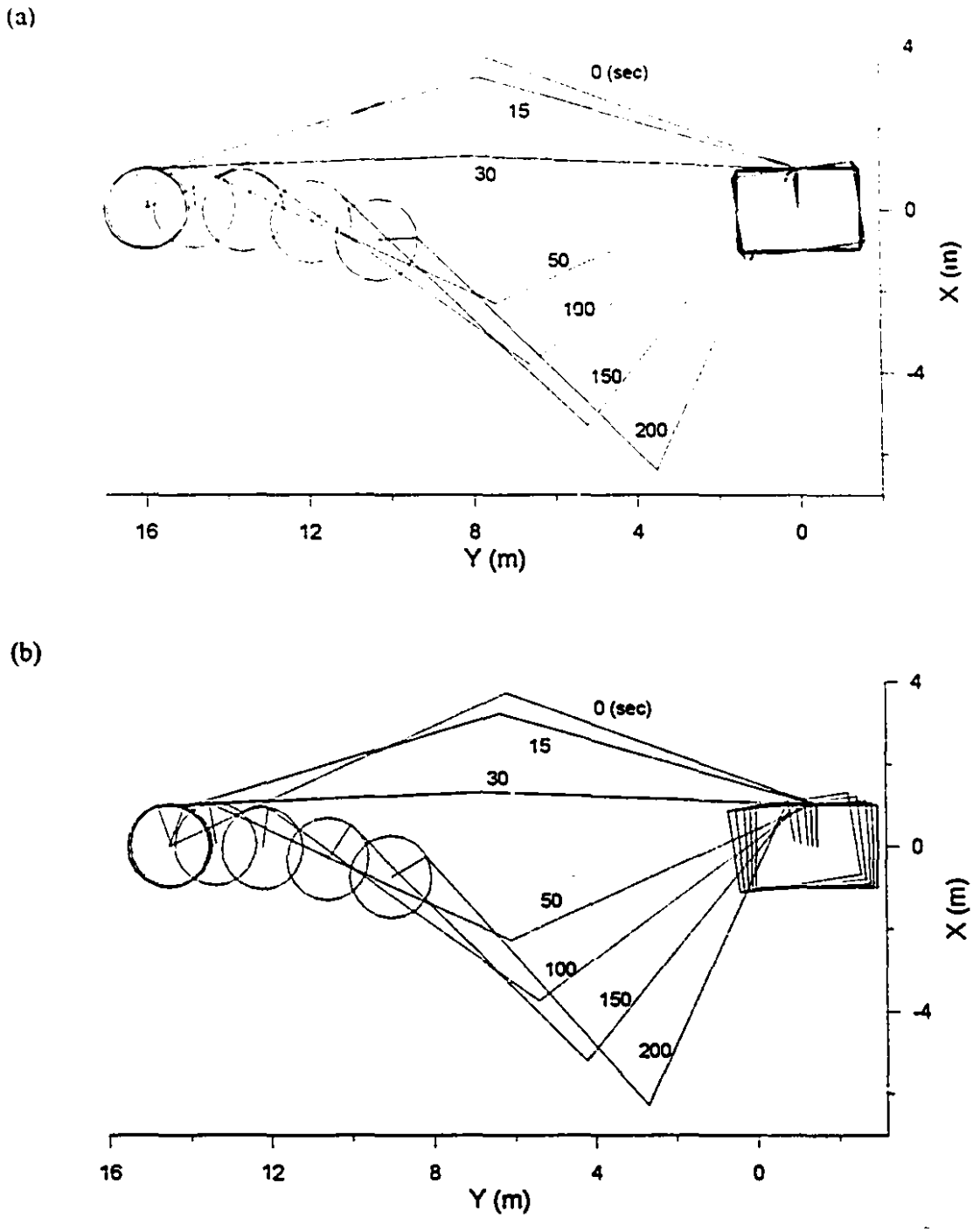

Figure 6.2 Simulation of the uncontrolled capturing process with a rigid manipulator: (a) case 1, spacecraft center of mass has the prescribed orbit; (b) case 3, entire system's center of mass has the prescribed orbit.

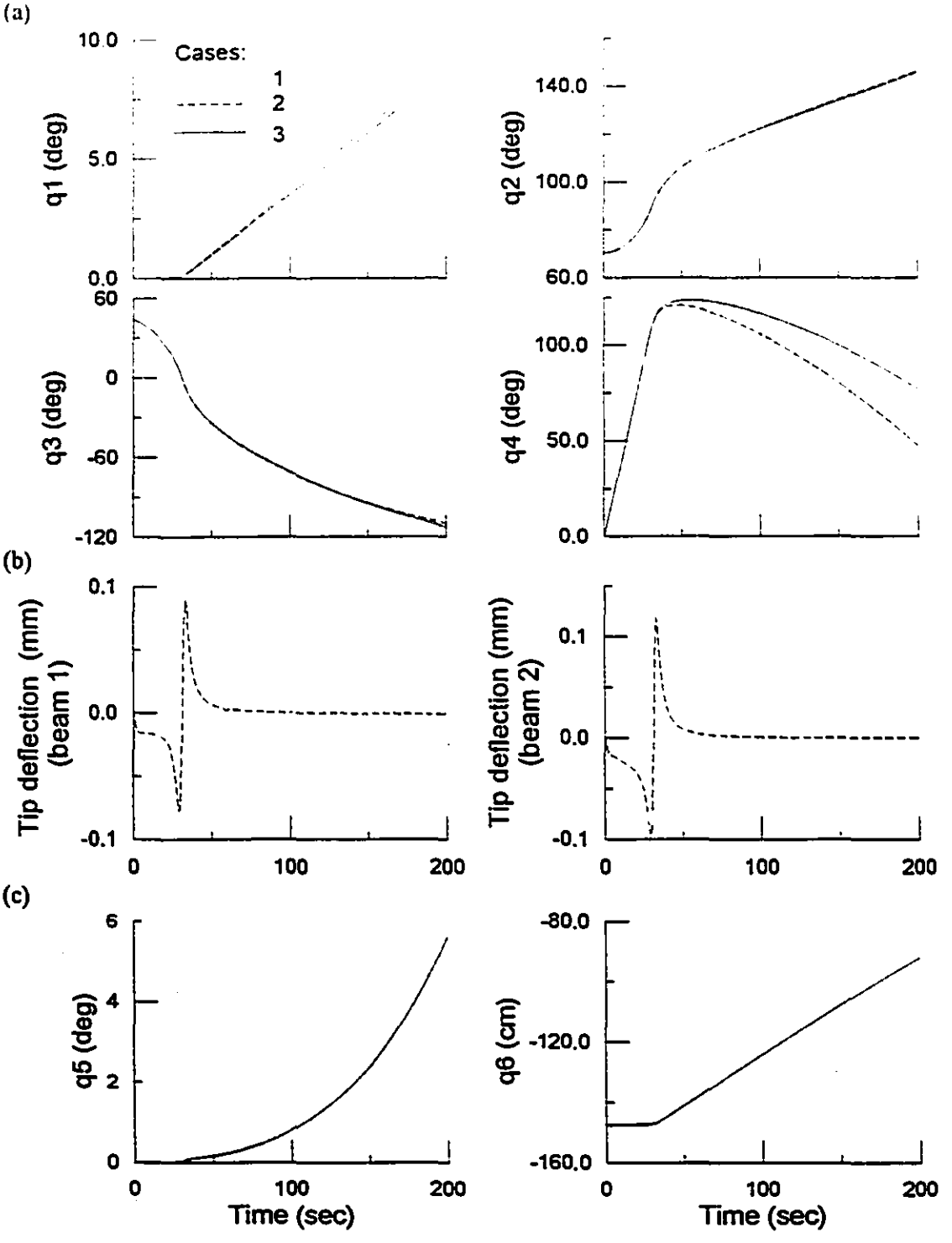

Figure 6.3 Time history of the uncontrolled capturing process: (a) joint angles, cases 1, 2, and 3; (b) tip deflection, case 2; (c) spacecraft position, case 3.

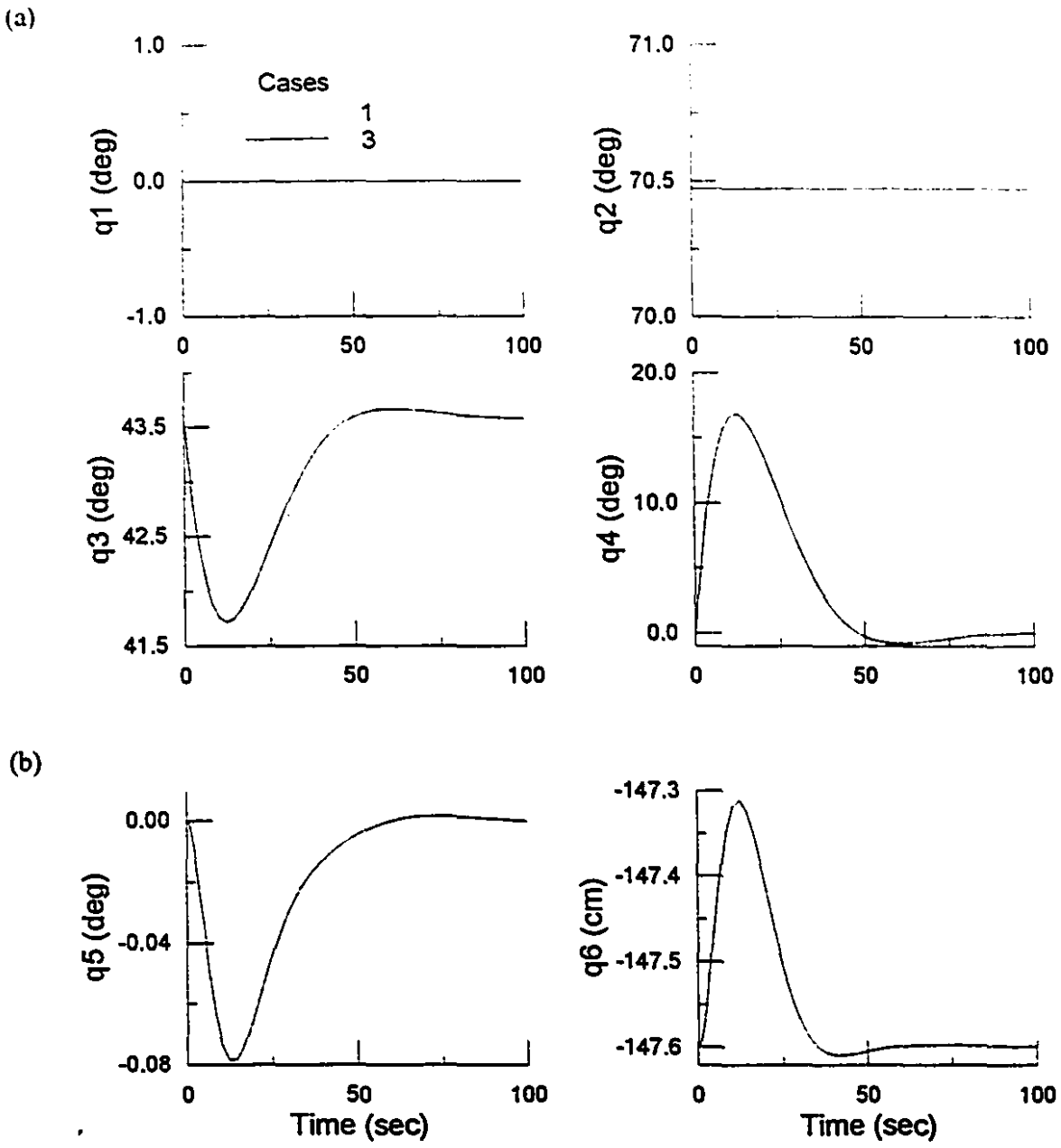

Figure 6.4 Simulation of the controlled motion during the post-capture phase: (a) joint angles, cases 1 and 3; (b) spacecraft position, case 3.

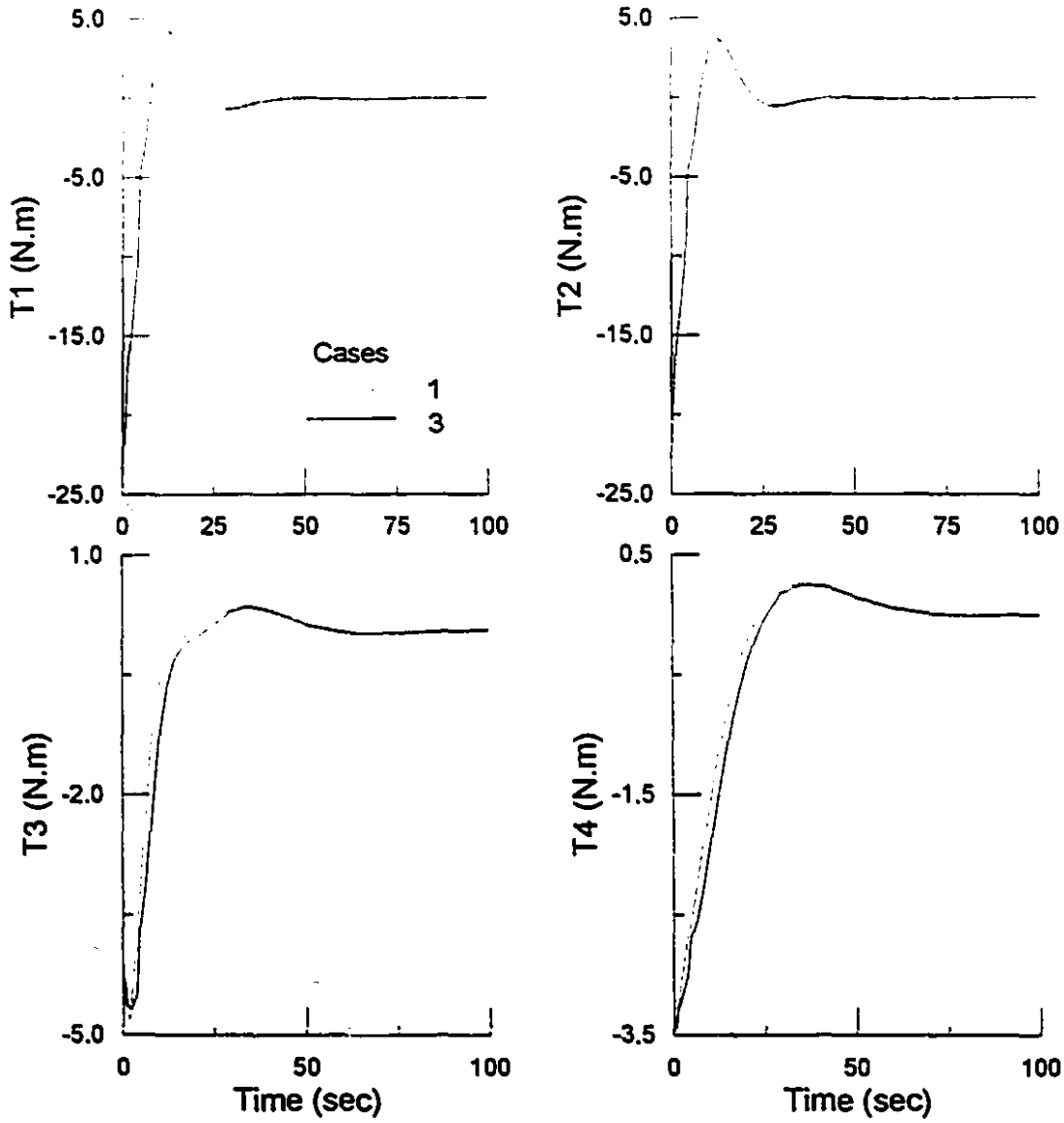

Figure 6.5 Time history of the actuator torques in the post-capture phase, cases 1 and 3.

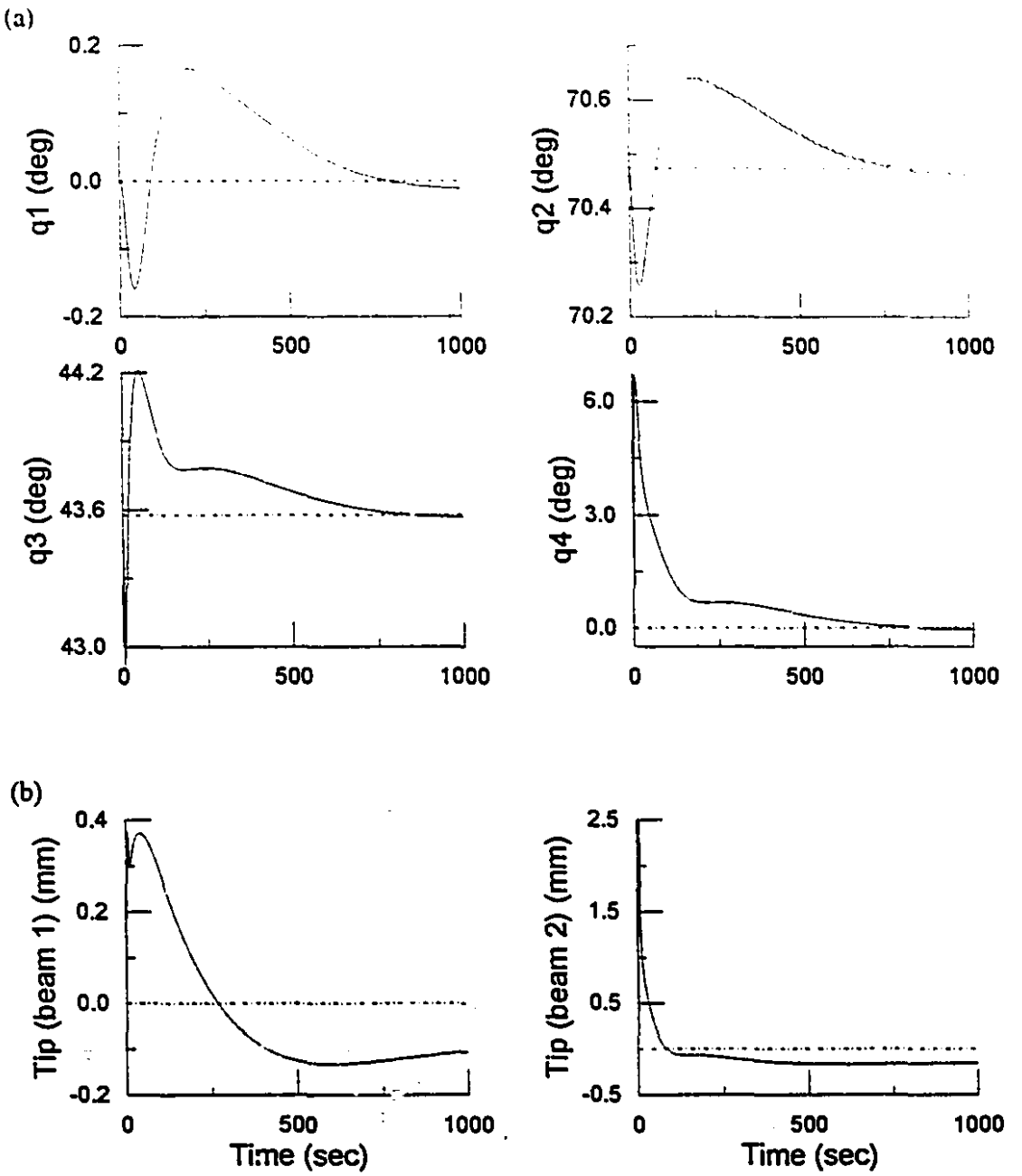

Figure 6.6 Simulation of the controlled motion in the post-capture phase, case 2: (a) joint angles; (b) tip deflection.

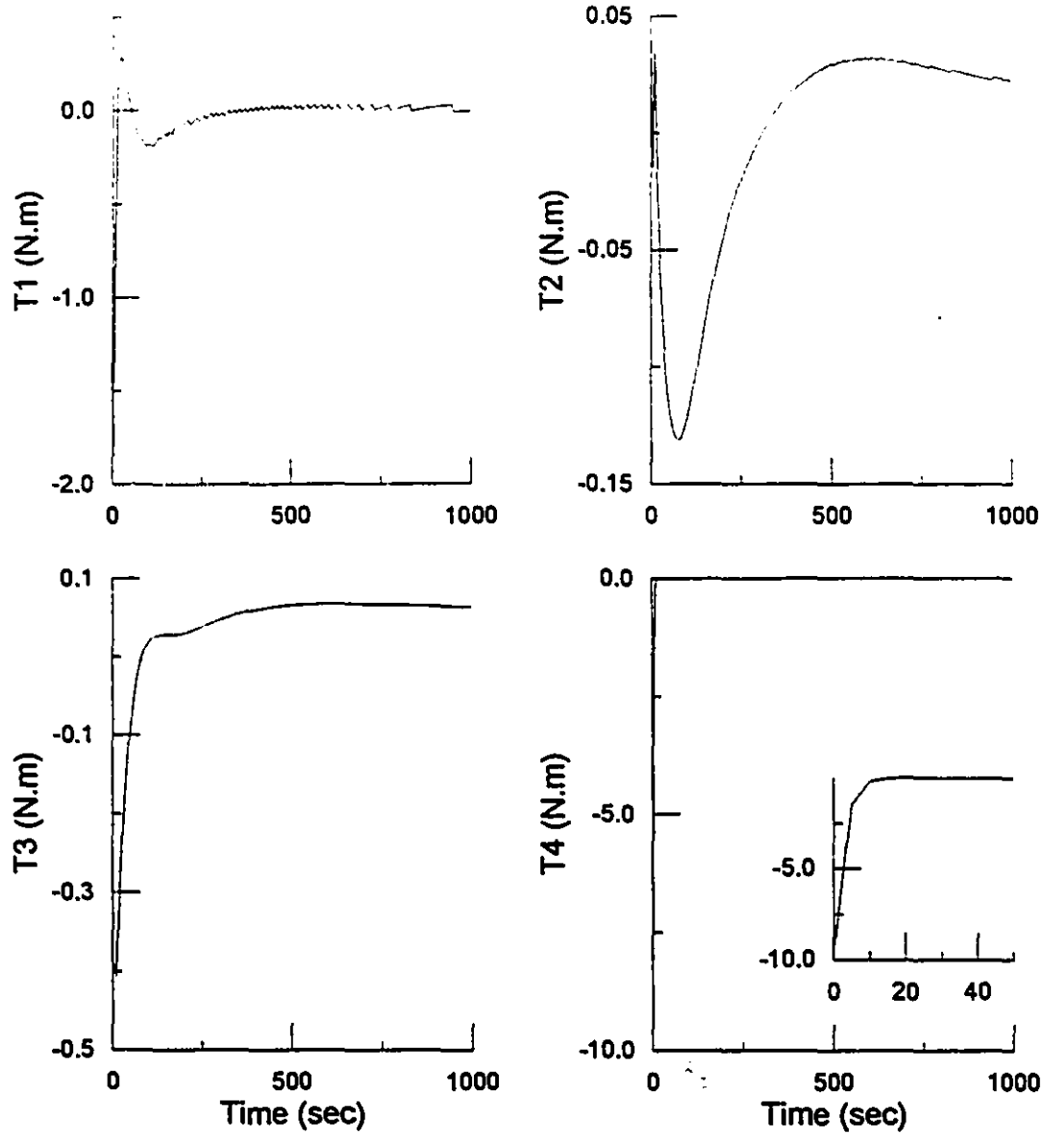

Figure 6.7 Time history of the actuator torques in the post-capture phase, case 2.

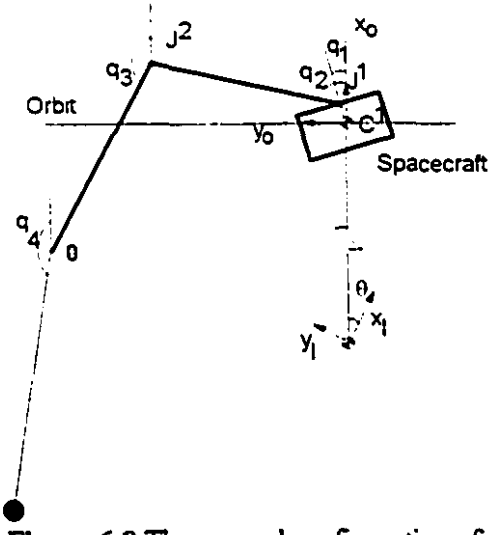

Figure 6.8 The general configuration of a TSS being controlled using a manipulator.

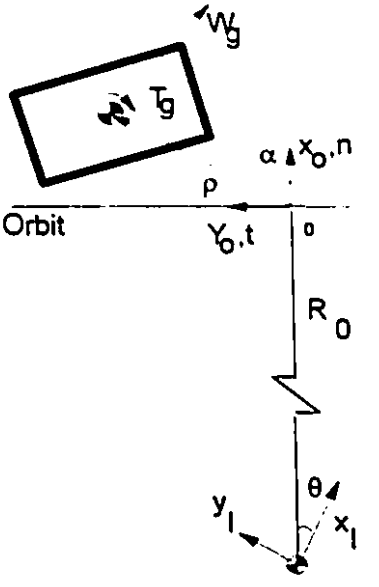

Figure 6.9 Gravitational forces applied on a rigid body, considering the effect of gravity gradient.

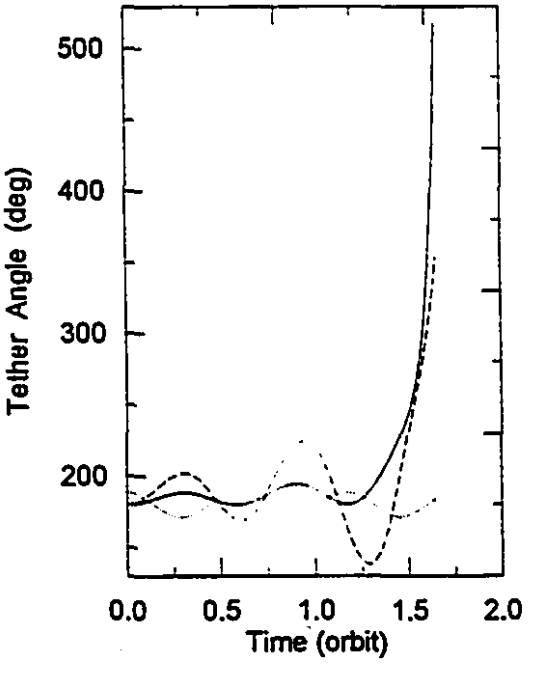

Figure 6.10 Uncontrolled motion of a tethered satellite system; dotted line: stationkeeping; dashed line: retrieval with exponential rate; solid line: retrieval with constant rate.

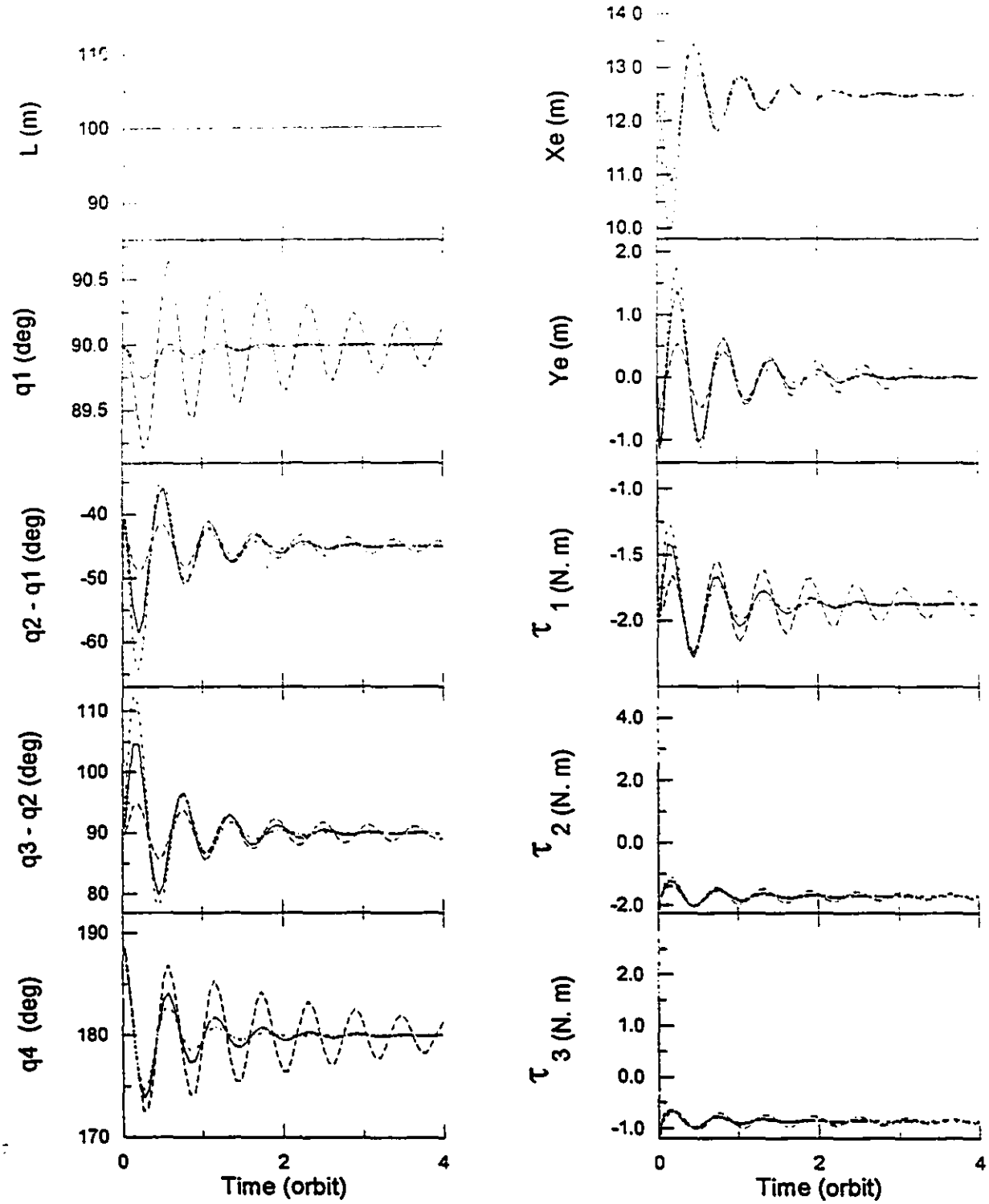

Figure 6.11 Stationkeeping at L=100 m, controlled motion, with different feedback gains; dotted line: Q_1, solid line: Q_2, dash-dotted line: Q_3. Time history of tether length, DOFs, end effector position in the orbital frame (Xe and Ye), and torques.

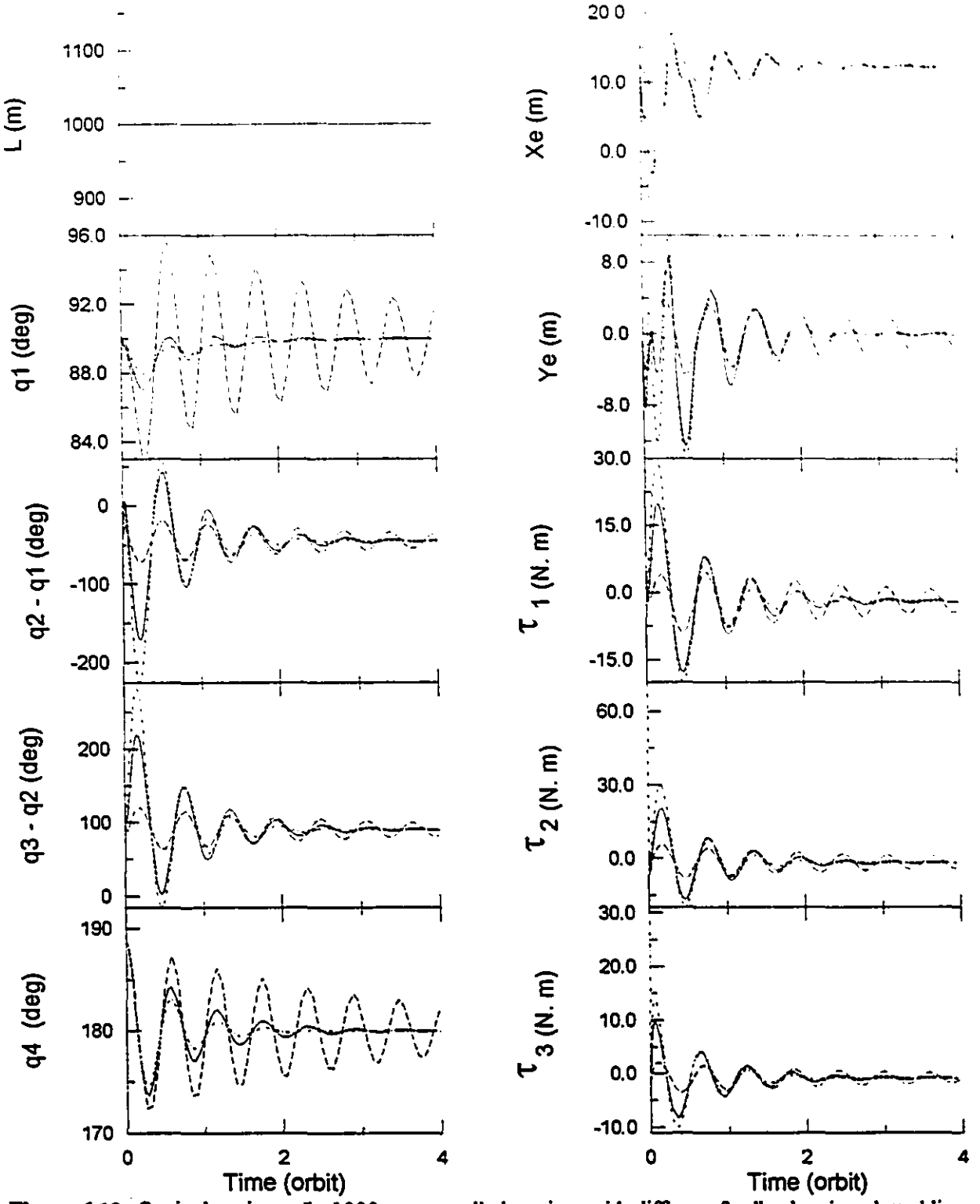

Figure 6.12 Stationkeeping at L=1000 m, controlled motion, with different feedback gains; dotted line: Q_1, solid line: Q_2, dash-dotted line: Q_3. Time history of tether length, DOFs, end effector position in the orbital frame (Xe and Ye), and torques.

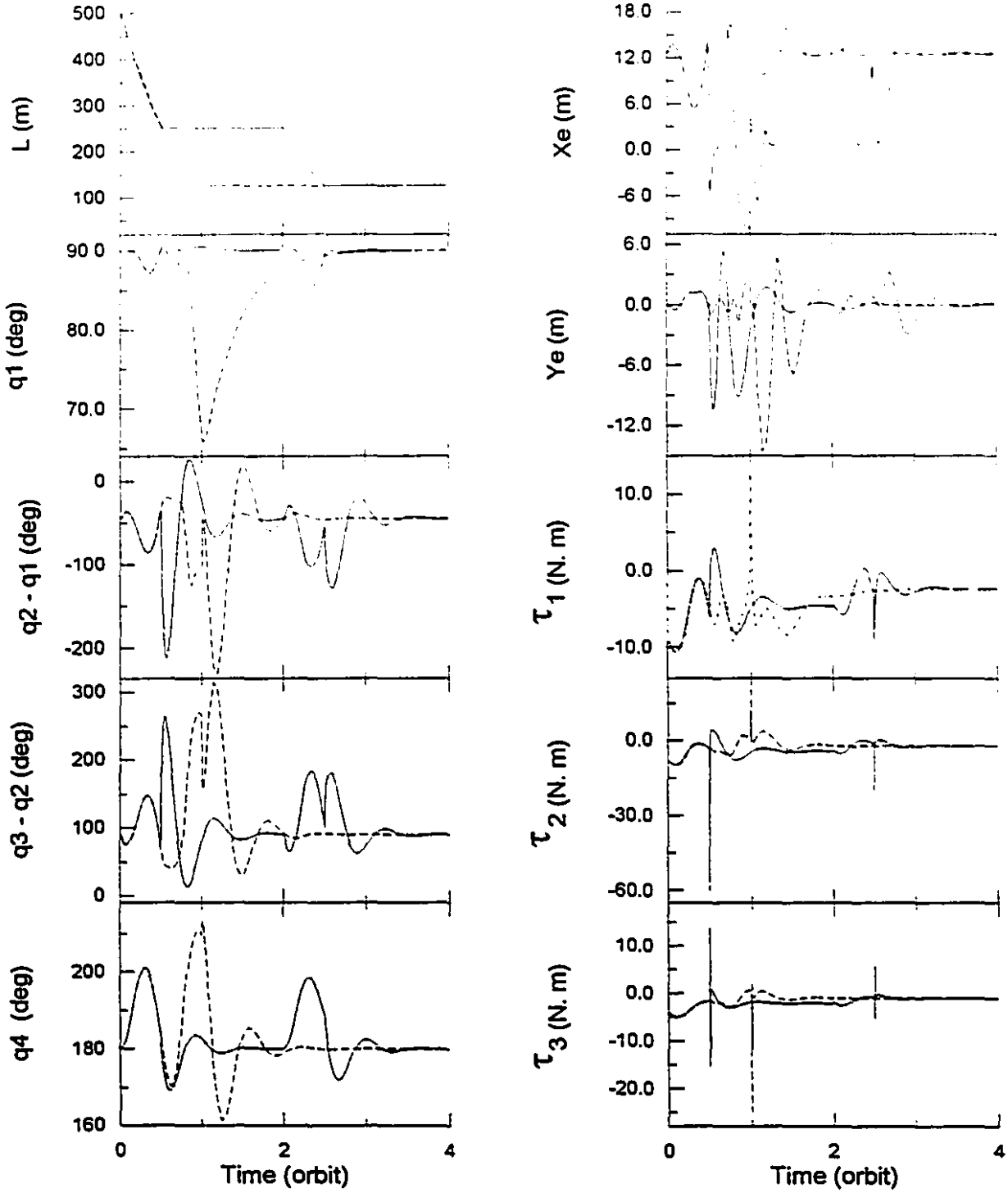

Figure 6.13 Comparison between one-step and multi-step retrieving; dotted line: single-step, solid line: multi-step. Time history of tether length, DOFs, end effector position in orbital frame (Xe and Ye), and torques.

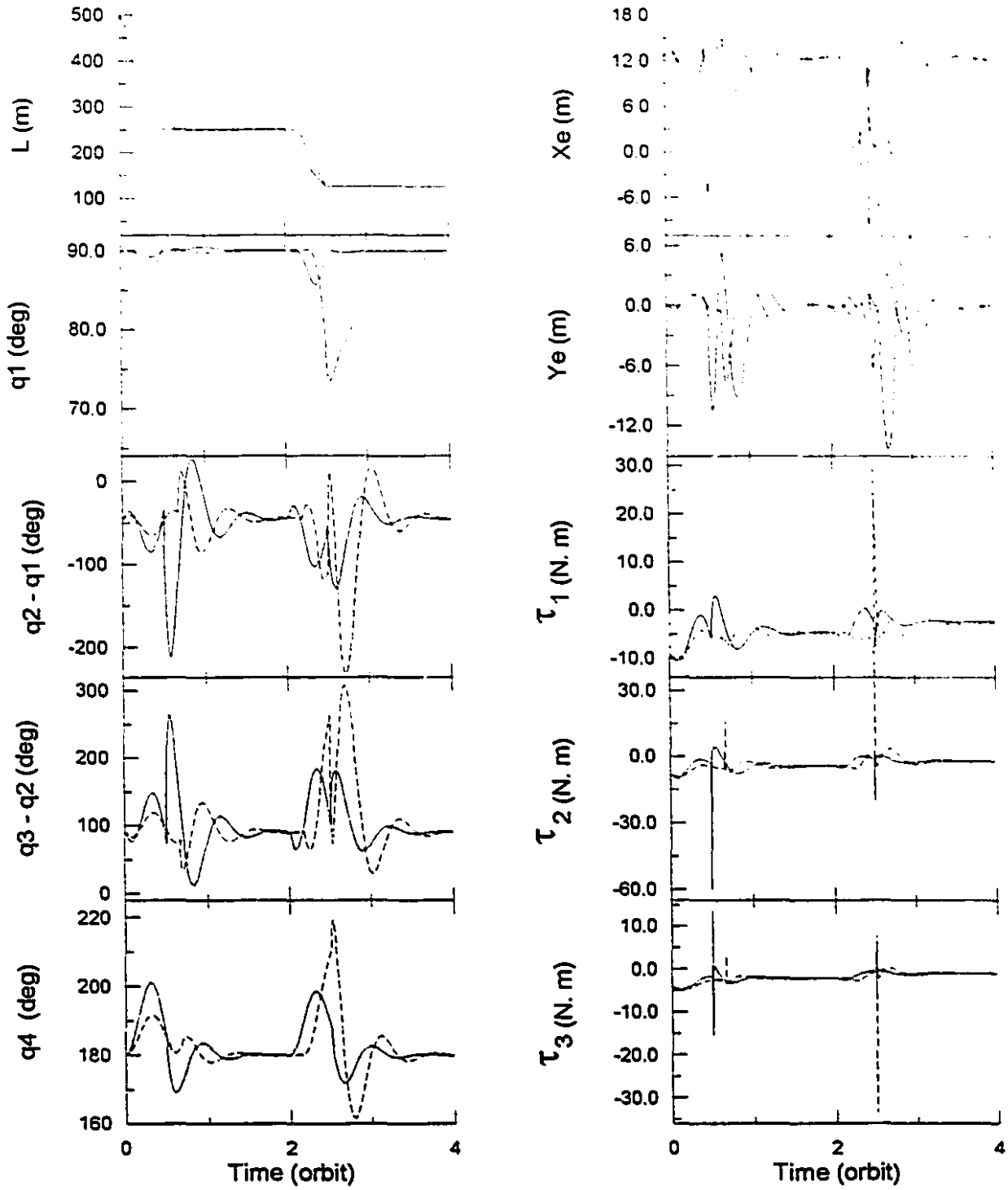

Figure 6.14 Comparison of different retrieval profiles; dotted line: constant rate, solid line: exponential rate. Time history of tether length, DOFs, end effector position in orbital frame (Xe and Ye), and torques.

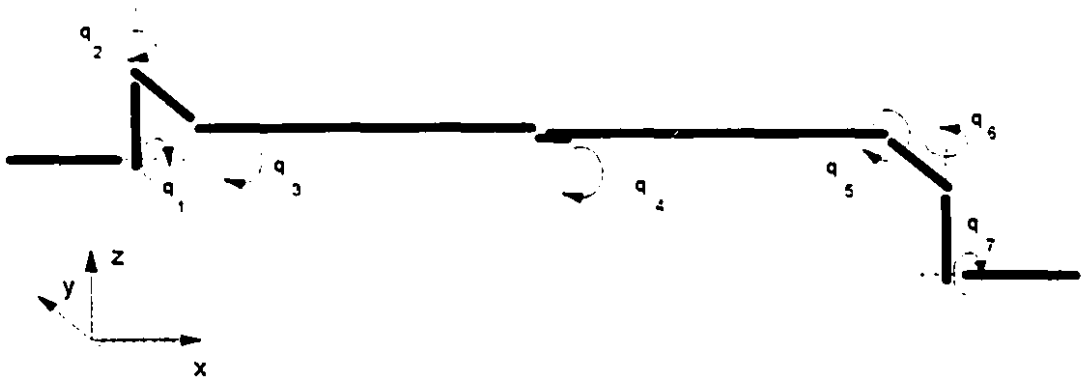

Figure 6.15 Schematic of a spatial, seven-revolute-joint manipulator in straight-out configuration.

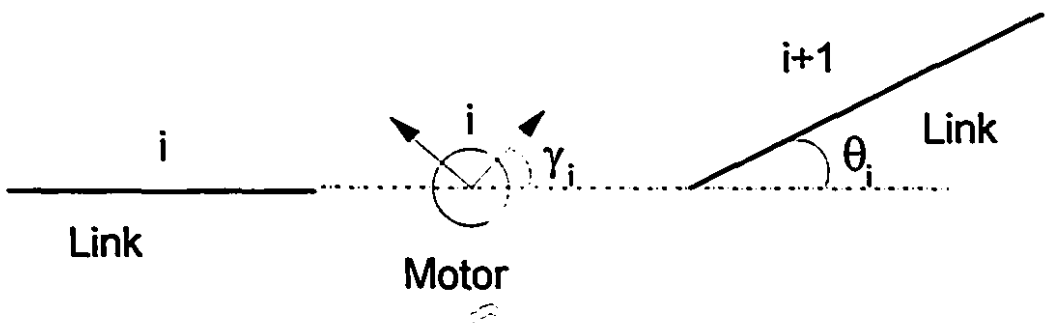

Figure 6.16 Schematic of a flexible joint, definition of the motor and joint angles.

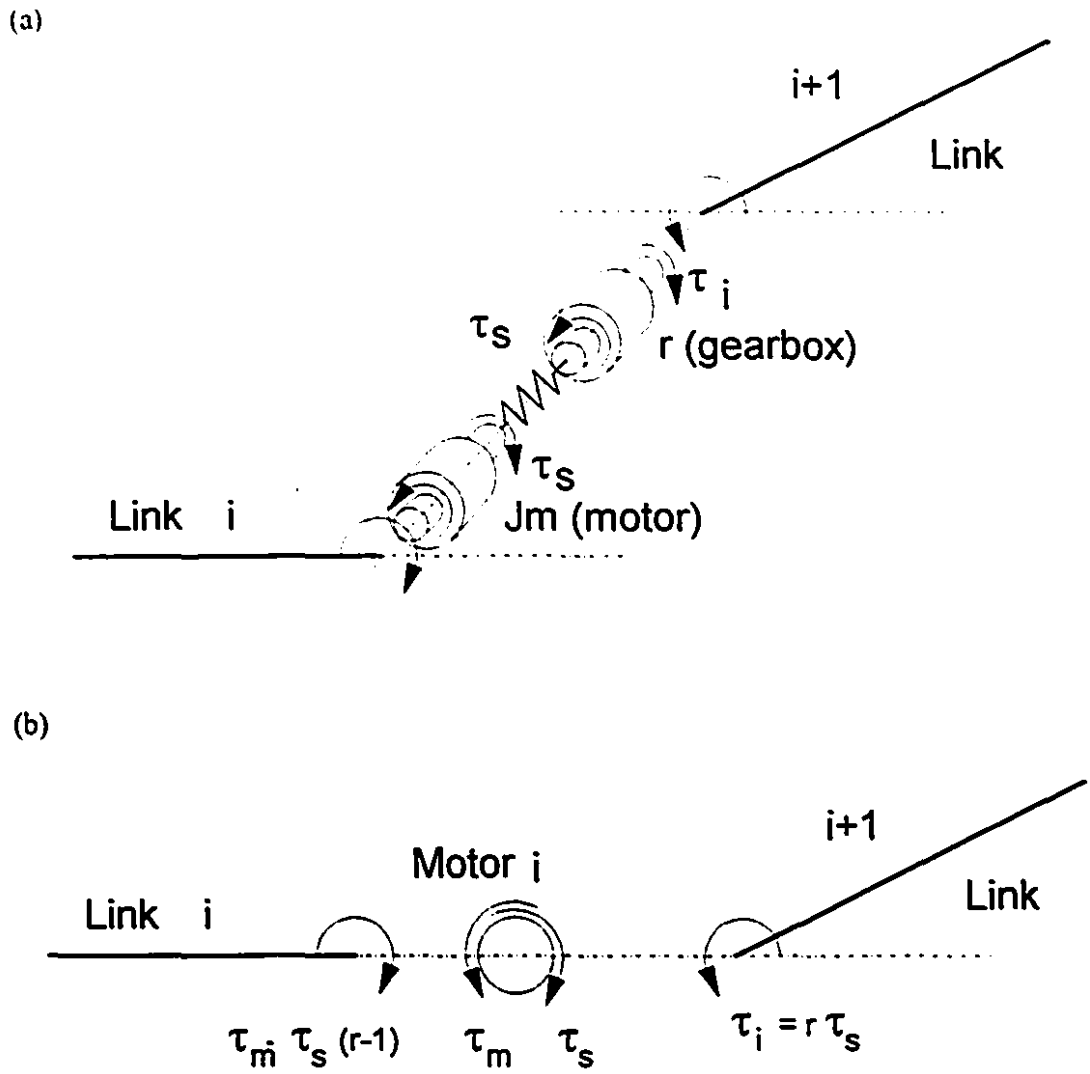

Figure 6.17 Schematic of a flexible joint: (a) the mass-spring model; (b) the free-body diagram of the elements of the joint.

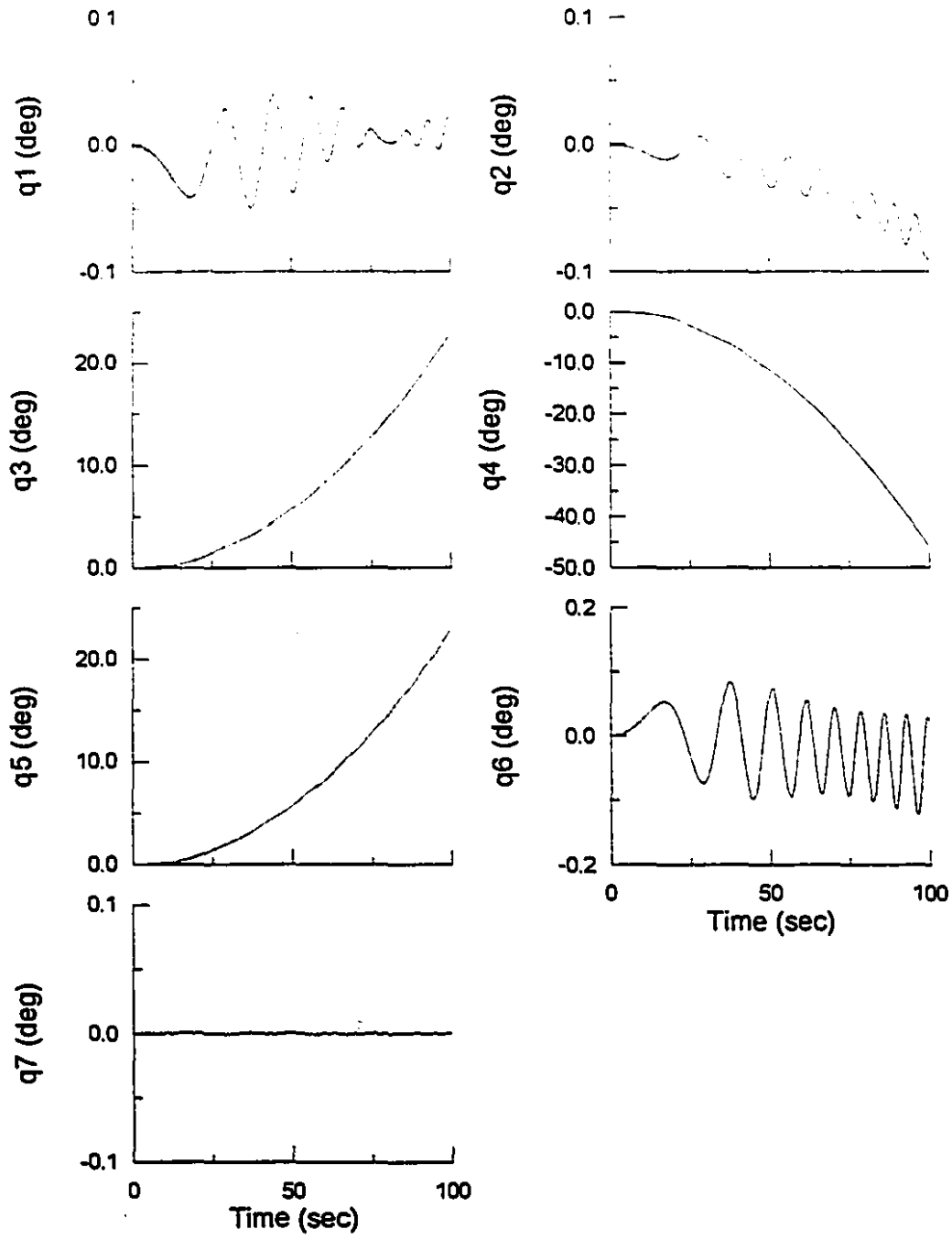

Figure 6.18 Simulation of the seven-revolute-joint, flexible manipulator: time history of the joint angles.

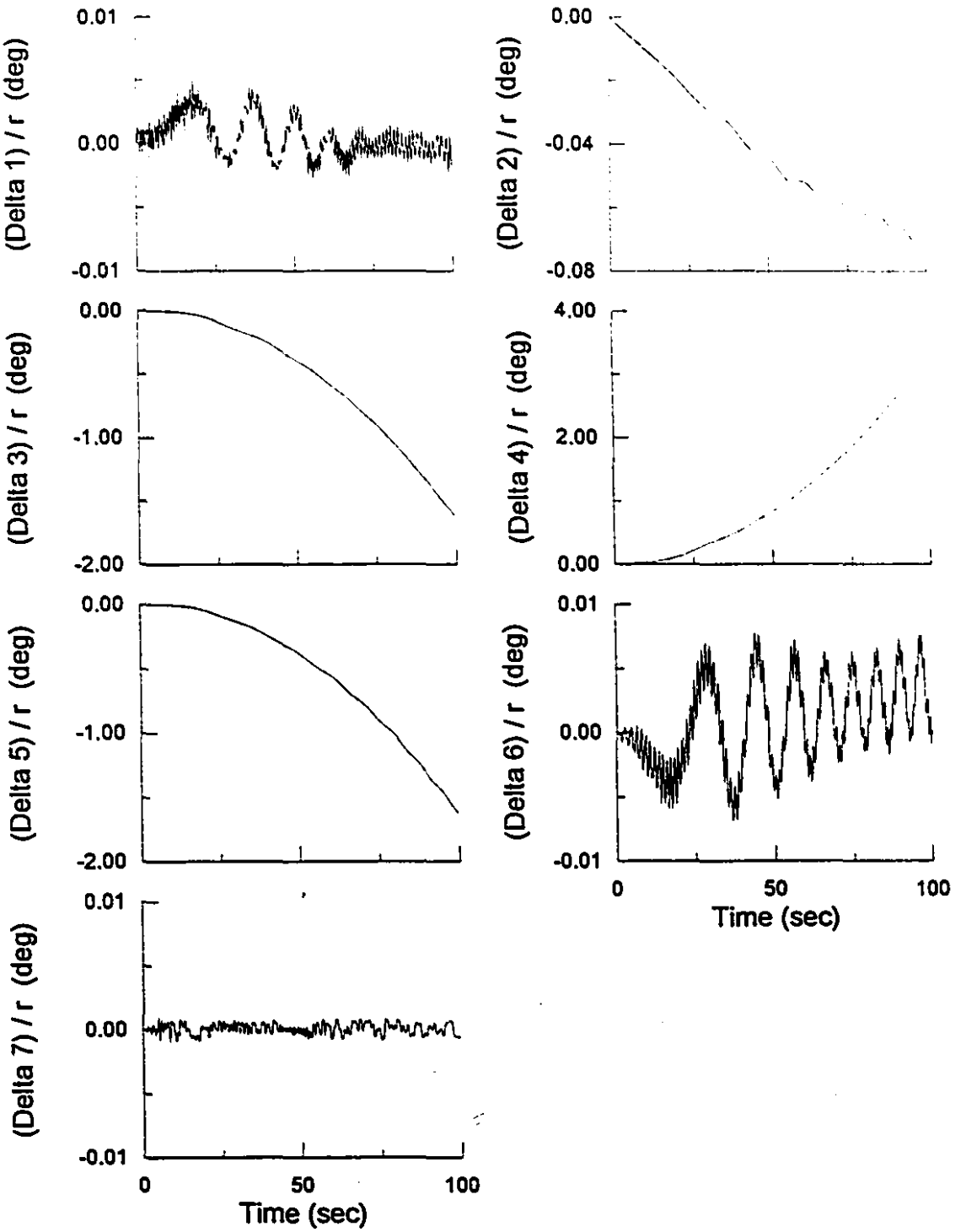

Figure 6.19 Simulation of the seven-revolute-joint, flexible manipulator: time history of elastic deflections of the joints as seen from the gearbox output, $\delta_i/r = \gamma_i/r - \theta_i$.

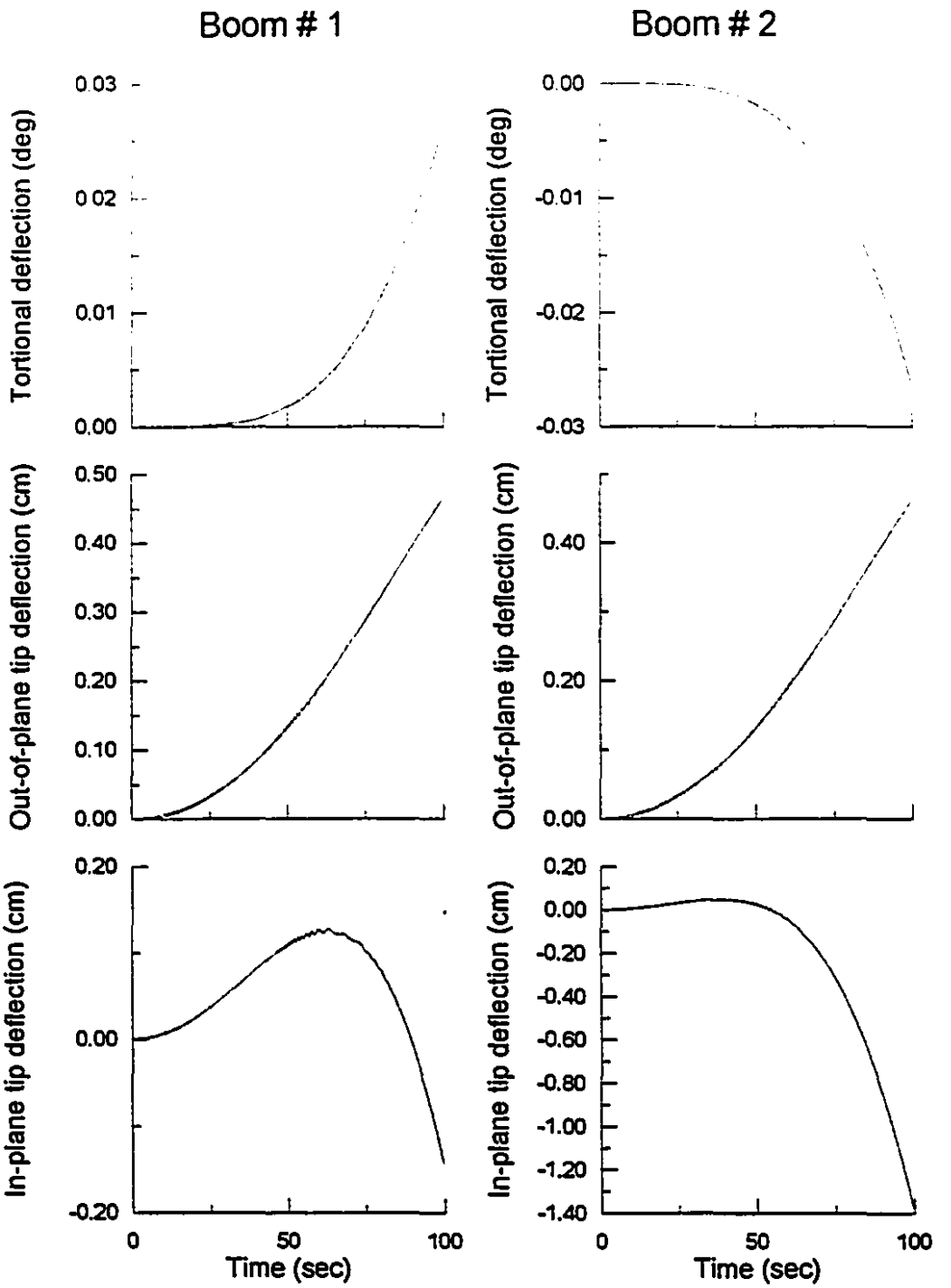

Figure 6.20 Simulation of the seven-revolute-joint, flexible manipulator: time history of the elastic deflections of the long booms.

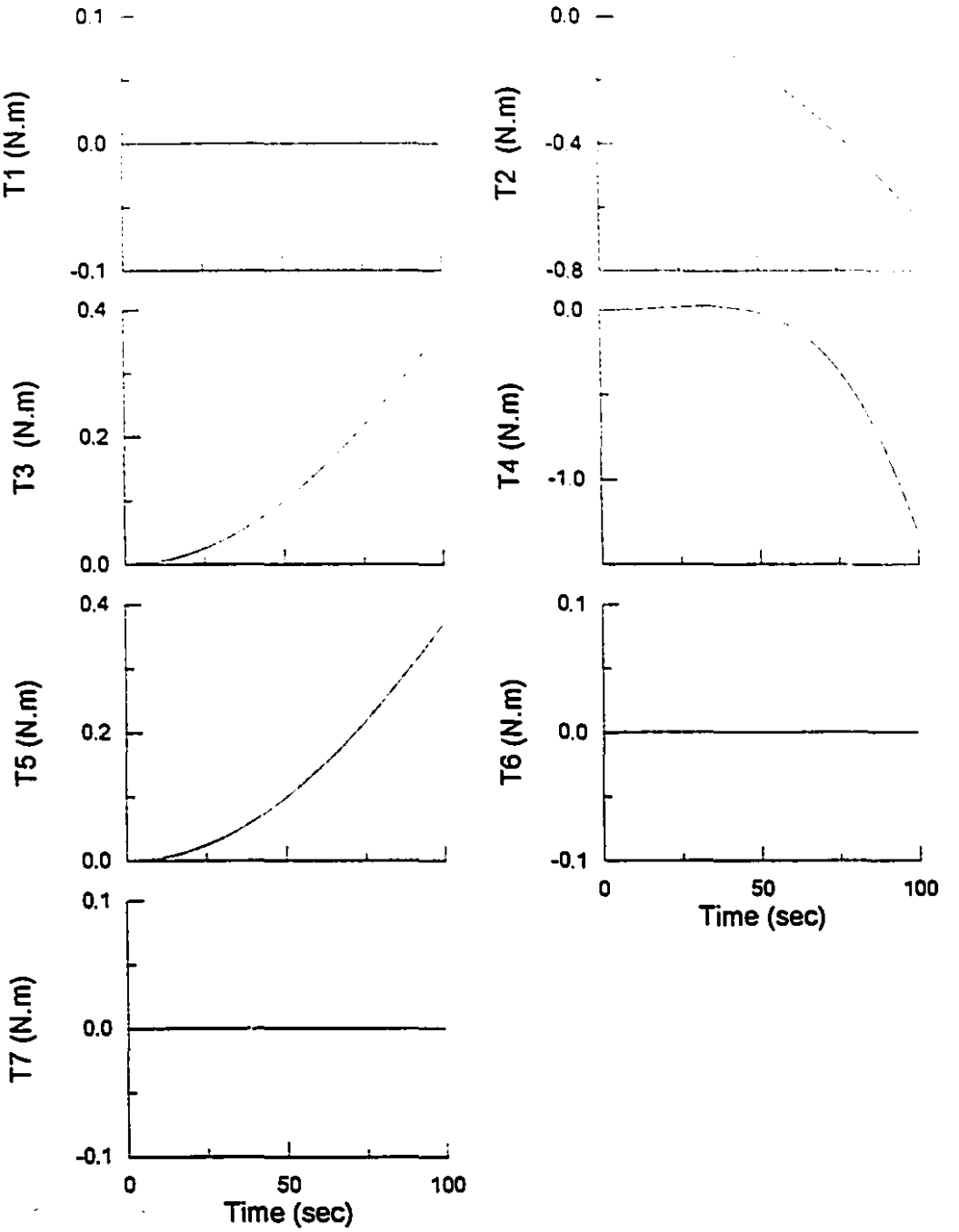

Figure 6.21 Simulation of the seven-revolute-joint, flexible manipulator: time history of the actuator torques.

Chapter 7

Application of Constrained Motion in the Control of Flexible Structures

7.1 Introduction

In Chapter 3 a new method was introduced for developing the minimum-order set of equations of motion for systems with both artificial and natural constraints. The proposed method can find several applications in position and force control of robots (see Craig [1989] and Raibert and Graig [1981]). This chapter presents an interesting application of that method in the position control of flexible manipulators.

In practice, there are cases where maintaining a nominal trajectory of a system during the entire interval of motion is important. Preserving the direction of an antenna during the maneuver of a satellite and moving the end effector of a manipulator along a prescribed trajectory are typical examples of this sort of problems, which are also referred to as tracking problems. One way of achieving an accurate tracking of the output trajectory is to track all of the states of the system in a way that the desired output is generated. This can be accomplished via a feedback linearization technique, provided that the system is not under-actuated (i.e., the number of independent inputs is not less than the number of degrees of freedom of the system).

In contrast to rigid-body systems, feedback linearization technique does not guarantee an accurate tracking of the output for flexible systems, which are normally under-actuated.

Another approach for tracking problems, which is introduced in this chapter, is to consider the equations which describe the desired trajectories as some constraints on the motion of the system. Due to the imposition of constraints, some of the DOFs of the system, as many as the number of the constraint equations, become dependent on the others. In this approach, the states do not have to follow prescribed trajectories to ensure tracking of the output, but the dependent states are always determined such that the constraints are satisfied, or in other words, the desired output trajectory is perfectly tracked.

To apply this method, one has to recognize the input forces which have the potential to act as the constraint forces, and to obtain the relations which give the magnitude of the inputs in terms of the states of the system. Next, the minimum-order equations of motion of the constrained system, which is an *artificially* constrained one, has to be developed. This set of equations can then be employed to manipulate the system, while the tracking of the desired trajectory is assured by imposition of constraints. The method presented in Chapter 3 for deriving the equations of motion of artificially constrained systems can provide us with both the equations of motion of the constrained system and the expressions for constraint forces.

The approach presented in this chapter has two advantages which are due to the fact that, to have a desired trajectory tracked by the output, the states do not have to follow prescribed trajectories. The first advantage is that one can use any arbitrary type of control scheme to manipulate the independent states of the system without being concerned about violating the prescribed evolution of the output. The second advantage is that to track a desired trajectory the system does not have to be fully actuated, so the method can work equally well work for rigid and flexible systems.

7.2 Analytical Development

Consider a system with $\mathcal{N}$ degrees of freedom which has μ inputs denoted by $\tau = \tau_1,\ldots,\tau_\mu$. The system is required to move such that its outputs track prescribed trajectories described by P equations as follows:

$$g_i(\mathbf{q},t) = 0, \quad i = 1,\ldots,P, \quad P < \mu \tag{7.1}$$

in which $\mathbf{q} = q_1,\ldots,q_\mathcal{N}$ is the array of generalized coordinates of the system, and t is time. This system can be viewed as a constrained system whose motion is subjected to P constraints described by Eq.(7.1). In practice, however, to impose the constraints, we must find P inputs of the system which can act as constraint forces. Assuming $\tau_1,\ldots,\tau_P$ to be the set of inputs that are acting as constraint forces, one can use Eq.(3.28) to develop the equations of motion of this constrained system as

$$\sum_{s=1}^{N} \tilde{\tilde{M}}_{rs}\dot{u}_s = \tilde{\tilde{f}}_r(\mathbf{q},\mathbf{u}_1,\tau_{P+1},\ldots,\tau_\mu,t), \quad r = 1,\ldots,N, \tag{7.2}$$

in which $N = \mathcal{N} - P$ is the number of degrees of freedom of the constrained system, and $\mathbf{u}_1 = u_1,\ldots,u_N$ denotes the array of independent generalized speeds. The $\mu - P$ inputs in Eq.(7.2), $\tau_{P+1},\ldots,\tau_\mu$, can be used to manipulate the system (to control the motion of the constrained system), while tracking of prescribed trajectories is guaranteed through imposition of artificial constraints by application of $\tau_1,\ldots,\tau_P$.

The constraint forces $(\tau_1,\ldots,\tau_P)$ can be found using Eq.(3.35). These forces are functions of the generalized coordinates and generalized speeds of the system and the other inputs - i.e., $\tau_i = \tau_i(\mathbf{q},\mathbf{u}_1,\tau_{P+1},\ldots,\tau_\mu,t), i = 1,\ldots,P$. Calculation of $\tau_1,\ldots,\tau_P$ based on Eq.(3.35) represents a model-based, open-loop control law for the system which, in theory, guarantees the motion of the system to comply with the constraints (desired trajectory). In practice, however, a perfect tracking of prescribed trajectories is pending upon the accuracy of

the model, the availability of input forces that are supposed to act as the constraint forces, and availability of the states of the system.

7.3 Illustrative Examples

Two examples are given to illustrate how the method works, and how it can be employed to control a flexible structure.

7.3.1 A rigid, two-link manipulator

Consider a rigid, two-link manipulator, shown in Figure 7.1, which is employed to move a point mass M, at the tip of the second link, along the X axis. The main objective is that the mass does not leave the X axis during the course of motion. Although, for this rigid manipulator, the maneuver can be accomplished by feedback linearization technique, we want to apply the method presented here for two reasons. First, to show, through a simple example, how the method works, and second, to show how this method enables us to use a mixed control strategy to control this system.

The prescribed trajectory can be described by the equation $\ell \sin(q_1) + \ell \sin(q_2) = 0$, in which ℓ denotes the length of the links and q_1 and q_2 are the generalized coordinates of the system as shown in Figure 7.1. Solving this relation, one gets the following constraint equation

$$q_1 + q_2 = 0 \cdot \tag{7.3}$$

Employing the method presented in Section 7.2 and choosing the torque τ_2 as the constraint force, we can find the magnitude of τ_2, using Eq.(3.35), in terms of the states of the system and the other input as

$$\tau_2 = \left[\cos(2q_1)(1/2 + M/m) - (M/m + 1/3)\right]\tau_1 - \ell^2 u_1^2 \sin(2q_1)(m/2 + M), \tag{7.4}$$

where m denotes the mass of each link, and $u_1 = \dot{q}_1$ is the independent generalized speed of the system. On the other hand, the equation of motion of the constrained system, with the constraints as described in Eq.(7.3), can be written, based on Eq.(3.28), as follows:

$$m\ell^2 \dot{u}_1 = \tau_1 \tag{7.5}$$

As one can see, Eq.(7.5) represents a one degree of freedom system with one input. This equation can be used to control the independent generalized coordinate (q_1), and, through that, to manipulate the payload, whereas the open-loop control law given by Eq.(7.4) guaranties the tracking of the prescribed trajectory (i.e., the mass M moves on the X axis). To control q_1, one can use any control law, even a simple PD controller which can be easily implemented in practice. This also allows us to control the system semi-manually – to control q_1 by a master and slave system, while q_2 is being controlled through proper evaluation and application of τ_2 such that the overall motion satisfies the constrained motion which describes the desired trajectory.

The validity of the above analysis can be verified by simulation. However, in this simple case, one may analytically verify that the equations of motion of the unconstrained system admits $q_1 = -q_2$ as its solution if the torque τ_2 is determined by the open-loop control law of Eq.(7.4). To this end, let us substitute τ_2 from Eq.(7.4) into the equations of motion of the unconstrained system given by

$$\begin{bmatrix} (4m/3+M)\ell^2 & \alpha\cos(q_1-q_2) \\ \alpha\cos(q_1-q_2) & (m/3+M)\ell^2 \end{bmatrix} \begin{bmatrix} \dot{u}_1 \\ \dot{u}_2 \end{bmatrix} = \begin{bmatrix} \tau_1 - \tau_2 - \alpha u_2^2 \sin(q_1-q_2) \\ \tau_2 + \alpha u_1^2 \sin(q_1-q_2) \end{bmatrix}, \tag{7.6}$$

which results in

$$\begin{bmatrix} (4m/3+M)\ell^2 & \alpha\cos(q_1-q_2) \\ \alpha\cos(q_1-q_2) & (m/3+M)\ell^2 \end{bmatrix} \begin{bmatrix} \dot{u}_1 \\ \dot{u}_2 \end{bmatrix} = \begin{bmatrix} (1-\beta)\tau_1 - \alpha[u_2^2 \sin(q_1-q_2) - u_1^2 \sin(2q_1)] \\ \beta\tau_1 + \alpha u_1^2[\sin(q_1-q_2) - \sin(2q_1)] \end{bmatrix}, \tag{7.7}$$

where $\alpha = (m/2 + M)\ell^2$ and $\beta = \cos(2q_1)(1/2 + M/m) - (M/m + 1/3)$. Upon substituting $q_1 = -q_2$, $u_1 = -u_2$, and $\dot{u}_1 = -\dot{u}_2$ in Eq.(7.7), after some mathematical manipulation, one gets the following consistent, over-determined set of equations

$$\begin{bmatrix} m\ell^2 \\ m\ell^2 \end{bmatrix} \dot{u}_1 = \begin{bmatrix} \tau_1 \\ \tau_1 \end{bmatrix}. \tag{7.8}$$

which shows that $q_1 + q_2 = 0$ is a solution to Eq.(7.6) if τ_2 is determined by Eq.(7.4).

7.3.2 Control of a flexible manipulator

In this example we consider a manipulator with two flexible links and a rigid end effector which are connected through revolute joints in a planar configuration as shown in Figure 7.2. The data of the manipulator are given in Table 7.1. The flexible links of the manipulator are modeled as Euler-Bernoulli beams. Transverse vibration in the plane of motion is the only elastic motion which is considered. Assumed modes method, with one elastic DOF for each link, is used to relate the elastic deflections of the beams to the elastic generalized coordinates of the system. The normalized first mode shape of a cantilever beam, given in Eq.(5.36), is used as the shape function. The system has five DOFs, which can be identified by the definition of the following generalized coordinates:

q_1: shoulder joint angle,

q_2: elastic tip deflection of the first link,

q_3 : elbow joint angle,

q_4: elastic tip deflection of the second link,

q_5: wrist joint angle.

The generalized speeds of the system are defined as the time derivatives of the generalized coordinates (i.e., $u_i = \dot{q}_i, i = 1,\ldots,5$). The system has three inputs denoted by τ_1, τ_2, and τ_3

which are the actuator torques applied at the shoulder, elbow, and wrist joints, respectively. This system is under-actuated, i.e., has fewer inputs than the number of DOFs.

Table 7.1 Three-link flexible manipulator: the physical data.

Description	Mass (kg)	Length (m)	Flexural rigidity ($N.m^2$)	Structural damping
Link 1	2.51	0.8	930	2%
Link 2	2.51	0.8	930	2%
End effector & Payload	5	0.15	-	-

We intend to perform a rest-to-rest maneuver which moves the end effector of the manipulator from point A ($y = 5$ cm) to point B ($y = 80$ cm) along the Y axis, see Figure 7.2. The objective is to keep the tip of the end effector on the Y axis. The desired trajectory can be described by $X_e = 0$, where X_e denotes the X-component of the position vector of the end effector tip. Using forward kinematics, one can expand the constraint equation as follows:

$$\begin{aligned} X_e = {} & 0.8[\cos(q_1) + \cos(q_1 + \gamma q_2 + q_3)] - q_2 \sin(q_1) - q_4 \sin(q_1 + \gamma q_2 + q_3) \\ & + 0.15\cos(q_1 + \gamma q_2 + q_3 + \gamma q_4 + q_5) = 0 \end{aligned} \tag{7.9}$$

in which γ is a constant dependent on the choice of the shape function (using the shape function given in Eq.(5.36), $\gamma = 1.72$).

Applying the method presented in Section 7.2, while considering τ_3 as the constraint force, one can develop the equations of motion of the constrained system as

$$\sum_{n=1}^{4} \tilde{\tilde{M}}_{rn} \dot{u}_n = \tilde{\tilde{f}}_r + \sum_{i=1}^{2} \tilde{\tilde{T}}_{ri} \tau_i, \quad r = 1,\ldots,4. \tag{7.10}$$

Equations (7.10) can be used to control the independent DOFs of the system (here, $q_1,\ldots,q_4$). Different control schemes can be used to control this system. For instance, the computed torque method can be employed to manipulate q_1 and q_3 (joint angles) such that the wrist joint moves close to a desired trajectory (with deviations due to elastic fluctuations). The wrist joint angle

(q_5) will be accordingly determined, through application of τ_3, such that the end effector tip follows the prescribed trajectory.

A simpler method, used in this example, for controlling the constrained motion of the system (given by Eq.(7.10)) is to employ a PD controller. The control law can be expressed as

$$\begin{aligned} \tau_1 &= k_1(\bar{q}_1 - q_1) + c_1(\bar{u}_1 - u_1), \\ \tau_3 &= k_2(\bar{q}_3 - q_3) + c_2(\bar{u}_3 - u_3), \end{aligned} \tag{7.11}$$

where $\bar{q}_i$ and $\bar{u}_i$ are the desired final values for q_i and u_i. This type of controller, apparently, does not force the states of the system to follow prescribed trajectories; moreover, it does not control the elastic vibrations directly. However, the dependent generalized coordinate (q_5) will always be determined, by applying the proper value of the constrained force (τ_3), such that the end effector moves along the Y axis, the prescribed trajectory.

The initial and final conditions for this maneuver, which are chosen arbitrarily, are given in Table 7.2. The results of the simulation of the system for the aforementioned maneuver are shown in Figure 7.3, while Figure 7.4 shows the input torques which are applied to accomplish the maneuver. The controller gains for this simulation are chosen as $k_1 = 120, k_2 = 80, c_1 = 22$, and $c_2 = 16$.

Table 7.2 Initial and final conditions for moving the end effector of a flexible manipulator along the Y axis

	q_1 (rad)	q_2	q_3 (rad)	q_4	q_5 (rad)
Initial conds.	0.1253	0	2.8909	0	1.6961
Final conds.	0.5421	0	1.8964	0	1.7503

Now, let us repeat the same maneuver, moving the end effector from point A to point B along the Y axis), but with a different objective. This time we would like to maintain the end effector parallel to the X axis, see Figure 7.2. Repositioning a spacecraft antenna, while preserving its orientation, is an interesting application for this type of maneuver.

The desired prescribed motion can be expressed as $\theta_e = \pi$, where θ_e denotes the angle of the end effector measured from the X axis. As before, the constraint equation can be expanded as follows:

$$\theta_e = q_1 + \gamma q_2 + q_3 + \gamma q_4 + q_5 = \pi \tag{7.12}$$

in which $\gamma = 1.72$. The independent DOFs of the constrained system is controlled using the same PD controller as defined in Eq.(7.11), but with a different set of controller gains chosen as $k_1 = 30$, $k_2 = 20$, $c_1 = 11$, and $c_2 = 8$. The initial and final conditions for this maneuver, which are chosen arbitrarily, are given in Table 7.3. The simulation results for this maneuver are shown in Figures 7.5 and 7.6.

Table 7.3 Initial and final conditions for moving the end effector of a flexible manipulator parallel to the X axis

	q_1 (rad)	q_2	q_3 (rad)	q_4	q_5 (rad)
Initial conds.	-1.15	0	2.9436	0	1.348
Final conds.	0.3483	0	2.0742	0	0.7190

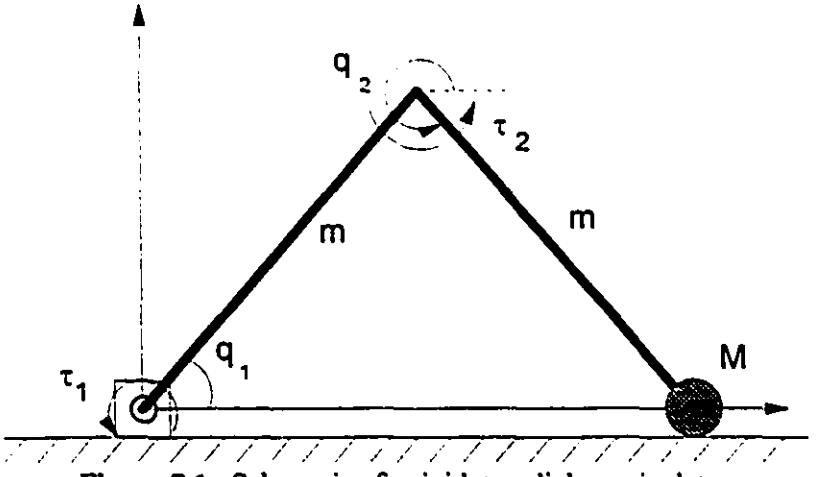

Figure 7.1 Schematic of a rigid, two-link manipulator.

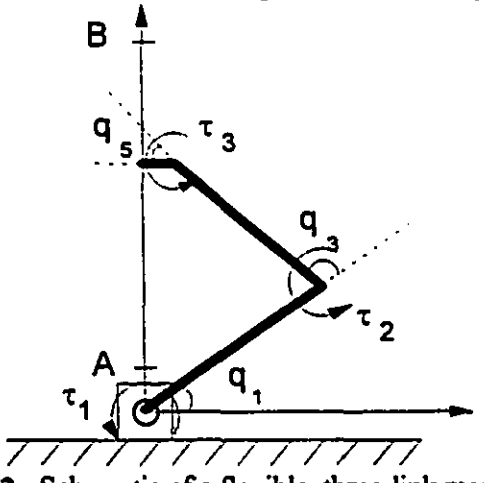

Figure 7.2 Schematic of a flexible, three-link manipulator.

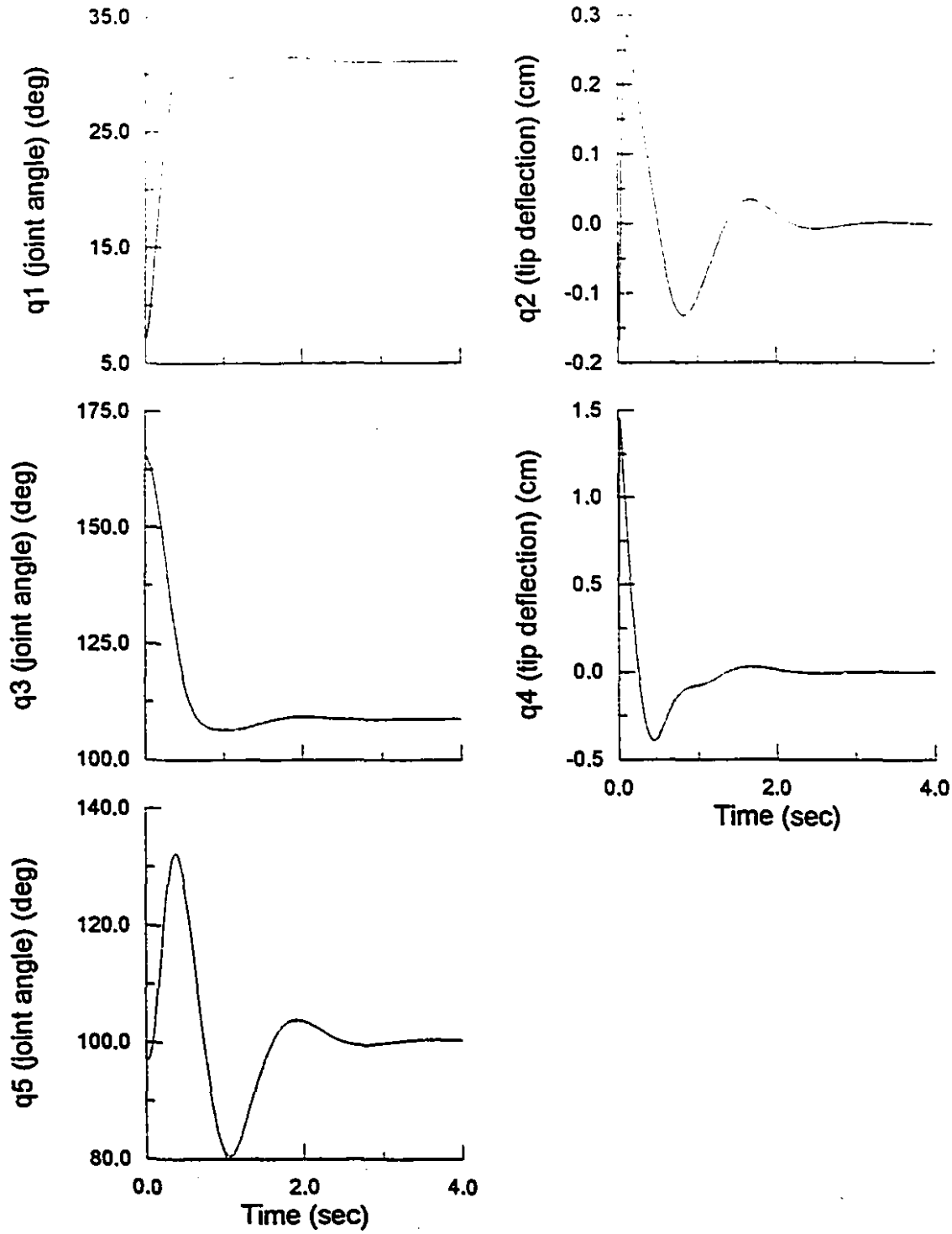

Figure 7.3 Simulation results for maneuver of a flexible manipulator, while keeping the end effector tip on the Y axis; time history of the generalized coordinates.

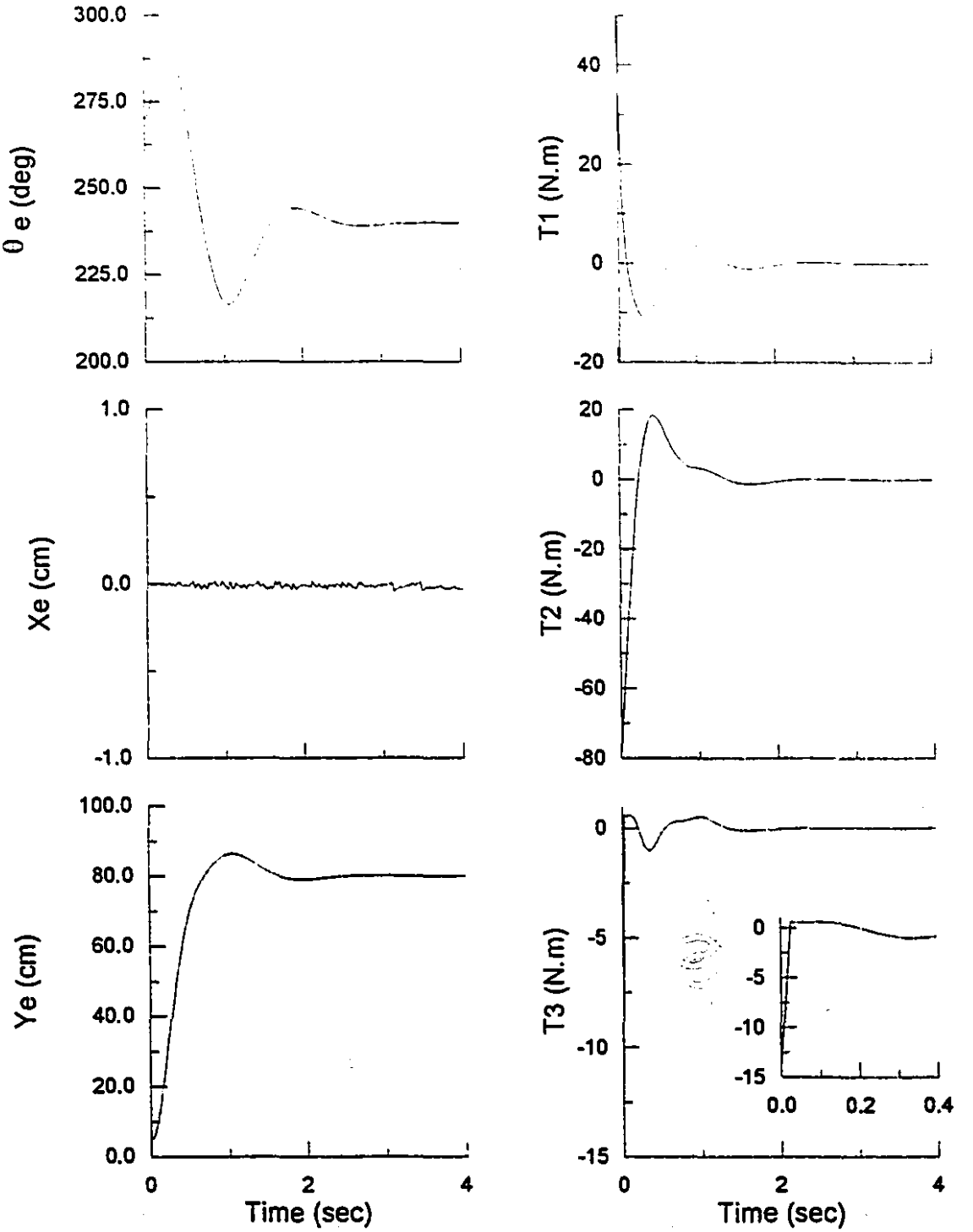

Figure 7.4 Simulation results for maneuver of a flexible manipulator, while keeping the end effector tip on the *Y* axis; time history of the position of the end effector tip and the actuator torques.

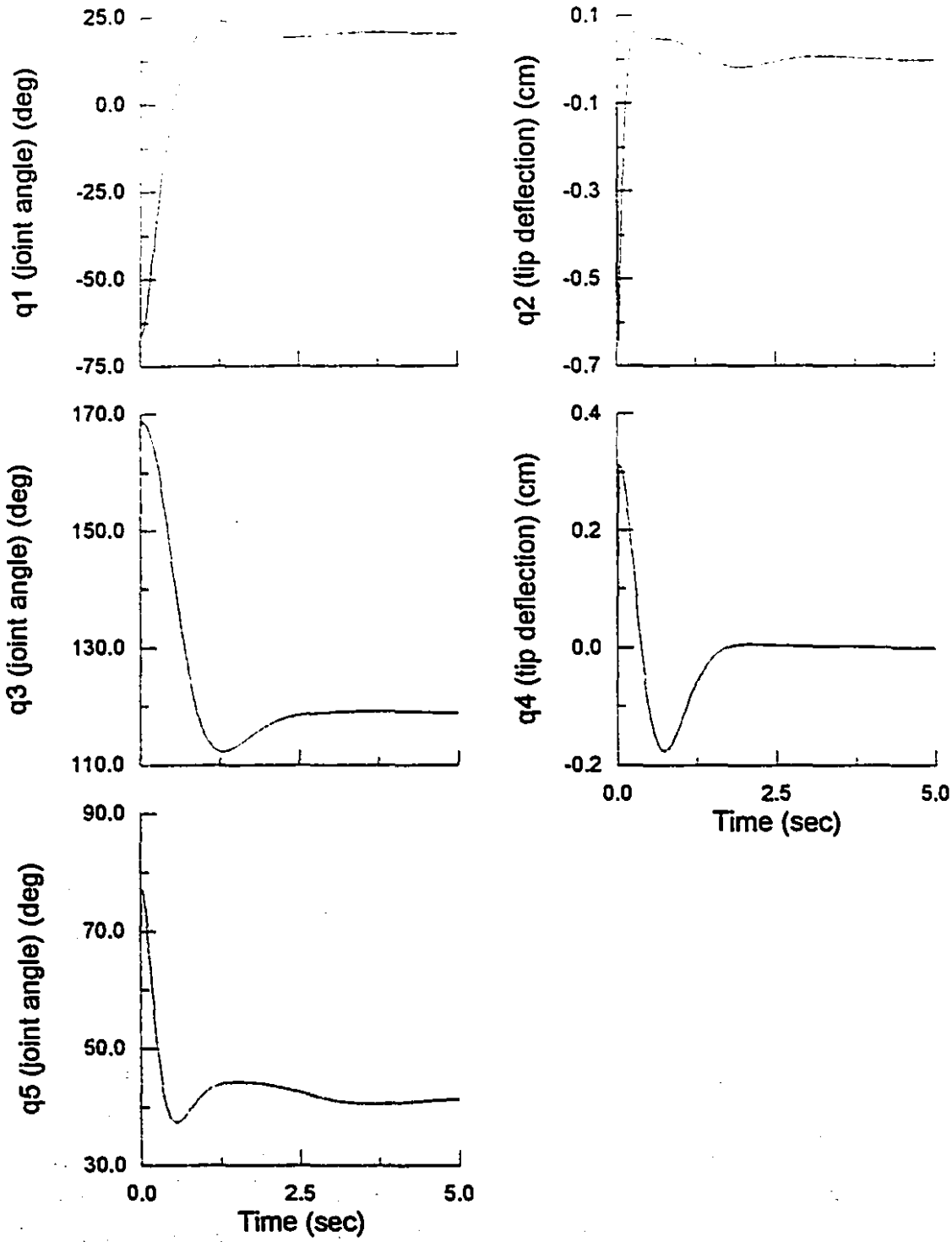

Figure 7.5 Simulation results for maneuver of a flexible manipulator, while keeping the end effector parallel to the X axis; time history of the generalized coordinates.

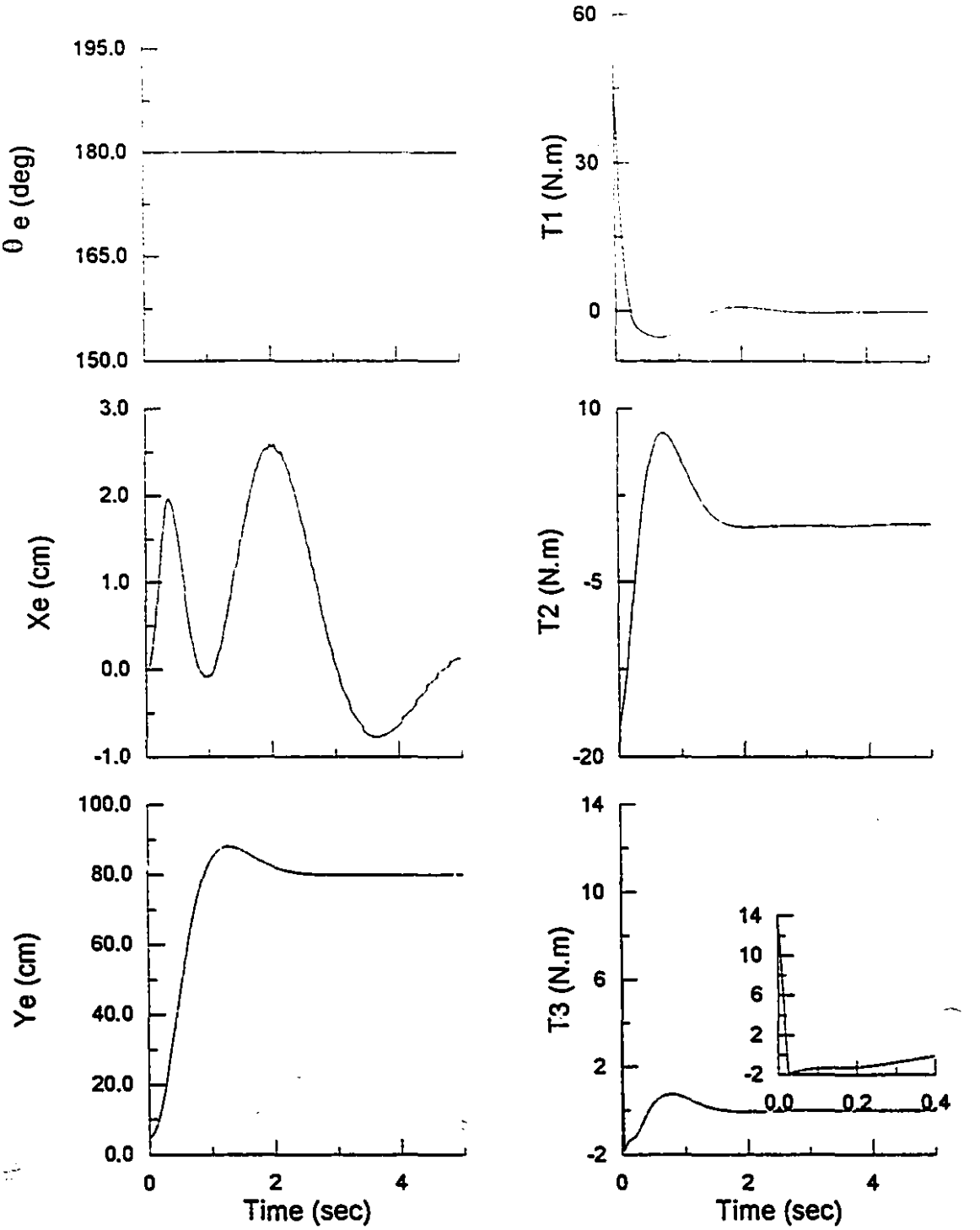

Figure 7.6 Simulation results for maneuver of a flexible manipulator, while keeping the end effector parallel to the *X* axis; time history of the position of the end effector tip and the actuator torques.

Chapter 8

Time-Optimal Maneuvering of Flexible Multibody Systems

8.1 Introduction

The problem of minimum-time maneuvering of space systems has gained a lot of attention in the past. Depending on the complexity of the system, the optimal solution might become very complicated and difficult, if not impossible, for practical implementation as a feedback control of the system. Yet, the same solution is important because it can provide a limit on the achievable performance for the maneuver at hand; moreover, in some cases it can be a guide for modifying the practical maneuvers to achieve a better performance.

In Chapter 1 it was mentioned that most of the research works in the area of time-optimal control of flexible multibody systems were directed towards solving the problem of maneuvering of systems with a special configuration, i.e., a rigid hub with some flexible appendages. On the other hand, multibody systems with general configuration, such as space manipulators, have received comparatively less attention. In this chapter we try to use optimal control theory to maneuver a multibody system along a prescribed trajectory.

Instead of finding the minimum-time solution using numerical methods, a near-minimum-time solution is attempted. The solution is found by employing a perturbation

technique to subdivide the equations of motion into two sets: zero-order equations (governing the rigid body motion) and first-order equations (describing the elastic vibrations).

The time-optimal solution to the zero-order part is found by applying nonlinear optimal control theory, while the unwanted elastic fluctuations are damped by a controller designed using a linear control theory such as the LQR method. The actuator forces† are then found by superposing the forces found from the open-loop control law of the zero-order system and the closed-loop control law of the first-order system.

8.2 Theoretical Development

The problem at hand can be stated as follows:

(P1): *For a system S with N DOFs (N^R rigid DOFs and $(N - N^R)$ elastic DOFs) and N^R inputs, determine the inputs which can drive the system from its specified initial condition to the desired final condition in minimum time.*

To express the problem mathematically, let us assume that the DOFs of the system are described by N generalized coordinates denoted by $\mathbf{q} = q_1,\ldots,q_N$, of which the first N^R describe the rigid body DOFs of the system. Furthermore, the magnitudes of the actuator forces denoted by $\tau = \tau_1,\ldots,\tau_{N^R}$ are the inputs of the system. The equations of motion of this system can be written as

$$\sum_{s=1}^{N} M_{rs}(\mathbf{q},t)\ddot{q}_s = f_r(\mathbf{q},\dot{\mathbf{q}},t) + \sum_{i=1}^{N^R} \mathcal{T}_{ri}\,\tau_i, \quad r = 1,\ldots,N. \tag{8.1}$$

We further assume that the maneuver starts at $t = 0$ from $\mathbf{q}_0$ and $\dot{\mathbf{q}}_0$ and ends at $t = t^f$ in $\mathbf{q}_f$ and $\dot{\mathbf{q}}_f$, where all the quantities $\mathbf{q}_0$, $\dot{\mathbf{q}}_0$, $\mathbf{q}_f$, and $\dot{\mathbf{q}}_f$ are specified. With these definitions, problem (P1) can be restated as

† In this context, the term "actuator force" refers to both actuator force and actuator torque.

(P2). *For the system S, we seek to find the input* $\boldsymbol{\tau} = \boldsymbol{\tau}(t)$ *which minimizes the performance index function* $J = \int_0^{t_f} dt$, *with* $\mathbf{q}(0) = \mathbf{q}_0$, $\dot{\mathbf{q}}(0) = \dot{\mathbf{q}}_0$, $\mathbf{q}(t_f) = \mathbf{q}_f$ *and* $\dot{\mathbf{q}}(t_f) = \dot{\mathbf{q}}_f$, *subject to the following constraints*

$$\sum_{s=1}^{N} M_{rs}(\mathbf{q},t)\ddot{q}_s = f_r(\mathbf{q},\dot{\mathbf{q}},t) + \sum_{i=1}^{N^R} \mathcal{T}_{ri}\,\tau_i, \quad r = 1,\ldots,N \tag{8.2}$$

and

$$\tau_{i_{min}} \le \tau_i \le \tau_{i_{max}}, \quad i = 1,\ldots,N^R. \tag{8.3}$$

This problem can be solved using Pontryagin's minimum principle, which results in a bang-bang solution (Meirovitch [1990]). However, determining the number of switches and the switching times can be a challenging problem. In the case of complicated problems, such as multibody flexible systems, not only a closed form solution can not be reached, but even the numerical methods often fail to give the switching times.

For flexible systems, a near-minimum-time solution can be obtained by using the perturbation technique to partition the equations of motion into a zero-order and a first-order set of equations. This technique is discussed in the following section.

8.2.1 Perturbation technique

In this section we first show how the technique can be used to partition the equations of motion into two sets of zero-order and first-order equations. Then, it will be discussed how the method can be used to find the near-minimum-time solution for a flexible system.

The technique is based on the assumption that the difference between the response of a flexible system and its rigid counterpart is of the first-order (i.e., one order of magnitude smaller than the rigid-body motion). This is true only if the magnitudes of the elastic vibrations are much smaller than those of the rigid-body motion. According to this assumption, if the array $\mathbf{q}$ is the solution to Eqs.(8.1), which describe the motion of the flexible system, then it can be expressed as

$$\mathbf{q} = \bar{\mathbf{q}} + \tilde{\mathbf{q}} \tag{8.4}$$

where $\tilde{\mathbf{q}}$ is an array of some first-order terms (i.e., $\|\tilde{\mathbf{q}}\| << \|\mathbf{q}\|$), and $\bar{\mathbf{q}}$ is the solution to the equations of motion of the rigid counterpart of the system S given by

$$\sum_{s=1}^{N^R} \bar{M}_{rs}(\bar{\mathbf{q}},t)\ddot{\bar{q}}_s = \bar{f}_r(\bar{\mathbf{q}},\dot{\bar{\mathbf{q}}},t) + \sum_{i=1}^{N^R} \bar{\mathcal{T}}_{ri}(\bar{\mathbf{q}},t)\bar{\tau}_i, \quad r = 1,\ldots,N^R, \tag{8.5}$$

in which N^R is the number of the rigid DOFs of the system. Substituting $\mathbf{q}$ from Eqs.(8.4) and $\dot{\mathbf{q}}$ and τ by their equivalents $\bar{\mathbf{q}} + \dot{\tilde{\mathbf{q}}}$ and $\bar{\tau} + \tilde{\tau}$ in Eq.(8.1), using Taylor expansion up to the first order to expand Eq.(8.1), and collecting the zero-order and first-order terms, one gets

$$\sum_{s=1}^{N} M_{rs}(\bar{\mathbf{q}},t)\ddot{\bar{q}}_s = f_r(\bar{\mathbf{q}},\dot{\bar{\mathbf{q}}},t) + \sum_{i=1}^{N^R} \mathcal{T}_{ri}(\bar{\mathbf{q}},t)\bar{\tau}_i, \quad r = 1,\ldots,N, \tag{8.6.a}$$

$$\sum_{s=1}^{N}\left[M_{rs}(\bar{\mathbf{q}},t)\ddot{\tilde{q}}_s + K_{rs}(\bar{\mathbf{q}},\dot{\bar{\mathbf{q}}},t)\tilde{q}_s + C_{rs}(\bar{\mathbf{q}},\dot{\bar{\mathbf{q}}},t)\dot{\tilde{q}}_s\right] = \sum_{i=1}^{N^R} \mathcal{T}_{ri}(\bar{\mathbf{q}},t)\tilde{\tau}_i, \; r = 1,\ldots,N, \tag{8.6.b}$$

where

$$K_{rs} = \left[\left(\sum_{i=1}^{N} \frac{\partial M_{ri}}{\partial q_s}\ddot{\bar{q}}_i\right) - \frac{\partial f_r}{\partial q_s} - \frac{\partial \mathcal{T}_{ri}}{\partial q_s}\bar{\tau}_i\right]_{\bar{\mathbf{q}},\dot{\bar{\mathbf{q}}}}, \quad r,s = 1,\ldots,N, \tag{8.7}$$

and

$$C_{rs} = \left[\frac{\partial f_r}{\partial \dot{q}_s}\right]_{\bar{\mathbf{q}},\dot{\bar{\mathbf{q}}}}, \quad r,s = 1,\ldots,N. \tag{8.8}$$

One can see that using this technique, the equations of motion of the system, Eq.(8.1), have been split into two sets of equations, Eqs.(8.6). Considering that $\bar{q}_i = \dot{\bar{q}}_i = \ddot{\bar{q}}_i = 0$ for $i = N^R + 1,\ldots,N$ (the elastic DOFs), one can reduce the first set of equations, Eq.(8.6.a), which describes the motion of the system in the absence of elastic vibrations, to the equations of motion of the rigid counterpart of the system, Eq.(8.5). This set of equations is, obviously, a nonlinear set, but of the lower dimension, N^R, compared to the original system with dimension N. On the other hand, the second set, given by Eq.(8.6.b), which describes the first-order motion induced by the flexibility of the system, is a linear set of equations of the same dimension as the original system.

The problem can, now, be solved in two steps to give a near-minimum-time solution. The first step would be to find a $\bar{\tau}$ which drives the rigid counterpart of the system from its initial condition $(\bar{q}_0, \dot{\bar{q}}_0)$ to the final condition $(\bar{q}_f, \dot{\bar{q}}_f)$ in minimum time. In the second step, we seek to find $\tilde{\tau}$, using the LQR method, such that the vibrations induced by the flexibility effect get damped. The desired control law which accomplishes the maneuver in near-minimum-time is given as $\tau = \bar{\tau} + \tilde{\tau}$

8.2.2 Minimum-time, rigid-body maneuver

The minimum-time maneuvering problem for the rigid counterpart of the system S can be stated as follows:

(P3): *Find the actuator torque* $\bar{\tau} = \bar{\tau}(t)$ *which minimizes the index function* $J = \int_0^{t_f} dt$, *with* $\bar{q}(0) = \bar{q}_0, \dot{\bar{q}}(0) = \dot{\bar{q}}_0, \bar{q}(\bar{t}_f) = \bar{q}_f$, *and* $\dot{\bar{q}}(\bar{t}_f) = \dot{\bar{q}}_f$, *subject to the following constraints*

$$\sum_{s=1}^{N^R} \bar{M}_{rs}(\bar{q},t)\ddot{\bar{q}}_s = \bar{f}_r(\bar{q},\dot{\bar{q}},t) + \sum_{i=1}^{N^R} \bar{T}_{ri}(\bar{q},t)\bar{\tau}_i, \quad r = 1,\ldots,N^R, \tag{8.9}$$

and

$$\bar{\tau}_{i_{min}} \le \bar{\tau}_i \le \bar{\tau}_{i_{max}}, \quad i = 1,\ldots,N^R. \tag{8.10}$$

The solution to this problem is a bang-bang control law; however, finding the switching points can still be a challenging problem. In fact, for systems with $N^R > 1$, not only a closed form solution may not be found in general, but , in some cases, even numerical methods fail to give the solution. For instance, Bobrow et al.[1985] reported that even for a rigid manipulator with three DOFs, several numerical methods were tested, but all of them failed to give the switching points.

Here, instead of using numerical routines to solve the problem in its general form, we try to find the time-optimal solution for the system along a prescribed trajectory. Although this method does not yield the global solution for problem (P3), it is still a useful method because it is computationally advantageous and can find practical applications. The method is specially

convenient for cases where the path of maneuver is either prescribed or has to be selected from a few possible paths. Such cases are likely to be encountered in maneuver of robotic manipulators. Apart from robotics applications, the method can also be used in cases such as minimum-time, rest-to-rest, 3-D maneuvering of a rigid body around the Euler axis, with specified initial and final conditions.

In this method, application of the constraints, which describes the path, reduces the degrees of freedom of the system from N^R to one. However, due to the presence of several actuators, which together should drive the system along the prescribed path, the time-optimal solution for this one-DOF system is not as straightforward as a simple one-DOF system (with no constraint). What follows is a brief discussion of the method. A simpler, and yet more detailed version of the method can be found in the paper published by Bobrow et al.[1985]. The above mentioned time-optimal problem can be stated as follows:

(P4): *Find the actuator torque* $\bar{\tau}$ *which minimizes the index function* $J = \int_0^{t_f} dt$, *with* $\bar{q}(0) = \bar{q}_0, \dot{\bar{q}}(0) = \dot{\bar{q}}_0, \bar{q}(t_f) = \bar{q}_f$, *and* $\dot{\bar{q}}(t_f) = \dot{\bar{q}}_f$, *subject to the following constraints*

$$\sum_{s=1}^{N^R} \bar{M}_{rs}(\bar{q},t)\ddot{\bar{q}}_s = \bar{f}_r(\bar{q},\dot{\bar{q}},t) + \sum_{i=1}^{N^R} \bar{T}_{ri}(\bar{q},t)\bar{\tau}_i, \quad r = 1,\ldots,N^R, \tag{8.11}$$

$$g_i(\bar{q},s,t) = 0, \quad i = 1,\ldots,N^R, \tag{8.12}$$

and

$$\bar{\tau}_{i_{min}} \le \bar{\tau}_i \le \bar{\tau}_{i_{max}}, \quad i = 1,\ldots,N^R. \tag{8.13}$$

In Eq.(8.12) the scalar s denotes a pseudo-generalized coordinate which can uniquely determine the configuration of the constrained system. For instance, the length measured along the path or one of the generalized coordinates of the system can be a candidate for the scalar s. This means that given a value of s, one should be able to find corresponding values of $q_1,\ldots,q_{N^R}$.

To solve problem (P4) we try to express it as a one-DOF problem in terms of the pseudo-generalized coordinate s. To this end, $\bar{q}, \dot{\bar{q}}$, and $\ddot{\bar{q}}$ must be substituted in Eq.(8.11) by

their equivalents in terms of $s, \dot{s}$, and $\ddot{s}$. Differentiating the constraint equations with respect to time, one can write

$$\left[\mathcal{A}_1(\bar{\mathbf{q}},s,t) \quad \mathcal{A}_2(\bar{\mathbf{q}},s,t)\right]\begin{bmatrix}\dot{\bar{\mathbf{q}}}\\ \dot{s}\end{bmatrix} = \mathcal{B}(\bar{\mathbf{q}},s,t). \tag{8.14}$$

This equation can be solved for $\dot{\bar{\mathbf{q}}}$, provided that the constraints are independent (i.e., $\mathcal{A}_1$ is invertible), which results in

$$\dot{\bar{\mathbf{q}}} = \mathbf{A}(\bar{\mathbf{q}},s,t)\dot{s} + \mathbf{B}(\bar{\mathbf{q}},s,t), \tag{8.15}$$

where $\mathbf{A} = -\mathcal{A}_1^{-1}\mathcal{A}_2$ and $\mathbf{B} = \mathcal{A}_1^{-1}\mathcal{B}$. Differentiating Eq.(8.15) with respect to time, one gets

$$\ddot{\bar{\mathbf{q}}} = \mathbf{A}(\bar{\mathbf{q}},s,t)\ddot{s} + \dot{\mathbf{A}}(\bar{\mathbf{q}},s,\dot{\bar{\mathbf{q}}},\dot{s},t)\dot{s} + \dot{\mathbf{B}}(\bar{\mathbf{q}},s,\dot{\bar{\mathbf{q}}},\dot{s},t). \tag{8.16}$$

Substituting for $\dot{\bar{\mathbf{q}}}$ and $\ddot{\bar{\mathbf{q}}}$ from Eqs.(8.15) and (8.16) into Eq.(8.11), one can rewrite the equations of motion, Eq.(8.11), as

$$\mathbf{C}\ddot{s} = \bar{\boldsymbol{\tau}} - \mathbf{D}, \tag{8.17}$$

in which $\mathbf{C}$ and $\mathbf{D}$ are $N^R \times 1$ matrices given by

$$\begin{aligned}\mathbf{C} &= \bar{T}^{-1}\bar{\mathbf{M}}\mathbf{A},\\ \mathbf{D} &= \bar{T}^{-1}\left[\bar{\mathbf{M}}(\dot{\mathbf{B}} + \dot{\mathbf{A}}\dot{s}) - \bar{\mathbf{f}}\right].\end{aligned} \tag{8.18}$$

Given the values of $s, \dot{s}$, and $\ddot{s}$, Eq.(8.18) shows the unique values of the actuator forces, τ, which are needed to produce the specified motion. However, taking the actuator limits, Eq.(8.13), into consideration, certain patterns of motion may not be achievable. In other words, for a given pair of s and $\dot{s}$, there is a bound of admissible accelerations, where an admissible acceleration for given s and $\dot{s}$ is defined as any acceleration which can drive the system without violating the constraints. To find the bound of admissible accelerations, let us substitute the actuator force limits from Eq.(8.13) into Eq.(8.17)

$$\bar{\tau}_{i_{\min}} - D_i \le C_i\ddot{s} \le \bar{\tau}_{i_{\max}} - D_i, \quad i = 1,\ldots,N^R. \tag{8.19}$$

Since for any s and $\dot{s}$, $\bar{\mathbf{q}}$ and $\dot{\bar{\mathbf{q}}}$ can be computed using Eqs.(8.12) and (8.15), all quantities in the above equation can be considered as functions of s and $\dot{s}$. If $C_i \neq 0$, Eq.(8.19) can be rewritten as

$$h_i(s,\dot{s}) \le \ddot{s} \le g_i(s,\dot{s}), \quad i = 1,\ldots,N^R, \tag{8.20}$$

where

$$h_i(s,\dot{s}) = \begin{cases} (\bar{\tau}_{i_{max}} - D_i)/C_i, & C_i > 0, \\ (\bar{\tau}_{i_{min}} - D_i)/C_i, & C_i < 0, \end{cases} \tag{8.21}$$

and

$$g_i(s,\dot{s}) = \begin{cases} (\bar{\tau}_{i_{min}} - D_i)/C_i, & C_i > 0, \\ (\bar{\tau}_{i_{max}} - D_i)/C_i, & C_i < 0. \end{cases} \tag{8.22}$$

Any admissible acceleration must satisfy all of the inequalities give by Eq.(8.20), which means that

$$h(s,\dot{s}) \le \ddot{s} \le g(s,\dot{s}), \tag{8.23}$$

in which $h(s,\dot{s}) = \max_i(h_i(s,\dot{s}))$ and $g(s,\dot{s}) = \min_i(g_i(s,\dot{s}))$, with the maximum and minimum taken over those i for which $C_i \neq 0$.

On the other hand, if $C_i = 0$, the i-th inequality of Eq.(8.20) reduces to

$$\bar{\tau}_{i_{min}} < D_i < \bar{\tau}_{i_{max}}, \tag{8.24}$$

so the selection of $\ddot{s}$ can not depend on whether Eq.(8.20) holds for that i or not. In this case, while choosing $\ddot{s}$ the i-th inequality has to be overlooked. However, there might be cases where for a given pair of s and $\dot{s}$ no admissible acceleration can be found. This can happen when irrespective of the value of $\ddot{s}$, a given pair of s and $\dot{s}$ violates either the inequality given by Eq.(8.24) or the inequality given by Eq.(8.23) (i.e., makes $g(s,\dot{s}) < h(s,\dot{s})$). Such a pair of s and $\dot{s}$ is nonfeasible, which means that if the system gains the velocity $\dot{s}$ at the point s, the actuators can no longer hold the system on the prescribed trajectory. This divides the phase plane ($s-\dot{s}$ plane) into feasible and nonfeasible regions. In practice, for most of the points on

the path, there is a certain velocity $\dot{s}$ above which no combination of admissible actuator forces can hold the system on the prescribed trajectory.

Now, we come to the point when we can restate problem (P4) in terms of s.

(P5): *Given $s(0)$ and $\dot{s}(0)$, choose $\ddot{s}(t)$ to minimize the final time $\bar{t}_f$ for which $s(\bar{t}_f) = s_f$ and $\dot{s}(\bar{t}_f) = \dot{s}_f$, subject to the following inequality constraints*

$$h(s,\dot{s}) \le \ddot{s} \le g(s,\dot{s}) \tag{8.25}$$

It can be proved that (see Bobrow et al.[1985]) to minimize the maneuver time, $\ddot{s}$ must always takes either its minimum or its maximum possible value; that is, either $\ddot{s} = g(s,\dot{s})$ or $\ddot{s} = h(s,\dot{s})$. Therefore, finding the optimal control law amounts to finding the times at which $\ddot{s}$ switches between maximum acceleration and maximum deceleration.

The best way to find the switching points of this problem is to construct the switching curve in the phase plane. This method is motivated by the fact that for a maneuver, the higher the phase-plane trajectory, the shorter the traveling time. The method can be stated in terms of the following algorithm:

Step 1: Integrate the equation $\ddot{s} = h(s,\dot{s})$ backward in time from $s = s_f$ and $\dot{s} = \dot{s}_f$ until either the line $s = s_0$ is reached or the solution curve (c_1) enters the non feasible region of the phase plane (Figures 8.1 and 8.2).

Step 2: Integrate the equation $\ddot{s} = g(s,\dot{s})$ forward in time from $s = s_0$ and $\dot{s} = \dot{s}_0$ until either the solution curve (c_2) intersects the solution curve c_1 (see Figure 8.1), or it enters the non-feasible region of the phase plane at some point a (Figure 8.2). In the first case, the solution is complete; the problem has one switch which takes place at the intersection of curves c_1 and c_2. In the second case, the problem is multi-switching.

Step 3: From point a on the curve c_2, drop to some lower velocity on the dotted vertical line (see Figure 8.2). Then, integrate the equation $\ddot{s} = h(s,\dot{s})$ forward in time until either the solution curve (c_3) intersects the s axis, or it enters the nonfeasible region of the phase plane. The objective is to find, by iteration, the point b such that the decelerating trajectory, c_3, starting from point b just touches the boundary of the non feasible region at a single point s_2.

Step 4: From point s_2 integrate the equation $\ddot{s} = h(s,\dot{s})$ backward in time until the solution curve intersects the solution curve c_2 at some point s_1 (see Figure 8.2).

Step 5: From point s_2 integrate the equation $\ddot{s} = g(s,\dot{s})$ forward in time† until either the solution curve (c_4) intersects the solution curve c_1 at some point s_3 (see Figure 8.2) or it again enters the nonfeasible region of the phase plane. In the first case, the solution is complete, and the three switches are determined to be at points s_1, s_2, and s_3. In the second case, however, the system has more switches which can be found by repeating the Steps 3 to 5.

This algorithm involves a tedious iteration procedure for multi-switching case. A much better method for finding the switching points of this type of problems is proposed by Pfeiffer and Johanni [1987].

8.2.3 Vibration suppression

Two different strategies can be adopted to design the feedback control to damp the unwanted elastic vibrations. The first is to control the elastic vibrations while the rigid-body maneuver is in progress, and the other strategy is to start damping the elastic vibrations after

† It can be proved, see Bobrow et al.[1985], that it is possible to resume maximum acceleration at point s_2 without immediately entering the nonfeasible region.

the rigid body maneuver is finished. The corresponding formulation, advantages and disadvantages of each method are discussed below.

8.2.3.1 Vibration suppression during the minimum-time maneuver

In this approach one has to spare some of the actuator capabilities for the feedback control ($\bar{\tau}$) for vibration suppression. This reduces the limits on the actuator forces available to the rigid-body maneuver (i.e., $\bar{\tau}_{max} < \tau_{max}$ and $\bar{\tau}_{min} > \tau_{min}$). For instance, one might choose $\bar{\tau}_{max} = \alpha \tau_{max}$ and $\bar{\tau}_{min} = \alpha \tau_{min}$ where $0 < \alpha < 1$. Suppose that $\bar{\tau}_1(t)$ is the actuator force which accomplishes the rigid-body maneuver in a minimum time denoted by $\bar{t}_1^f$, according to a certain selection of $\bar{\tau}_{max}$ and $\bar{\tau}_{min}$. Then, the feedback control law for the vibration suppression can be obtained by solving the following time-varying LQR problem:

Find $\bar{\tau}$ which minimizes the performance index function

$$J = \int_0^{\bar{t}^f} (\bar{\mathbf{X}}^T \mathbf{Q} \bar{\mathbf{X}} + \bar{\tau}^T \mathbf{R} \bar{\tau}) dt, \tag{8.26}$$

subject to following time-varying linear equations

$$\sum_{s=1}^{N} \left[M_{rs}(\bar{\mathbf{q}}^*, t)\ddot{\bar{q}}_s + K_{rs}(\bar{\mathbf{q}}^*, \dot{\bar{\mathbf{q}}}^*, t)\bar{q}_s + C_{rs}(\bar{\mathbf{q}}^*, \dot{\bar{\mathbf{q}}}^*, t)\dot{\bar{q}}_s \right] = \sum_{i=1}^{N^R} \mathcal{T}_{ri}(\bar{\mathbf{q}}^*, t)\bar{\tau}_i, \quad r = 1, \ldots, N, \tag{8.27}$$

in which $\bar{\mathbf{q}}^* = \bar{\mathbf{q}}^*(t)$ denotes the time-optimal solution to the rigid-body maneuver, and the matrices $\mathbf{K}$ and $\mathbf{C}$ are as defined in Eqs.(8.7) and (8.8).

The quantities $\bar{\mathbf{X}} = [\dot{\bar{\mathbf{q}}}, \bar{\mathbf{q}}]$, $\mathbf{Q} \geq 0$, and $\mathbf{R} > 0$ appearing in Eq.(8.26) are, respectively, the state vector of the system and some weight functions.

In this approach the final time of the maneuver ($\bar{t}_1^f$) would be equal to the final time of the rigid-body maneuver ($\bar{t}_1^f$). Due to simultaneous vibration suppression and rigid-body

maneuver, which prevents build up of elastic vibrations, this method can work even for highly flexible systems which may go unstable (develop large elastic vibrations) in the absence of feedback control during the rigid-body maneuver.

A disadvantage of this method is that one has to decide a priori what percentage of the actuator capacity should be allocated to the rigid-body maneuver task. Apparently, the lower this percentage is, the longer the maneuver time would be, and the higher this percentage is, the higher the chance for the actuators to get saturated during the maneuver would be (recall that the actuator force is the sum of $\bar{\tau}$ and $\tilde{\tau}$).

8.2.3.2 Vibration suppression after finishing the minimum-time maneuver

In this approach the actuator forces for the entire maneuver are given by

$$\tau_i = \begin{cases} \bar{\tau}_i, & 0 \le t \le \bar{t}_2^f \\ \tilde{\tau}_i, & \bar{t}_2^f \le t \ge t^f \end{cases}, \quad i = 1,\ldots,N^R, \tag{8.28}$$

where $\bar{t}_2^f$ denotes the minimum-time for the rigid-body maneuver. In this case, due to the absence of feedback control during the rigid-body maneuver we have $\bar{\tau}_{max} = \tau_{max}$ and $\bar{\tau}_{min} = \tau_{min}$, which, clearly, makes $\bar{t}_2^f$ smaller than $\bar{t}_1^f$, the rigid-body maneuver time obtained in the previous approach. The feedback control law for vibration suppression can be obtained by solving the following time-invariant, LQR problem

Find $\tilde{\tau}$ which minimizes

$$J = \int_0^{t_f} (\tilde{\mathbf{X}}^T \mathbf{Q} \tilde{\mathbf{X}} + \tilde{\tau}^T \mathbf{R} \tilde{\tau}) dt, \tag{8.29}$$

subject to the following time-invariant linear equations

$$\sum_{s=1}^{N} \left[M_{rs}(\bar{\mathbf{q}}^d, t)\ddot{\tilde{q}}_s + K_{rs}(\bar{\mathbf{q}}^d, \dot{\bar{\mathbf{q}}}^d, t)\tilde{q}_s + C_{rs}(\bar{\mathbf{q}}^d, \dot{\bar{\mathbf{q}}}^d, t)\dot{\tilde{q}}_s \right] = \sum_{i=1}^{N^R} \mathcal{T}_{ri}(\bar{\mathbf{q}}^d, t)\tilde{\tau}_i, r = 1,\ldots,N \tag{8.30}$$

in which $\bar{\mathbf{q}}^d$ *and* $\dot{\bar{\mathbf{q}}}^d$ *are the desired final values of* $\bar{\mathbf{q}}$ *and* $\dot{\bar{\mathbf{q}}}$ *(given constants), and the matrices* $\mathbf{K}$ *and* $\mathbf{C}$ *are as defined in Eqs.(8.7) and (8.8).*

In this approach, the final maneuver time is $t^f = t_2^f + t^s$, where t^s indicates the settling time of the vibration suppression maneuver. Although the final time of the maneuver is larger than the minimum-time for rigid-body maneuver($t^f > \bar{t}_2^f$), it may not be larger than the final time obtained in the previous approach. This is due to the larger rigid body-maneuver time for the previous approach ($\bar{t}_1^f$) compared to the $\bar{t}_2^f$. On the other hand, the feedback controller designed based on this approach is both easier to design and to implement. However, lack of vibration suppression during the rigid-body maneuver may make this approach an improper choice for highly flexible systems. This approach can be used only for those systems whose response to the open-loop bang-bang control, in the absence of feedback control for vibration suppression, falls within a first-order neighborhood of the response of the rigid-body counterpart of the system.

8.3 Application: Retrieving a Satellite in Minimum Time, Using a Flexible Manipulator

Consider the system shown in Figure 8.3 in which a satellite (a rigid payload) is grasped by a flexible, spacecraft mounted manipulator. The main spacecraft is orbitting the earth in a 104.72 min. circular orbit. The system is initially at rest, with respect to the orbital frame. We intend to use the manipulator to retrieve the satellite from point A ($y_o = 15$ m) to point B ($y_o = 3$ m) along the local horizontal (y_o axis), while preserving the orientation of the satellite during the maneuver.

In this example, it is assumed that the orbital motion and attitude of the main spacecraft are not affected by the motion of the manipulator and the satellite. The in-plane, transverse

vibrations of the manipulator links are approximated using the assumed modes method. One elastic DOF is considered for each link and the normalized first mode shape of a cantilever beam, given in Eq.(5.36), is used as the shape function. The system has five DOFs, which can be identified by the definition of the following generalized coordinates:

q_1: shoulder joint angle,

q_2: elbow joint angle,

q_3 : wrist joint angle,

q_4: elastic tip deflection of the first link,

q_5: elastic tip deflection of the second link.

The system has three inputs denoted by τ_1, τ_2, and τ_3 which are the actuator torques applied at the shoulder, elbow, and wrist joints, respectively. The actuator bounds are

$$\begin{aligned} |\tau_1| &\le 800\ N.m \\ |\tau_2| &\le 800\ N.m \\ |\tau_3| &\le 400\ N.m \end{aligned} \tag{8.31}$$

To find a near-minimum-time solution for this maneuver, we first find the minimum-time solution for a similar maneuver performed by the rigid counterpart of the system S (problem P4 stated in Section 8.2.2). The constrained equations (Eq.(8.12) and (8.13) in problem P4) for this system are given as

$$\begin{aligned} & q_1 + q_2 + q_3 = \pi, \\ & d + \ell\cos(q_1) + \ell\cos(q_1 + q_2) - R = 0, \\ & \ell\sin(q_1) + \ell\sin(q_1 + q_2) - s = 0, \end{aligned} \tag{8.32}$$

and

$$\begin{aligned} |\overline{\tau}_1| &\le 800\ N.m, \\ |\overline{\tau}_2| &\le 800\ N.m, \\ |\overline{\tau}_3| &\le 400\ N.m, \end{aligned} \tag{8.33}$$

in which the quantities d, R, ℓ, and s indicate, respectively, the offset of the shoulder joint from the spacecraft center of mass, the distance from the wrist joint to the payload center of mass, the length of the manipulator links, and the pseudo generalized coordinate which is the distance measured along the Y axis. The physical data of the system are given in Table 8.1, and the initial and final conditions for this maneuver(i.e., $\bar{q}_0$, $\dot{\bar{q}}_0$, $\bar{q}_f$, and $\dot{\bar{q}}_f$) are given in Table 8.2.

Table 8.1 Spacecraft mounted flexible manipulator: the physical data.

Description	Mass (kg)	Length (m)	Flexural rigidity ($N.m^2$)	Structural damping
Spacecraft	100000	$d = 1$	-	-
Link 1	80	$\ell = 8.13$	1×10^5	1%
Link 2	80	$\ell = 8.13$	1×10^5	1%
Payload	4000	$R = 1$	-	-

Table 8.2 Time-optimal retrieval maneuver: the initial and final conditions.

	q_1 (rad)	q_2 (rad)	q_3 (rad)
Initial cond.	1.175	0.7925	1.175
Final cond.	0.1856	2.7705	0.1856

The solution to this minimum-time problem is a single switching, bang-bang maneuver with the final time $\bar{t}^f = 40.37(s)$ and the switching time $t_s = 14.61(s)$.

Applying the open-loop control $\bar{\tau}$, the input torques obtained from the rigid-body minimum-time maneuver, to the flexible system shows that the system is stiff enough to withstand the bang-bang, open-loop control, so the vibration suppression is carried out after finishing the rigid-body maneuver. Figures 8.4 and 8.5 show the simulation results for the near-minimum-time maneuver. The results show that some of the capabilities of the second and third actuators are not used during the maneuver. This suggests that one can obtain a shorter maneuver time by selecting another path for going from point A to point B.

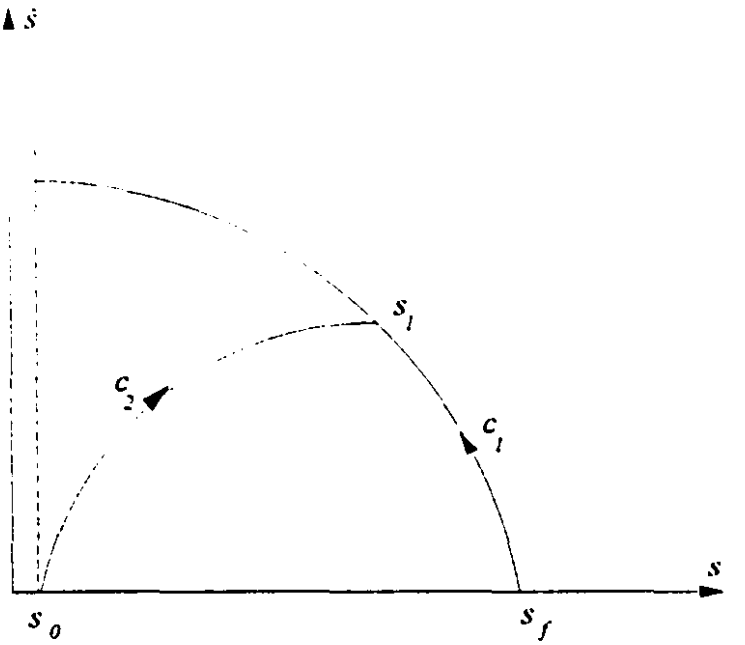

Figure 8.1 Minimum-time trajectory construction; a single-switching case

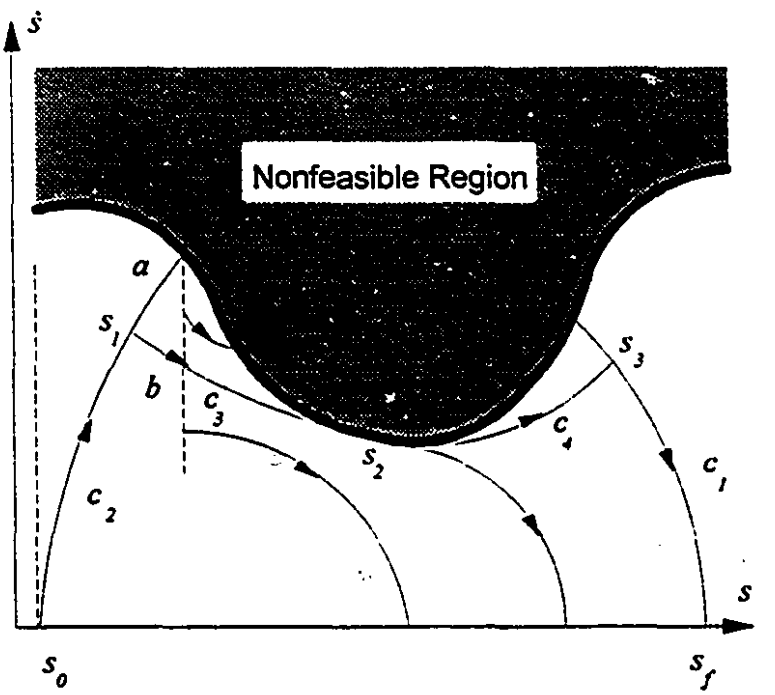

Figure 8.2 Minimum-time trajectory construction; a multi-switching case

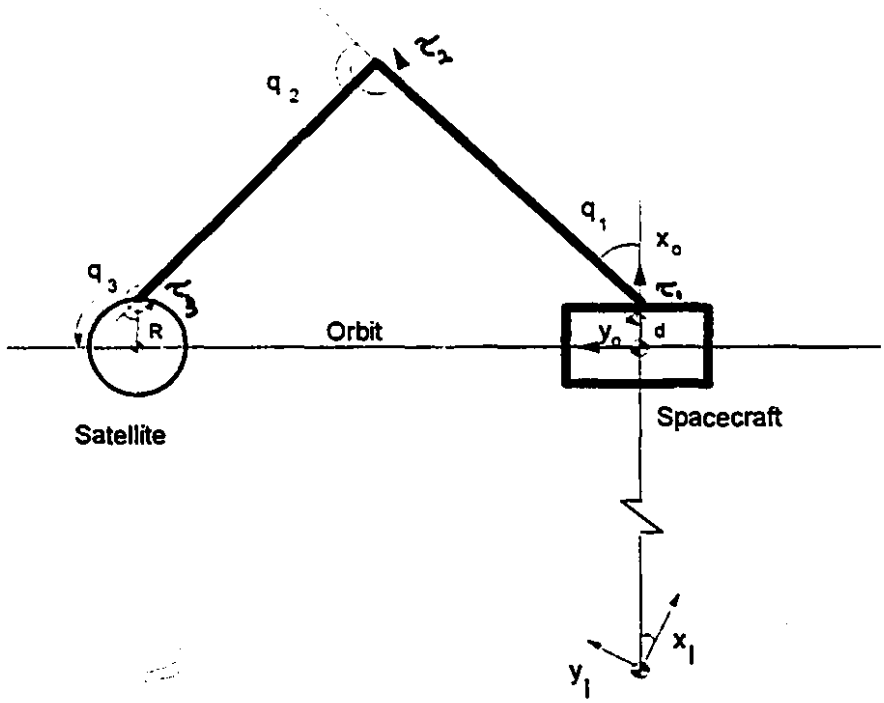

Figure 8.3 Retrieval of a satellite by a spacecraft mounted manipulator; a schematic of the system.

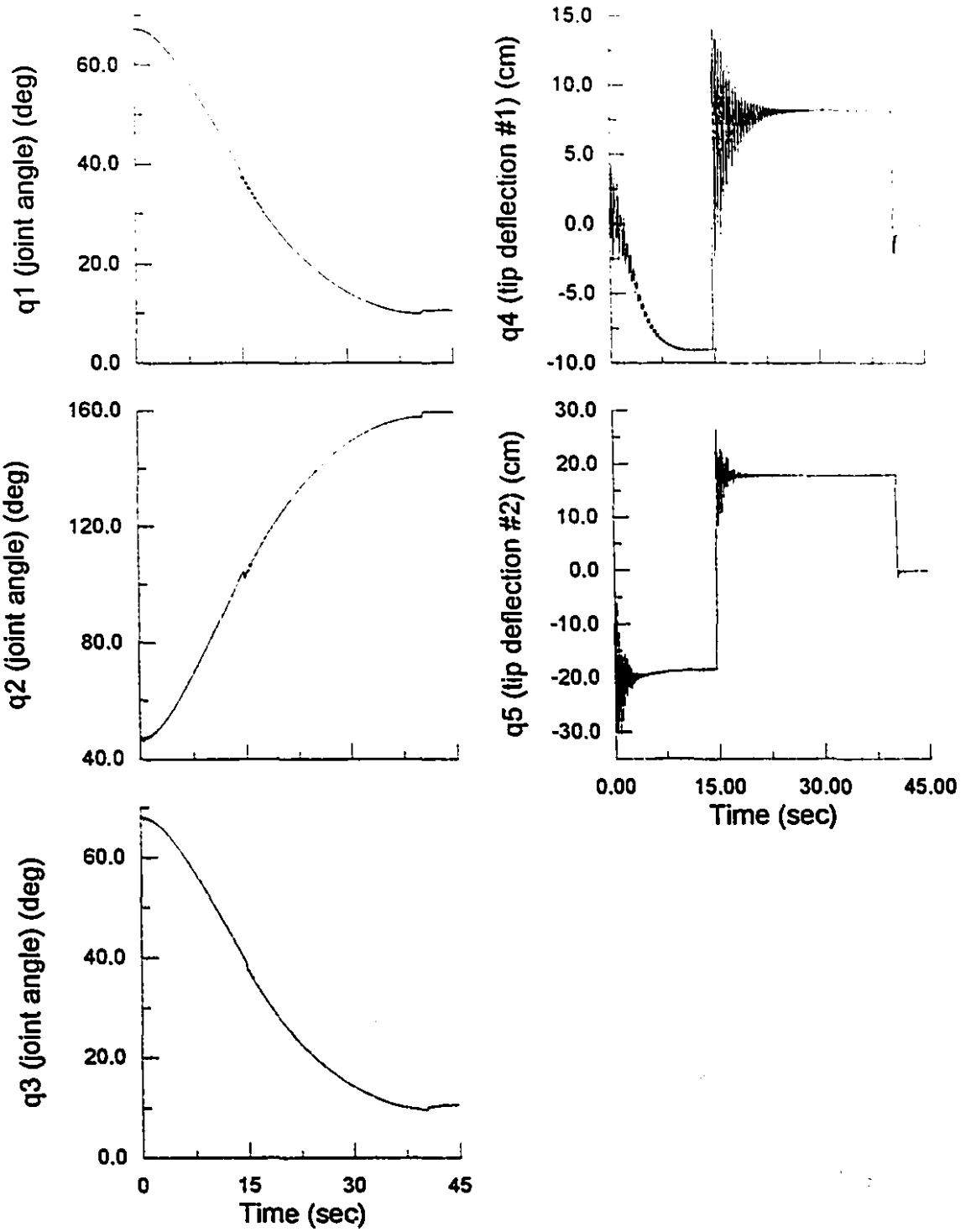

Figure 8.4 Simulation results for moving the satellite along the local horizontal; time history of the generalized coordinates.

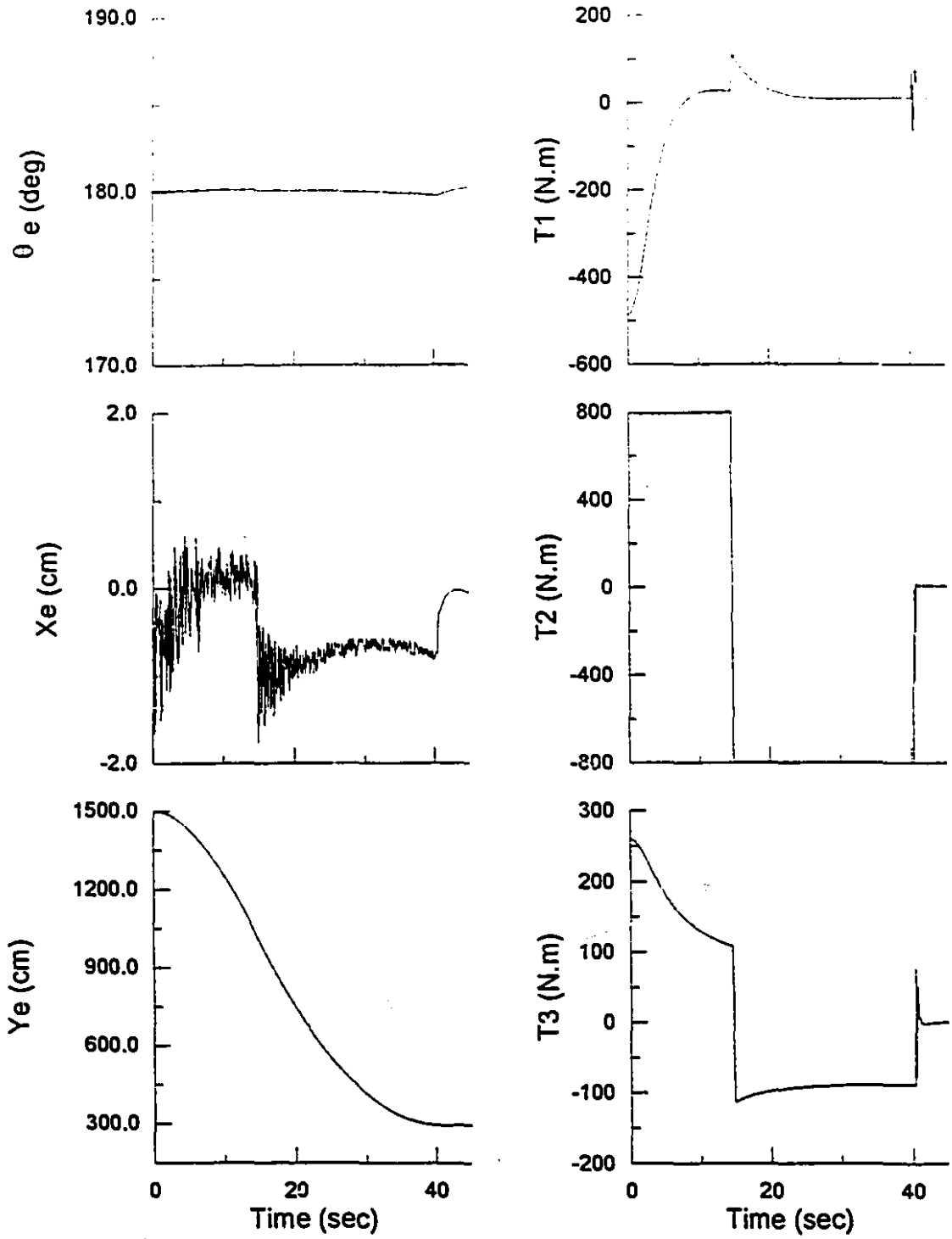

Figure 8.5 Simulation results for moving the satellite along the local horizontal; time history of the position of the satellite and the actuator torques.

Chapter 9

Conclusions and Recommendations for Future Work

9.1 Summary and Conclusions

The problem of attitude dynamics and maneuvering of flexible, multibody space systems was considered in this thesis. The main problems which were examined in detail are the constrained motion, the effect of rigid-body base motion on the dynamical characteristics of a flexible structure, application of constrained motion in control of flexible space systems, and the time-optimal maneuvering of flexible systems along a prescribed trajectory. A formulation for deriving the equations of motion of flexible multibody systems was presented based on the above developments. The formulation was implemented in a symbolic computer code, FLXSIM, which was employed to solve several problems.

The following points were concluded from the study of the constrained motion.

- Constrained motion is of particular importance in the analysis of motion of space systems. That is because, even in the absence of any closed kinematic loop, the motion of a spacecraft during certain modes of operation can be regarded as a constrained motion. For

example, in the free-flying mode, that is to fly with no thruster firings, the component bodies of the system move such that the center of mass of the entire system remains on the orbit.

- The method of implementation of the constraint forces (naturally or artificially) has an important effect on the response of the system.
- The available methods for constrained motion cannot, in general, produce a complete set of equations (with as many equations as the number of unknowns) for systems subjected artificial constraints.

This investigation led to the development of a novel method which can be applied to generate directly the complete, minimum-order set of equations of motion of systems with artificial and/or natural constraints. The method automatically reduces to the conventional methods of formulation for constrained motion if all of the constraints are natural. As a spin-off of this formulation, some analytical measures were developed for testing the adequacy and redundancy of the constraint forces.

The effect of negligence of the second-order elastic deflections* on the equations of motion of flexible systems which undergo rigid-body motion is another topic which was studied in detail. From this study the following points were concluded

- Improper linearization (i.e., a linearization which is started prior to the calculation of partial derivatives in the process of deriving the equations of motion using an energy based method) is a source of flaw in dynamic analysis of flexible systems undergoing rigid-body motion.

* The term "second-order elastic deflections" refers to some small quantities (of the order ε^2) which are quadratic functions of the elastic generalized coordinates. These terms are normally neglected in the linear analysis of the elastic systems with fixed base.

- Using a nonlinear strain energy expression (up to the third order) to compensate for this deficiency is a weak remedy, which can produce wrong results unless special care is taken in choosing the elastic DOFs of the system. For instance, in the case of beams, this method can only produce acceptable results when the elongation of the beam is not ignored. This, clearly, is not convenient for cases where the elongation of the beam is of no practical importance, such as flexible space manipulators. Another drawback of this remedy is that considering elongation of the beam as a degree of freedom makes the differential equations of motion numerically stiff and inconvenient for simulation purposes –recall that the frequencies of longitudinal vibration of a beam can be several hundred times larger than those of its lateral vibrations.

- The stiffness of an elastic system may or may not be increased due to the base motion. In fact, the stiffness of the system might be reduced in some cases or it might become time varying, depending on the base motion. Thus, the general use of the term "geometric stiffening" or "nonlinear stiffening" is not strictly valid. Furthermore, rigid-body base motion, if not prescribed, might even change the generalized mass matrix of the system.

- Contrary to the common belief, it was shown that the importance of the nonlinear coupling between elastic and rigid-body motions is not restricted to spinning systems; any type of rigid-body acceleration of the base might change the dynamic behaviour of the system. For example, if a constant velocity perturbation is applied to the orbital motion of a non-spinning satellite, the flexible appendages of the satellite might become either stiffer or softer (they may even collapse) due to the effect of Coriolis acceleration of the satellite during this maneuver.

To prevent improper linearization and to derive the correct form of equations of motion for elastic systems undergoing rigid body motion, a novel method based on nonlinear strain-displacement relations was presented in this thesis. The method can be used either to derive the

correct equations directly, or to find the correction terms for an improperly linearized set of equations. The method is geometry-independent and can be used for any arbitrary type of elastic media. Specializations of the method for beams and plates are provided for convenience.

The computer code FLXSIM, developed based on the formulation presented in this thesis, was applied to study several problems. One of them was the study of capture of a spinning satellite by a flexible space manipulator, from which we concluded the following.

- If the approach trajectory (i.e., the initial condition) is chosen properly, the rotational kinetic energy of the captured satellite can be used in the retrieval process.
- The uncontrolled post-capture response of the system strongly depends on the approach trajectory. This induces a challenging problem of choosing the best approach trajectory to achieve the most desirable system response.
- Considering the free flying mode as a constrained motion can be helpful both in control synthesis as well as the simulation of the dynamics of the system by reducing the order of the equations of motion. For instance, regulation† of a space structure during its free flying mode, using feedback linearization technique, can be carried out without thruster firing.

Another application was the examination of the problem of using space manipulators in stabilizing tethered satellite systems (TSS), through offset control. A standard LQR method was used to asymptotically stabilize the librational motion of the tether during the stationkeeping phase, marginally stable if uncontrolled. A *modified* feedback linearization technique was employed to keep the response of the system during the retrieval phase –an unstable one if uncontrolled– bounded. The results indicate the possibility of using space manipulators to control tethered satellite systems with short tether lengths. Some of the points learned from this study are the following:

† Regulation refers to a control problem in which we intend to keep the states of the system close to some *constant* target values.

- Shorter tethers are easier to control (demand less control effort and induce smaller motion in the rest of the system).
- A *multi-step* retrieval–stationkeeping gives better results than retrieving the same length in one step followed by a period of controlled stationkeeping.
- The performance of retrieval with exponential rate is better, both in terms of the system response and the required actuator torques, compared to the retrieval with constant rate.

The idea of using artificial constrained motion to devise open-loop control laws for tracking problems was introduced in this thesis. Using this approach, the output can track the desired trajectory without requiring all of the states of the system to track prescribed trajectories. This method can find interesting applications in semi-manual control of manipulators and in fine tracking of flexible manipulators. In the case of flexible manipulators, the controller does not try to prevent elastic vibrations; instead, it tries to compensate for the effect of the elastic vibrations by necessary corrections in the joint angles so that the output tracks the desired motion. This method was employed to control a flexible manipulator such that its end effector follows a prescribed trajectory.

A perturbation technique in conjunction with a phase-plane based optimal control analysis was proposed for near-minimum time maneuvering of flexible multibody systems moving along a prescribed trajectory. The idea was successfully employed to devise a control law for a typical retrieval maneuver performed by a Shuttle-based three link, flexible manipulator.

9.2 Suggestions for Future Work

Perhaps one of the reasons for the exponential growth in the knowledge is that any research activity introduces more new questions than answers. This is true for the research work presented in this thesis as well. Here are some of these questions and problems which

might provide a platform for new research activities and advancements in the analysis of dynamics and maneuvering of flexible space systems.

- Development of a method based on Lagrange's equations for deriving the complete minimum-order equations of motion of *artificially* constrained systems. This, perhaps, can be done by premultiplying the equations of motion by the orthogonal complement of a modified constraint matrix. The problem amounts to modifying the Jacobian matrix of the constraints in such a way that its orthogonal complement is normal to the matrix of influence of the constrained forces[‡].
- Adopting Eulerian description (i.e., considering the shape functions as functions of current configuration as opposed to the reference configuration) in calculating the second-order elastic deflections based on the nonlinear strain-displacement relations. This can help to develop a more accurate, but more complex theory for correct analysis of two and three-dimensional elastic members, such as plates and shells, undergoing overall rigid body motion.
- Extension of the dynamic formulation by giving the specialized relations for contribution of a shell type member to the mass matrix and generalized force vector, and the specialization of the method presented in Section 5.4 for calculating the second order elastic deflections of shells.
- Development of an order-n formulation, while incorporating the theories for constrained motion and geometric nonlinearities presented in this thesis.
- Development of numerically efficient methods for calculation of the constraint forces for *artificially* constrained systems.

[‡] The matrix of influence of the constrained forces is the matrix of coefficients of constraint forces in the equations of motion.

- Development of the equations of motion governing the tracking errors of an artificially constrained system. These equations can be used to devise a feedback control law for better tracking and damping the deviations of the output from the desired trajectory due to the disturbances and uncertainties of the model.

Bibliography

Amirouche, F.M.L., Jia, T., and Ider, .S.K., 1988, "Recursive Householder Transformation for Complex Dynamical Systems with Constraints," *Journal of Applied Mechanics*, Vol.55, pp.729-734.

Angeles, J., and Lee, S., 1988, "The Formulation of Dynamical Equations of Holonomic Mechanical Systems Using Natural Orthogonal Complements," *J. Applied Mechanics*, Vol.55, pp.243-244.

Bainum, P., and Li, F., 1991, "Optimal Large Angle Maneuvers of a Flexible Spacecraft," *Acta Astronautica*, Vol.25, No.3, pp.141-148.

Bainum, P., Li, F., and Xu, J., 1992, "A Combined Algorithm for Minimum-Time Slewing of Flexible Spacecraft," *NASA Workshop on Distributed Parameter Modeling and Control of Flexible Aerospace Systems*, Williamsburg, Virginia.

Banerjee, A.K., and Kane, T.R., 1989," Dynamics Of a Plate in Large Overall Motion," *Journal of Applied Mechanics*, Vol.56, pp.887-892.

Banerjee, A.K., and Dikens, J.M., 1990, "Dynamics of an Arbitrary Flexible Body in Large Rotation and Translation," *Journal of Guidance, Control, and Dynamics*, Vol.13, pp.221-227.

Banerjee, A.K., and Singhose, W., 1994, "Slewing and Vibration Control of a Nonlinearly Elastic Shuttle Antenna," AIAA/AAS Astrodynamics Conference, Scottsdale , AZ, AIAA 94-3752.

Bang, H., Junkins, J.L., and Fleming, P.J., 1993, "Lyapunov Optimal Control Laws for Flexible Maneuver and Vibration Control," *Journal of the Astronautical Sciences*, Vol.41, No.1, pp.91-118.

Barbieri, E., and Ozguner, U., 1988, "Rest to Rest Slewing of Flexible Structures in Minimum Time," *IEEE, Proceedings of 27th Conference on Decision and Control*, pp.1633-1638.

Bejczy, A.K., 1974, "Robot Arm Dynamics and Control," Jet Propulsion Lab., Pasadena, Calif., TM-33-669.

Bell, M. J., and Junkins, J.L., 1993, "Near-Minimum-Time Three-Dimensional Maneuvers of Rigid and Flexible Spacecraft," AAS/AIAA Astrodynamics Specialist Conference, Victoria, B.C., Canada, AAS 93-586.

Ben-Asher, J., Burns, J.A., and Cliff, E.M., 1987, "Time-Optimal Slewing of Flexible Spacecraft," *IEEE, Proceedings of 26th Conference on Decision and Control*, Vol.1, pp.524-528.

Bobrow, J.E., Dubowsky, S., and Gibson, J.S., 1985, "Time-Optimal Control of Robotic Manipulators," *International Journal of Robotic Research*, Vol.4, No.3, pp.3-17.

Bodley, C.S., Devers, A.D., Park, A.C., and Frisch., H.P., 1978, "A Digital Computer Program for the Dynamic Interaction Simulation of Controls and Structures (DISCOS)," NASA T-1219, Vol.1&2.

Carington, C.K., and Junkins J.L., 1986, "Optimal Nonlinear Feedback Control of Spacecraft Attitude Maneuvers," *Journal of Guidance, Control, and Dynamics*, Vol.9, No.1, pp.99-107.

Chen, J., and Kane T.R., 1980, "Slewing Maneuvers of Gyrostat Spacecraft," *Journal of the Astronautical Sciences*, Vol.28, pp.267-281.

Craig, J., 1989, "*Introduction to Robotics: Mechanics and Control*," Addison-Wesley, Reading

Cyril, X., Angeles, J., and Misra, A.K., 1991, "Dynamics of Flexible Mechanical Systems," *Transactions of the Canadian Society of Mechanical Engineering*, Vol. 15, pp. 235-256.

D'Amario, L.A., and Stubbs, G.S., 1979, "A New Single Rotation Autopilot for Rigid Spacecraft Attitude Maneuvers," *Journal of Guidance, Control, and Dynamics*, Vol.2, pp.339-346.

Dikmanns, E.D., and Well, H., 1975, "Approximate Solution of Optimal Control Problems Using Third-Order Hermit Polynomial Functions," *Proc. of the 6-th Technical Conference on Optimization Techniques*, Springer-Verlag, New York.

Dodds, S., Williamson, S., 1984, "A Signed Switching Time Bang-Bang Attitude Control Law for Fine Pointing of Flexible Spacecraft," *International Journal of Control*, Vol.49, No.4, pp.795-811.

Donaldson, B.K., 1993, "*Analysis of Aircraft Structures; An Introduction*," McGraw-Hill, New York.

Flisher, G.E., and Likins P.W., 1974, "Attitude Dynamics Simulation Subroutines for Systems of Hinge-Connected Rigid Bodies," *JPL Technical Report*, No.32-1592, Pasadena, California.

Fox, C.H., and Burdess, J.S., 1978, "The Natural Frequencies of a Thin Rotating Cantilever with Offset Root," *Journal of Sound and Vibration*, Vol.65, No.2, pp.151-158.

Frisch., H.P., 1975, " A Vector Dyadic Development of the Equations of Motion for N-Coupled Flexible Bodies and Point Masses," *NASN TN D-8047*.

Goldstein, H, 1950, "*Classical Mechanics*," Addison-Wesley Publishing Company, Reading, Mass.

Hanagud ,S., and Sarkar, S., 1989, "Problem of the Dynamics of a Cantilever Beam Attached to a Moving Base," *Journal of Guidance, control, and Dynamics*, Vol.12, pp.438-441.

Hargraves, C.R., and Paris S.W., 1981, "Direct Trajectory Optimization Using Nonlinear Programming and Collocation," *Journal of Guidance and Control*, Vol.10, No.4, pp.406-414.

Hecht, N.K., and Junkins, J.L., 1992, "Near-Minimum-Time Control of a Flexible Manipulator," *Journal of Guidance, Control, and Dynamics*, Vol.15, No.2, pp.477-481.

Hoa, S.V., 1979, "Vibration of a Rotating Beam with Tip Masses," *Journal of Sound and Vibration*, Vol.67, pp.369-381.

Hooker, W.W., and Margulies, G., 1965, "The Dynamical Attitude Equations for n-Body Satellite," *Journal of the Astronautical Sciences*, Vol 12, No.4, pp.123-128.

Horn, B.K.P., and Raibert, M.H., 1978 "Configuration Space Control," *The Industrial Robot*, pp.69-73.

Hughes, P.C., and Cherchas, D.B., 1970, "Spin Decay of Explorer XX," *Journal of Spacecraft and Rockets*, Vol. 7, No.1, pp.92-93.

Hughes, P.C., 1972, "Attitude Dynamics of a Three-Axis Stabilized Satellite with Large Flexible Solar Array," *Journal of the Astronautical Sciences*, Vol.20, No.3, pp.166-189.

Hughes, P.C., 1986, "*Spacecraft Attitude Dynamics*," John Whiley & Sons, New York.

Ider, .S.K., and Amirouche, F.M.L., 1988, "Coordinate Reduction in the Dynamics of Constrained Multibody Systems – A New Approach," *Journal of Applied Mechanics*, Vol.55, pp.899-904.

Ider, S.K., and Amirouche, F.M.L., 1989, "Nonlinear Modeling of Flexible Multibody Systems Dynamics Subjected to Variable Constraints," *Transactions of the ASME*, Vol.56,pp.444-450.

Junkins, J.L., Rahman, Z., and Bang, H.C., 1990, "Near-Minimum-Time Maneuvers of Flexible Vehicles: A Lyapunov Design Method," *AIAA Dynamics Specialist Conference*, AIAA, Washington, DC., pp.565-593.

Junkins, J.L., Rahman, Z.H., and Bang, H., 1991, "Near-Minimum-Time Control of Distributed Parameter Systems: Analytical and Experimental Results," *Journal of Guidance, Control, and Dynamics*, Vol.13, No.1, pp.406-415.

Kahan, M.E., 1969, "The Near-Minimum-Time Control of Open-Loop Articulated Kinematic Chains," Stanford Artificial Intelligence Memo., AIM 106.

Kamman, J.W., and Huston, R.L., 1984, "Constrained Multibody Systems Dynamics- An Automated Approach," *Journal of Computers and Structures*, Vol.18, No.6, pp.899-903.

Kammer, D.C., and Schlack, A.L.Jr., 1986, "Critical Spin Rate of Rotating Beams by Lyapunov's Direct Method," *Journal of Vib., Acoustics, Stress and Reliability in Design*, Vol.108, pp.389-393.

Kane, T.R., Ryan, R.R., and Banerjee, A.K., 1987, "Dynamics Of a Cantilever Beam Attached to a Moving Base," *Journal of Guidance, control, and Dynamics*, Vol.10, pp.139-151.

Kane, T.R., 1961, "Dynamics of Nonholonomic Systems," *Journal of Applied Mechanics*, Vol.28, pp.574-578.

Kamton, J., 1970, "Minimum-Time Attitude Maneuvers with Control Moment Gyroscopes," *AIAA Journal*, Vol.8, pp.1523-1525.

Kim, S S , and Vanderploeg, M.J., 1986, "QR Decomposition for State Space Representation of Constrained Mechanical Dynamic Systems," *Journal of Mechanisms, Transmissions, and Automation in Design*, Vol.108, pp.183-188.

Kirk, D.E., 1970, "*Optimal Control*," Englewood Cliffs, N.J., Prentice Hall.

Li, F., and Bainum, P.M., 1990, "Numerical Approach for Solving Rigid Spacecraft Minimum Time Attitude Maneuvers," *Journal of Guidance, Control and Dynamics*, Vol.13, No.1, pp.38-45.

Li, F., and Bainum, P., 1993, "Analytical Time-Optimal Control Synthesis of a Fourth-Order System and Maneuvers of Flexible Structures," AAS/AIAA Astrodynamics Specialist Conference, Victoria, B.C., Canada, AAS 93-585.

Likins, P.W., 1966, Effects of Energy Desipation on the Free-Body Motions of Spacecraft," Jet Propulsion Lab., Pasadena, Calif., TR-32-860.

Likins, P.W., 1974, "Geometric Stiffening Characteristics of a Rotating Elastic Appendage," *International Journal of Solids and Structures*, Vol.10, pp.161-167.

Likins, P.W., 1988, "Multibody Dynamics -An Historic Perspective," Proceedings of the workshop on the Multibody Simulation, Jet Propulsion Lab., Pasadena, Calif.

Mani, N.K., 1984, "Use of Singular Value Decomposition for Analysis and Optimization of Mechanical System Dynamics," Ph.D. thesis, The University of Iowa.

Meier, E.B., and Bryson, A.E.Jr., 1990, "Efficient Algorithm for Time-Optimal Control of a Two-Link Manipulator," *Journal of Guidance, Control, and Dynamics*, Vol.13, No.5, pp.859-866.

Meirovitch, L., and Nelson, H.D., 1966, "High-Spin Motion of a Satellite Containing Elastic Parts," *Journal of Spacecraft and Rockets*, Vol.3, No.11, pp.1597-1602.

Meirovitch, L., 1967, "*Analytical Methods in Vibrations*," The McMillan Company, New York.

Meirovitch, L., 1970, "*Analytical Methods in Dynamics*," The McGraw-Hill Book Company, New York.

Meirovitch, L., 1970, "Stability of a Spinning Body Containing Elastic Parts via Lyapunov's Direct Method," *AIAA Journal*, Vol.8, pp. 1193-1200.

Meirovitch, L., and Calico, R.A., 1973, "A Comparative Study of Stability Methods for Flexible Satellites," *AIAA Journal*, Vol.11, No.1, pp.91-98.

Meirovitch, L., and Quinn, R.D., 1987, "Maneuvering and Vibration Control of Flexible Spacecraft," *Journal of the Astronautical Sciences*, Vol.35, No.3, pp.301-328.

Meirovitch, L., 1990, "*Dynamics and Control of Structures*," John Whiley & Sons, New York.

Meirovitch, L., and Kwak, K., 1990, "Control of Spacecraft with Multi-Targeted Flexible Antennas," *Journal of the Astronautical Sciences*, Vol.38, No.2, pp.187-199.

Meirovitch, L., and Sharony, Y., 1990, "A Perturbation Approach to the Maneuvering and Control of Space Structures," *Advances in Aerospace Systems, Control and Dynamic Systems*, Vol.33, pp.247-293.

Miele, A., and Iyer, P.R., 1970, "General Technique for Solving Nonlinear Two-Point Boundary Value Problems, via the Method of Particular Solutions," *Journal of Optimization Theory and Applications*, Vol.5, No.5, pp.382-399.

Misra, A.K., and Modi, V.J., 1986, "A Survey on the Dynamics and Control of Tethered Satellite Systems," *Advanced in the Astronautical Sciences, Tethers in Space*, Vol.62, pp.667-719.

Modi, V.J., 1974, "Attitude Dynamics of Satellites with Flexible Appendages -A Brief Review," *Journal of Spacecraft and Rockets*, Vol.11, No.11, pp.743-751.

Modi, V.J., and Suleman, A., 1991, "An Approach to Dynamics of Flexible Orbiting Systems with Application to the Proposed Space Station," *42nd Congress of the International Astronautical Federation*, Montreal, Canada, IAF-91-293.

Modi, V.J., Lakshamanan, P.K. and Misra, A.K., 1990, "Offset Control of Tethered Satellite Systems: Analysis and Experimental Verification," *Acta Astronautica*, Vol.21, No.5, pp.283-294.

Nikravesh, P.E., and Haug, E.J., 1983, "Generalized Coordinate Partitioning for Analysis of Mechanical Systems with Nonholonomic Constraints," *Journal of Mechanisms, Transmissions, and Automation in Design*, Vol.105, pp379-384.

Padilla, C.E., and von Flotow, A.H, 1992," Nonlinear Strain Displacement Relations and Flexible Multibody Dynamics," *Journal of Guidance, Control, and Dynamics*, Vol.15, pp.128-136.

Paul, R.P., 1972, "Modeling, Trajectory Calculation, and Servoing of Computer Controlled Arm," Stanford University, Artificial Intelligence Lab., AIM 177.

Peters, D.A., and Hodges, D.H, 1980, "In-plane Vibration and Buckling of a Rotating Beam Clamped off the Axis of Rotation," *Journal of Applied Mechanics*, Vol.47, pp.398-402.

Pfeiffer, F., and Johanni, R., 1987, "A Concept for Manipulator Trajectory Planning," *IEEE Journal of Robotics and Automation*, Vol. RA-3, No.2, pp.115-123.

Raibert, M.H., 1977, " Analytical Equations vs. Table Look-up for Manipulation: A Unifying Concept," Proceedings of IEEE Conf. Decision and Control, New Orleans, pp.576-579.

Raibert, M., and Craig, J., 1981, "Hybrid Position/Force Control of Manipulators," ASME Journal of Dynamic Systems, Measurement and Control.

Robert, S. M., Shipman, J. S., and Elis, W. J., 1969, "A Perturbation Technique for Nonlinear Two-Point Boundary Value Problems," SIAM *Journal of Numerical Analysis*, pp.347-358.

Rosenthal, D.E., and Sherman, M.A., 1986, "High Performance Multibody Simulation via Symbolic Equation Manipulation and Kane's Method," *Journal of the Astronautical Sciences*, Vol.34, pp.223-239

Sayers, M.W., 1991, "Symbolic Vector/Dyadic Multibody Formalism for Tree-Topology Systems," *Journal of Guidance, Control, and Dynamics*, Vol.14, pp.1240-1250.

Schaechter, D.B., and Levinson D.A., 1988, "Interactive Computerized Symbolic Dynamics for the Dynamicist," *Journal of the Astronautical Sciences*, Vol.36, No.4, pp.365-388.

Schiehlen, W.O., and Kreuzer, E.J., 1977, "Symbolic Computerized Derivation of Equations of Motion," *Dynamics of Multibody Systems*, Springer Verlag, New York, pp.290-305.

Scrivener, S., and Thompson, R.C., 1992, "Survey of Time-Optimal Attitude Maneuvers," AAS/AIAA Spaceflight Mechanics Meeting, Colorado Springs, Colorado.

Scrivener, S.L., and Thompson R.C., 1993, "Time Optimal Attitude Maneuvers of Rigid Spacecraft Using Collocation and Nonlinear Programming," AAS/AIAA Astrodynamics Specialist Conference, Victoria, B.C., Canada, AAS 93-584.

Shiller, Z., and Dubowsky, S., 1989, "Robot Path Planning with Obstacles, Actuator, Gripper, and Payload Constraints," *International Journal of Robotic Research*, Vol.8,No.6, pp.3-18.

Shiller, Z., 1984, "Optimal Dynamic Trajectories and Modeling of Robotic Manipulators," M.S. Thesis, Department of Mechanical Engineering, Massachuset Institute of Technology, Cambridge, Mass.

Singer, N.C., and Seering, W.P., 1990, "Preshaping Command Inputs to Reduce System Vibration," *Journal of Dynamic Systems, Measurement, and Control*

Singh, R.P., Voort, R.J.V., and Likins, P.W., 1985, "Dynamics of Flexible Bodies in Tree Topology - A Computer Oriented Approach," *Journal of Guidance, Control, and Dynamics*, Vol. 8, pp. 584-590.

Singh, R.P., and Likins, P.W., 1985, "Singular Value Decomposition for Constrained Dynamical Systems," *Journal of Applied Mechanics*, Vol.52, pp.943-948.

Singh, G., Kabamba, P.T., and Maclanroach, N.H., 1989, "Planar, Time-Optimal, Rest-to-Rest Maneuvers of Flexible Spacecraft," *Journal of Guidance, Control, and Dynamics*, Vol.12, No.1, pp.71-81.

Spong, M.W., and Vidyasagar, M., 1989, "*Robot Dynamics and Control*," John Whiley & Sons, New York.

Storm, J. E., 1973, "CSMP III Optimum System Control," *Summer Computer Simulation Conference*, pp.429-435.

Subrahmanyam, M.B., 1986, "Computation of Optimal Controls by Newton's Method Using a Discretized Jacobian," *Journal of Guidance, control, and Dynamics*, Vol.9, No.3, pp.371-374.

Tan, Z., Bainum, P.M., and Li, F., 1991, "Minimum-Time Large Angle Slew of an Orbiting Flexible Shallow Spherical Shell System," *Advances in the Astronautical Sciences*, Vol.75, pp.589-608.

Thompson, R.C., Junkins, J.L., and Vadali, S.R., 1989, "Near-Minimum-Time Open-Loop Slewing of Flexible Vehicles," *Journal of Guidance, Control, and Dynamics*, Vol.12, No.1, pp.82-88.

Tiesenhausen, G.von , 1984, "Tethers in Space: Birth and Growth of a New Avenue to Space Utilization", *NASA*, TM-82571.

Uicker, J.J., 1965, "On the Dynamic Analysis of Spatial Linkages Using 4×4 Matrices," Ph. D. Dissertation, Northwestern University.

Uicker, J.J., 1969, "Dynamic Behaviour of Spatial Linkages," *Journal of Engineering for Industry*, pp.251-265.

Vadali, S.R., and Junkins, J.L, 1983, "Spacecraft Large Angle Rotational Maneuvers with Optimal Momentum Transfer," *Journal of the Astronautical Sciences*, Vol.31, No.2, pp. 217-235.

Vadali, S.R., and Junkins, J.L, 1984, "Optimal Open-Loop and Stable Feedback Control of Rigid Spacecraft Attitude Maneuvers," *Journal of the Astronautical Sciences*, Vol.32, No.2, pp. 105-122.

Vadali, S.R., 1986, "Variable Structure Control of Spacecraft Large Angle Maneuvers," *Journal of Guidance, Control, and Dynamics*, Vol.9, pp.235-239.

Vigneron, F.R., 1970, "Stability of a Freely Spinning Satellite of Crossed-Dipole Configuration," *C.A.S.I Transaction*, Vol.3, No.1.

Walton, W.C., and Steeve, E.C., 1969, "A New Matrix Theorem and its Application for Establishing the Independent Coordinates for Complex Dynamical Systems with Constraints," NASA TR R-326.

Wehage, R.A., and Haug, E.J., 1982, "Generalized Coordinate Partitioning for Dimension Reduction in Analysis of Constrained Dynamic Systems," *Journal of Mechanical Design*, Vol.104, No.1, pp.247-255.

Wie, B., Chaung, C.H., and Sunkel, J., 1990, "Minimum-Time Pointing Control of a Two-Link Manipulator," *Journal of Guidance, Control, and Dynamics*, Vol.13, No.5, pp.867-873.

Wie, B., and Barbara, P.M., 1985, "Quaternion Feedback for Spacecraft Large Angle Maneuvers," *Journal of Guidance, Control, and Dynamics*, Vol.8, pp.360-365.

Wittenburg, J., and Wolz, U., 1985, "MESA VERDA: A Symbolic Program for Nonlinear Articulated Rigid-Body Dynamics," *Proc. of the 10-th Design Engineering Division Conference on Mechanical Vibration and Noise*, Cincinnati, Ohio.

Yeo, B. P., Waldron, K. J., Goh, B. S., 1974, "Optimal Initial Choice of Multipliers in the Quasilinearization Method for Optimal Control Problems with Bounded Controls," *International Journal of Control*, Vol.20, No.1, pp.12-23.

Appendix A:

Proof of Equation 3.10

To prove the validity of the Eq. (3.10), we begin with substitution of Eq.(3.20) in Eq.(3.10) which yields

$$\sum_{i=1}^{v}\left(\tilde{\mathbf{V}}_r^i\cdot\mathbf{e}^r-\sum_{s=1}^{P}\sum_{k=1}^{P}\tilde{T}_{rk}\left(\mathcal{T}'^{-1}\right)_{ks}\tilde{\mathbf{V}}_{s-N}''\cdot\mathbf{e}^r\right)=0. \tag{A1}$$

Now substitution of $\mathbf{e}^r$ from Eq.(3.11) gives

$$\sum_{i=1}^{v}\left[\tilde{\mathbf{V}}_r^i\cdot\left(\sum_{j=1}^{P}\mathbf{n}^jC_j\right)-\sum_{s=1}^{P}\sum_{k=1}^{P}\tilde{T}_{rk}\left(\mathcal{T}'^{-1}\right)_{ks}\tilde{\mathbf{V}}_{s-N}''\cdot\left(\sum_{j=1}^{P}\mathbf{n}^jC_j\right)\right]=0. \tag{A2}$$

Changing the order of summations and recalling the definition of $\tilde{\mathcal{T}}$ (Eq.(3.14)) and $\mathcal{T}'$ (Eq.(3.17)) we arrive at

$$\sum_{j=1}^{P}\tilde{T}_{rj}C_j-\sum_{j=1}^{P}\sum_{s=1}^{P}\sum_{k=1}^{P}\tilde{T}_{rk}\left(\mathcal{T}'^{-1}\right)_{ks}\mathcal{T}'_{sj}C_j=0. \tag{A3}$$

The left hand side (LHS) of Eq.(A3) is identically zero which completes the proof.

Appendix B:

Independent Additional Equations for Constraint Forces

In this section we prove that for a system with N DOFs and P simple nonholonomic constraints, using $\tilde{\mathbf{V}}_r''$, defined as in Eq.(3.15), one can generate P additional equations independent of the nonholonomic equations of motion, given in Eq.(3.13). To this end, we define a new set of generalized speeds for the system, containing P additional generalized speeds. The new set, $u_1',\ldots,u_{N+2P}'$, and the original set of generalized speeds, $u_1,\ldots,u_{N+P}$, are related to each other through the following relations:

$$\begin{aligned}
&\mathbf{u}_1' = u_1',\ldots,u_N' \equiv \mathbf{u}_1 = u_1,\ldots,u_N\ ,\\
&\mathbf{u}_2' = u_{N+1}',\ldots,u_{N+P}' \equiv \text{New}\ ,\\
&\mathbf{u}_3' = u_{N+P+1}',\ldots,u_{N+2P}' \equiv \mathbf{u}_2 = u_{N+1},\ldots,u_{N+P}\ .
\end{aligned} \tag{B1}$$

The new P generalized speeds, $u_{N+1}',\ldots,u_{N+P}'$, are defined such that they satisfy the following $2P$ simple nonholonomic constraints

$$\begin{bmatrix} [\mathcal{A}_1(\mathbf{q},t)]_{P\times N} & -[\mathbf{I}]_{P\times P} & [\mathcal{A}_2(\mathbf{q},t)]_{P\times P} \\ [0]_{P\times N} & [\mathbf{I}]_{P\times P} & [0]_{P\times P} \end{bmatrix} \begin{bmatrix} [\mathbf{u}_1']_N \\ [\mathbf{u}_2']_N \\ [\mathbf{u}_3']_N \end{bmatrix} = \begin{bmatrix} [\mathcal{B}(\mathbf{q},t)]_P \\ [0]_P \end{bmatrix}, \tag{B2}$$

in which $[\mathbf{I}]$ and $[0]$ are the unity and zero matrices, respectively, whereas $\mathcal{A}_1, \mathcal{A}_2$ and $\mathcal{B}$ are as defined in Eq.(3.1). The new system with the $2P$ constraints defined in Eq.(B2) is exactly equivalent to the original system if $\mathbf{u}_1'$ and $[\mathbf{u}_2', \mathbf{u}_3']^T$ are considered as independent and dependent generalized speeds, respectively. On the other hand, this definition provides the capability of violating the j-th original constraint simply by relaxing the new constraint of $u_{j+P}' = 0$, the $(j+P)$-th row in the new set of constraint equations. One should note that, without this approach, it can be a difficult task to define some P independent generalized speeds which

can violate the desired constraints in the case of complex systems. This can be even more difficult if one wants to violate some of the constraints while leaving the rest to remain in effect.

The velocity of the i-th particle of the system in terms of the original generalized speeds is defined as

$$\mathbf{V}^i = \sum_{r=1}^{N-P} \mathbf{V}_r^i u_r + \mathbf{V}_t^i, \tag{B3}$$

in which $\mathbf{V}_t^i$, the remainder of velocity of particle i, is the term which does not depend on the generalized speeds. Substituting for u_r from Eq.(B1), one can express the velocity in terms of the new set of generalized speeds as follows

$$\mathbf{V}^i = \sum_{r=1}^{N} \mathbf{V}_r^{ii} u_r' + \sum_{r=N-P+1}^{N+2P} \mathbf{V}_r^{ii} u_r' + \mathbf{V}_t^i. \tag{B4}$$

The partial velocities associated with the new generalized speeds can be found, simply by inspection of Eq.(B4), to be

$$\begin{aligned} &\mathbf{V}_r^{ii} = \mathbf{V}_r^i, \quad r = 1,\ldots,N, \\ &\mathbf{V}_r^{ii} = 0, \quad r = N+1,\ldots,N+P, \\ &\mathbf{V}_r^{ii} = \mathbf{V}_{r-P}^i, \quad r = N+P+1,\ldots,N+2P. \end{aligned} \tag{B5}$$

Now, let us relax the last P constraints in Eq.(B2) which is equivalent to relaxing the P constraints of the original system. The new constraint equations are

$$\left[[\mathcal{A}_1(\mathbf{q},t)]_{P\times N} \quad -[\mathbf{I}]_{P\times P} \quad [\mathcal{A}_2(\mathbf{q},t)]_{P\times P}\right] \begin{bmatrix} [\mathbf{u}_1']_N \\ [\mathbf{u}_2']_N \\ [\mathbf{u}_3']_N \end{bmatrix} = [\mathcal{B}(\mathbf{q},t)]_P, \tag{B6}$$

in which $\mathbf{u}_1'$ and $\mathbf{u}_2'$ are considered as independent and $\mathbf{u}_3'$ as dependent generalized speeds. We may generate $N+P$ independent nonholonomic equations of motion for the above system using the new nonholonomic partial velocities which are defined (with the help of Eq.(B6)) as:

$$\tilde{\mathbf{V}}_r'' = \mathbf{V}_r'' + \sum_{s=1}^{P} \bar{A}_{rs} \mathbf{V}_{s+N}'', \quad r = 1,\ldots,N+P, \tag{B7}$$

where

$$\bar{\mathbf{A}}_{P\times(N+P)} = \left[\left[-\mathcal{A}_c^{-1}\mathcal{A}_t\right]_{P\times N} \quad \left[\mathcal{A}_c^{-1}\right]_{P\times P}\right]. \tag{B8}$$

Equation (B7) can be expressed in terms of partial velocities of the original system as follows:

$$\begin{aligned} \tilde{\mathbf{V}}_r'' &= \mathbf{V}_r'' + \sum_{s=1}^{P} A_{sr} \mathbf{V}_{s+N}'' = \tilde{\mathbf{V}}_r', \quad r = 1,\ldots,N \\ \tilde{\mathbf{V}}_r'' &= 0 + \sum_{s=1}^{P} A_{sr}' \mathbf{V}_{s+N}', \quad r = N+1,\ldots,N+P. \end{aligned} \tag{B9}$$

It can be observed from (B9) that using $\tilde{\mathbf{V}}_1'',\ldots,\tilde{\mathbf{V}}_{N+P}''$, one can generate $N+P$ *independent* equations of which the first N of them are exactly equivalent to the nonholonomic equations of motion (Eq.(3.13)), and the last P of them are those used to calculate the constraint forces (Eq.(3.16)). This completes the proof of independence of Eq.(3.13) from Eq.(3.16).